ESTABLISHING A PILOT PLANT FACILITY FOR POST COMBUSTION CARBON DIOXIDE CAPTURE STUDIES

by

LIAAN RUDOLF KRITZINGER

Thesis presented in partial fulfilment

of the requirements for the Degree

of

MASTER OF SCIENCE IN ENGINEERING

(CHEMICAL ENGINEERING)

in the Faculty of Engineering

at Stellenbosch University

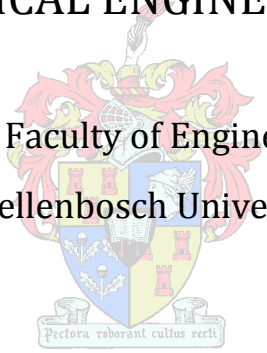

SUPERVISOR

Prof. J.H. Knoetze

CO-SUPERVISOR

Dr. L.H. Callanan

March 2013

Declaration

By submitting this thesis electronically, I declare that the entirety of the work contained therein is my own, original work, that I am the sole author thereof (save to the extent explicitly otherwise stated), that reproduction and publication thereof by Stellenbosch University will not infringe any third party rights and that I have not previously in its entirety or in part submitted it for obtaining any qualification.

Liaan Rudolf Kritzinger

March 2013

……

Signature

……

Date

ABSTRACT

Carbon dioxide (CO_2) is seen as one of the main contributors to global warming. The use of fossil fuels for power production leads to large quantities of carbon dioxide being released into the atmosphere. The released CO_2 can, however, be captured by retrofitting capture units downstream from the power plant called Post Combustion Carbon Dioxide Capturing.

Post combustion CO_2 capture can involve the reactive absorption of CO_2 from the power plant flue gas steam. Reactive solvents, such as monoethanolamine (MEA), are used for capturing the CO_2 and the solvent is regenerated in a desorber unit where the addition of heat drives the reverse reaction, releasing the captured CO_2. However, the large energy requirement for solvent regeneration reduces the viability of employing CO_2 capture on an industrial scale.

This study focused on establishing a facility for CO_2 capture studies – the main aim being the construction and validation of the results produced by the pilot plant facility. A secondary aim of this study was developing an Aspen Plus® Simulation method that would simplify simulating the complex CO_2 capture process. Results from the simulation were to be compared to that of the pilot plant experiments.

A pilot plant facility with a closed gas system, allowing gas recycling from both the absorber and the stripping columns, was set up. The absorber column (internal diameter = 0.2 m) was set up to allow one to obtain information regarding gas- and liquid temperatures and compositions at various column heights. Online gas analysers are used for analysing the gas composition at various locations in the absorber column.

The pilot plant was initially commissioned with 20 weight % MEA in aqueous solution; however the main validation experiments were conducted with 30 weight % MEA in aqueous solution. 30 weight % MEA (aq) is generally used as the reference solvent for pilot plant studies. Pilot plant results with regards to the carbon dioxide concentration profiles for the absorber column as well as the regeneration energy requirement and capture rates compared well to literature data.

The Aspen Plus® simulation was also set up and validated using published pilot plant data. The comparison of the pilot plant results from this study, to the results from the Aspen Plus® Simulation, showed good agreement between the two. The Aspen Plus® Simulation could further be used to validate pilot plant data that has been gathered outside the range of reported CO_2 capture efficiencies.

The Aspen Plus®model was evaluated at liquid-to-gas ratios of 1.7 and regeneration energies matching the pilot plant results. It was found that the model under predicts the capture

efficiency of CO_2 with an average of 4.0%. The model was corrected for this error at liquid-to-gas ratios of 2 and the fit of the model to pilot plant results improved considerably (R^2-value = 0.965).

Pilot plant repeatability was investigated with both 20 weight %- and 30 weight % MEA in aqueous solution. Temperature- and gas concentration profiles from the absorber column showed good repeatability. The maximum deviation of the regeneration energy and the capture efficiency from the calculation means were ±0.72% and ±1.40% respectively.

The aims of this study have been met by establishing, and validating the results of a pilot plant facility for carbon dioxide capture studies. It has been shown that the pilot plant produces repeatable results. Results from the Aspen Plus® Simulation were validated and also match results from the established pilot plant setup. The simulation may prove to provide valuable information regarding the optimal operating conditions for the pilot plant and may aid in performing a full parametric study on the CO_2 capture process.

OPSOMMING

Koolstofdioksied (CO_2) word geklassifiseer as een van die bekendste kweekhuisgasse wat ’n groot bydra lewer tot aardverwarming. Die gebruik van fossielbrandstowwe om na die energiebehoeftes van die mens om te sien lei daartoe dat groot hoeveelhede koolstofdioksied, hoofsaaklik vanaf kragstasies, vrygestel word in die atmosfeer. Daar is verskeie maniere hoe die CO_2 uit die uitlaatgas van kragstasies verwyder kan word – die vernaamste hiervan is bekend as die Na-verbranding opvangs metode.

Die opvangs van CO_2 na verbranding van fossielbrandstowwe vir kragproduksie kan vermag word deur van reaktiewe absorpsie tegnieke gebruik te maak. Mono-etanol-amien (MEA) kan vir hierdie doeleindes aangewend word deur dit, in ’n absorpsiekolom, in kontak te bring met die CO_2. Die gereageerde oplosmiddel word geregenereer deur die oplosmiddel te verhit in ’n stropingskolom. ’n Bykans suiwer CO_2 stroom word vrygestel. Die implementering van hierdie opvangtegniek op industriële skaal lei egter tot groot energieverliese vir die kragstasies. Die hoofrede hiervoor is die hoeveelheid energie wat benodig word om die oplosmiddel te regenereer vir hergebruik.

Die hoofdoel van hierdie studie was gemik op die oprigting en inwerkstelling van 'n navorsingsfasiliteit vir studies aangaande die na-verbranding opvangs van CO_2. Dit het behels die ontwerp, konstruksie en stawing van gelewerde resultate met resultate in die literatuur. 'n Sekondêre doel van hierdie studie was die metode-ontwikkeling vir die opstel van 'n Aspen Plus® Model wat die simulasie van die CO_2 opvangsproses met ’n reaktiewe oplosmiddel, MEA, vereenvoudig. Gesimuleerde resultate is vergelyk met resultate uit die literatuur.

Die toetsaanleg, met 'n geslote gas stelsel, maak voorsiening vir die hersirkulering van gas wat vir eksperimentele doeleindes gebruik word. Die absorpsie kolom (interne diameter van 0,2 m) is opgestel sodat informasie aangaande die gas- en vloeistof temperature, sowel as gas- en vloeistof komposisies vanaf verskillende kolomhoogtes, bekom kan word. ’n Aanlyn CO_2 analiseerder word gebruik om vir CO_2 in die prosesgas te analiseer.

Die toetsaanleg is aanvanklik in bedryf gestel met ’n 20 massa % MEA in waterige oplossing; die hoof eksperimente is egter uitgevoer deur van 30 massa % MEA in waterige oplossing gebruik te maak. Die laasgenoemde oplosmiddel word algemeen gebruik in die CO_2 opvangs verwante navorsingsveld. Die resultate van die toetsaanleg, vergelyk goed met resultate in die literatuur.

Die gesimuleerde Aspen Plus® resultate is ook vergelyk met resultate in die literatuur en die gevolgtrekking is gemaak dat die simulasie gebruik kan word om redelike akkurate voorspellings van die werklike prosesresultate te gee. Die simulasie is verder ook gebruik om

resultate, verkry vanaf die opgerigte toetsaanleg, te verifieer en ’n goeie ooreenstemming tussen die gesimuleerde en die eksperimentele resultate is waargeneem. ’n Verder gevolgtrekking aangaan die Aspen Plus® simulasie metode was dat dit in die toekoms ’n groot doel kan dien in die optimeringsproses van toetsaanlegte waar navorsing aangaande die na-verbranding opvang van CO_2 gedoen word.

Die Aspen Plus® model is geëvalueer by ‘n vloeistof-tot-gas-verhouding van 1,7 en ooreenstemmende toetsaanleg resultate, aangaande die hoeveelheid energie wat ingesit is vir die regenerasie van die oplosmiddel. Die onakkuraathede in die model, met betrekking tot die voorspelling van die hoeveelheid CO_2 wat vasgevang sal word, is hierdeur bepaal en die model is daarvoor aangepas. Resultate van die verbeterde model vergelyk baie goed met die toetsaanleg resultate – ’n R^2-waarde van 0.965.

Die herhaalbaarheid van die toetsaanleg resultate is ondersoek en ’n goeie herhaalbaarheid van die temperatuur- en CO_2 konsentrasieprofiele is verkry. Die toetsaanleg dui ook goeie herhaalbaarheid met betrekking tot die effektiwiteit waarmee die CO_2 uit ’n gasstroom verwyder word (± 1,40%), sowel as die hoeveelheid energie wat benodig word vir regenerering van die oplosmiddel (± 0,72%).

Die doelwitte van hierdie studie is bereik deur die oprigting en verifiëring van resultate gelewer deur 'n toetsaanleg vir studies aangaande die na-verbrandingsopvang van CO_2. Die herhaalbaarheid van toetaanleg resultate is bewys. Resultate van die Aspen Plus® simulasie stem ooreen met resultate in die literatuur sowel as resultate van die toetsaanleg wat opgerig is in hierdie studie.

CONTENTS

LIST OF FIGURES

LIST OF TABLES

CHAPTER 1
INTRODUCTION

1.1. BACKGROUND

Emissions of Greenhouse gases into the atmosphere are a growing concern for the current and future generations. CO_2 is one of the major greenhouse gases that are emitted to the atmosphere on a daily basis due to human activity. A continuous increase in the demand for energy leads to a continuous increase in the amount of CO_2 that is released into the atmosphere by point source emitters such as natural gas and coal-fired power plants. Abuzahra et al.(2007) state that more than 80 % of the world's energy demands are met by the use of fossil fuels, and it is thus a difficult task to reduce the amount of CO_2 currently released into the atmosphere.

Therefore, in order to reduce the amount of CO_2 that is released into the atmosphere, a sufficient capturing technique would be required. According to Allam et al.(2005), CO_2 capturing from industrial process flue gas streams has been studied for 80 years, but due to a lack of application for captured CO_2 it has been released into the atmosphere. **Figure 1** shows a simplified block diagram of the CO_2 capturing process, where the use of a sorbent of some kind is utilized. From **Figure 1** it can be seen that the sorbent removes the CO_2 from the flue gas, after which it is regenerated by the addition of energy. The regenerated sorbent can once again be recycled back for CO_2 capture from the incoming flue gas.

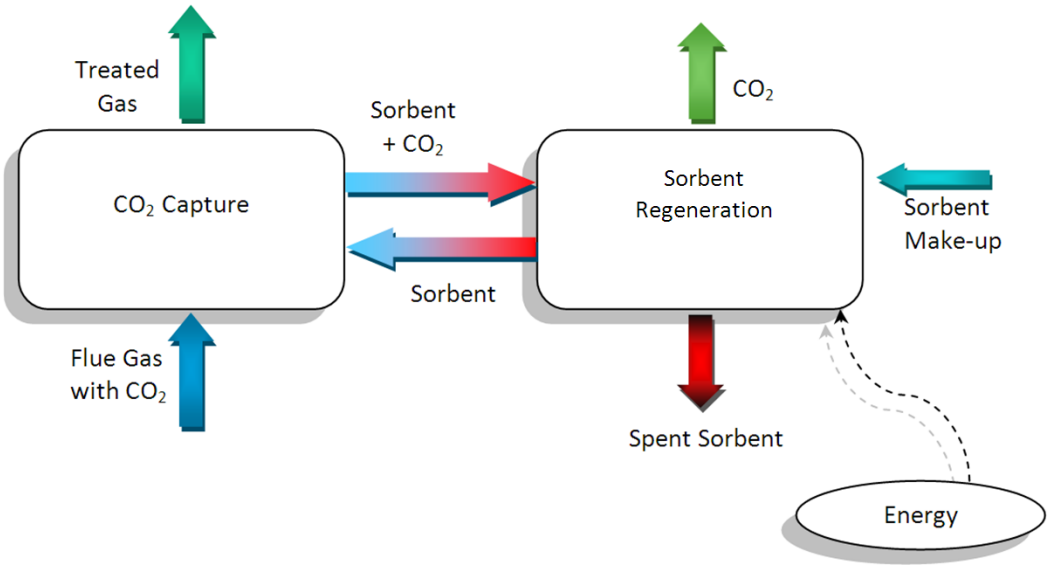

FIGURE 1 SIMPLIFIED CO_2 CAPTURE PROCESS USING SORBENTS (ADAPTED FROM (OLUJIĆ ET AL., 1999))

Various sorbents have been used for the absorption of CO_2. These include solvents for physical absorption, solid adsorbents, membrane facilitated processes, and reactive solvents, to name a few. The study will focus primarily on the latter namely reactive solvents.

One major drawback when using a reactive solvent for CO_2 absorption is the high desorption energy of the solvents used. The amount of energy required for solvent regeneration is so much that it negatively affects the overall efficiency of the industrial process (Wang et al., 2010).

Many authors (Aronu et al., 2009; Chen and Rochelle, 2005; Mangalapally et al., 2009; Notz et al., 2007; Oexmann and Kather, 2010; Rochelle et al., 2011) have performed studies on the solvent choice for the CO_2 absorption process, in order to minimize the energy penalty that is associated with solvent regeneration. Numerous optimization studies have also been done in order to determine the optimum operating conditions for the absorption process..

1.2. OBJECTIVES

The main objective of this study is focused on establishing a CO_2 capture pilot plant at the Process Engineering Department of the University of Stellenbosch. The pilot plant will be commissioned using 30 wt% monoethanolamine (MEA) as the reference solvent and the results will be compared to literature data. The pilot plant will be set up allowing for proper data acquisition in order to perform in-depth optimisation- and parametric studies on the CO_2 capture process. The established pilot plant can in future be used to study the effect of various process parameters, process configurations, solvent blends and column internals on the energy requirement for solvent regeneration. This will provide a platform for research in the field of post combustion CO_2 capture.

Another objective of this study is to develop a simplified method of simulating the CO_2 capture process using Aspen Plus®. The outcomes from this objective will be detailed in this work and is presented in Chapter 6. Results from the simulation will be compared to the results from pilot plant studies reported in literature. This will be done in order to validate the method of simulating the CO_2 capture process. The simulation will further be used to compare the performance of various column internals with respect to the energy requirement for solvent regeneration.

For the third objective the Aspen Plus® Simulation will be set up to match the configuration of the established pilot plant. The pilot plant results will be compared to results from the simulation, and this will serve as further validation of the obtained pilot plant results. Depending on the agreement between the simulated- and the pilot plant results, conclusions

will be made regarding whether or not the simulation can be used at a later stage to aid in the process of pilot plant optimization.

1.3. MIND MAP

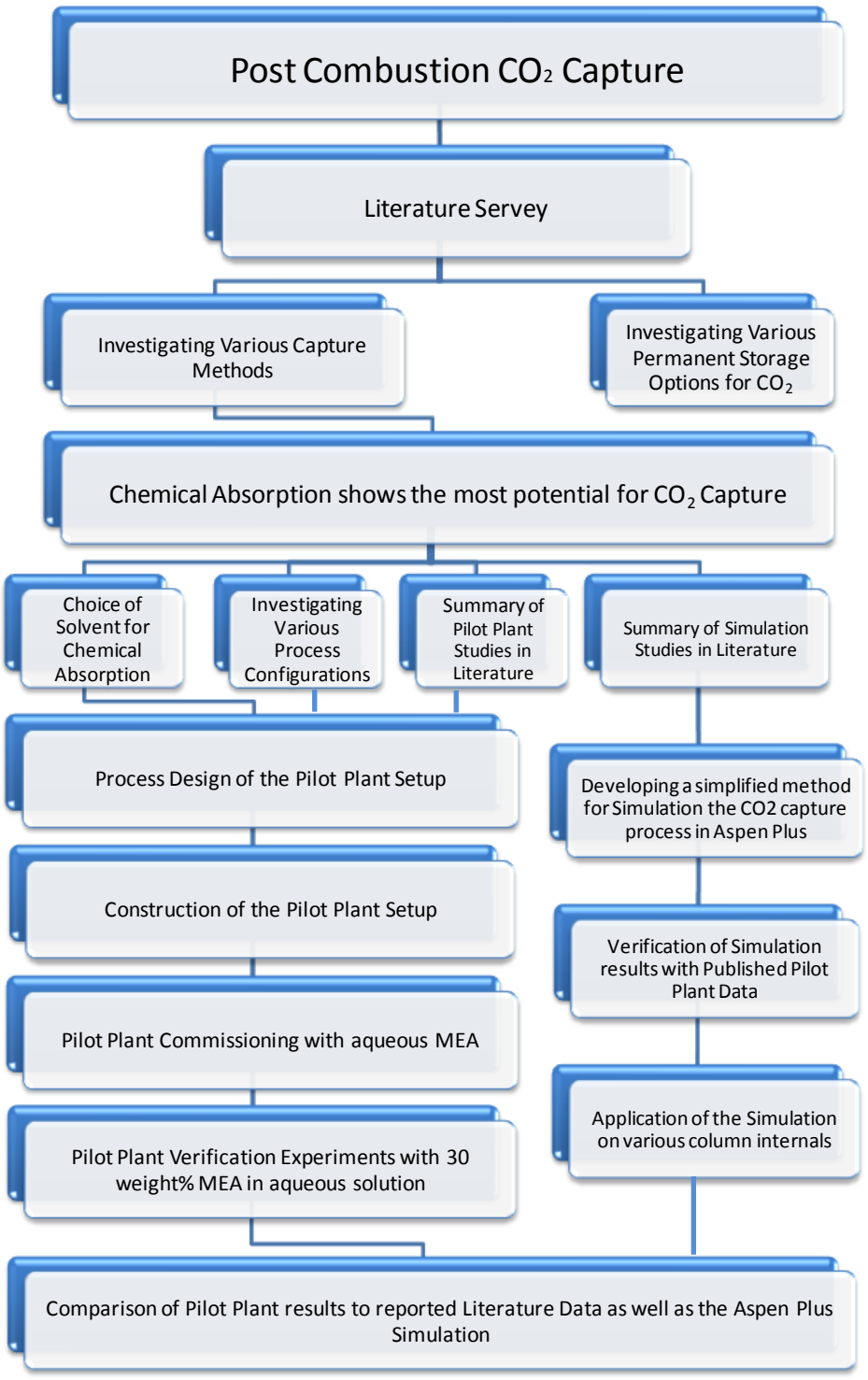

FIGURE 2 MIND MAP OF THE PROJECT OUTLINE

CHAPTER 2

LITERATURE REVIEW AND THEORETICAL FRAMEWORK

2.1. BACKGROUND

2.1.1. HISTORY OF CO_2 EMISSIONS

Human activity has increased the amount of greenhouse gases that is released into the atmosphere between 1970 and 2004 by 70 % (Liu et al., 2011). Brewer et al.(2005) report that the atmospheric CO_2 content has increased from 280 ppm in 1800 to 380 ppm in 2004. Pieter Tans, NOAA/ESRL (www.esrl.noaa.gov/gmd/ccgg/trends) reports the most recent (September 2012) recorded atmospheric CO_2 concentration of 390.53 ppm. The average rate at which the global atmospheric CO_2 increased for the years 1991 to 2000 was 1.48 ppm/year. For the years 2001 to 2010 the average increase rate was 2.05 ppm/year. **Figure 1** shows the rising trend of the atmospheric CO_2 concentration from the years 1980 to the latest recorded concentrations in 2012.

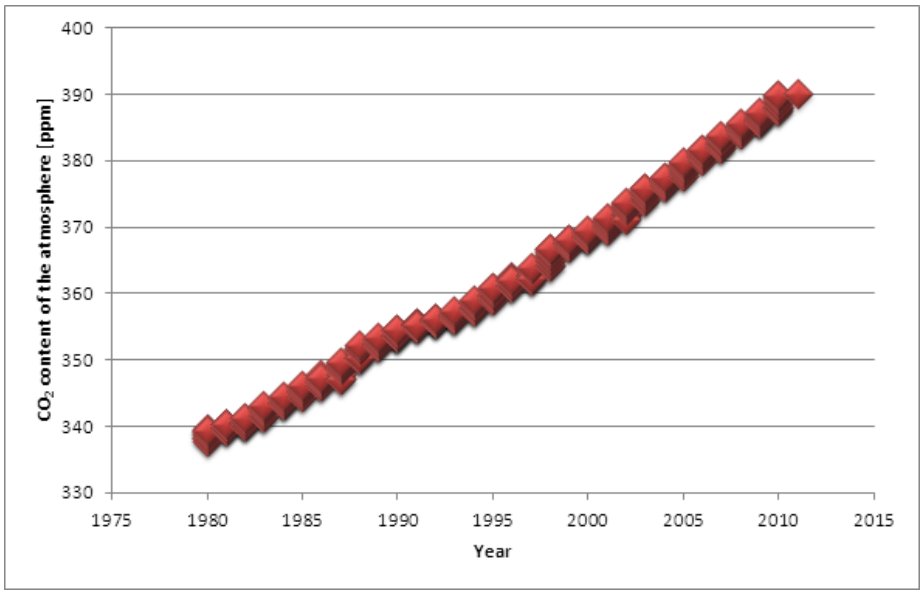

FIGURE 3 RISING TREND IN THE ATMOSPHERIC CO_2 CONCENTRATION (REPRODUCED FROM DATA BY PIETER TANS, NOAA/ESRL (WWW.ESRL.NOAA.GOV/GMD/CCGG/TRENDS))

These reported data sets on the atmospheric CO_2 concentrations, indicate not only an increase in the atmospheric CO_2 concentration, but also an increase in the rate at which the CO_2 concentration in the atmosphere is increasing. If something is not done in order to break this trend, the existence of life on earth as it is, for future generations, might be compromised.

2.1.2. MAIN SOURCES OF CO_2

The combustion of fossil fuels is the main source of CO_2 release into the atmosphere. Fossil fuels such as coal, natural gas and oil are used in power plants and in almost every facet of mankind's daily lives (Abuzahra et al., 2007). CO_2 emissions from large point sources, such as power stations and cement plants, are the main contributors to the build-up of CO_2 in the atmosphere. Metz et al.(2005) report the CO_2 emissions that can be allocated to different point sources. A summary of all point sources with annual emissions higher than 0.1 million tons of CO_2, as well as their relative contributions, is given and can be seen in **Figure 4**.

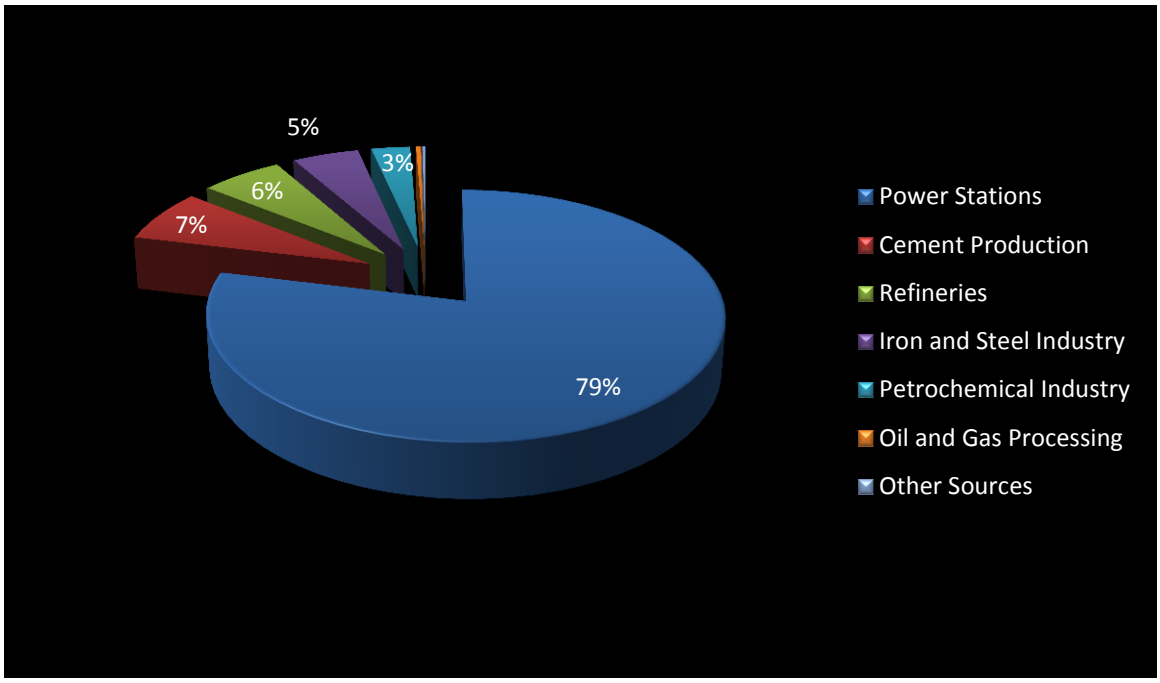

FIGURE 4 COMPARISON OF THE ANNUAL CO_2 EMISSIONS BY VARIOUS POINT SOURCES (DRAWN WITH DATA FROM (METZ ET AL. 2005))

From **Figure 4** it is clear that the emissions from power plants are the greatest contributor to CO_2 release into the atmosphere. Thus, the great dependency of the human race on fossil fuels for energy requirements necessitates an effective method of reducing the amount of CO_2 that are released into the atmosphere. Abuzahra et al.(2007) state that the only way this can be achieved is by producing power plants and production facilities with increased efficiency and combining this with CO_2 capture for long term storage.

2.2. CO_2 CAPTURE AND STORAGE

CO_2 Capture and Storage (CCS) can be described as the use of technology for the capture of CO_2 from point source emitters, the transportation of the captured CO_2 to an identified storage location and finally long term storage, preventing CO_2 release into the atmosphere (Allam et al., 2005). The post-combustion capture of CO_2 is the simplest method for capturing CO_2, seeing that it can merely be installed at the end of the line of an excising industrial process without any major modifications (Cottrell et al., 2009).

In this section the capture process will be discussed in short, considering various processes that are currently in use. Several long term storage options will also be considered, mentioning the feasibility, but also uncertainties and potential dangers involved.

2.2.1. TRADITIONAL METHODS FOR CO_2 CAPTURE

Different techniques are available for carbon dioxide capture. Some of the techniques include physical adsorption utilizing pressure and temperature swing technology, cryogenic separation as well as molecular sieve and membrane based separations. Absorption techniques are probably the most commonly used technique for CO_2 absorption. Both physical and chemical absorption are used, but chemical absorption proved to be the best option for post combustion CO_2 capture from flue gas streams (Mores et al., 2010; Wang et al., 2010). Each technique will be discussed briefly, while considering the advantages and disadvantages each one holds.

2.2.1.1. PHYSICAL ADSORPTION

The phenomenon of physical CO_2 adsorption can be described as the physical attachment of the gas to the surface of a solid or liquid sorbent (Wang et al., 2010). Two different techniques can be employed for regeneration of the adsorbents – pressure swing adsorption (PSA) or temperature swing adsorption (TSA). According to Allam et al.(2005), TSA is the less attractive option of the two due to the longer cycle times required for heating the bed when regenerating the adsorbent. Adsorbents that are currently being studied for application of CO_2 adsorption include activated carbon, metal oxides and zeolites (Allam et al., 2005).

Studies on CO_2 absorption from the flue gas streams of power plants have been performed by various authors reporting on R&D studies using PSA in combination with super cold separator technology (Takamura et al., 2001). Another option is combining PSA and TSA with the use of a zeolites as adsorbent (Yokoyama, 2003) for CO_2 removal from flue gas streams of power plants.

These pilot-scale studies have shown that it might be feasible to construct a full scale adsorption process (Allam et al., 2005).

The adsorption process does however have some drawbacks. One of these is the fact that the flue gas has to be pre-treated prior to being exposed to the adsorbent (Allam et al., 2005). Adsorbents, like zeolites for instance, have low selectivity and also have a greater affinity for moisture than for CO_2; thus the gas has to be dried, increasing the energy penalty of this CO_2 capture technology (Wang et al., 2010). Another drawback as mentioned by Wang et al.(2010) is most adsorbents' low adsorption capacity when considering large scale plants. This increases the required size of the adsorption plant. Riemer and Ormerod (1995), state that the use of gas-solid adsorption would only be practical for gas steams with a low CO_2 concentration, up to a maximum of 1.5 volume % CO_2.

Yokoyama (2003) states that in comparing physical adsorption of CO_2 from flue gas streams to the use of chemical absorption processes; physical adsorption seems like the less attractive option. However, the development of adsorbents that have an improved affinity and selectivity for CO_2 will allow this method of separation to compete with other methods such as chemical absorption (Allam et al., 2005).

2.2.1.2. CRYOGENIC SEPARATION

The principle of condensation is utilized when considering cryogenic separation. CO_2 condenses at temperatures of -56.6°C. Low temperatures achieved by refrigeration cycles are used to condense CO_2 from flue gas streams. However a major drawback of cryogenic separation is the cost of refrigeration to achieve these low temperatures (Wang et al., 2010). For this reason the use of cryogenic separation for CO_2 capture would only be practical when the gas stream CO_2 concentration is very high (Riemer and Ormerod, 1995).

2.2.1.3. MEMBRANE SEPARATION

Membranes can be used in various ways to achieve or facilitate separation of CO_2 from flue gas streams. In the first application of membrane separation, the membrane itself provides the selectivity for the separation process. Membranes usually consist of polymeric films. The different compounds that are contained within the gas mixture permeate at different rates based on the sizes of the various molecules (Wang et al., 2010). However, the feasibility of this separation process is highly dependent on the pressure at which it is operated as well as the amount of CO_2 in the gas stream. According to (Allam et al., 2005) membrane separation with

these polymeric membranes bring about large energy penalties when compared to the conventional chemical absorption processes.

A further application of using membranes for CO_2 capture can be referred to as membrane facilitated absorption. This process uses a combination of membranes and solvents. The membrane serves as the gas permeable device that contacts the gas and the liquid stream, allowing gas molecules to pass through, but preventing the liquid form permeating through the membrane. These membranes are used to provide large surface area to volume ratios for mass transfer from the gas phase to the liquid (Allam et al., 2005; Wang et al., 2010). The process efficiency does however still depend on the partial pressure of the CO_2 and the process would be suitable for flue gas streams with CO_2 concentrations well above 20 volume % (Wang et al., 2010). Some of the advantages of the membrane/solvent system are the elimination of operational problems like column flooding, entrainment, channelling and foaming, problems that are relevant when considering the conventional, chemical absorption method of CO_2 capture. The use of membranes also allows for smaller, compact equipment which in effect leads to reduction in overall capital cost (Allam et al., 2005).

2.2.1.4. PHYSICAL ABSORPTION

Physical absorption refers to the absorption of CO_2 into the solvent, and this can be described by Henry's Law. Due to the physical nature of this process, regeneration of the solvent can easily be obtained by applying heat, reducing the pressure or a combination of the two. The biggest energy penalty with physical absorption lies in the pressurization of the flue gas stream (Chakravarti et al., 2001; Wang et al., 2010). Wang et al.(2010) also state that physical absorption would not be feasible for flue gas streams with a CO_2 concentration lower than 15 volume %.

2.2.1.5. CHEMICAL ABSORPTION

This method of CO_2 capture involves the chemical reaction of the solvent used with the CO_2 in the flue gas stream to form compounds that can easily be regenerated (Wang et al., 2010; Yokoyama, 2003). Chemisorption with a reactive solvent, amine-based in particular, is currently the conventionally preferred method of capturing CO_2 from flue gas streams of fossil-fueled power plants (Allam et al., 2005). A study, comparing the efficiencies of four different CO_2 capture technologies – adsorption, cryogenics, membrane separations and absorption was performed by Riemer and Ormerod (1995). The results indicated that the chemical absorption process with monoethanolamine (MEA) as a solvent proved to be the most energy efficient way to capture CO_2 from power plant flue gas streams (Riemer and Ormerod, 1995).

The general flow scheme for CO_2 capture with a reactive solvent will be explained based on a capture plant using monoethanolamine (MEA). **Figure 5** shows a simplified flow diagram of this CO_2 capture process. The aqueous solution of MEA counter currently contacts the flue gas in an absorber column. The CO_2 in the flue gas reacts with the MEA and forms a water soluble salt product. The stream leaving the bottom of the absorber column is referred to as the 'rich' MEA stream. The rich MEA is pre-heated by the stream leaving the bottom of the stripper - the lean MEA. Rich MEA is then fed to the top of the stripper column where more heat is added in order to promote the reverse reaction. The CO_2 that forms as a product from the reverse reaction leaves the top of the stripper column, while the lean MEA solvent from the bottom is recycled back to the top of the absorber column (Alie et al., 2005).

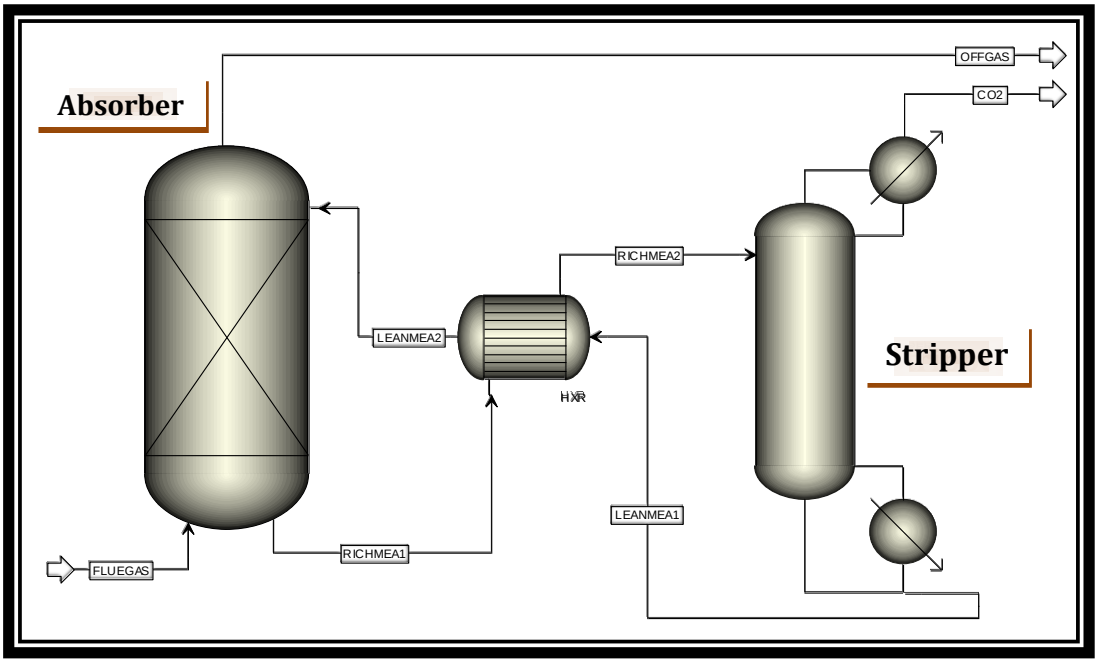

FIGURE 5SIMPLIFIED FLOW DIAGRAM FOR THE POST COMBUSTION CO2 CAPTURE PROCESS WITH MEA (ADAPTED FROM (ALIE ET AL. 2005))

One of the most important factors that needs to be considered when opting for chemical absorption of CO_2 is the choice of solvent. A solvent with a low desorption energy, a high cyclic capacity for CO_2, fast reaction kinetics, as well as a relatively low decomposition rate and minimal by-product formation is preferred (Allam et al., 2005; Chakravarti et al., 2001). Multiple studies (Aronu et al., 2009; Chen and Rochelle, 2005; Mangalapally et al., 2009; Notz et al., 2012, 2007; Oexmann and Kather, 2010; Rochelle et al., 2011) have been performed and Section 2.4 will provide an in-depth discussion on these studies and the outcomes thereof.

Some of the advantages of this CO_2 capture technology include superior selectivity and high capture efficiency when compared to the other methods of CO_2 capture mentioned above

(Allamet al., 2005; Wang et al., 2010). The obtainment of a relatively pure CO_2 gas stream from the top of the stripping column is one of the great advantages. This reduces the cost of further processing in order to commercially use the produced CO_2 (Wang et al., 2010).

However, some drawbacks related to the chemical absorption technology include the following: Pre-treatment of the flue gas in order to remove pollutant compounds such as SO_2 and NO_X – these compounds may potentially degrade the solvent. The solvent may react to form heat stable compounds that cannot be regenerated. It may be subjected to thermal degradation at high temperatures, and this limits the temperature at which regeneration can occur, subsequently increasing the energy requirement. The biggest drawback is said to be the high desorption energy of the solvents used, thus large amounts of energy are required for the regeneration of the solvent (Allam et al., 2005; Aronu et al., 2009; Notz et al., 2007; Rochelle et al., 2011; Wang et al., 2010).

Seeing that this method of CO_2 capture would induce a smaller energy penalty on the power production and other CO_2 emitting industrial processes (Yokoyama, 2003), this will be the method considered and the main focus of this study.

2.2.2. PERMANENT STORAGE

Various options are currently under investigation as potential storage for captured CO_2. Some of these options include storage in geological formations, ocean storage, reacting CO_2 to form mineral carbonates and industrial use of captured CO_2 (Bradshaw et al., 2005).

2.2.2.1. GEOLOGICAL STORAGE

After capturing CO_2 from flue gas streams, the gas needs to be stored. Geological storage of captured CO_2, in order to decrease the amount of greenhouse gases that is emitted into the atmosphere, was already proposed in the 1970's. However, extensive research only began in the early 1990's (Anderson et al., 2005). This might be due to a 70% increase in the greenhouse gas emissions from 1970 to 2004 (Liu et al., 2011). Geological storage can be seen as the injection of captured CO_2 into deep rock formations, suitable for trapping the injected gas.

CO_2 TRAPPING MECHANISMS

The trapping mechanisms for CO_2 can be sub-divided into two categories: Physical and Geochemical trapping (Anderson et al., 2005).

Various ways of physical CO_2 trapping in geological formations has been identified. The first can be explained as the injection of CO_2 into formations that is covered with a layer of low-

permeability rocks, called caprocks. According to Liu et al.(2011), the existence of these so-called caprocks is of extreme importance for safely sequestrating the CO_2 gas. An example of this caprocks is low-permeable shale, as is the case for Mt. Simon sandstone formation in Midwest USA, a major candidate for large scale CO_2 storage. Stratigraphic trapping is another way of physically trapping CO_2. These traps are formed by variations in the rock types due to different setting conditions when the rocks were formed (Anderson et al., 2005). The last physical mechanism is hydrodynamic trapping. This method of trapping can occur in saline formations with no prominent caprocks, but where the fluid can slowly move for long distances with time. Liu et al.(2011) simulated this multi-phase, multi-component mass transport of CO_2 into the sandstone formations of Mt. Simon. The results indicated that the CO_2 plume migrates about 700 meters in the first 10 years, 2200 meters in 100 years and 3000 meters after 1000 years, after which further migration of the CO_2 plume becomes almost insignificant (Liu et al., 2011). Caprocks covers this particular sandstone formation, thus the migration of injected CO_2 would only be distributed horizontally around the point of injection. This makes the location ideal for CO_2 Storage.

Geochemical trapping is related to the geochemical interactions and reactions that involve the injected CO_2. **Figure 6** summarizes the sequence for geochemical trapping. The process starts off by CO_2 dissolving in the formation water, known as solubility trapping. The weak acid formed by the solution of CO_2 in the water reacts with metal silicate or carbonate minerals to form ions. In the last step some of the ions can be trapped in stable carbonate minerals – mineral trapping(Anderson et al., 2005).

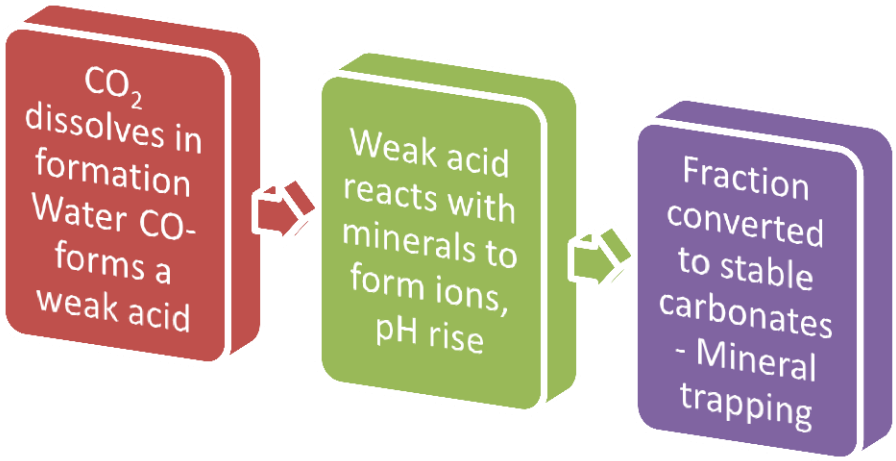

FIGURE 6 THE SEQUENCE OF GEOCHEMICAL TRAPPING

One of the advantages of geochemical trapping is the fact that once the CO_2 has dissolved in the formation water, it is no longer present as a separate phase and would not be subjected to the upward buoyant forces; thus a reduced possibility for any leakages to occur (Anderson et al., 2005).

Liu et al.(2011) found that the main threat of CO_2 injection for geological storage is not leakage of the buoyant plume, but rather leakage of the acidic plume that is a result of the dissolution of CO_2. Leakage of this acidic brine into drinking water may result in the release of toxic metals and other contaminants.

2.2.2.2. ENHANCED OIL RECOVERY

CO_2 can be used in the recovery of oil that is still trapped in the original oil reservoir. 5-40 % of the original amount of oil can usually be recovered through primary oil production. Secondary production by water flooding can be as much as 10-20 %. Enhanced recovery using CO_2 can be utilized to recover a further 13% of the oil originally present (Anderson et al., 2005).

CO_2 is injected into the oil reservoir where enhanced oil recovery is required. Through complex interactions between the injected gas and the oil trapped in the reservoir (which will not be discussed for the purpose of this study) additional oil can be recovered, while at the same time, storing some of the injected CO_2 in the reservoir (Anderson et al., 2005).

Some of the advantages related to EOR and storing CO_2 in depleted oil reservoirs can be summarized as follows (Anderson et al., 2005; Ferguson et al., 2009):

- Establishing a stronger market for buying captured CO_2 from coal fired power plants;
- Oil that otherwise would be trapped in the reservoir can be recovered while simultaneously storing CO_2 and thus reducing emissions to the atmosphere;
- Reservoirs provide a more secure storage space for CO_2 than geological storage, seeing that oil that was originally tapped in such reservoirs did not escape for long periods of time;
- The physical properties and geological content of the oil field has normally been studied in depth and is well characterized;
- Infrastructure that has been used for oil recovery might be used for storing the CO_2, thus reducing the capital cost required for the project.

Two projects where EOR has been implemented in industry include the Weyburn CO_2-EOR Project in the Williston Basin, extending from southern Canada to north United States and also the Rangely, Colorado CO_2-EOR Project. It is expected that the Weyburn Project would allow for

storing 20 $MtCO_2$ for a project life of 20-25 years. The Rangely Project, operating from 1986, has stored an estimated amount of 22.2 $MtCO_2$ to date (Anderson et al., 2005).

2.2.2.3. OCEAN STORAGE

Already in 1977 Marchetti(1977) proposed the long term storage of CO_2 in the ocean. The ocean occupies 71% of the earth's surface with an averaged depth of 3800 meters, thus providing great potential for storage of large quantities of CO_2. To date the amount of research done in the field of ocean storage is limited to modelling studies, laboratory work and small-scale experiments.

One of the principles that might be utilized for ocean CO_2 storage is the increasing density of CO_2 with ocean depth. At depths of 3000 meters and more, CO_2 is subjected to supercritical conditions, thus having a density higher than that of the ocean water. This will allow CO_2 that has been injected to depths deeper than 3000 meters to sink to the bottom of the ocean, forming a CO_2 lake. This method of CO_2 storage might however have adverse effects on the ecosystems of the ocean floor (Brewer et al., 2005).

Another storage method to consider is the dissolution of CO_2 in the ocean water by direct injection from a ship carrying the captured and compressed CO_2. The CO_2 can be injected in various phases. When considering the gas phase, the injection depth should be less than 500 meters but still be deep enough to allow dissolution of the CO_2 before any bubbles reaches the surface. In case of injecting CO_2 to depths greater than 500 meters, the CO_2 can exist as a liquid still less dense than the sea water surrounding it. Shrinking droplets, due to dissolution, would thus rise to depths of 500 meters, when it will change to the gas phase. Another method of CO_2 dissolution involves injecting CO_2 to depths greater than 3000 meters. Sinking droplets will dissolve, and the droplet size could be controlled to ensure that all CO_2 has been dissolved before reaching the ocean floor (Brewer et al., 2005). One of the disadvantages of this method is possible mortality of ocean organisms at the point of injection.

The additions of mineral carbonates to sea water are also considered. Studies have shown that this would reduce the effects of CO_2 injection on the pH and the CO_2 partial pressure of the ocean water (Brewer et al., 2005). Studies by Kheshgi and Archer(2004) have shown that with the use of carbonate neutralization, the amount of CO_2 that could be dissolved in the ocean would increase. Each mole of $CaCO_3$ that is added to the ocean, would allow for storing and additional 0.8 moles of CO_2 in the sea water. This would however require an extensive amount of limestone handling, which might not be desired (Brewer et al., 2005).

This method of permanently storing CO_2 still requires lots of research and trial run experimentation. Even so, it is still not known whether this would be an acceptable method of reducing CO_2 emissions to the atmosphere, due to the unknown biological effects it might have on the ocean's ecosystems.

2.2.2.4. MINERAL CARBONATE FORMATION

Mineral carbonization is very similar to mineral trapping in the sense that the CO_2, present in high concentrations, reacts with metal oxide bearing minerals, forming carbonates that are insoluble. Calcium and magnesium is mainly considered when mineral carbonization is involved (Abanades et al., 2005).

Even though this method of storing CO_2 would be ideal, Abanades et al. (2005) states that this is still a new technology with many uncertainties. Future research in mineral carbonization will shed light on the feasibility and practicality of this technology for long term CO_2 storage.

2.2.2.5. INDUSTRIAL USE OF CO_2

Carbon Dioxide (CO_2) is a valuable industrial gas that is used in many applications and processes. Some of these include the following: The production of chemicals such as urea and methanol; the use of CO_2 in refrigeration cycles to replace other, more harmful ozone damaging products; the use of CO_2 as an inert gas for packaging in the food industry; sparkling beverages; the contents of fire extinguishers and it is also used in the water treatment and paper production industries. Larger quantities of CO_2 might be used industrially in the future for enhanced oil recovery (EOR) (Abanades et al., 2005).

With the exclusion of EOR, Abanades et al. (2005) states that the other mentioned industrial uses for CO_2 is of a scale non-comparable to the amount of CO_2 that could be captured. There is a great chance that the industrial applications of CO_2 gas will not have any considerable contribution to CO_2 storage in the future.

2.3. REACTION MECHANISMS AND PILOT PLANT SETUP

The chemical absorption of CO_2 is based on the use of a thermally regenerable, reactive solvent. The solvent can thus be regenerated at elevated temperatures. A strong affinity for CO_2 is another requirement of an appropriate solvent (Abuzahra et al., 2007). The main reactions for the process that uses MEA in aqueous solution as the solvent will first be considered after which the CO_2 absorption process will be described with reference to **Figure 7**.

2.3.1. REACTIONS INSIDE THE ABSORBER AND STRIPPING COLUMNS

When an aqueous MEA solution is used as the solvent of choice, the following reactions, given by Equations (1) – (7), should be considered (Mores et al., 2010).

$$2\,H_2O \leftrightarrow H_3O^+ + OH^- \quad \ldots(1)$$

$$2\,H_2O + CO_2 \leftrightarrow H_3O^+ + HCO_3^- \quad \ldots(2)$$

$$H_2O + HCO_3^- \leftrightarrow H_3O^+ + CO_3^{2-} \quad \ldots(3)$$

$$H_2O + MEAH^+ \leftrightarrow H_3O^+ + MEA \quad \ldots(4)$$

$$MEAH^+ + HCO_3^- \leftrightarrow H_2O + MEACOO^- \quad \ldots(5)$$

$$MEA + CO_2 + H_2O \leftrightarrow MEACOO^- + H_3O^+ \quad \ldots(6)$$

$$CO_2 + OH^- \leftrightarrow HCO_3^- \quad \ldots(7)$$

From these reactions it can be seen that the reaction of CO_2 with MEA is a reversible reaction. This means that the equilibrium of the reaction can be disturbed in order to obtain the required products. Thus in the absorber column, which is operated at lower temperatures, the exothermic reaction of CO_2 with MEA occurs, forming water soluble products. The reaction of the CO_2 with the MEA facilitates a high mass transfer rate into the solvent, preventing the absorption being limited by the saturation of the solvent with CO_2.

In the stripping column, heat is added to the process and this drives the reaction given by Equation (6) in the reverse direction. This occurrence is in accordance to what would be predicted for exothermic reactions by Le Chatelier's principle. The promotion of the reverse reaction means that the CO_2 is driven from the solvent and the solvent can be recycled back to the absorber column where it can be used once again for the absorption process.

2.3.2. PROCESS DESCRIPTION

In this process description reference will be made to different streams by referring to the corresponding numbers given in **Figure 7**.

Flue gas (stream 1), at a temperature of about 40°C is contacted counter currently with the reactive solvent (stream 4) in the absorber column. The operating temperature of the absorber is normally between 40 and 60°C. The CO_2 in the flue gas stream is transferred to the solvent where it reacts with the MEA to form water soluble salt products. Treated gas leaves the top of the absorber, see stream 2 in **Figure 7**. The liquid leaving the bottom of the absorber column (stream 5), contains the water soluble salts and is called the "rich MEA" stream (stream 5).

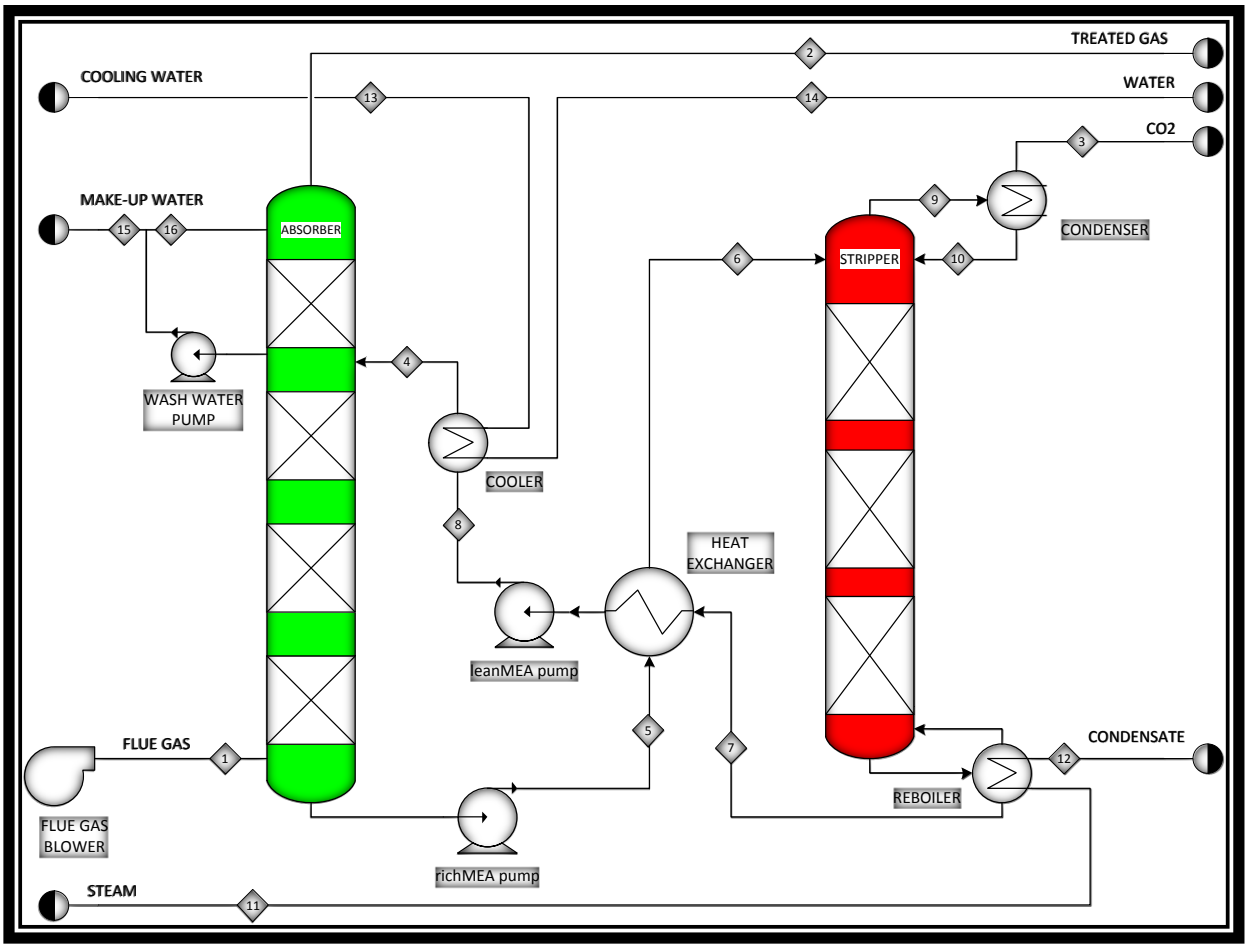

FIGURE 7 PROCESS FLOW DIAGRAM OF A BASIC CO2 CAPTURE PILOT PLANT

This liquid is pumped to a rich-lean cross flow heat exchanger where it is preheated prior to entering the top of the stripping column. The rich MEA stream (stream 6) can be preheated to temperatures of close to 100°C. At the bottom of the stripping column more heat is supplied by the reboiler, normally operated with steam. The reboiler facilitates a rise in temperature, thus promoting the reverse reaction as explained in the previous section. Regeneration of the solvent is usually done at temperatures between 100 and 120°C for MEA systems. At temperatures

higher than 120°C, MEA is subjected to thermal degradation (Notz et al., 2007; Rochelle et al., 2011). The vapour from the top of the column is sent to a condenser where most of the water vapour is condensed and recycled back to the stripping column. The gaseous stream (stream 3) from the condenser contains almost pure CO_2. The liquid stream from the bottoms of the stripping column (stream 7) is sent to the rich-lean heat exchanger, where it is used to preheat the rich MEA stream, while simultaneously being cooled to about 80°C. Further cooling of this stream is necessary to obtain a temperature of about 40-50°C for the stream entering the top of the absorber column (stream 4).

The top section of the absorber column is used as a water wash section. This packed section is washed with water to remove any possible entrained MEA. Make-up water and -MEA are also added to the system to ensure a perfect water and MEA balance in the system (Abuzahra et al., 2007; Allam et al., 2005; Idem et al., 2009).

2.3.3. VARIATION IN PILOT PLANT SETUPS

The setup of the ITC pilot plant in Canada is almost identical to what is given in **Figure 7** (Kittel et al., 2009). The pilot plant for the Castor project at the Esbjerg Power station in Denmark looks very similar to what is given in **Figure 7**, but some components that have been added to this pilot plant are the use of a wash section for the stripping column as well. The pilot plant also employs a reclaiming system. The degradation of some reactive solvents leads to the formation of heat stable and insoluble products. Reclaiming is required in order to remove these insoluble products from the solvent stream and thus preventing accumulation thereof in the closed solvent recycle loop. Reclaiming was a necessity for this setup, seeing that each experiment had a duration of 1000 hours (Knudsen et al., 2009).

The SINTEF-NTNU pilot plant setup at Tiller, Trondheim, recycles the CO_2 that is released from the top of the stripping column back to the flue gas stream that is fed to the bottom of the absorber column. This is a convenient method of keeping track of all the CO_2 that is present in the system. This setup does however not use any water wash sections or reclaiming of degenerated solvent (Luo et al., 2009). **Table 1** summarizes the variations observed in various pilot plant setups.

TABLE 1 SUMMARY OF THE VARIATIONS OBSERVED FOR THE DIFFERENT PILOT PLANT SETUPS

Pilot Plant Setup	Water Wash Section		Reclaiming	CO2 Recycle
	Absorber	Stripper		
CASTOR Pilot Plant at Esbjerg in Denmark	✓	✓	✓	✗
SINTEF/NTNU in Norway	✗	✗	✗	✓
University of Regina in Canada	✓	✗	✗	✗
University of Texas at Austin	✗	✗	✗	✓
University of Kaiserslautern in Germany	✓	✓	✗	✓

2.3.4. PACKING MATERIAL

Some studies have been done on the effect of packing material on the CO_2 absorption process. Studies by Mimura et al.(1995) aimed at not only reducing the amount of energy required for solvent regeneration, but also the amount of power required for the CO_2 absorption process. This was done by developing packing material that reduces the pressure drop across the absorber column, thus reducing the power requirement of the blower that sends the flue gas through the column. The new packing material for the absorber, called KP-1, also allowed a reduction in the absorber diameter and higher absorbing performances were reported, when compared to the random packing that was originally used.

The pilot plant at the University of Texas used Flexipac 1Y structured packing for in the absorber column, while the stripping column was set up with sieve trays (Chen and Rochelle, 2005). In other pilot plants such as NTNU/SINTEF and ITT, Stuttgart Mellapak 250Y is used in both the absorber and stripping columns. For the Castor project IMPT50 are used in both columns, and the ITC pilot plant in Regina makes use of Flexipac 700Y (Luo et al., 2009).

It seems that the various pilot plants use various packing material for the CO_2 absorption process, but studies on the effect of the type of packing material on the process performance are limited. However, studies (Mangalapally and Hasse, 2011a; Mangalapally et al., 2009; Notz et al., 2012) at the University of Kaiserslautern in Germany investigate the effect of various packing materials on the energy requirement for solvent regeneration. Absorption and desorption columns with internal diameters of 0.125 meters are used for the CO_2 capture studies. Mangalapally and Hasse (2011a) report results of the comparison between packing materials Mellapak 250Y and BX500. The results show that at higher CO_2 capture rates, the performance of the BX500-type packing material is superior to that of the 250Y-type packing. This can be explained with reference to the higher surface area provided by the 500BX packing material. **Table 2** gives a summary of the various column internals that are being used in various pilot plant studies.

TABLE 2 SUMMARY OF PACKING MATERIAL USED IN THE VERIOUS PILOT PLANT STUDIES

Pilot Plant	Packing Material Used	
	Absorber Column	**Stripping Column**
CASTOR Pilot Plant at Esbjerg in Denmark	IMTP50	IMTP50
SINTEF/NTNU in Norway	Mellapak 250Y	Mellapak 250Y
University of Regina in Canada	Flexipac 700Y	Flexipac 700Y
University of Texas at Austin	Flexipac 1Y	Sieve Trays
University of Kaiserslautern in Germany	Mellapak 250Y/BX500	Mellapak 250Y/ BX500

2.4. SELECTION OF A REACTIVE SOLVENT FOR CO_2 ABSORPTION

Monoethanolamine (MEA) is the most widely used reactive solvent in industry for capturing CO_2 from flue gas streams. It is suitable for this application due to the high rate of the reactive CO_2 absorption. However, some of the drawbacks of using MEA as the reactive solvent includes a very high heat of desorption and that the maximum loading capacity of CO_2 is limited to about 50%, because MEA reacts with CO_2 in a 2:1 ratio. MEA is also known to degrade when exposed to oxygen (O_2) and other impurities like sulphur dioxide (SO_2) in the flue gas (Lawal et al., 2005).

As a result, various authors have been involved in a search for a solvent that would reduce the thermal energy requirements of the desorption process. The solvent selection also depends on factors such as the flue gas composition, effect of impurities in the gas stream on the specific solvent, the cost of the preferred solvent, solvent degradation, tendency of the solvent to corrode process equipment as well as the reaction kinetics (Mores et al., 2010). In a study by Retief (2012), a solvent screening method has been developed that is based on the use of partial solubility parameters. This method of solvent screening highlighted the potential of using ionic liquids for the CO_2 absorption process. This has however not been verified in any pilot plant studies.

2.4.1. ENERGY REQUIREMENTS FOR REGENERATION

Pilot plant studies on the post combustion CO_2 capture process, performed by a team from the University of Regina, report regeneration energy of 3.9 GJ/ton CO_2 when 30 wt% MEA solvent is used to capture 90% of the CO_2(Adams et al., 2009).

The CAPRICE Project is a combined study by various researchers from the EC CASTOR project and also the team from the University of Regina. The study aimed at integrating the post combustion CO_2 capture process into the heat cycle and gas path of a power plant. It was found that optimisation of the two processes combined led to a reduction in solvent regeneration energy requirement of about 7.5 %. The energy requirement for solvent regeneration was reported to be 3.6 GJ/ton of CO_2 (Adams et al., 2009).

Process developers claim that the required regeneration energy can be reduced by process optimization to about 3 GJ/ton of CO_2 captured (Reddy, 2008).

Rochelle et al.(2011) performed an energy analysis on a proposed flow scheme when using piperazine as a solvent. The energy analysis resulted in a reduction of required regeneration energy to about 2.6 GJ/ton CO_2 removed. The process requires a different experimental setup to those conventionally used for MEA based capture plants. This is however not included in the scope of this study.

2.4.2. INFLUENCE OF GAS COMPOSITION ON THE SOLVENT SELECTION

In a study on simplifying the simulation of the post combustion CO_2 capture process using Aspen Plus®, gas compositions of 3, 14 and 25 % CO_2 were investigated. These can be related to flue gas streams from a natural gas power plant, a coal power plant and a cement plant. The simulation was performed using a process flow sheet decomposition method. This can be better explained as simulating a standalone absorber, and a standalone stripper column. The simulation process was performed with 30 wt% MEA as the solvent. It was found that for 3 volume % CO_2 in the gas stream, the solvent regeneration energy requirement per unit mass of captured CO_2, was higher than that of the 14 and 25 volume % CO_2 streams (Alie et al., 2005). This corresponds well to what was found by Idem et al.(2009) in a study on reducing the amount of steam required for regeneration of the solvent.

2.4.3. SOLVENT DEGRADATION

In a study by Rochelle et al.(2011) on the robustness of MEA and piperazine solvents to oxidative degeneration, piperazine proved to be superior to the 30 wt % aqueous MEA solution. The test performed involved bubbling a gas, containing 98 mole% oxygen and 2 mole% CO_2 through the well mixed solvents. Tiny amounts of Fe^{2+}, Cr^{3+} and Ni^{2+} were added to the mixed solvents, as these might be present due to the corrosion effect of aqueous amine solutions on stainless steel. These ions catalyse the oxidation reactions in the solvent. Piperazine is less sensitive to the effects of contaminants such as SO_x and NO_x in the flue gas than MEA (Oexmann, 2008).

Lawal et al.(2005) performed a comparative study on MEA and blends of MEA and MDEA considering oxidative degradation. The results from the study indicated that fewer degradation products resulted from exposing a MEA-H_2O solution to oxygen than for the case where MEA-MDEA-H_2O was considered. It was also clear from the results that oxidative degradation is more apparent when the solvent is lean in CO_2 than for a CO_2 loaded solvent.

In Australia, development of post-combustion CO_2 capture plants is subjected to problems concerning the power plant flue gas compositions. Coal fired power plants do not have processing for desulphurization and denitrification of the flue gas due to limited emissions control. This provides difficulties for implementing amine based CO_2 capture processes on an industrial scale. The limits for SO_2 in the flue gas when considering an MEA-based process is 100 ppm. For newly developed processes with different amines and other solvents, SO_2 levels of less than 10 ppm is required (Cottrell et al., 2009). Thus, pre-treatment of the flue gas from these coal-fired power stations are a necessity, adding to the capital cost for implementation of the CO_2 capture process.

Thermal degradation is another important factor that needs to be considered. Notz et al. (2007), states that due to thermal degradation, regeneration of the solvent is not normally performed at temperatures higher than 120°C. According to what is reported by Rochelle et al. (2011), MEA thermally degrades at a rate of 1.7% per week, when regenerated at 120°C. However, when the regeneration temperature is increased to 135 and 150°C, MEA degrades at 8% and 50% per week respectively.

2.4.4. REACTION KINETICS

Rochelle et al.(2011) reports that, the kinetics of the reaction between piperazine and CO_2 when compared to that of MEA with CO_2 is considerably faster. It is predicted that the absorption rate when using piperazine as a solvent would be twice as fast as MEA.

Aronu et al.(2009) investigated a variety of solvents in order to compare their absorption and desorption potentials. One of the solvents that were investigated, tetraethylenepentamine (TEPA) showed exceptional CO_2 absorption potentials. TEPA maintained a high absorption rate and the cyclic capacity also proved superior to all the other solvents. However, it was suggested that working with TEPA at high concentrations would be a challenging task, due to its high viscosity.

2.4.5. ECONOMICS

One major drawback for using piperazine as opposed to MEA in the absorption process is cost related. Rochelle et al.(2011) state that the cost of piperazine is about three times that of MEA. Another drawback is the fact that when using piperazine as the solvent, the process flow scheme needs to be adapted by constructing different absorber- and stripper columns to replace the existing columns of the conventional CO_2 capture process. This brings about high capital costs investments.

A thermodynamic and economic study was performed by Oexmann and Kather (2009) in order to determine the viability of using piperazine promoted potassium carbonate as an alternative solvent to MEA. Equipment sizing and cost, total capital investment and the operating cost of the two different processes were compared. It was found that a 30 wt% MEA solvent would be superior to using aqueous solutions of potassium carbonate and piperazine. The optimized amount of energy required for regeneration of MEA was found to be 4.2 % lower than that of a 2.5M potassium carbonate/2.5M piperazine solution. The cost of equipment as well as the total capital cost required is 11.7 % higher than the MEA process, and the operational and CO_2 avoidance costs were respectively 8 % and 18 % higher than the MEA case.

2.5. OPTIMISING OPERATING CONDITIONS USING SIMULATIONS

2.5.1. PARAMETRIC STUDY: OPTIMISING THE THERMAL ENERGY REQUIREMENTS

Abuzahra et al.(2007) performed a parametric study on the CO_2 capture process using Aspen Plus® with a RADFRAC subroutine. The operating conditions that were investigated and optimised include the percentage of CO_2 removed, the MEA solvent concentration, operating pressure of the stripper, as well as the lean solvent loading and its temperature. The flue gas flow rate and CO_2 concentration were kept constant throughout. To investigate the optimum process, the CO_2 removal rate was set to 90% and the solvent flow rate were varied in order to acquire this specification. Thus, in effect the L/G-ratio in the absorber column was optimised. Even though this was not specifically reported, back-calculations allow for the determination of the optimum L/G ratios as seen in **Table 3**.

The optimised model was compared to a base case, which was selected based on the energy requirements of CO_2 capture plants in industry – about 3.9 GJ/ton CO_2. It was found that the energy requirements could be reduced by optimisation to 3.3 GJ/ton CO_2 for a 30 wt% MEA solution and to about 3.0 GJ/ton CO_2 for a 40 wt% MEA solution.

In this study by Abuzahra et al.(2007) it was found that the optimum CO_2 capture process, with regards to thermal energy requirement, would have operating conditions as shown in Table 3.

TABLE 3: SUMMARY OF THE RESULTS FOR THE OPTIMISED PROCESS

Operating condition	30 wt% MEA	40 wt% MEA
CO_2 removal (%)	90	90
MEA solvent concentration (wt.%)	30	40
Absolute Operating Pressure of Stripper (kPa)	210	210
Loading of the lean solvent (mol CO_2/mol MEA)	0.32	0.30
Lean solvent Temperature (°C)	30	25
L/G-ratios for optimum process (mass/mass)	5.25	4.15

2.5.2. OPTIMISATION OF OPERATING CONDITIONS

The following ratios can be used for optimisation of the absorption process. The first ratio needs to be minimized and the second maximized in order to obtain the optimum operating conditions (Mores et al., 2010).

a. The ratio between the total amount of CO_2 absorbed and the total heating and cooling utilities that is required.
b. The ratio between the total amount of CO_2 absorbed and the total solvent flow rate.

2.5.3. OPTIMISING WITH REGARDS TO LEAN MEA LOADING

A simulation study by Alie et al.(2005), with gas streams containing 3, 14 and 25 % CO_2, showed that the energy required for regeneration of the solvent is a minimum at a lean MEA loading of 0.25 mol of CO_2 per mole of amine. For the case with 14 % CO_2 in the gas stream, the minimum regeneration energy required was found to be 4 GJ per ton of CO_2 captured. This corresponds well with other sources from literature.

2.6. PILOT PLANT STUDIES

Various pilot plant studies have been performed. **Table 4** gives a summary of the column diameters, packing material used and the packed bed heights of various pilot plants. This section will discuss in short the published research work that has been performed by researchers working on these CO_2 absorption pilot plants. The pilot plant setup, the experimental studies performed and the research outcomes in each case will be discussed.

TABLE 4 SUMMARY OF THE COLUMN DIAMETERS, PACKING MATERIAL USED AND PACKED BED HEIGHTS FOR VARIOUS PILOT PLANTS

Pilot Plant	Column Diameter		Packing Material Used		Packed Bed Height	
	Absorber	Stripper	Absorber	Stripper	Absorber	Stripper
CASTOR Pilot Plant at Esbjerg in Denmark	1.1 m	1.1 m	IMTP50	IMTP50	17.0 m	10.0 m
SINTEF/NTNU in Norway	0.15 m	0.1 m	Mellapak 250Y	Mellapak 250Y	4.36 m	3.98 m
University of Regina in Canada	0.33 m	0.33 m	Flexipac 700Y	Flexipac 700Y	7.05 m	9.97 m
University of Texas at Austin	0.42 m	0.42 m	Flexipac 1Y	Sieve Trays	6.00 m	-
University of Kaiserslautern in Germany	0.125 m	0.125 m	Mellapak 250Y	Mellapak 250Y	4.20 m	2.52 m

2.6.1. CASTOR PROJECT AT ESBJERG POWER STATION

The CASTOR project involves a CO_2 absorption pilot plant operating alongside the Esbjerg power station in Denmark. The pilot plant was commissioned in 2005 and in the period from 2006-2007 a total of 4000 hours experimental work were performed. The main focus of the pilot plant was to investigate the operation of such a CO_2 absorption plant in conjunction with a full scale power station. The CASTOR project made use of only a portion of the flue gas from the coal fired power station for CO_2 absorption studies. The split stream was channelled to the absorption plant and the captured CO_2 was reintroduced into the flue gas stream after passing through the pilot plant set-up (Knudsen et al., 2009).

2.6.1.1. PILOT PLANT SETUP

The pilot plant has a total maximum capacity of 1 ton of CO_2 per hour to be absorbed from the incoming flue gas stream. It consists of an absorber and a stripper column both with internal diameters of 1.1 meters. The absorber has a total of four sections, each 4.25 meters high,

packed with IMTP50 random packing. The stripper column is also packed with IMTP50 random packing and consists of 2 sections of 5 meters each. Both columns have wash sections installed above the packed beds. Structured- and random packing (IMTP50) are used respectively for the wash sections of the absorber and the stripper. The stripper makes use of a thermosyphon reboiler, driven by 2.5 bar(g) saturated steam. The columns are joined by a rich/lean plate heat exchanger with a delta T of about 10°C (Knudsen et al., 2009).

2.6.1.2. EXPERIMENTAL STUDIES PERFORMED AND OUTCOMES

CASTOR 1 and CASTOR 2 are new blends of amine solvents. These solvents were developed in the CASTOR project in order to find the solvent that would improve the energy efficiency of the CO_2 capture process (Knudsen et al., 2009). This pilot plant was used to perform a comparative study when using these new solvents. Other studies on this pilot plant also include validating simulated data with actual data gathered from the pilot plant (Dugas et al., 2009).

BACKGROUND

The CASTOR project was divided into four 1000 hour test campaigns in order to provide sufficient data for a comparative study. The campaigns are summarised in **Table 5**.

TABLE 5 SUMMARY OF THE CAMPAIGNS OF THE CASTOR PROJECT

Campaign No.	Solvent Used	Description of the Campaign	Duration [h]
1	30 wt% MEA	Operating with the reference solvent	1000
2	30 wt% MEA	Operation with reference solvent (similar to Campaign#1)	1000
3	CASTOR 1	Experiments and operation with a new solvent	1000
4	CASTOR 2	Experiments and operation with a new solvent	1000

PHASE ONE: PARAMETRIC STUDY

The first 500 hours of each campaign were used to perform a parametric study in order to optimize the operating conditions of the process with regards to energy efficiency. The second 500 hours of the campaign was then used to study continuous operation in conjunction with the coal fired power station (Knudsen et al., 2009).

The parametric study was performed optimising the liquid-to-gas (L/G) ratio in the absorber column. Knudsen et al.(2009) report an optimum L/G ratio of 2.5 kg/kg for MEA. This limits the

steam requirement to 3.6 GJ/ton CO_2. CASTOR 1 showed a minimum steam requirement of 3.8 GJ/ton CO_2 at L/G ratios of between 2.5 and 3 kg/kg. CASTOR 2 appeared to be the more promising solvent of the two new ones with a minimum steam demand below 3.6 GJ/ton CO_2 at an L/G ratio of 2 kg/kg (Knudsen et al., 2009). This indicates that CASTOR 2 has a higher cyclic capacity for CO_2, seeing that the solvent flow rate can be lower for the same gas flow rate when compared to the other solvents.

The optimum L/G ratios for each solvent were used in order to investigate the effect of percentage CO_2 removed on the reboiler steam requirement. It was found that there is a considerable increase in the steam requirement when increasing the CO_2 captured from 90 to 95%. The target for CO_2 capture was thus set to be 90% (Knudsen et al., 2009).

PHASE TWO: CONTINUOUS OPERATION

The second phase of each campaign had objectives of continuous operation for 500 hours at the optimized conditions, investigating the corrosive nature of each solvent, as well as gathering some valuable information on solvent degradation (Knudsen et al., 2009).

The results showed that initially the steam demand of CASTOR 2 was the lowest with an average values of 3.5 - 3.6 GJ/ton CO_2. However, unexpected solvent losses from the process had a negative effect on the overall results for all 500 hours. The average steam demand of MEA for the 500 hours was reported to be 3.7 GJ/ton CO_2, while that of CASTOR 1 was slightly higher (Knudsen et al., 2009).

The corrosion monitoring was performed by strategically installing weight loss coupons in the pilot plant. The corrosion coupons were samples of carbon steel, stainless steel 304 and 316. Kittel et al.(2009) report on the results of exposing these weight loss coupons for the solvents during the 500 hours of operating. It was found that the stainless steel is superior to the carbon steel, as expected. It was also clear that temperature greatly affects the rate of corrosion. This is apparent when considering that the coupons at the stripper inlet and outlet were subjected to considerable corrosion (Kittel et al., 2009).

In monitoring the degradation rates of the different solvents, the presence of heat stable salts were used as an indication of the extent of solvent degradation (Knudsen et al., 2009). The results from this study showed that the concentration of the heat stable salts increased considerably faster for MEA when compared to using CASTOR 2. According to Knudsen et al.(2009), this is an indication that the new solvent, CASTOR 2, is chemically more stable than MEA.

VALIDATING SIMULATED DATA

Dugas et al.(2009) made and attempt at comparing simulated data to actual data obtained from the CASTOR pilot plant. The main experiments were performed at different solvent flow rates, varying between 13 and 24 $m^3/m^2.h$ as well as varying lean loading, between 0.16 and 0.28 mole CO_2/mole MEA. Twelve different runs were performed while running the CASTOR pilot plant project. The results obtained for the absorber gas temperatures and CO_2 concentrations were simulated using Aspen Plus®. The study showed that the simulation can be used to reliably model the absorber for a MEA-CO_2 capture system (Dugas et al., 2009).

OUTCOMES

The CASTOR project showed that there is potential for developing new solvents which require less energy for regeneration. It also provided some useful information on the corrosion effect and degradation of the various solvents that were investigated. The CASTOR project also provided a basis for comparison for simulations performed in Aspen Plus®.

2.6.2. UNIVERSITY OF REGINA

A pilot plant for CO_2 capture was used for experiments regarding minimizing the total amount of steam required in the reboiler for solvent regeneration in the stripping section. This pilot plant has a capacity of 1 ton CO_2 per day (Luo et al., 2009).

2.6.2.1. PILOT PLANT SETUP

The pilot plant consists of three absorber columns with internal diameters of 0.32 meters, with three packed sections each, equivalent to a total packing height of 10 meters per column. Any one of these three absorbers can be used. The stripper column has an internal diameter of 0.32 meters and a height of 10 meters. The column has two sections both packed with Flexipack 700Y structured packing (Idem et al., 2009). The pilot plant was also equipped with corrosion probes that were used to determine the corrosion effect of the solvent on the process equipment (Luo et al., 2009).

2.6.2.2. EXPERIMENTAL STUDIES AND OUTCOMES

The study by Idem et al.(2009) showed that in order to minimise the energy requirement, not only the solvent should be considered but also the optimum operating conditions. The steam requirement, when using 5 molar MEA (equivalent to 24 wt% MEA (aq)), was 2.03 and 1.43 kg/kg CO_2 for a flue gas stream of 4 and 8 % CO_2 respectively. This is an improvement considering a steam requirement of 1.9 – 2.5 kg/kg CO_2 for the conventional process setup.

When using RS-1, a proprietary solvent, in the optimised process the steam requirement for regeneration was reduced to only 1.74 and 1.35 kg/kg CO_2 for the previously mentioned compositions of the flue gas stream. However, the most important result from this study is the fact that after optimisation of the process configuration with RS-1, the steam requirement was further reduced to 1 kg/kg CO_2.

The results of the corrosion tests were reported by Kittel et al.(2009) and corresponded quite well to the corrosion tests that were done with the CASTOR pilot plant. The results show that the corrosion rate is directly proportional to the solvent temperature. It is also clear from the results that the combination of a high CO_2 loading and the high temperatures creates the most corrosive environment. This conclusion was made after observing that the stripper inlet showed the highest corrosion rate (Kittel et al., 2009).

2.6.3. DEVELOPMENTS AT THE UNIVERSITY OF TEXAS

2.6.3.1. EXPERIMENTAL STUDIES AND OUTCOMES

Various studies regarding post combustion CO_2 capture have been performed at the University of Texas. Some of these studies include pilot plant testing of new solvents to improve the energy efficiency of the capture process, as well as foaming tests with various solvents. In recent years the main focus was on the solvent piperazine.

2.6.3.2. NEW SOLVENTS EXPERIMENTS

Chen and Rochelle (2005) from the University of Texas at Austin report on setting up a pilot plant for performing pilot plant studies, investigating piperazine promoted potassium carbonate as an alternative solvent to the conventional aqueous MEA. Dugas and Rochelle(2009) performed wetted wall experiments measuring CO_2 absorption and desorption with various concentrations of MEA and piperazine at different CO_2 loadings. These studies showed that the 8 Molar solution of piperazine has a 75 % higher CO_2 capacity when compared to 7 molar (30 wt % MEA) solution of MEA (aq). Dugas and Rochelle(2009) also found that the absorption and desorption rates of CO_2 is 2-3 times faster with piperazine when compared to MEA solutions with an equivalent CO_2 partial pressure.

Rochelle et al.(2011) performed an energy analysis on the use of the various solvents, including piperazine and MEA, in the CO_2 absorption process. It was found that the energy required for solvent regeneration can be reduced to 2.6 GJ/(ton CO_2 removed) when using piperazine, compared to energy requirements of above 3 GJ/(ton CO_2 removed) for the use of MEA solvent.

2.6.3.3. OUTCOMES

The use of piperazine seems superior to MEA when considering the solvent robustness. MEA is very susceptible to thermal and oxidative degeneration when compared to piperazine. Piperazine can be regenerated at up to 150°C with minimal degeneration (Rochelle et al., 2011).

The use of piperazine as a solvent however has some drawbacks. One of these is higher capital cost due to a different flow scheme than that traditionally used for absorption with MEA. Pressure vessels that operate at pressures above 15 bar are required for desorption of CO_2 when piperazine is used. Heating the solvent to a temperature of 150°C would also require more steam than for a 30 wt% MEA solution. The cost of piperazine is also about three times that of MEA (Rochelle et al., 2011).

2.6.3.4. FOAMING TESTS

Studies on solvent foaming were performed by Chen et al.(2011). Both MEA and Piperazine were investigated and were exposed to various factors that are known to cause foaming. From this study it was found that foaming with piperazine increased with increasing concentration and also that the presence of oxidation products, specifically formaldehyde caused a significant increase in foaming.

Steel is the main material for construction of gas treating plants. Dissolved ions are thus likely to be present in the solvents streams. The effect of ferric and ferrous ions on foaming was investigated. Results showed that ferrous ions increase the foaminess of piperazine, while it had an insignificant effect on the foaming of MEA. The presence of the ferric ions did not contribute to foaming in either one of the solvents (Chen et al., 2011).

2.6.4. PILOT PLANTS IN AUSTRALIA

As previously mentioned, the post-combustion CO_2 capture process cannot be implemented on Australian coal fired power stations as is. Pre-treatment of the flue gas is required in order to reduce the SO_2 to acceptable levels. Two pilot plants was set up in 2008, one in the state of Victoria and the other in New South Wales. Construction of a third pilot plant in Queensland started in 2009. The pilot plants are used in combination with coal fired power stations and have CO_2 removal capacities ranging from 100 kg/h to 500 kg/h (Cottrell et al., 2009).

2.6.5. UNIVERSITY OF KAISERSLAUTERN IN GERMANY

Studies performed at the Laboratory of Engineering Thermodynamics are aimed at finding new solvents that allows for lower solvent regeneration energy requirements. Various packing materials were considered for the capture process (Mangalapally and Hasse, 2011a; Mangalapally et al., 2009; Notz et al., 2012).

2.6.5.1. PILOT PLANT SETUP

The pilot plant at the University of Kaiserslautern consists of an absorber- and stripping column with internal column diameters of 0.125 m. The absorber column has a packed height of 4.25 meters and the stripping column is packed to a height of 2.55 m. The flue gas for the pilot plant studies were produced by a gas burner. The bottom of the stripping column is fitted with electrical heating elements to add the required energy for solvent regeneration.

2.6.5.2. INVESTIGATING NEW SOLVENT BLENDS

CESAR 1 and CESAR 2 are both new amine blended solvents that are investigated for application in the CO_2 Capture process. Performance of these solvents was compared to results with 30wt% MEA (aq) which is used as the reference solvent in the comparative study. Solvents were evaluated by varying the solvent flow rate to the absorber column and maintaining a constant CO_2 capture rate of 90 % by adjusting the regeneration energy (Mangalapally and Hasse, 2011a).

2.6.5.3. INVESTIGATING VARIOUS COLUMN INTERNALS

The effect of the column internals on the absorption capacity of the absorber column was investigated. The performance of Mellapak 250Y packing was compared to that of BX500 packing material. It was found that a maximum capture rate of 88% could be obtained with the Mellapak 250Y packing, compared to the 90% for the BX500 packing. Furthermore, a steep increase in the regeneration energy requirement was obtained with Mellapak 250Y packing at capture rates close to 90%. The increase of regeneration energy with the BX500-type packing at capture rates close to 90% are much less when compared to the Mellapak 250Y.

This was explained by the lower surface area that is available for mass transfer with the Mellapak 250Y packing when compared to the higher surface area of BX500 (Mangalapally and Hasse, 2011b).

2.6.5.4. FULL PILOT PLANT PARAMETRIC STUDY

Notz et al. (2012) performed a full pilot plant parametric study. This was done by performing eight different variation studies. Thus, eight different studies were performed, each time varying one parameter or boundary condition while keeping the other 7 parameters constant. The varied process parameters include the stripping column pressure, solvent flow rate, solvent composition and -temperature. The boundary conditions that were investigated were CO_2 removal rate, CO_2 concentration of the flue gas, flue gas temperature and the fluid dynamic load in the absorber column.

2.7. CONCLUDING REMARKS

From the presented literature it is clear that there is extensive research being done in the field of post combustion CO_2 capturing. The main aim of all these research studies is focused on the minimization of the solvent regeneration energy requirement. This is done by considering various solvent blends, process configurations, operating- and boundary conditions as well as various column internals. Furthermore, the CO_2 capture process is investigated by performing parametric studies, like the one by Notz et al.(2012). This provides insight with reference to the interaction between various process parameters and boundary conditions. A proper understanding of these interactions will aid in the process of pilot plant optimisation.

With the exception of work done at the University of Kaiserslautern in Germany (Mangalapally and Hasse, 2011a; Mangalapally et al., 2009), there is limited comparative pilot plant studies on the effect of various column internals on the CO_2 capture efficiency and regeneration energy requirement. Pilot Plant studies using ionic liquids as potential solvents are also limited. This study was aimed at establishing a pilot plant facility for CO_2 capture studies. This pilot plant facility can be used in future to investigate the effect of various column internals, solvent blends and process configurations on the CO_2 capture process.

Literature also report on optimization studies that has been done by simulating the process in Aspen Plus®. Due to the complexity of simulating the CO_2 capture process Wang et al. (2010) state that most of the simulation studies performed are done by experts. A need for a simplified method of simulating the CO_2 capture process is identified.

CHAPTER 3

KEY QUESTIONS, RESEARCH AIMS AND OBJECTIVES

3.1. KEY QUESTIONS

The main focus of this study is establishing a pilot plant facility for CO_2 capture studies. In order to establish a pilot plant facility that will eventually serve in resolving some of the many questions that arise when considering the CO_2 capture process, the questions to be answered first need identification.

The key questions that arise from performing the literature survey can be sub-divided into two sets of questions; one set concerns the packing material used and the other set the choice of solvent. The main questions to be considered with regards to packing material are summarized below.

- What is the effect of the surface area of the structured packing, on the energy requirement for solvent regeneration?
- What effect does the type of packing material have on the rate of CO_2 absorption and thus the capture efficiency in the absorber column?
- What is the difference in absorption efficiency when comparing an absorber column packed with structured packing to one that is randomly packed?
- How do the optimum solvent flow rates for structured and random packing compare?
- What are the optimum liquid-to-gas (L/G) ratios fed to the absorber column for different packing materials?
- What is the effect of the specific gas load in the absorber column on the absorption process?
- How does the energy requirement for solvent regeneration compare when using structured and random packing respectively?
- How would the type of packing material, structured or random packing influence the performance of the stripping column?

Some key questions relating to the solvent choice as well as some questions on the operating conditions is stated below.

- Which amine blends would be preferred as opposed to the conventional 30 wt % MEA aqueous solution?
- Do amine blends provide a more energy efficient process when compared to 30 wt % MEA?

- Can the solvent regeneration energy requirement be reduce by using ionic liquids showing improved absorption potential, to replace conventional solvents?
- How do the rates of degradation of the various solvents under investigation compare?
- What is the effect of the MEA concentration on the key process parameters such as rate of CO_2 absorbed, the amount of CO_2 absorbed and the optimum solvent flow rate?
- What is the effect of solvent flow rates on the CO_2 absorbed?
- How does the absorber inlet solvent temperature influence the absorption process?
- How does the solvent temperature at the inlet of the stripping column influence the energy requirement for solvent regeneration?
- How does solvent performance decrease with time?
- What is the corrosive effect of any solvent blends used?

Establishing a pilot plant facility will eventually aid in finding the answers to the questions mentioned above.

3.2. AIMS AND OBJECTIVES

The aims and objectives of this project can be separated into two parts. The first part focuses on the design, construction and the commissioning of the pilot plant that needs to be set up. The second part focuses more on the experiments and process simulations that will be performed once the pilot plant is operational.

3.2.1. AIM 1: DESIGN, BUILD AND COMMISSION A PILOT PLANT WITH COLUMN DIAMETER OF 200MM

3.2.1.1. PILOT PLANT CONSTRUCTION

The main objective for the first part of the project was setting up the pilot plant. The pilot plant was to be set up by implementing modifications to two glass columns that were not used at the time. One of the columns had previously been used to perform hydrodynamic studies on packed columns, and the other column was set up for continuous distillation studies. These column configurations were to be modified to obtain an absorber and a stripping column respectively.

3.2.1.2. PILOT PLANT COMMISSIONING

The next objective was the commissioning of the pilot plant. This was done by initially running the process with water, ensuring that there were no leaks in the system and that the heating and cooling capabilities of the process equipment are sufficient.

After this, the pilot plant was to be commissioned with 20 wt% MEA, investigating the performance of the pilot plant when the reactive absorption is performed. The lower MEA concentration used for commissioning also provides data sets for comparison to results with the higher MEA concentrations. Commissioning with 30 wt% MEA (aq) was to follow and the pilot plant results were to be compared to published pilot plant data. In order for the pilot plant data to be comparable to that of other pilot plants in other parts of the world, it was required that similar results can be obtained with a reference solvent such as 30 wt% MEA. This serves as validation for the CO_2 capture pilot plant setup at the University of Stellenbosch.

3.2.1.3. PILOT PLANT EXPERIMENTS

Pilot plant experiments for this study mainly consisted of validation experiments with structured packing [Flexipac 250Y]. The experimental conditions were set up in order to allow comparison to other published pilot plant data.

The primary focus of the experiments was on reproducing literature results that relates the amount of solvent regeneration energy required and the CO_2 capture rate in the absorber column. A secondary objective was to perform a preliminary investigation on what effect the L/G-ratio in the absorber column has on the solvent regeneration energy requirement.

3.2.2. ASPEN PLUS® SIMULATIONS

Another objective for this study was the development of a method by which the CO_2 capturing process can accurately be simulated using Aspen Plus®. Published pilot plant data was to be used in order to validate the process simulation set up in Aspen Plus®. The rate based simulation was to be performed using 30wt% MEA as the reference solvent.

Depending on the agreement between the simulated and the published pilot plant data, the simulation was to be used for comparison and possible validation of the results from the established pilot plant.

The capabilities of the simulation to predict the solvent regeneration energy at various operating conditions were to be evaluated and compared to the results from the pilot plant setup.

3.3. SCOPE AND DELIVERABLES

3.3.1. PROJECT SCOPE

The scope of this study was limited to establishing a pilot plant facility for CO_2 capture studies. This includes the design, construction as well as setting up the control systems for the pilot plant setup. The controls will be set up to allow operation of four different systems; post combustion CO_2 capture plant, a continuous distillation column, column for hydrodynamic tests on column internals as well as a total reflux column. The post combustion CO_2 capture pilot plant will be commissioned with MEA (aq) and verification experiments will be performed. Results from the pilot plant will be validated using published data from similar pilot plant setups. Simulating the CO_2 capture process in Aspen Plus® also forms part of the scope of this study. The method of simulation will be validated by comparing the simulation results to real pilot plant data.

The validated simulation can be used as a tool in order to provide predictions of what the operating conditions for the pilot plant setup should be. The operating conditions will be adapted in order to minimize the solvent regeneration energy requirement. The simulation will also be used in order to provide insight on how various process parameters influence the energy requirement of the process. Finally, the simulation will be set up in order to match the configuration of the established pilot plant. Data comparison between the simulation and the newly established pilot plant will follow.

3.3.2. MAIN OBJECTIVES

The scope of this project defines the boundaries of the main objectives of this study. A summary with reference to the specific project objectives that falls within the project scope is summarised below.

1. Design a pilot plant facility for CO_2 capture studies. The absorber- and stripping columns both have inside diameters of 200 mm.
2. Build the pilot plant facility and commission with aqueous MEA solution as the reactive solvent.
3. Perform verification experiments and validate the pilot plant results by comparing it to pilot plant results in literature.
4. Develop a simplified method of simulation the CO_2 capture process using Aspen Plus®.
5. Verify the results from the Aspen Plus® Simulation with pilot plant results in literature.
6. Compare the Aspen Plus® Results to that obtained from the experimental runs with the established pilot plant.

3.3.3. PROJECT DELIVERABLES

In order to meet all the objectives of this study, some deliverables has to be met. The following list contains some of the design deliverables.

1. Design of the cross heat exchanger
2. Designing an absorber column that provides a packed bed length capable of capturing CO_2 from a flue gas stream containing up to 12 volume % CO_2.
3. Designing absorber column with sufficient sampling ports at various heights.
4. Designing gas- and liquid sample ports for the absorber column.
5. Design liquid sample ports to allow for sampling at various points across the diameter of the absorber column.
6. Measuring gas- and liquid temperatures at different heights in the absorber column.
7. Constructing distributors for the absorber column that will reduce wall flow.
8. Design of a surge tank / knock-out drum for gas recycling.
9. Specification of a gas blower unit to be used for gas recycling.
10. Designing a water wash section to be installed on top of the absorber column.
11. Employing safety measures with regards to over-pressurization of the glass columns.
12. Employing safety measures with regards to possible excessive energy input into the system.

Some of the deliverables related to pilot plant commissioning and validation are listed below.

1. Pilot plant commissioning with water to check for leaks and access the heating and cooling capabilities of the process equipment.
2. Pilot plant commissioning with low CO_2 concentrations and 20wt% MEA.
3. Validation of pilot plant data by comparison to published pilot plant data with 30 wt% MEA as the solvent.
4. Obtaining gas concentration profiles as well as temperature profiles of the gas- and liquid for the absorber column.
5. Obtaining temperature profiles for the stripping column.
6. Investigating the energy requirement for solvent regeneration at various CO_2 capture rates.

Deliverables related to simulating the CO_2 capture process using Aspen Plus®

1. Develop a method that simplifies the process of simulation and aid the convergence within the simulation, thus shortening the required simulation time.

2. Validation of the method of simulation using real pilot plant data published in literature.
3. Considering the capability of the simulation to predict solvent regeneration energy requirement for various packing materials.
4. Investigating the effect of various process parameters on the energy requirement for solvent regeneration.
5. Comparing simulation data to the results from the established pilot plant.

CHAPTER 4
EQUIPMENT DESIGN AND PILOT PLANT CONSTRUCTION

This section will focus on the design and the construction of the pilot plant facility. The flow scheme development with reference to the existing process equipment, and the necessary changes required will be discussed. The philosophy behind the design of the absorber column, gas recycling system, water wash section and gas sampling system are discussed in detail. Setting up the coupled absorption/stripping system is discussed along with the process flow diagrams. Sensor installation, placement and scaling are discussed. The final process and instrumentation diagrams are presented.

4.1. FLOW SCHEME DEVELOPMENT FOR THE POST COMBUSTION CO_2 CAPTURE PILOT PLANT

The initial focus of this particular study was aimed at making use of two existing glass columns with internal diameters of 200 mm, in order to set up a process configuration that can be used for CO_2 capture studies. This section sheds light on the scope development for this study.

4.1.1. HYPOTHETICAL PROCESS SETUP USING EXISTING PROCESS EQUIPMENT

4.1.1.1. AVAILABLE PROCESS EQUIPMENT

With reference to the literature review on the various post-combustion CO_2 capture plants set up at different research centres, some major process equipment are a necessity of performing CO_2 capture studies. The major process equipment units are listed below:

- Packed column for absorption;
- Packed column for solvent stripping;
- Solvent reboiler at the bottom of the stripping column;
- Gas blower unit feeding flue gas to the absorber;
- Rich-lean cross heat exchanger for process heat integration;
- A lean solvent cooler for solvent cooling prior to feeding absorber.

A glass column with an internal diameter of 200 millimetres packed with structured packing and previously used for hydrodynamic studies were available for use as an absorber. A glass

continuous distillation column (ID = 200 mm), fitted with a steam driven thermosyphon reboiler were available for use of a stripping column. The distillation column is also set up for operating with structured packing material. The process configuration was to be designed for use either as individual columns for hydrodynamic- and distillation studies respectively, or as a combination for CO_2 capture studies.

An air blower, initially used to feed the 200 mm hydrodynamic column, was available for providing gas flow to the absorption column. CO_2 can be fed into the air stream and carried to the absorber column.

Designing and installing a heat exchanger and a solvent cooling unit would complete a simple pilot plant setup for CO_2 capture studies.

4.1.1.2. PROBLEMS RELATED TO USING A SIMPLE PROCESS SETUP FOR CO_2 CAPTURE STUDIES

A diagrammatic representation of a simplified process setup that would mainly consist of already existing process equipment can be seen in **Figure 8**. Synthesized flue gas is fed to the bottom of the absorber column, and all gas fed to the system is vented to the atmosphere.

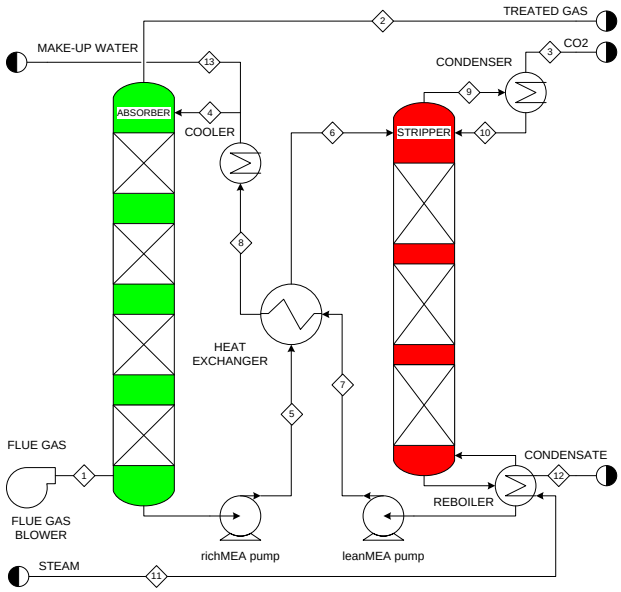

FIGURE 8 SIMPLIFIED PROCESS FLOW DIAGRAM OF A POST COMBUSTION CO2 CAPTURE PILOT PLANT

4.1.1.3. ABSORBER COLUMN

The hydrodynamic column available for absorption studies had a total packed bed length of 0.81 meters. A bed height this small would limit the CO_2 capture studies to CO_2 concentrations related to gas turbines and natural gas fired power stations (3-5 volume %). Coal fired power stations and cement factories produce flue gas streams with CO_2 concentrations of 13 and 25 volume % respectively (Alie et al., 2005). If studying these concentrations is of any interest, the length of the absorber column had to be increased.

4.1.1.4. STRIPPING COLUMN

Seeing that the stripping column normally is the smaller column of the two, the continuous distillation column with a packed bed length of 3.68 meters would be sufficient. The continuous distillation column is also equipped with a total of four condenser units for condensing solvent that evaporates due to boiling in the reboiler unit. The thermosyphon reboiler unit at the bottom of the stripping column is driven by steam from a boiler unit. Steam can be delivered to the reboiler unit at a maximum mass flow rate of 400 kg/h and a pressure of 8 bar.

4.1.1.5. SYNTHESIZING THE FLUE GAS

The initial idea was to enrich the air stream delivered by the air blower with CO_2 up to the desired concentration. Without the option of recycling any of the gas, all CO_2 fed to the system will be released into the atmosphere and evidently lost.

An economic analysis was done using a very simple experimental design (seen in **Table 6**) for testing different column internals with the pilot plant setup. The design only includes CO_2 concentrations and gas flow factors of 3 – 5 volume % and 1.2/1.6 $Pa^{0.5}$ respectively. An average time of 5 hours for the system to reach equilibrium was assumed in performing the cost estimation study. The calculations were also based on the cost of a 33.5 kg CO_2 cylinder being R300-00.

TABLE 6 SIMPLE EXPERIMENTAL DESIGN FOR THE PURPOSES OF THE ECONOMIC EVALUATION

Gas Flow Factor	1.2 $Pa^{0.5}$	1.6 $Pa^{0.5}$
3 volume % CO_2	Block 1	Block 2
5 volume % CO_2	Block 3	Block 4

TABLE 7: SHOWING THE COST OF THE VARIOUS OPTIONS

Option #	Block #				Cost [1packing]	Cost [2packings]	Cost [3packings]
	1	2	3	4			
1	■				R 4 166	R 8 331	R 12 497
2		■			R 5 554	R 11 108	R 16 662
3			■		R 6 922	R 13 844	R 20 767
4				■	R 9 230	R 18 459	R 27 689
5	■	■			R 9 720	R 19 439	R 29 159
6	■		■		R 11 088	R 22 176	R 33 263
7	■			■	R 13 395	R 26 790	R 40 185
8		■	■		R 12 476	R 24 953	R 37 429
9		■		■	R 14 784	R 29 567	R 44 351
10			■	■	R 16 152	R 32 304	R 48 455
11	■	■	■		R 16 642	R 33 284	R 49 925
12	■		■	■	R 20 317	R 40 635	R 60 952
13		■	■	■	R 21 706	R 43 412	R 65 118
14	■	■	■	■	R 25 871	R 51 743	R 77 614

Each block in **Table 6** represents 12 experimental runs – considering 4 different L/G-ratios and 3 different reboiler settings. **Table 7** shows the cost of the various experimental option combinations when considering each block of experiments on their own (Block 1 – 4). The cost increases as the number of column internals tested increase; this can be seen by moving from left to right in the last three columns of **Table 7**.

It can be seen from **Table 7** that the operating cost of the pilot plant would be quite significant if none of the CO_2 is recycled. Also considering that the pilot plant will be used in future for further CO_2 capture studies, gas recycling becomes a necessity.

4.1.2. CHANGES REQUIRED TO EXISTING PROCESS EQUIPMENT

With the main aim being to establish a pilot plant that can be used in future to perform various CO_2 capture studies, some changes to the existing equipment are required.

4.1.2.2. ABSORBER COLUMN

In order to allow for studying CO_2 concentrations higher than 3 – 5 volume %, the packed bed length of the absorber column needs to be increased. The column packed bed length needs to be increased to allow for treating a flue gas with CO_2 concentration of up to 12 volume %.

4.1.2.3. REDUCING OPERATING COSTS BY RECYCLING CO_2 GAS

The analysis of the operating costs related to fresh CO_2 fed to the system proves the viability of gas recycling even though this would increase the initial capital cost investment of the pilot plant. A closed gas cycle needs to be constructed in order to allow for recycling of all the CO_2 that are loaded into the system. The gas stream from the top of the absorber column as well as the gas stream from the top of the stripping column will be recycled back to a gas surge tank. The surge tank will also serve as a knock-out drum for any possible water that might condense in the gas lines.

Gas recycling will also allow for reducing the oxygen content of the process gas by adding nitrogen to the recycle loop. This is desired, seeing that some solvents, such as MEA, are prone to oxidative degradation.

4.1.2.4. INSTALLING WATER WASH SECTION ON TOP OF THE ABSORBER COLUMN

The installation of a water wash section is required when gas recycling is employed. The water wash section is packed with structured packing and is installed on top of the absorber column. This section is required in order to remove any solvent droplets that might be carried over from the absorber column into the gas lines. This section will also serve as a direct contact cooler, cooling the hot process gas from the absorber column before it is recycled back to the gas surge tank unit.

4.2. PILOT PLANT LAYOUT AND PROCESS FLOW DIAGRAM

The pilot plant layout is presented in the process flow diagram shown in **Figure 9**. The layout can be divided into four different subsections namely the solvent circulation loop, process gas-, carbon dioxide- (CO_2) and the wash water circulation loops. Each one of these subsections are discussed and as the chapter progress a more detailed explanation of the process equipment and sensors used in each specific section will be given.

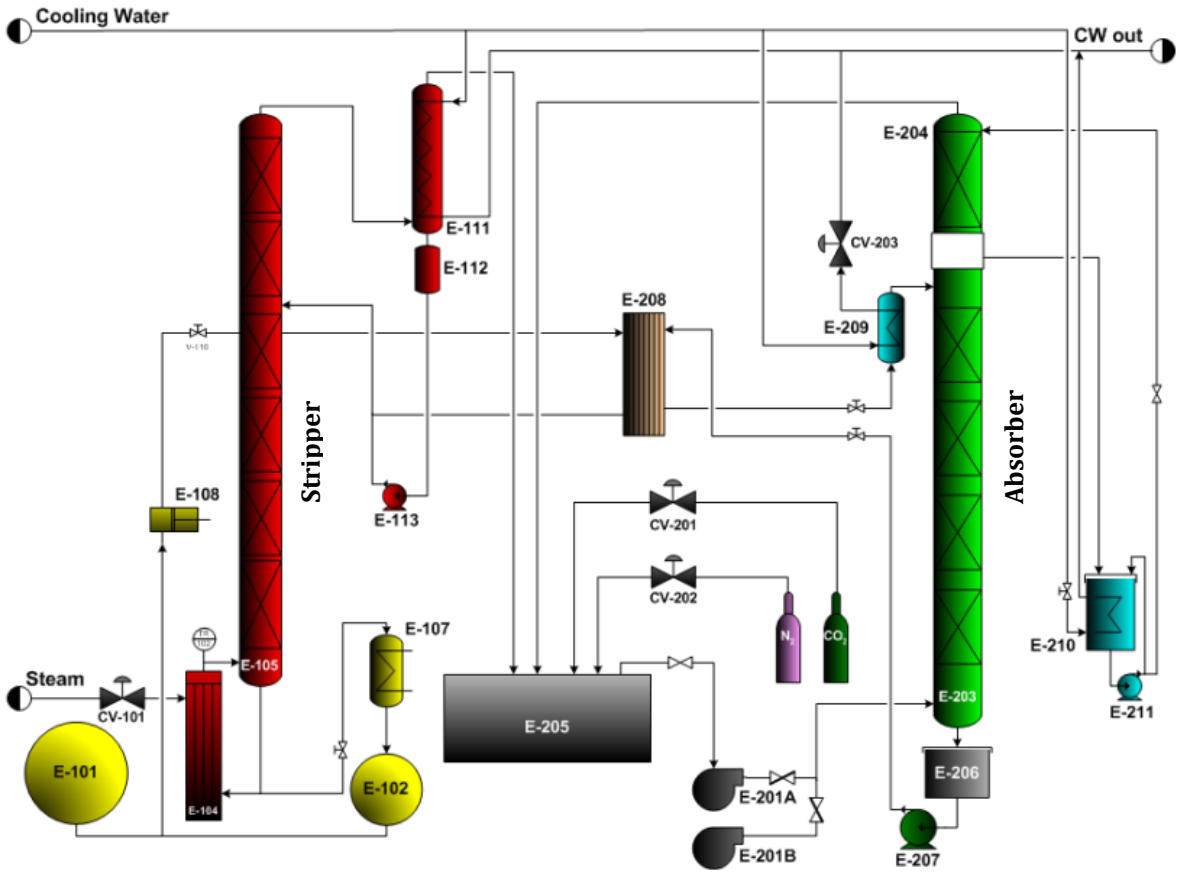

FIGURE 9 PROCESS FLOW DIAGRAM SHOWING THE PILOT PLANT LAYOUT

4.2.1. SOLVENT CIRCULATION LOOP

The solvent circulation loop starts from a point just before the absorption process and will end just prior to feeding solvent to the top of the absorber column. Reference will be made to the tags on the process equipment as presented in **Figure 9**.

Solvent, lean of CO_2, is fed to the top of the absorber column (E-203) and flows downward over the packing material, reacting with the CO_2 in the process gas. The rich solvent at the bottom of the absorber column flows to the rich solvent storage tank (E-206) before it is pumped with a

centrifugal pump (E-207) to a heat exchanger (E-208) for heat integration. After passing through the heat exchanger, the heated solvent is fed to the top of the stripping column (E-105). The solvent is heated further in the reboiler (E-104) at the bottom of the stripping column – driving off CO_2. The hot, lean solvent is then pumped with a pulsation pump (E-108) to the heat exchanger unit (E-208) for heat integration after which it is fed to the solvent cooler (E-209). The solvent is cooled before it is fed again to the top of the absorber column.

4.2.2. PROCESS GAS CIRCULATION LOOP

For the purpose of the circulation loop discussion, CO_2 will not be considered as part of the process gas. The process gas is referred to as all the inert components in the gas passing through the absorber column. This will mainly be nitrogen enriched air. The discharge from the gas recycle blower (E-201A) will be used as the reference point for this discussion.

Process gas passes through a venturi flow meter, is fed to the bottom of the absorber column (E-203) and passes through the column to the water wash section (E-204). Any entrained solvent is washed from the process gas after which it is sent through a second venturi flow meter before passing to the gas surge tank / knock-out drum (E-205). The suction side of the recycle blower (E-201A) is connected to the surge tank (E-205).

4.2.3. CO_2 CIRCULATION LOOP

The CO_2 circulation loop can be divided into two different sections, one with CO_2 in the gas phase (present in the process gas) and one in a reacted form (present in the liquid solvent). The two separate loops join up after the stripped CO_2 from the top of the stripping column (E-105) is combined once again with the process gas in the surge tank (E-205). From here it is fed to the absorber column again (E-203) where the loop splits once again.

4.2.4. WASH WATER CIRCULATION LOOP

The function of the wash water section is to remove any entrained solvent from the process gas. Water is pumped with a centrifugal pump (E-211) to the top of the water wash section (E-204). The water passes through the section and is gathered at the bottom of the wash section with a weir construction that allows gas from the absorber column (E-203) through but guides the wash water back to the wash water tank (E-210).

4.3. ABSORBER COLUMN DESIGN

The absorber column was designed in order to allow operation within certain boundary conditions. These boundary conditions were chosen in order to allow results from the pilot plant to be directly comparable to published data from other pilot plant setups. The column was sized using a rate based Aspen Plus® Simulation of the column. Gas- and liquid sample ports were designed to allow one to obtain concentration profiles across column height.

4.3.1. COLUMN REQUIREMENTS

From the literature study it is clear that the various pilot plant setups have differing process flow setups, column heights, column diameters, packing material, lean solvent loadings, L/G ratios, CO_2 capture rates and flue gas conditions. These factors were considered in the design of the absorber column.

4.3.1.1. CO_2 CONCENTRATION IN THE FLUE GAS STREAM

Natural gas- and coal fired power plants produce flue gas with CO_2 concentrations of 3 and 10 – 12 volume % respectively (Freguia and Rochelle, 2004). Pilot plant studies at the University of Regina were performed for flue gas with CO_2 concentrations of 4 and 8 volume % (Idem et al., 2009). The CASTOR project was performed with a flue gas split stream from an existing power plant (Knudsen et al., 2009). Mangalapally and Hasse, (2011b) and Notz et al.(2012, 2007) performed pilot plant studies with a maximum CO_2 concentration of 10 volume %.

Based on the literature presented, the absorber column was designed to allow the performing of test runs up to the CO_2 concentrations levels present in coal fired power plant flue gas (up to 12 volume % CO_2).

4.3.1.2. PACKING MATERIAL AND CO_2 CAPTURE RATE

In the pilot plants NTNU/SINTEF and ITT, Stuttgart Mellapak 250Y packing material was used for both the absorber and stripping columns. For the Castor project IMPT50 random packing was used in both columns and the CO_2 capture efficiency was set to 90%. Mangalapally and Hasse, (2011b) as well as Notz et al. (2012) considered the effect of various packing materials, in 125 mm internal diameter columns, on the energy efficiency of the process. Mellapak 250Y

and 500BX were compared. A maximum CO_2 removal efficiency of 88% were reported with the 250Y-type packing material, while the BX500 type packing allowed CO_2 removal efficiencies of up to 90%.

In this study 250Y-type packing will be used for the pilot plant verification studies. Considering that 250Y-type packing is less efficient when compared to others with higher surface areas, designing the column for 250Y packing will allow the column to be large enough for operation with more efficient packing materials. To prevent unnecessary overdesign for more efficient packing material, the capture rate with 250Y-type packing material was limited to 85%.

4.3.1.3. L/G RATIO AND LEAN SOLVENT LOADING

Various optimisation studies have been performed in order to determine the optimum liquid-to-gas mass flow rates (L/G-ratio) in the absorber column (Knudsen et al., 2009; Mangalapally and Hasse, 2011b; Notz et al., 2012, 2007). The L/G-ratio highly influences the energy efficiency of the process, and the optimum L/G-ratio has been found to decrease as the CO_2 concentration in the flue gas decrease. Knudsen et al. (2009) reports an optimum L/G-ratio of 2.5 kg/kg when MEA is the solvent of choice. An optimum L/G-ratio of between 2.5 – 2.8 kg/kg was also reported by Mangalapally and Hasse (2011a).

The lean solvent loading [moles CO_2/moles MEA] also greatly influences the energy efficiency of the capture process. Alie et al. (2005) performed simulations for optimisation studies and an optimum lean loading of 0.25 [moles CO_2/moles MEA] was one of the outcomes. Dugas et al. (2009) also performed Aspen Plus® simulations investigating a lean solvent loading within the range of 0.16 – 0.28 [moles CO_2/moles MEA].

Based on the literature presented here, the absorber column was designed for a maximum L/G-ratio of 3 kg/kg for 12 volume % CO_2 in the flue gas. Keep in mind that with decreasing CO_2 concentration the optimum L/G ratio also decreases. The column was designed for a lean solvent loading of 0.25 [moles CO_2/moles MEA].

4.3.2. ASPEN PLUS® ABSORBER COLUMN DESIGN

The rate-based Aspen Plus® simulation that was used for sizing the absorber column is presented in Chapter 6 and will not be discussed in this section. The simulation was used in order to determine the total bed height that would be required in order to achieve the design requirements.

The column diameter was constrained to an inside diameter of 0.2 m by the pre-existing process equipment. The parameters that were used as inputs into the Aspen Plus® Simulation model are summarised in **Table 8**.

TABLE 8 INPUT PARAMETERS FOR THE ASPEN PLUS® ABSORBER DESIGN SIMULATION

Parameter	Input into Aspen Plus®	Units
Packing material	250Y	-
Equilibrium stages	20	-
Column diameter	0.20	[m]
Solvent flow rate [min]	150	[kg/h]
Solvent flow rate [max]	650	[kg/h]
Liquid Load [min]	4.8	[$m^3/m^2.h$]
Liquid Load [max]	20.7	[$m^3/m^2.h$]
Lean solvent loading	0.25	[moles CO2/moles MEA]
L/G ratio	3	-
CO_2Removal efficiency	85%	[%]
CO_2 inlet concentration	12%	[%]
Flood dynamic load predicted	96 (L/G ratio of 2.5)	[%]
Operating in loading range	80 (L/G ratio of 3.0)	[%]

The simulation was set up with a design specification that set the CO_2 capture rate to 85%. The column height was varied iteratively in order to obtain the packed height that would be required for the specified capture rate. From the simulation it was found that a packed bed with a total height of 2.2 meters would be required.

Figure 10 and **Figure 11** show the CO_2 concentration- and gas temperature profiles from the Aspen Plus® simulation for the designed absorber column. The trend for the temperature profile across the column height, shown in **Figure 11**, also corresponds well to data published in literature (Mangalapally and Hasse, 2011a; Notz et al., 2012). From **Figure 12** it can be seen that the requirement of an 85% CO_2removal efficiency is satisfied.

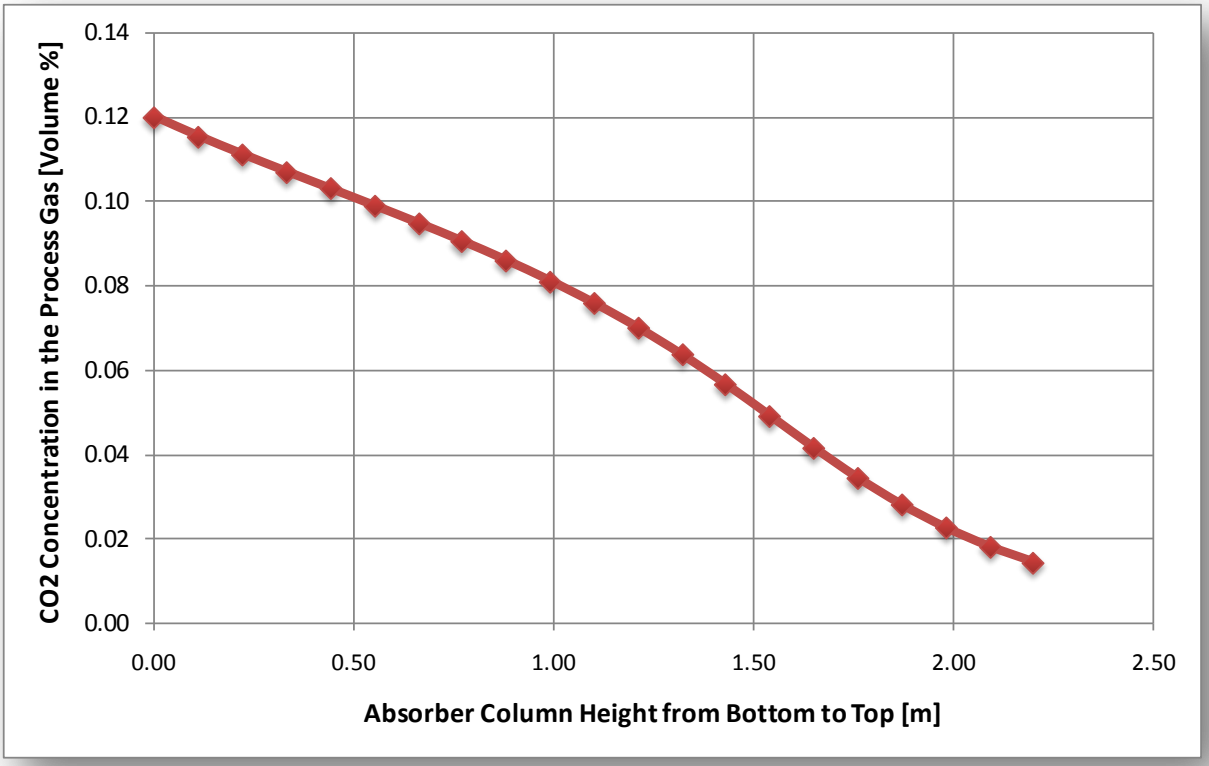

FIGURE 10 CO_2 CONCENTRATION PROFILE AS PREDICTED BY THE ASPEN PLUS® SIMULATION

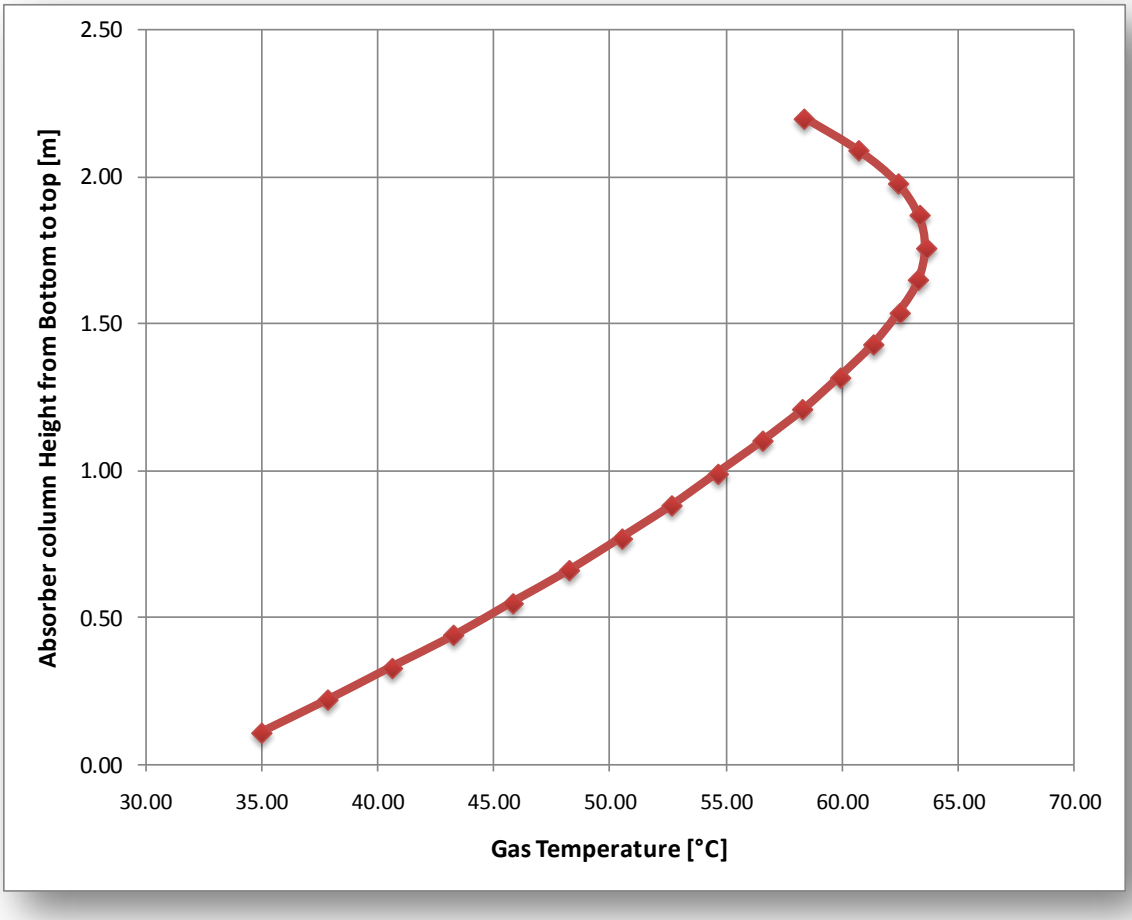

FIGURE 11 GAS TEMPERATURE PROFILE AS PREDICTED BY ASPEN PLUS® SIMULATION

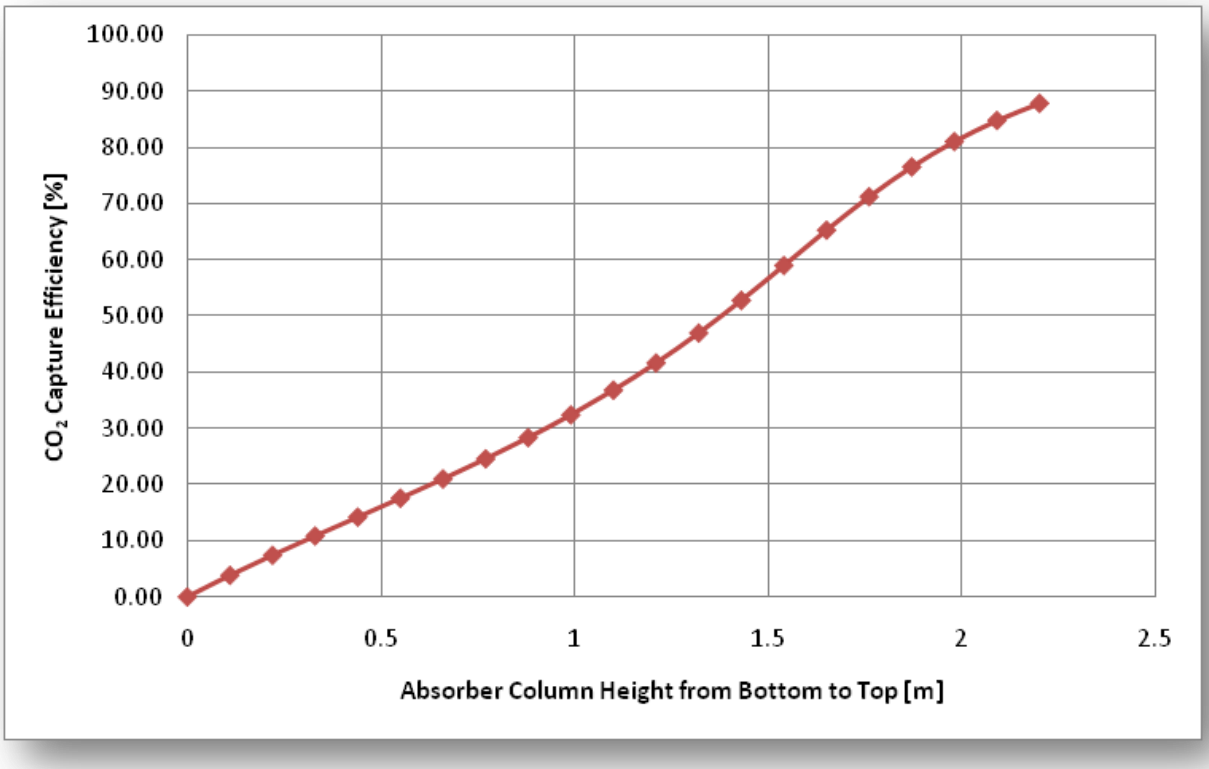

FIGURE 12 CO_2 CAPTURE EFFICIENCY FOR VARIOUS COLUMN HEIGHT FOR THE CONDITIONS SPECIFIED IN **TABLE 8**

4.3.3. GAS / LIQUID SAMPLING AND DISTRIBUTION

In order to properly evaluate results from the pilot plant setup, sample points across the height of the absorber column would be required. This will allow setting up temperature, liquid- and gas composition profiles.

Glass sections with an internal diameter of 0.2 meter were manufactured in lengths of 1 meter per section. Each meter section was designed with three possible ports, at three different heights, where samples can be extracted or a temperature reading can be taken. Thus, each glass section has nine different ports. **Figure 13** shows a schematic diagram of one of the glass sections. The absorber column consists of three one meter glass sections as seen in **Figure 14**.

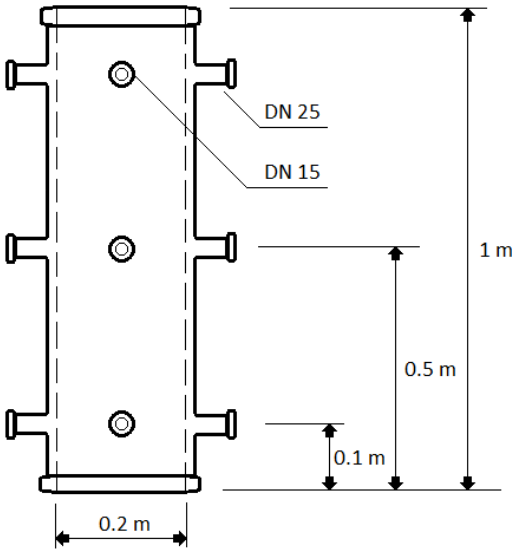

FIGURE 13 SCHEMATIC DIAGRAM OF THE GLASS SECTIONS FOR ABSORBER COLUMN

The number of ports that can be used for sampling or temperature readings is however limited by the fixed dimensions of the structured packing. The 250Y-type packing material sections used for pilot plant commissioning has a height of 0.27 m per section. Packing the column in such a way, that allows direct contact between at least two 0.27m packing sections before having a sampling section results in four sample points across the bed height. An additional data point is obtained by analysing the outlet from the top of the column. The configuration of the sampling ports for the absorber column can be seen in **Figure 14**.

Gas- and liquid sample ports were designed to allow sample extraction from the various column heights. Gas sample ports were designed to prevent solvent from entering the gas sample tubes. Liquid sampling devices were designed to allow sampling from any position across the diameter in the column. This will allow liquid sampling from the middle of the column as well as from the wall. It was thought that this sampling technique might provide more information regarding the influence of wall flow on the absorption process. **Figure 15** and **Figure 16** show drawings of the designed sample ports that were used for the construction of the gas- and liquid sample ports respectively. Stainless Steel 304 was used as the material of construction due to the corrosive nature of monoethanolamine (MEA).

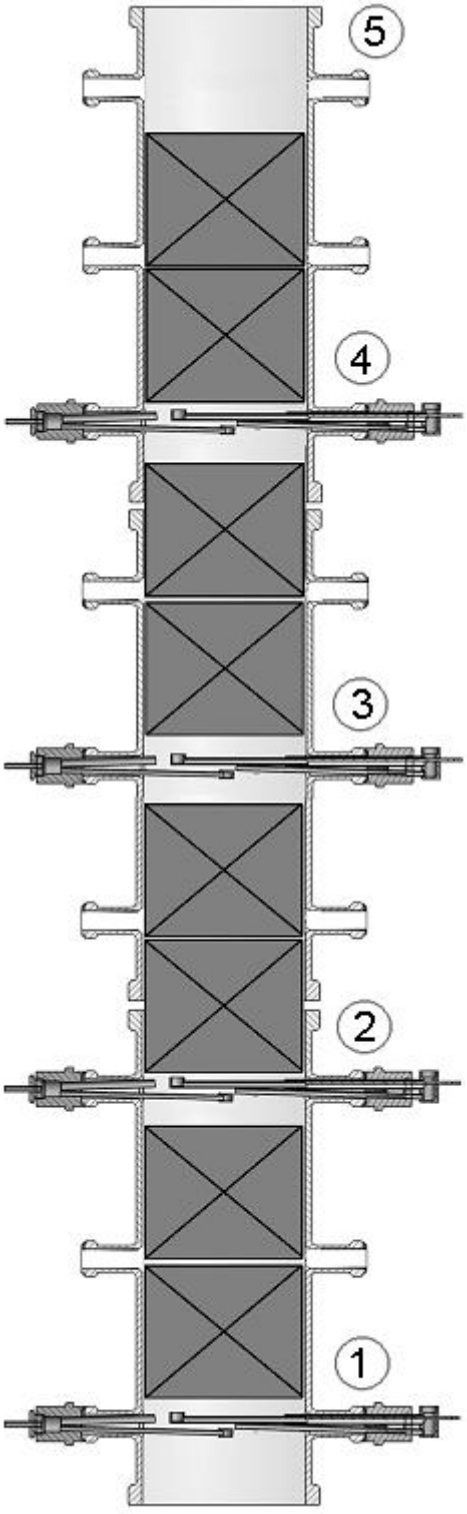

FIGURE 14 ABSORBER COLUMN CONFIGURATION OF SAMPLING POINTS

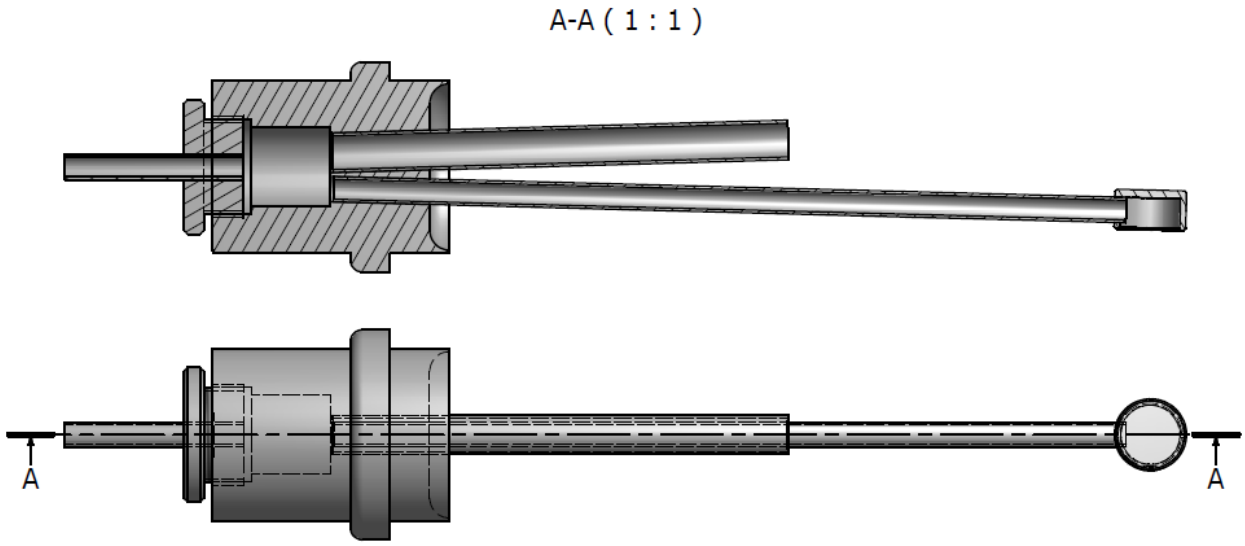

FIGURE 15 TOP- AND SIDE SECTION VIEW OF GAS SAMPLE PORT

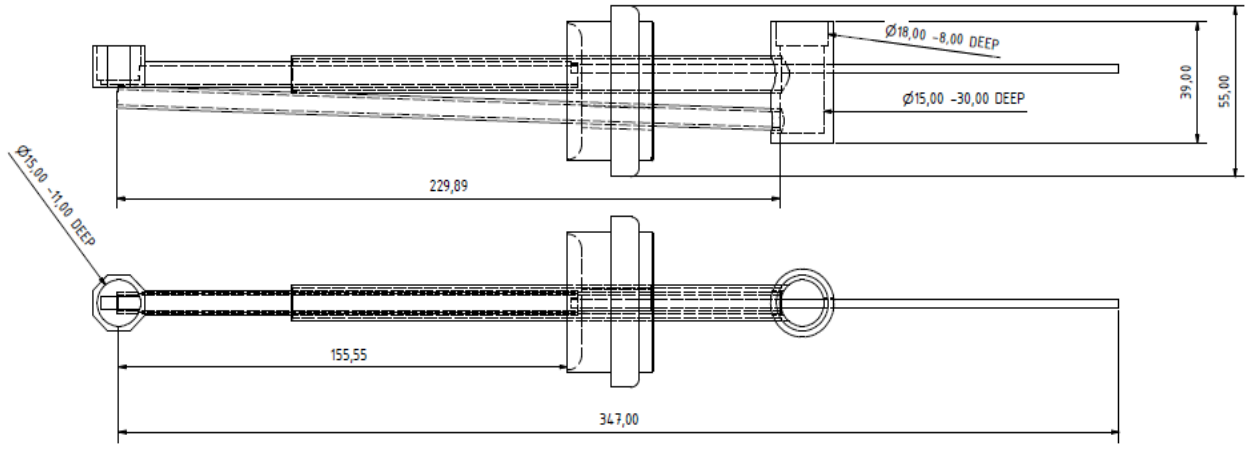

FIGURE 16 TOP- AND SIDE SECTION VIEW OF LIQUID SAMPLE PORT

Figure 17 shows a cross-section view of the bottom part of one of the glass sections with the gas- and liquid sample ports installed. The liquid sample pot (1) can be moved to pass over the gas sample pot (4). The liquid sample passes through the tube into the sample holding pot (2) from which a sample can be extracted with a syringe. The liquid sample, in the sampling holding pot (2), is continuously replaced with fresh sample by continuous circulation out through the liquid return tube (3).

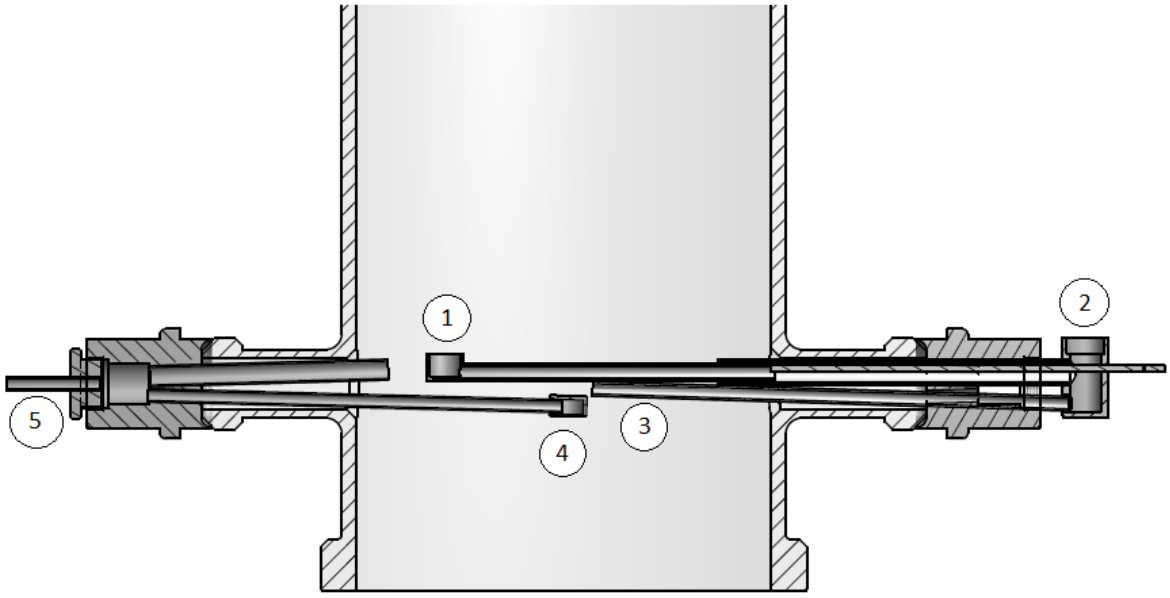

FIGURE 17 SCHEMATIC OF GAS- (LEFT) AND LIQUID (RIGHT) SAMPLE PORTS INSTALLED IN GLASS SECTION

The gas samples are extracted from the column through the gas sampling pot (4). The gas sample tube is manufactured with a slope to return any liquid that enters at (4) back to the column. Gas samples are pumped from (5) with a gas sample pump to the online gas analysers.

The gas- and liquid sample ports were installed in the absorber column, below every second section of structured packing. In order to evaluate the distribution in the column, water was fed to the top of the column. It became clear that the wall wipers on the packing material cannot guide the water from the walls onto the packing once a sampling section has been reached. Stainless steel wall wipers were designed in order to guide liquid back onto the packing material after each sampling section. **Figure 18** shows one of the manufactured stainless steel wall wipers. These wall wiper were installed prior to performing any of the reactive absorption experiments.

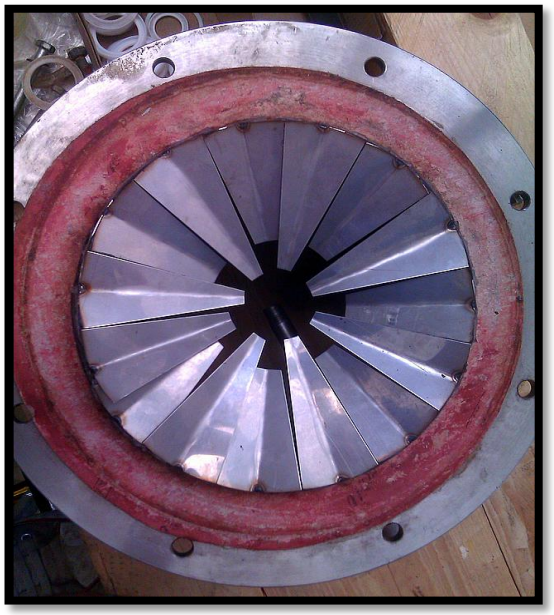

FIGURE 18 STAINLESS STEEL WALL WIPERS

Figure 19 shows the CAD drawing that was used for manufacturing the stainless steel plate wall wipers. Preliminary tests with water indicate that the wall wipers are effective in returning the liquid from the column walls back onto the packing material. The current design presented in **Figure 19** limits the gas flow rate to a maximum of about 300 kg/h. At higher gas flow rates flooding occur, starting from where the wall wipers are installed. This limitation on the gas flow rate can at a later stage be resolved by adapting the wall wiper design to allow for higher gas flow rates and lower pressure drop.

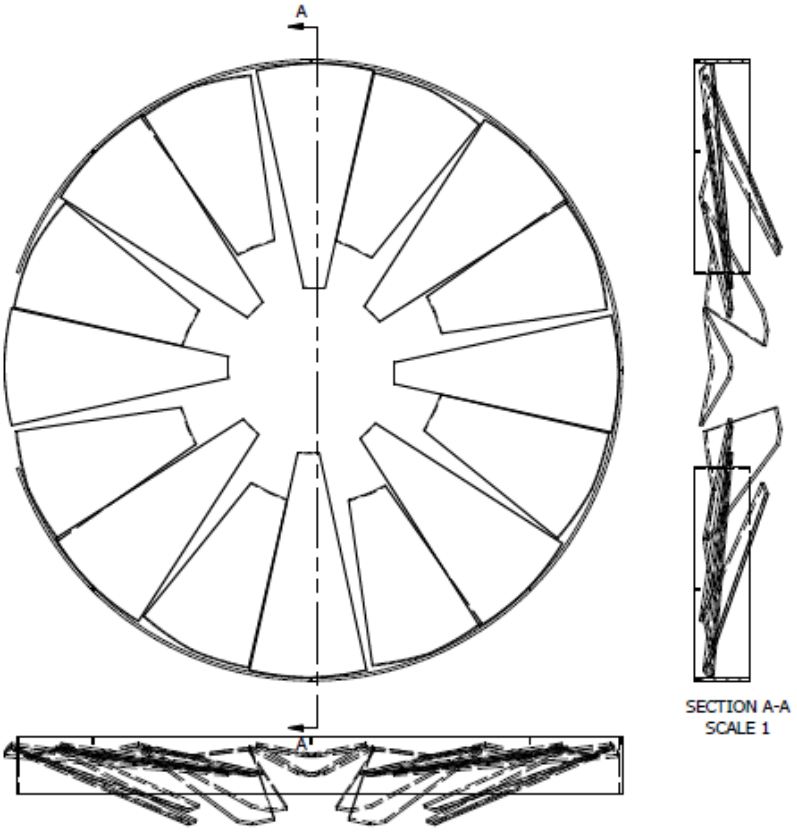

FIGURE 19 SCHEMATIC DIAGRAM OF THE STAINLESS STEEL PLATE WALL WIPERS

Temperature measurements across the height of the absorber column are done using PT100 temperature probes. In an attempt to obtain separate temperature profiles for both the liquid- and the gas streams in the column, temperature probe isolation devices were designed. The devices separate the two PT100 probes and prevent direct contact with the liquid (for the bottom probe) and

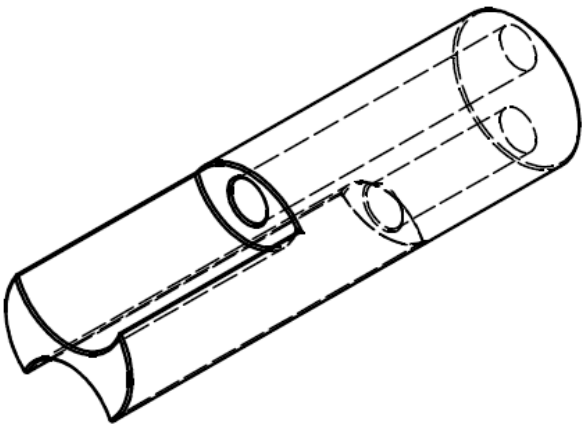

FIGURE 20 TEMPERATURE PROBE ISOLATION

with the gas (for the probe on top). The probe on top will measure the liquid temperature, while the probe at the bottom, exposed to the upward flowing gas, will be used to measure the gas temperature in the absorber column. The device, used to separate the temperature probes measuring gas- and liquid temperatures respectively is shown in **Figure 20**.

Proper distribution in the absorber column is ensured by designing, manufacturing and installing a stainless steel liquid distributor in the middle of the packed bed. The design of the liquid distributor was based on work done by (Erasmus, 2004). **Figure 21** shows the drawings of the designed liquid distributor.

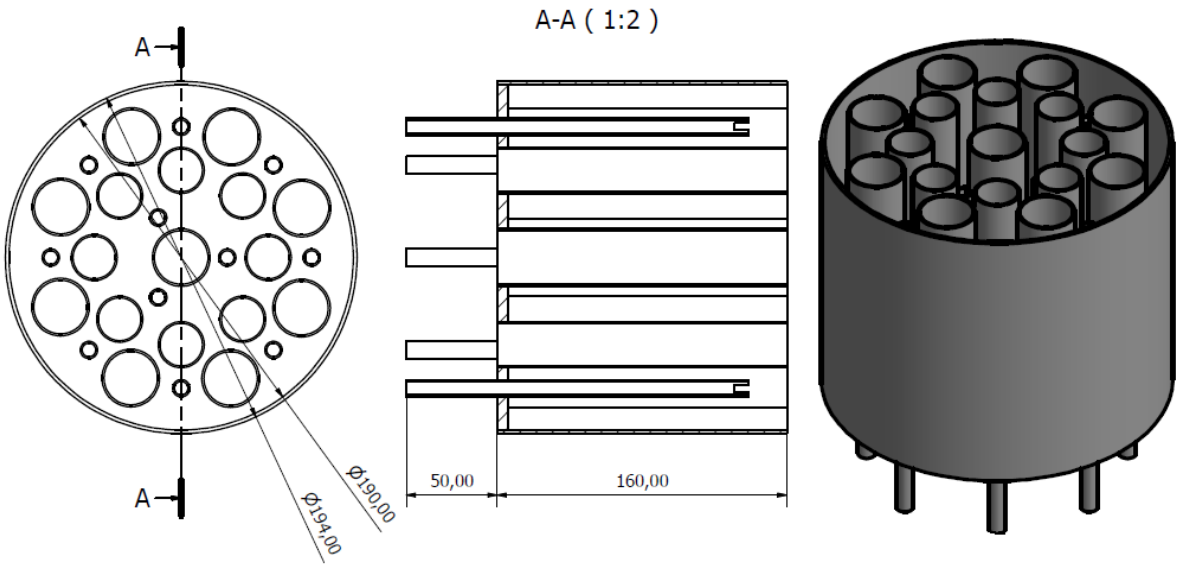

FIGURE 21 DRAWINGS OF THE DESIGNED LIQUID DISTRIBUTOR

4.4. GAS RECYCLING SYSTEM

At the start of this chapter the reasoning with regards to employing a gas recycling system was discussed in detail. This section covers the design and construction of the gas recycling system with reference to the surge tank, the venturi tubes and water wash section. Reference will also be made to the specifications of the gas recycle blower.

4.4.1. OVERVIEW OF GAS RECYCLING SYSTEM

Installing a closed gas recycle loop requires the installation of some extra equipment that otherwise would not be necessary.

Figure 22 gives a 3-dimensional representation of the gas recycle loop that is required. A recycle blower unit (1) is one of the additional requirements. The decision was made to keep the air blower (2) available for operation. This will be used when tests with air are conducted. The butterfly valves (6, 7, 8 and 9) installed in the PVC gas lines give the option of operating with an either closed or open gas system, depending on the specific tests performed.

Gas is fed to the absorber column (3) and passes to the water wash section (4) where any entrained solvent will be washed from the gas stream.

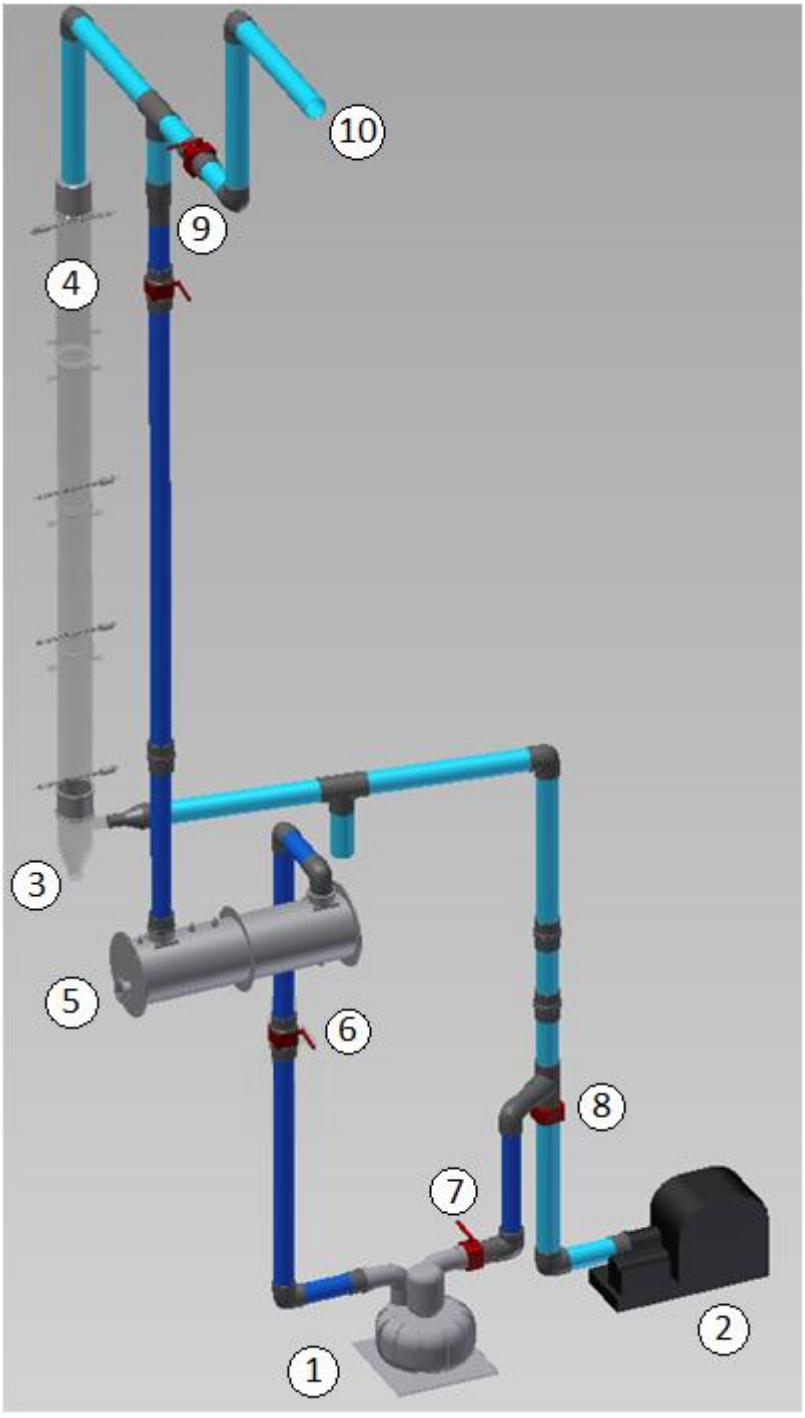

FIGURE 22 3D REPRESENTATION OF THE GAS RECYCLING SYSTEM

The surge tank (5) serves as a horizontal knock-out drum as well as a gathering vessel for recycled gas from the top of the absorber- and stripping columns. With a closed loop configuration, gas is returned from the top of the absorber column to the surge tank (5) which is connected to the suction side of the recycle blower unit (1). When operating with an open gas system, gas is vented to the atmosphere (10).

4.4.2. SURGE TANK DESIGN

A surge tank for gas recycling was designed with a dual function, the first being the gathering of the gas recycled from the absorber- and stripping columns. Furthermore the tank is installed on the suction side of the recycle blower, completing the gas recycle loop. The second function of the designed tank is to serve as a knock-out drum for any liquid droplets that might be present in the process gas. This is done by sufficiently reducing the gas velocity by increasing the cross-sectional area available for flow – allowing droplet settling.

The design of the surge tank was based on baselines given in Sinnot and Towler, (2009). The design for a horizontal liquid-gas separator was followed, leading to a smaller tank when compared to vertical tank designs. This was done due to space requirements around the already existing process equipment. **Figure 23** shows the drawings of the designed horizontal liquid-gas separator tank. The design calculations are summarised in Appendix A.

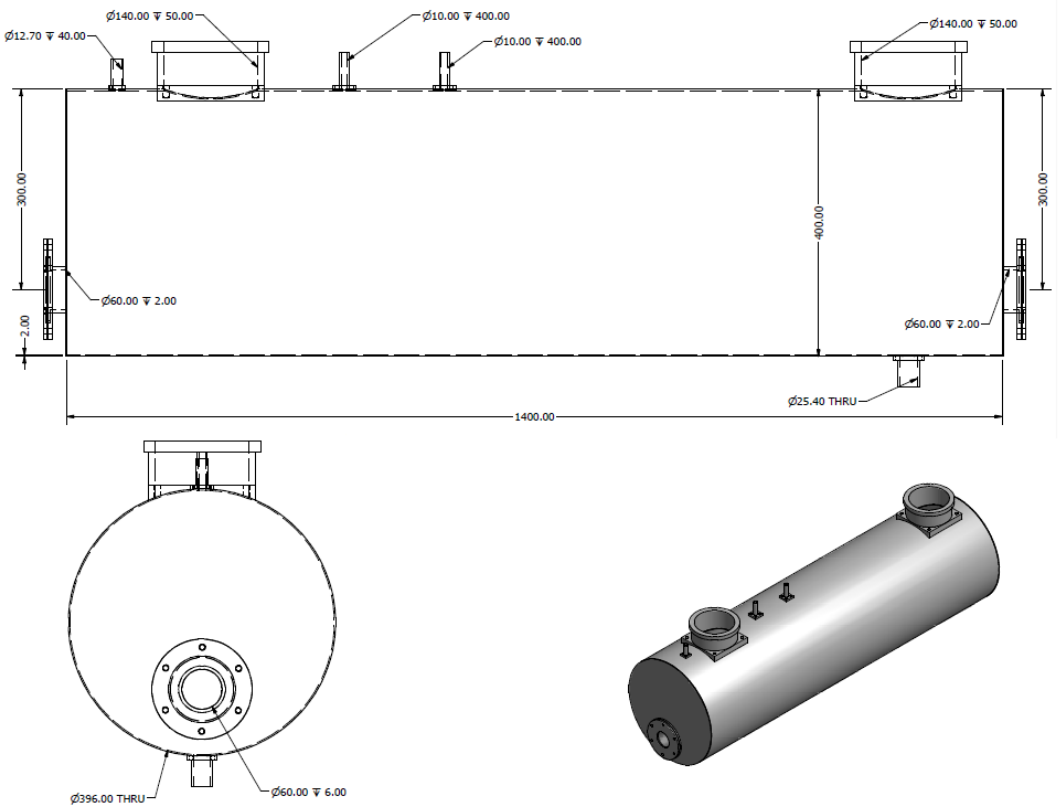

FIGURE 23 DIAGRAM OF THE DESIGN HORIZONTAL SURGE TANK

4.4.3. VENTURI MASS FLOW METER DESIGN

The mass flow rate of the process gas stream is determined using venturi mass flow meters. Two identical venturi tubes were constructed; one is installed in the gas feed line to the absorber column and the other in the line returning gas from the top of the absorber column to the surge tank. A comparison between readings from the two flow meters allows one to keep track of the amount of gas absorbed in the absorber column.

The venturi tubes were manufactured from PVC and details regarding the design and flow calculations can be seen in Appendix A. **Figure 24** shows the drawings that were used for manufacture of the venturi mass flow meters. The pressure taps are however not indicated on the drawing. Details regarding the calibration method used for the venturi flow meters can also be found in Appendix A.

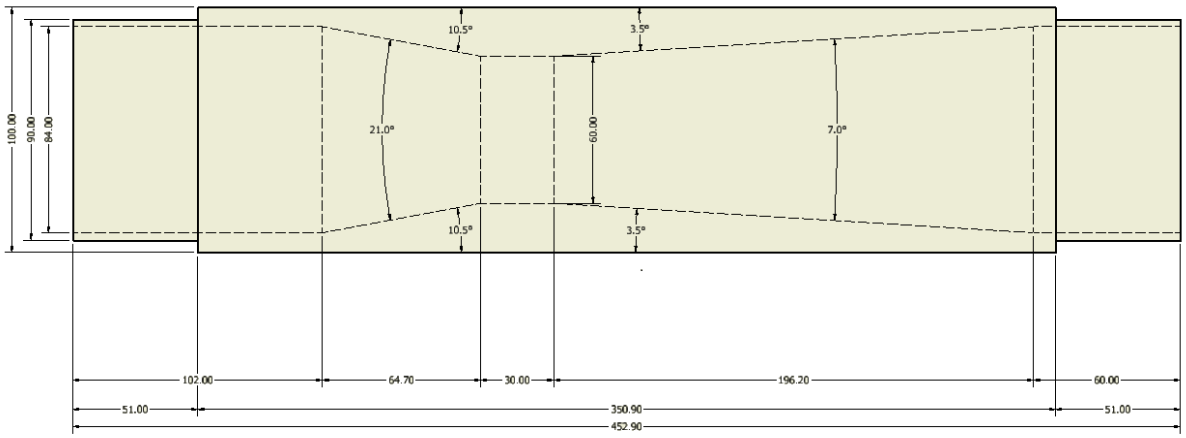

FIGURE 24 DESIGN FOR THE VENTURI TUBES INSTALLED

4.4.4. WATER WASH SECTION

The main function of the water wash section is to remove any entrained solvent from the process gas stream before it enters the PVC gas lines. Monoethanolamine (MEA) is a corrosive solvent and may damage the lines with continuous exposure.

The water wash section consists of a one meter glass section packed with 350Y type packing (total bed length of 0.54 m). Water is continuously circulated by the wash water pump from a wash water holding tank to the top of the water wash section. The water is then distributed across the packing material and a weir configuration at the bottom of the water wash section allows the water to return to the wash water tank and not pass into the absorber column.

4.4.5. BLOWER SPECIFICATION

The recycle blower specifications were prepared by evaluating the pressure drop across the packed column, the two venture mass flow meters, and the process gas lines set up for recycling. An overdesign factor was also included in the specifications to account for possible unforeseen pressure drops in the system, or future tests requiring higher gas flow rates. The blower specifications that were sent to the supplier, together with the calculations on which the specification was based, can be seen in Appendix A.

Seeing that the blower unit is installed inside the laboratory area sound isolation was also one of the main requirements. A recycle blower with a 7.5 kW motor was purchased and installed. Further specifications on the blower unit can also be seen in Appendix A.

4.5. GAS SAMPLING

Analysis of the gas compositions at various times and at various locations in the process is very important in order to properly evaluate the absorption process. Analysis for both carbon dioxide (CO_2) and oxygen(O_2) content are performed. Results from the CO_2 analysis are then used in order to determine the CO_2 capture rate. The method of sampling will also be discussed in this section.

4.5.1. CO_2 CONCENTRATION

Gas sampling is mainly performed in order to determine the CO_2 content of the process gas. It is of great importance that the CO_2 concentration of the flue gas being fed to the bottom of the absorber column is known. One of the main control objectives is to obtain a constant CO_2 content in the feed gas at steady state. This necessitates the use of an online CO_2 analyser – continuously analysing the CO_2 concentration in the feed gas. The CO_2 content of the process feed gas will eventually influence the energy requirement for solvent regeneration.

Furthermore, in order to properly evaluate the absorption process, it is very important to determine the amount of CO_2 that has been absorbed from the process gas. Thus, online analyses of the CO_2 content in the gas passing through the absorber column and leaving the top of the absorber column are also required.

An online analyser (Drager, 7200) was installed for analysing the CO_2 content of the process gas at various locations in the process. The accuracy of the CO_2 sensor is reported to be $< \pm 1.5$ % of the measured value with a repeatability of $\leq \pm 0.05$ % volume and a long-term drift of < 0.03 %

volume over a twelve month period. Gas sampling from the various locations will be discussed in the section on the gas sampling method, Section 4.5.3.

4.5.2. O_2 CONCENTRATION

As stated in the literature survey of this study, MEA and other amine solvent blends are subjected to oxidative degradation (Lawal et al., 2005; Rochelle et al., 2011). For this reason, in this study, the oxygen (O_2) content of the synthesized process gas is reduced by adding nitrogen gas (N_2) to the air.

The importance of continuously monitoring the O_2 content of the process gas thus becomes apparent. For this purpose an online O_2 analyser (Drager, VarioGard) is installed in series with the CO_2 analyser.

4.5.3. GAS SAMPLING METHOD

In order for the online gas analysis to provide valuable information regarding the gas composition and of the absorption process, the sampling method has to be set up properly. Due to limited resources, only one CO_2- and O_2 analyser could be purchased, even though composition analyses from various locations are necessary. This problem was however overcome by constructing a gas sampling manifold setup as seen in **Figure 25**.

The valve manifold setup shown in **Figure 25** allows composition analysis not only from the top of the absorber column (5), but also from four other locations (at different heights) in the absorber column (1 – 4). The operator can manually select the location for sample analysis by switching the valves. Samples are drawn from the various locations with a gas sample pump (Drager, PSD3000) (6), through the CO_2 analyser and from the pump discharge the sample is blown over the O_2 analyser (7).

FIGURE 25 GAS SAMPLING VALVE MANIFOLD SETUP

As previously mentioned, continuous analysis of the feed gas to the bottom of the absorber column and analysis of the stream leaving the top of the absorber column is required. This allows for proper evaluation of the overall absorption process. To overcome the problem of only having one CO_2 analyser, two control valves are used to automatically switch the location from where the sample is drawn. In doing this, the two streams are analysed in a time sequence that can be set by the user. More information on the control will be discussed in Chapter 5 which covers setting up the control of the pilot plant.

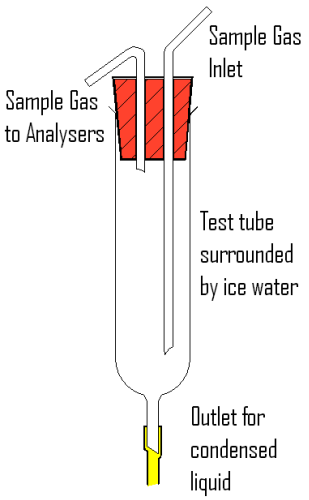

FIGURE 26 SCHEMATIC DIAGRAM OF WATER TRAP FOR GAS SAMPLES

The gas samples that are drawn from the column are sent to a water trap where most of the moisture content that might be present in the gas sample stream due to the elevated temperatures (40 – 60°C) is condensed. **Figure 26** shows a schematic diagram of the devices used for trapping volatile liquids in the sample gas. All gas

sample streams, from all locations in the absorber column, pass through one of these water traps. The ice water on the outside of the test tubes ensures that any moisture content present in the sampled gas condense inside of the test tube. This prevents any interference that the moisture content of the gas might have on the accuracy and reliability of the sample analysis. After passing through the gas analysers the gas sample stream is recycled back to the gas recycle loop.

4.5.4. CO_2 CAPTURE EFFICIENCY

The CO_2 capture efficiency can be defined as the efficiency of CO_2 removal from the process gas passing through the absorber column. This is usually expressed as a percentage value, relating the amount of CO_2 in the outlet gas to the amount of CO_2 in the feed gas. The CO_2 capture efficiency (α) can be calculated using only the gas compositions of the two streams as given by Equation (1).The derivation of Equation (1) can be seen in Appendix A.

$$\alpha = \frac{CO_{2\ vol\%\ [IN]} - CO_{2\ vol\%\ OUT}}{CO_{2\ vol\%\ [IN]} \times \left(1 - CO_{2\ vol\%\ OUT}\right)} \times 100$$

Gas sample analyses from the bottom and the top of the absorber column can thus be used to evaluate the CO_2 capture efficiency. This will be done until steady state, and thus a constant CO_2 removal efficiency, is reached. At steady state the manifold of sampling valves may be used to analyse samples from different heights in the absorber column. In this way a CO_2 concentration profile over the height of the absorber column can be obtained.

4.6. STRIPPING COLUMN AND REBOILER UNIT

The stripping column is used for regeneration of the rich solvent by the addition of energy in the form of heat. Heat is added to the solvent by means of a steam driven thermosyphon reboiler unit. Steam at a pressure of 8 bar (gauge) can be delivered to the reboiler unit at a mass flow rate of up to 400 kg/h.

Heating the rich solvent promotes the reverse reaction, thus releasing the CO_2 from the solvent mixture. The CO_2 and some of the evaporated solvent (mostly water) pass upward through the column and most of the water is condensed in the condensers at the top of the stripping column. The condensed water is returned to the stripping column with a centrifugal reflux pump, while CO_2 is directed toward the surge tank for gas recycling (back to the bottom of the absorber column).

Minimal adjustments were required to utilize the already existing continuous distillation setup as a stripping column for the CO_2 capture process. The main adjustment that was required is the installation of a gas line directing the CO_2 product to the surge tank. A non-return valve was installed in this line to allow flow in only one direction – that of the surge tank and no flow from the surge tank back into the stripping column. The higher temperature of the stripping column, and the suction created by the blower (suction-side connected to the surge tank) creates a natural pressure gradient between the column and the surge tank, thus driving the flow of the CO_2 in the correct direction.

The stripping column is packed with 250Y-type structured packing material and has a total packed bed height of 3.68 meters. The column is fitted with liquid sample ports and thermocouples for temperature measurements after every one meter packed section.

Calculations were performed in order to determine the capability of the steam operated reboiler unit for solvent regeneration. The calculations were based on the process design specifications for the absorber column. A process gas stream with CO_2 concentration of 12% and an 85% CO_2 capture rate. Furthermore it was assumed that 98% of absorbed CO_2 are removed in the stripping column with a desorption energy of 5 500 MJ/kg CO_2 removed. A reboiler efficiency of 75% was also assumed as any lower value than this would be unrealistic.

It was found that for the specifications given and the assumptions mentioned a steam flow rate of 200 kg/h would be required for solvent regeneration. Thus the reboiler unit is able to provide the energy required for solvent regeneration. Detailed calculations can be seen in Appendix A.

4.7. LINKING THE ABSORBER AND STRIPPING COLUMNS

One of the major concepts that make the process of capturing the CO_2 more efficient is energy recovery by heat integration. This is mainly done by using heat from the regenerated solvent to heat the cooler, rich solvent from the bottom of the absorber column. A heat exchanger, linking the absorption- and the desorption sections, is used for this type of heat integration.

4.7.1. HEAT EXCHANGER DESIGN

The heat exchanger that creates the link between the absorption- and stripping sections of the process was designed using Aspen Plus®. This method of design was used due to the limited availability of heat capacity data for 30 wt % MEA solvent with various CO_2 loadings.

The approach followed mainly consists of simulating the reaction process in the absorber column until the required rich- (stream from the bottom of the absorber column) and lean loadings (stream from the bottom of the stripping column) were obtained. The stream compositions and properties were then used as inputs to the heat exchanger design with a temperature approach of 10K. The stream temperatures that were considered can be seen in the diagram showing the Aspen Plus® simulation of the heat exchanger - **Figure 27**.

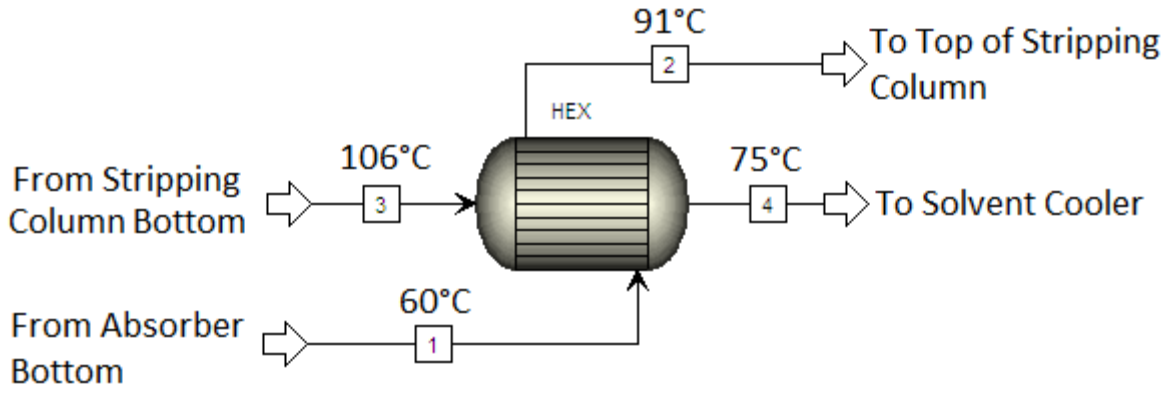

FIGURE 27 HEAT EXCHANGER IN-AND OUTLET TEMPERATURES AS IN ASPEN PLUS®

A plate heat exchanger with a heat duty rating of 8 kW was purchased. EPDM was used as the material for the gasket seals between the plates of the exchanger; as this would be chemically stable in an MEA rich environment. The heat exchanger was installed just before the inlet of the stripping column, limiting the heat lost in the pipes prior to the solvent entering to stripping column.

4.7.2. MEA COOLER UNIT

The temperature of the solvent entering the top of the absorber column needs to be as low as possible. This will promote the exothermic absorption reaction between the MEA and the CO_2 fed to the bottom of the column. The temperature of the stream leaving the heat exchanger will not be cooled sufficiently and thus a cooling unit is installed prior to feeding the solvent to the top of the absorber column. From the outlet of the MEA cooler the solvent is fed to the top of the absorber column, thus completing the solvent recycle stream for the pilot plant setup.

4.8. SENSORS FOR DATA ACQUISITION

The pilot plant is set up with a variety of sensors – differential pressure, absolute pressure- and steam pressure transmitters as well as temperature sensors, online composition analysers and flow meters. All sensors were placed and sized to allow for proper data acquisition of all sections of the CO_2 Capture pilot plant.

In setting up the P&IDs for the pilot plant setup, the process areas were sub-divided into three different areas – 100, 200 and 300. Areas 100, 200 and 300 represent the stripping section, absorption section and the total reflux column respectively. Every sensor in a specific area is tagged accordingly (For Example, TR-101 will be in Area 100, and TR-201 will be in Area 200), this can be seen in **Figure 28**.

All sensors installed in the pilot plant setup are recorded on a combined P&ID for all three 200 mm columns. All utility streams are also included on the P&ID.

4.8.1. SENSOR PLACING

The absorption- and stripping columns are both fitted with temperature sensors in order to obtain temperature profiles. Both column pressures are also recorded using absolute pressure cells and the pressure drop across each column are gathered. Furthermore absolute pressure- and differential pressure transmitters are used to calculate the mass flow rates of the process gas streams. This section summarises the placement of all sensors in the pilot plant setup. All sensor related accuracies are reported in Appendix A.

4.8.1.1. DIFFERENTIAL PRESSURE TRANSMITTERS

Area 100

dPR-101 - Measures the pressure drop across the stripping column (E-105);

dPR-102 - Measures the liquid level in liquid holding T-piece (E-112);

Area 200

dPR-201 - Measures the pressure drop across the absorption column (E-203);

dPR-202 - Measures the pressure drop across venturi flow meter (I-1), used for flow rate calculation of stream 2;

dPR-203 - Measures the pressure drop across venturi flow meter (I-2), used for flow rate calculation of stream 5;

Can also be used to measure the pressure drop across the water wash section installed at the top of the absorber column by switching manual ball valves (Close V-235, Open V-236).

Area 300

dPR-101 - Uses the same differential pressure transmitter as Area 100 with a manual valve switch setup (Open V-304 and V-305, Close V-121 and V-122)

4.8.1.2. ABSOLUTE PRESSURE TRANSMITTERS

Area 100

PIR-101 - Measures absolute pressure of the stripping column (E-105);

Area 200

PIR-201 - Measure absolute pressure of the absorber column (E-203);

Can be used to measure the absolute pressure of the process gas stream at the inlet of the venturi flow meter (I-2) by manipulating the installed ball valves (Open V-239, Close V-240);

PIR-202 - Measure absolute pressure of venturi flow meter (I-1) for density calculation of the process gas;

Area 300

PIR-101 - Uses the same absolute pressure transmitter as in Area 100, manual ball valves are switched to measure the relevant pressure (Open V-306, Close V-123)

4.8.1.3. PRESSURE TRANSMITTERS FOR STEAM PRESSURE

Area 100

PR-101 - Measures steam pressure prior to feeding reboiler (E-104);

Area 300

PR-301 - Measures steam pressure prior to feeding reboielr (E-301)

4.8.1.4. TEMPERATURE SENSORS PLACING

The temperature sensors installed consist of a mixture of PT100s (platinum resistance thermometers) and thermocouples. The thermocouples still installed are sensors that have been there prior to starting this project. It was found that the thermocouples give relatively good temperature readings if properly calibrated with an offset value. The list of all the temperature sensors and their various placements can be seen in Appendix B.

4.8.1.5. ONLINE GAS ANALYSERS

E-214 - DragerVarioGard O_2 analyser (0 – 25 vol%)

E-215 - Drager 7200 CO_2 analyser with process cuvet (0 – 20 vol%)

The accuracy of the CO_2 sensor is reported to be < ±1.5 % of the measured volume percentage value with a repeatability of ≤ ±0.05 % volume and a long-term drift of < 0.03 % volume over a twelve month period. The reported accuracy for the O_2 analyser is ≤ 0.4 volume %, with a resolution of ≤ 0.1 % volume.

These analysers are installed in series with a sample pump feeding gas samples to both of them. For both these units, samples can be extracted from various locations in the absorber column.

4.8.1.6. FLOW METERS

FIR-101 - Cooling water supply line (Stream 31)

I-1 - Venturi flow meter in process gas feed line (Stream 2)

I-2 - Venturi flow meter in treated process gas line (Stream 5)

The accuracy of the absolute pressure- and differential pressure transmitters that are used for the flow rate calculations are specified by the supplier (Siemens) to be ≤ 0.15% of the measured values.

4.8.2. SENSOR SIZING, SCALING AND CALIBRATIONS

In considering the sensor sizing and finally scaling in the PLC (programmable logic controller) programs, the operating ranges of each sensor were kept in mind. The same was done for the calibrations of the thermocouples. More detail regarding the sensor ranges and temperature calibrations can be seen in Appendix A.

4.8.3. PROCESS AND INSTRUMENTATION DIAGRAM (COMBINED: AREAS 100, 200 AND 300)

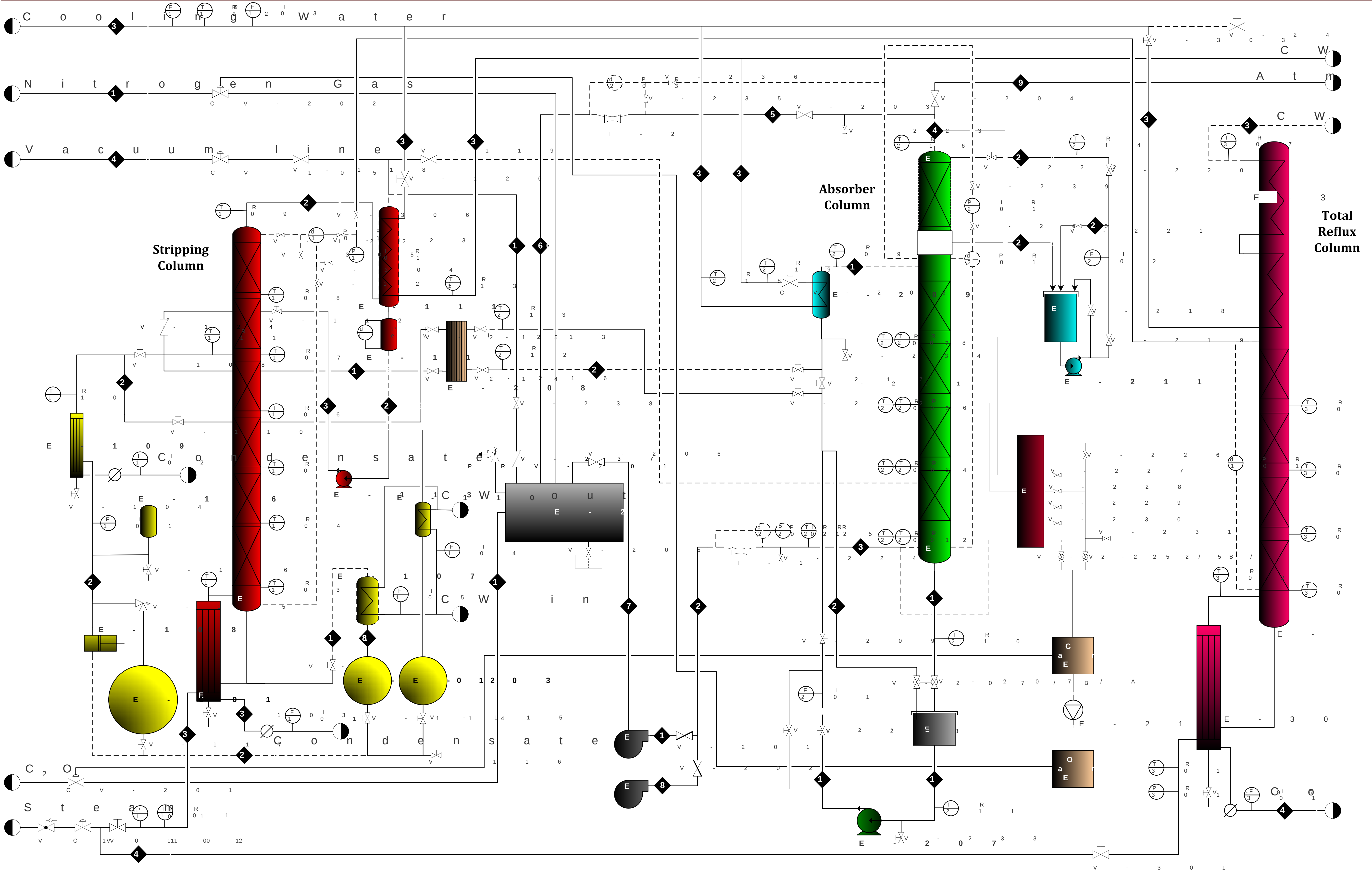

FIGURE 28 PROCESS AND INSTRUMENTATION DIAGRAM (P&ID) OF ALL PROCESSES (AREAS 100, 200 AND 300). PROCESS EQUIPMENT LIST PRESENTED IN APPENDIX B, **TABLE B.30**

4.9. CHAPTER SUMMARY

In this chapter the main focus was on the design and the construction of a pilot plant facility for CO_2 capture studies. The flow scheme development and design was of utmost importance seeing that the existing process equipment had to be adapted to form part of the CO_2 capture plant, but the design needed to allow one to operate the columns as stand-alone units as well.

The design of the pilot plant layout was presented and thoroughly discussed. The re-design of the column to be used as an absorber column was presented. The absorber design was performed using the Aspen Plus® simulation discussed in Chapter 6. The designed gas sampling method was discussed as well as the liquid distribution in the absorber column.

A gas recycle system was developed, designed and constructed. Developing the gas recycling system included the design, construction and installation of a gas surge tank, two venturi mass flow meters and a recycling gas blower unit. The gas recycle system allows gas recycling from the top of both the stripping and the absorption columns to a surge tank. The venturi mass flow meters measure the mass flow rates prior to feeding the absorber column and at the top of the absorber column. The suction side of the gas recycle blower unit is connected to the surge tank from where it feeds the bottom of the absorber column.

A heat exchanger was designed and installed for heat integration between the hot stripping section and the colder absorption section. A solvent cooler, cooling the solvent before it is fed to the top of the absorber column was also installed.

After discussing the developed flow scheme and the designed- and installed process equipment, the final P&ID was presented. All sensor placements for proper data acquisition were presented and discussed.

CHAPTER 5

CONTROL SYSTEMS AND COMMISSIONING PROCEDURE FOR THE PILOT PLANT SETUP

In setting up the control system for the Pilot Plant setup all possible applications of the process equipment available were taken into consideration. Three different glass columns with internal diameter of 200 mm are available. These columns can all be operated as stand-alone units allowing Continuous Distillation-, Total Reflux Distillation- and Column Hydrodynamic/Absorption Studies. The continuous distillation- and the hydrodynamic column can in turn be used together as a stripping and an absorber column in a coupled closed loop system for CO_2 capture studies.

5.1. INTRODUCTION TO THE DIFFERENT MODES OF OPERATION

The control structure required for operating all of the above mentioned columns, for their various applications, were divided into four different modes of operation. The four modes include the following processes:

- *Mode 1:* Post Combustion CO_2 Capture Pilot Plant
- *Mode 2:* Continuous Distillation Column
- *Mode 3:* Total Reflux Column
- *Mode 4:* Absorption / Hydrodynamic Column

All four modes will be discussed with reference to the specific application. The main screen that appears on the touch panel of the PLC unit for each mode will be shown as an introduction to the human-machine-interface (HMI) program that was set up.

5.1.1. MODE 1: PILOT PLANT FOR POST COMBUSTION CO_2 CAPTURE STUDIES

Mode 1 is set up for the control of the post combustion CO_2 capture pilot plant. The pilot plant consists of two different glass columns with internal diameter of 200 mm. The columns are used as an absorber and a stripping column respectively. In the absorber column, CO_2 is absorbed from a synthetically generated flue gas, using a reactive solvent. The reactive solvent is then sent to the stripping column where it is regenerated by the addition of heat. The regenerated solvent is recycled back to the top of the absorber column, where it is reused for absorption purposes.

The main screen of the HMI (human-machine-interface) program for mode 1 can be seen in **Figure 29**.

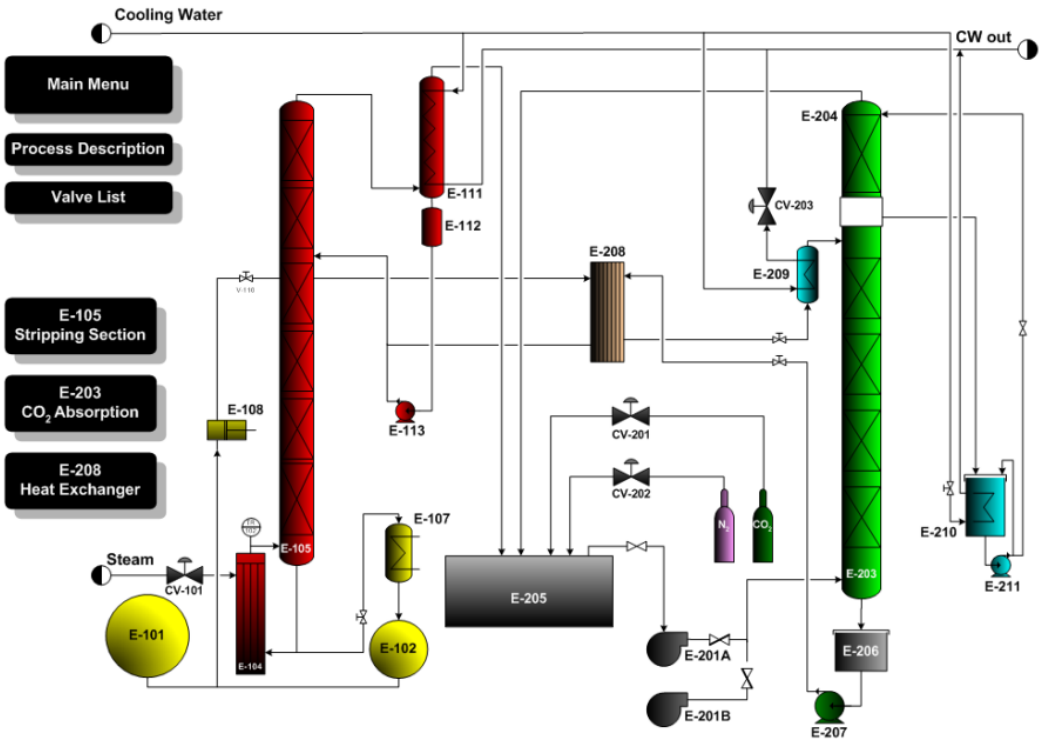

FIGURE 29 MAIN SCREEN OF POST COMBUSTION CO_2 CAPTURE PILOT PLANT

The post combustion CO_2 capture pilot plant can be operated with either a closed or an open gas cycle. With the closed cycle setup, gas from the top of the absorber and stripping columns is recycled back to a knock-out drum (E-205). E-205 is installed on the suction side of the recycle blower unit (E-201A).

Online gas composition analysis of the gas passing through the absorber column is made possible by the manifold valve system that allows the drawing of gas samples from different heights in the column. Analysis for both CO_2 and O_2 content are available.

5.1.2. MODE 2: CONTINUOUS DISTILLATION COLUMN

The continuous distillation column setup can be used by operating the stripping column from Mode 1 as a stand-alone unit. The column can be isolated from the absorber column by closing screw down valves installed between these two columns. **Figure 30** shows the main screen of this mode.

The continuous distillation column is operated with the steam valve CV-101. This valve is used to control the steam flow to the reboiler unit (E-104). The mixture to be separated is fed to the top of the column by a pulse pump (E-108). The distillate from the top of the column is

condensed in the condenser unit (E-111) after which it is sent to the distillate pot (E-103). The bottoms product is drawn from the bottom of the column and is sent to the bottoms pot (E-102).

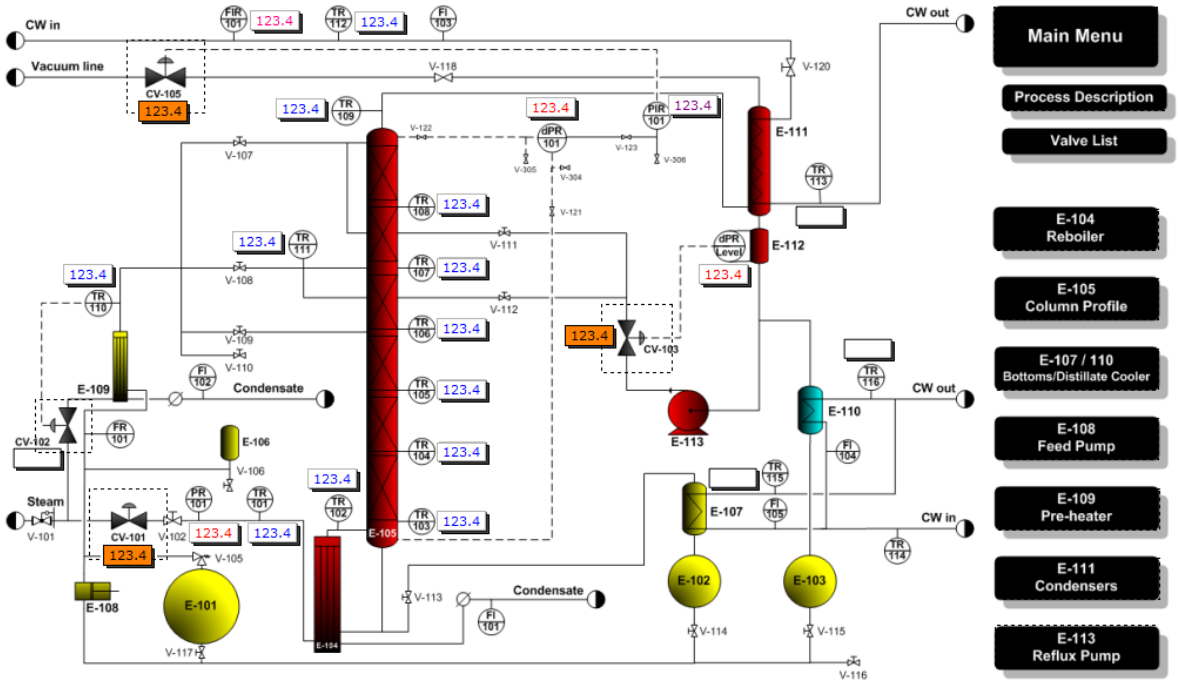

FIGURE 30 MAIN SCREEN OF MODE 2, CONTINUOUS DISTILLATION COLUMN

5.1.3. MODE 3: TOTAL REFLUX COLUMN

Mode 3 makes provision for the operation of the total reflux distillation column. The control valve used for steam supply to the reboiler of the 200 mm internal diameter glass column is CV-101. The steam isolation valve to the continuous distillation column should be closed, and the one to the reboiler of the total reflux column opened to operate in Mode 3. The main screen from Mode 3 can be seen in **Figure 31**.

The control for the total reflux setup is relatively simple. The only variable that requires adjusting is the setpoint on the control valve, CV-101, which supplies the reboiler with steam. The setpoint can be adjusted between 0 – 100 %. Furthermore, the control valve is interlocked with the flow meter in the cooling water supply line. This prevents adding heat to the column without extracting any energy from the system. In the process of total reflux distillation, all the distillate that condenses in the condenser at the top of the column is returned back to the column.

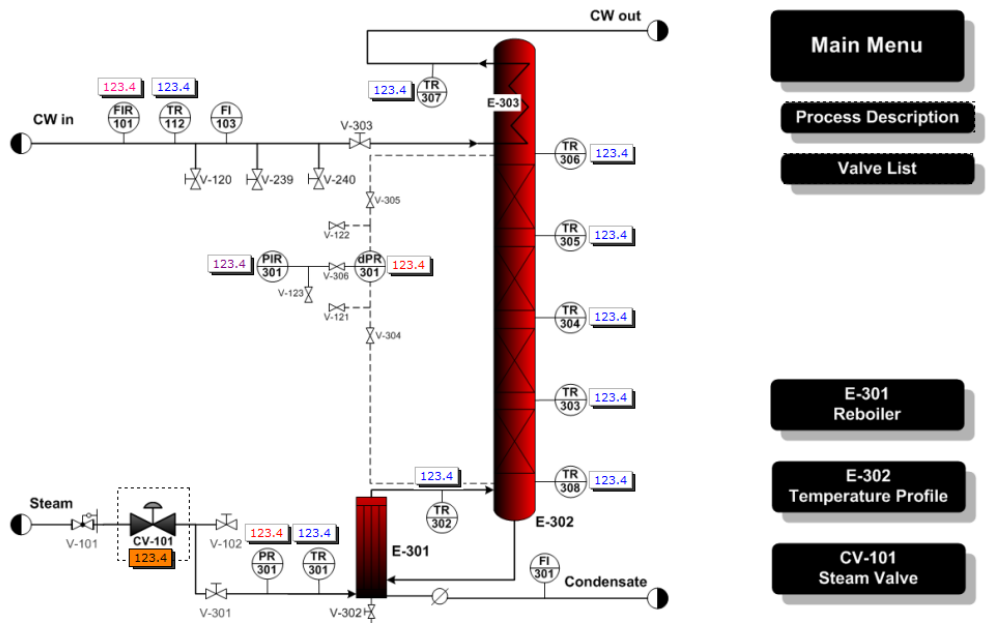

FIGURE 31 MODE 3 MAIN SCREEN FOR OPERATING THE TOTAL REFLUX DISTILLATION COLUMN

5.1.4. MODE 4: 200 MM COLUMN FOR HYDRODYNAMIC STUDIES

Mode 4 is set up for operating the absorber column from Mode 1 as a stand-alone column. The absorber column is isolated from the stripping column by closing the relevant screw down valves. The hydrodynamic column can be operated with an open or a closed gas cycle. The main screen for the hydrodynamic column can be seen in **Figure 32**.

This setup can be used in order to study the hydrodynamic behaviour of various structured and random packing materials. The setup can also be used for absorption studies. The air blower unit (E-201A) can be used when air is the preferred gas for a particular study.

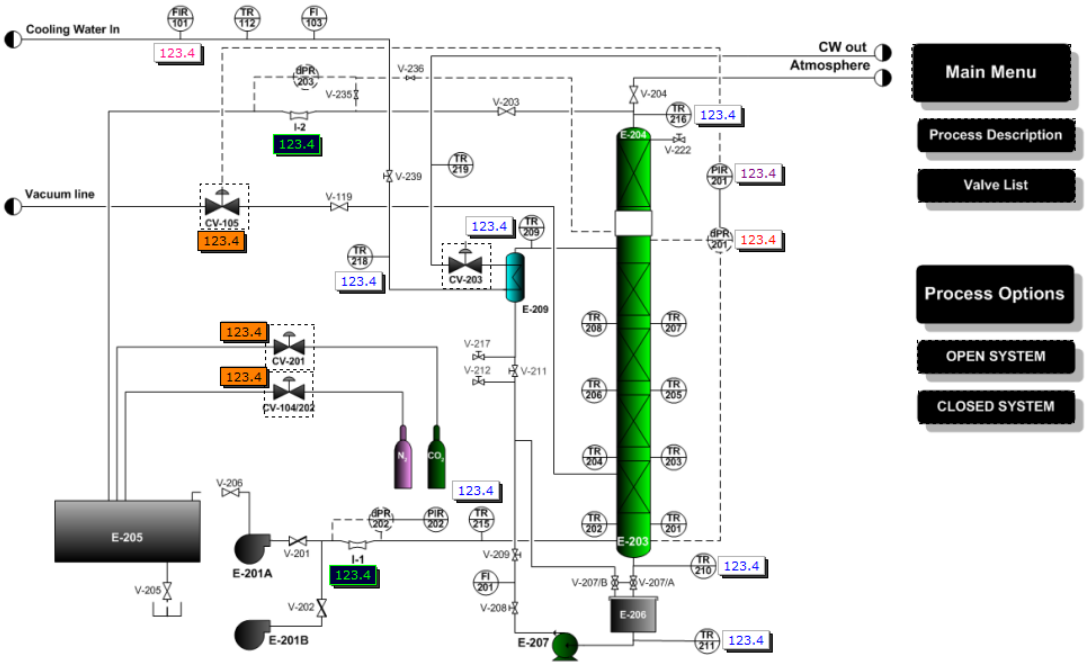

FIGURE 32 MODE 4 MAIN SCREEN, HYDRODYNAMIC COLUMN

5.2. CONTROL STRUCTURE OF THE VARIOUS MODES

This section summarises the control structure as it was set up for the four different modes of operation. The logic followed when setting up the control structure in the form of these block diagrams, were followed through when the HMI program was put together for installation on the PLC unit. The structures given in these block diagrams roughly summarizes how navigation though the HMI program can be achieved. It also gives an indication of the displayed and gathered sensor data.

The block diagrams given in **Figure 33** to **Figure 36** contain all the information regarding each one of the different modes of operation. The block diagrams were set up to be self-explanatory and further discussion thereof will be very brief in an attempt to be concise.

The control structures for the various modes were set up with reference to the main sections of each mode. This brief discussion is focussed on **Figure 33** which gives the control structure developed for the CO_2 capture pilot plant. The main sections that were identified include the gas recycle loop, utilities, sensors, P&ID, valves and sampling. Each of the sections was divided into sub-sections that give information regarding the control or data acquisition required for that particular sub-section. The HMI program installed on the touch panel of the PLC unit was set up with reference to the block diagrams given in **Figure 33** to **Figure 36**.

5.2.1. BLOCK DIAGRAM OF MODE 1

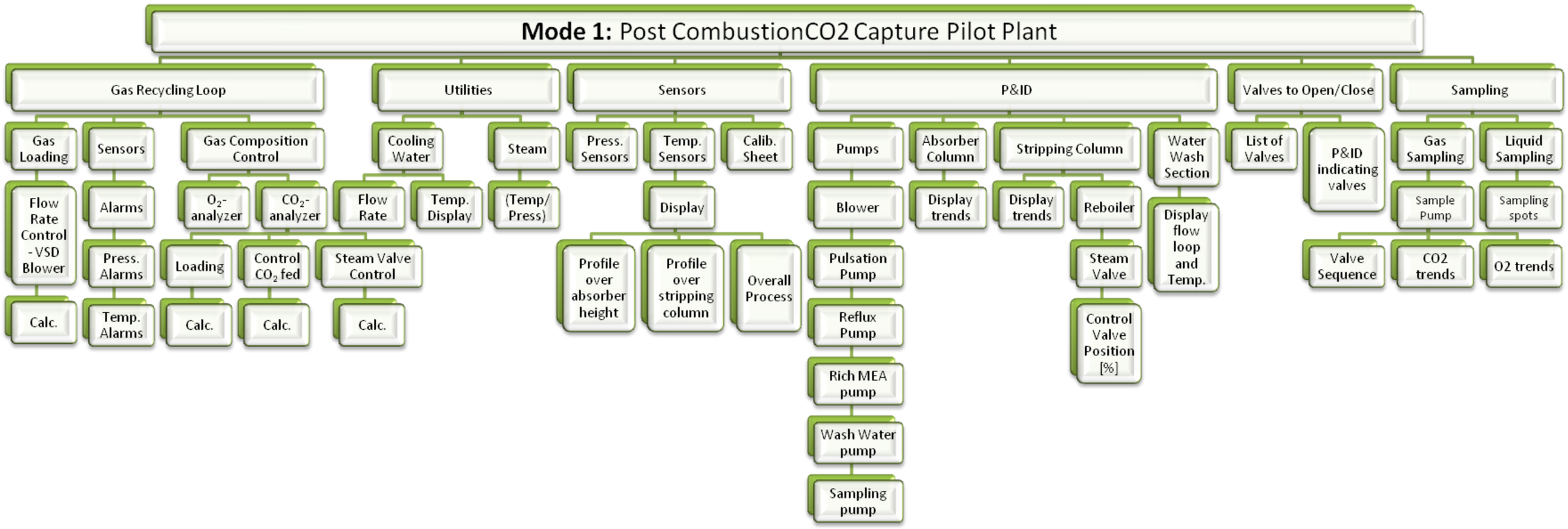

FIGURE 33 BLOCK DIAGRAM OF CONTROL STRUCTURE FOR MODE 1

5.2.2. BLOCK DIAGRAM OF MODE 2

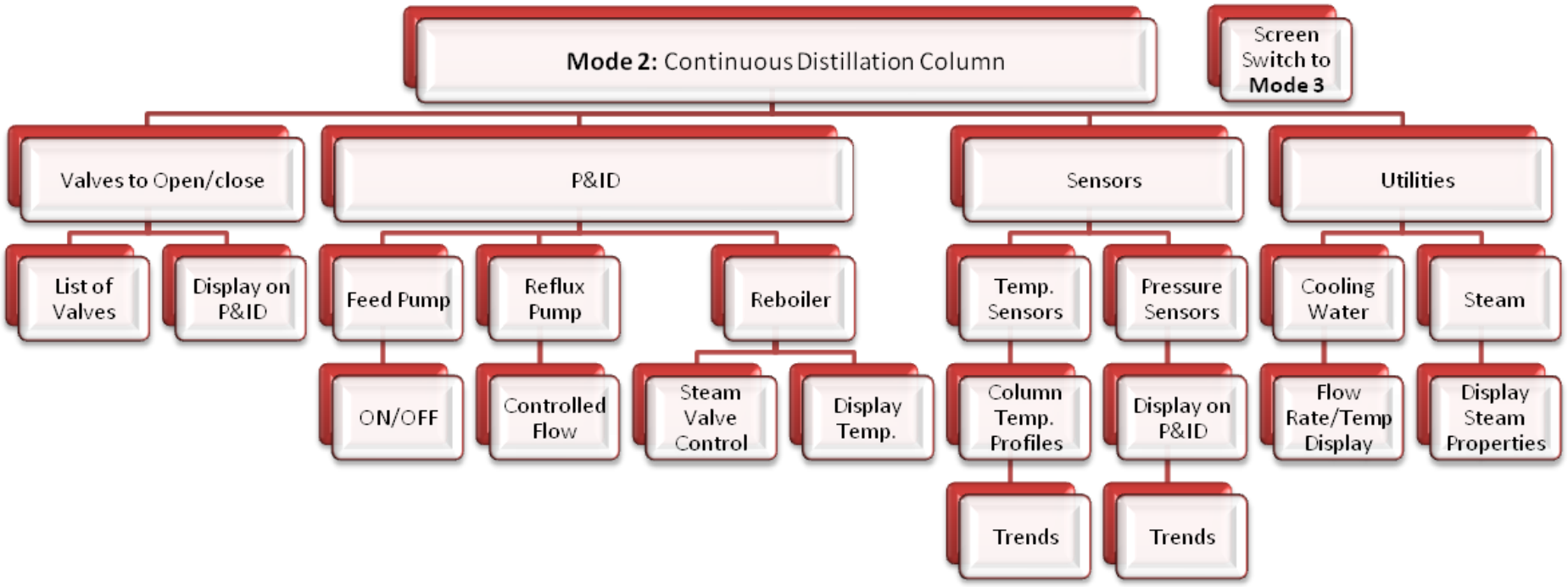

FIGURE 34 BLOCK DIAGRAM FOR CONTROL STRUCTURE OF MODE 2

5.2.3. BLOCK DIAGRAM OF MODE 3

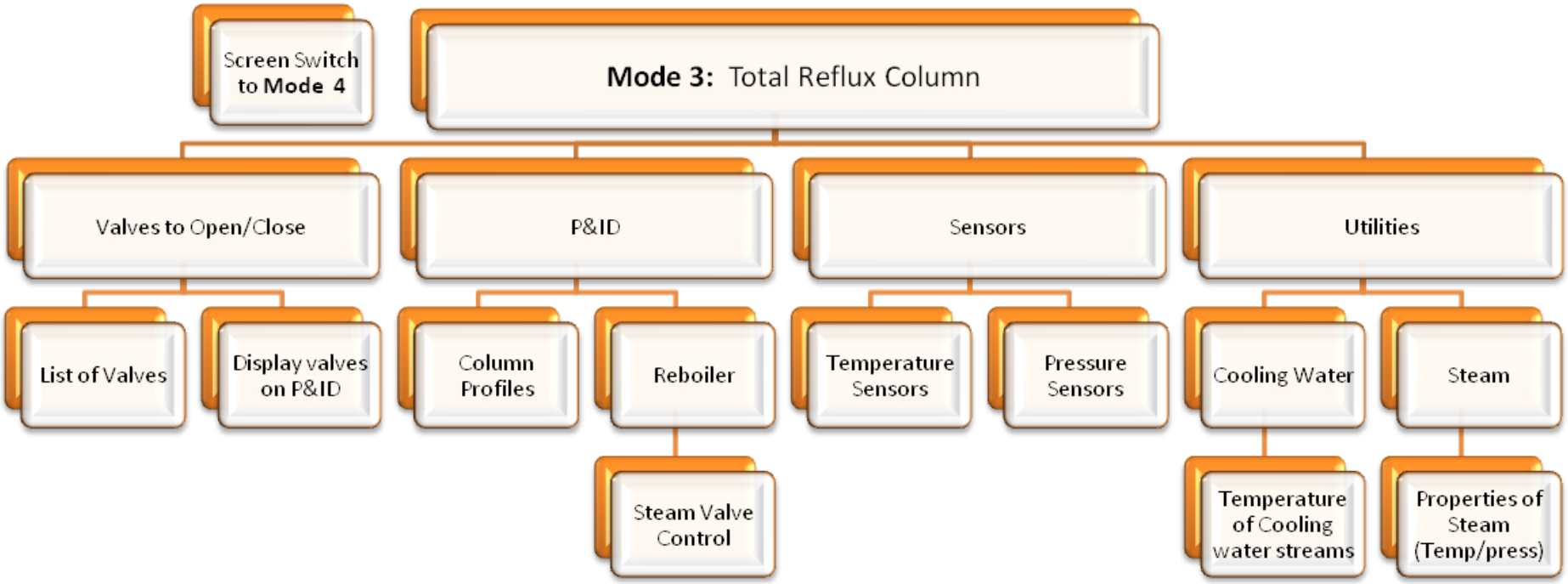

FIGURE 35 BLOCK DIAGRAM FOR CONTROL STRUCTURE OF MODE 3

5.2.4. BLOCK DIAGRAM OF MODE 4

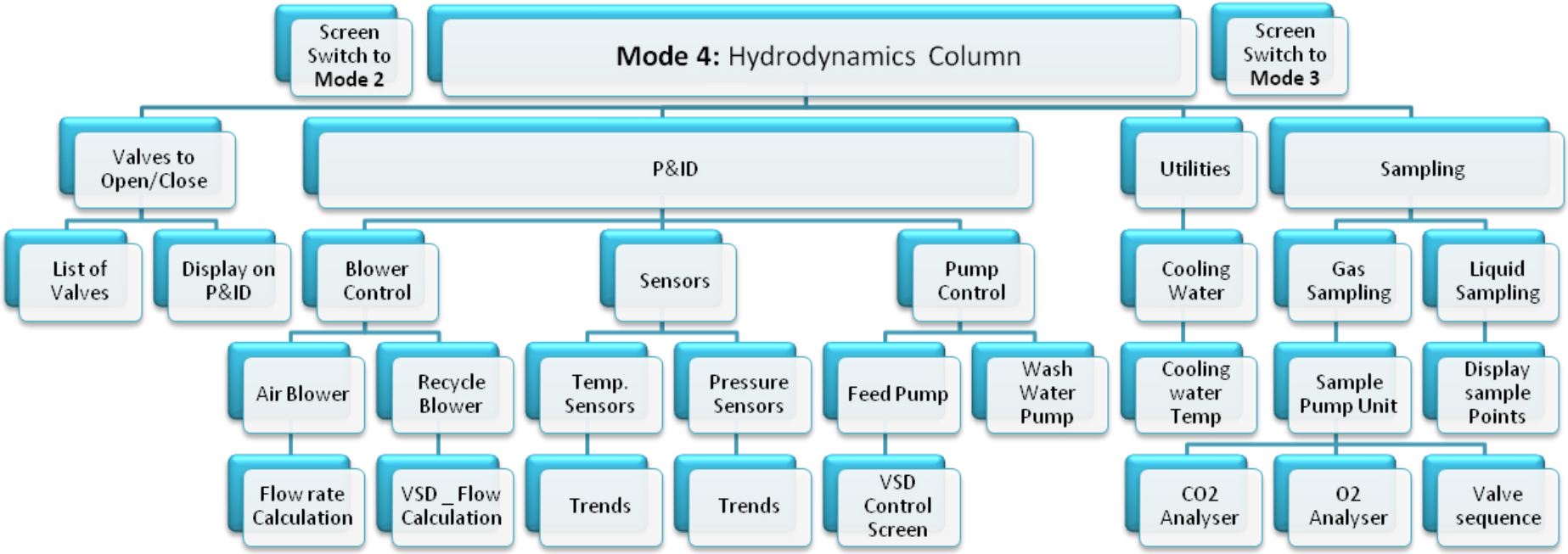

FIGURE 36 BLOCK DIAGRAM FOR CONTROL STRUCTURE OF MODE 4

5.3. HUMAN-MACHINE-INTERFACE (HMI)

This section gives examples of some of the screens in the human-machine-interface (HMI) program. The full collection of screens along with a discussion on each can be found in the operating manual for the pilot plant setup. Reference will also be made to sub-screens that are used to manipulate control valves and the variable speed drives (VSD) installed on some of the pumps.

5.3.1. ABSORPTION SECTION OF MODE 1

The absorption section is discussed as an example to how the HMI program was set up. The screens considered include the main screen for the absorption section of Mode 1 and screens for operating the blower units, showing the column temperature profiles and gas sampling process.

5.3.1.1. MAIN SCREEN FOR THE ABSORPTION PROCESS

Figure 37 shows the main screen for the absorption section of the post combustion CO_2 capture process. Navigation from this screen to screens giving a more detailed view on specific process equipment can be carried out by using the buttons on the right-hand side of the screen. Access to the Mode Menu (**Figure 29**) or to the stripping section can also be obtained from this screen.

Furthermore, the pumps and blowers can be started or stopped from this screen by pressing the red button above or below the corresponding pump or blower unit. The button will turn green once the pump is running in order to indicate its state (GREEN – Running, RED – Not running). Access to the control screens of the control valves appearing on screen can be obtained by touching on the particular control valve. A sub-screen will pop up where the valve position can be adjusted.

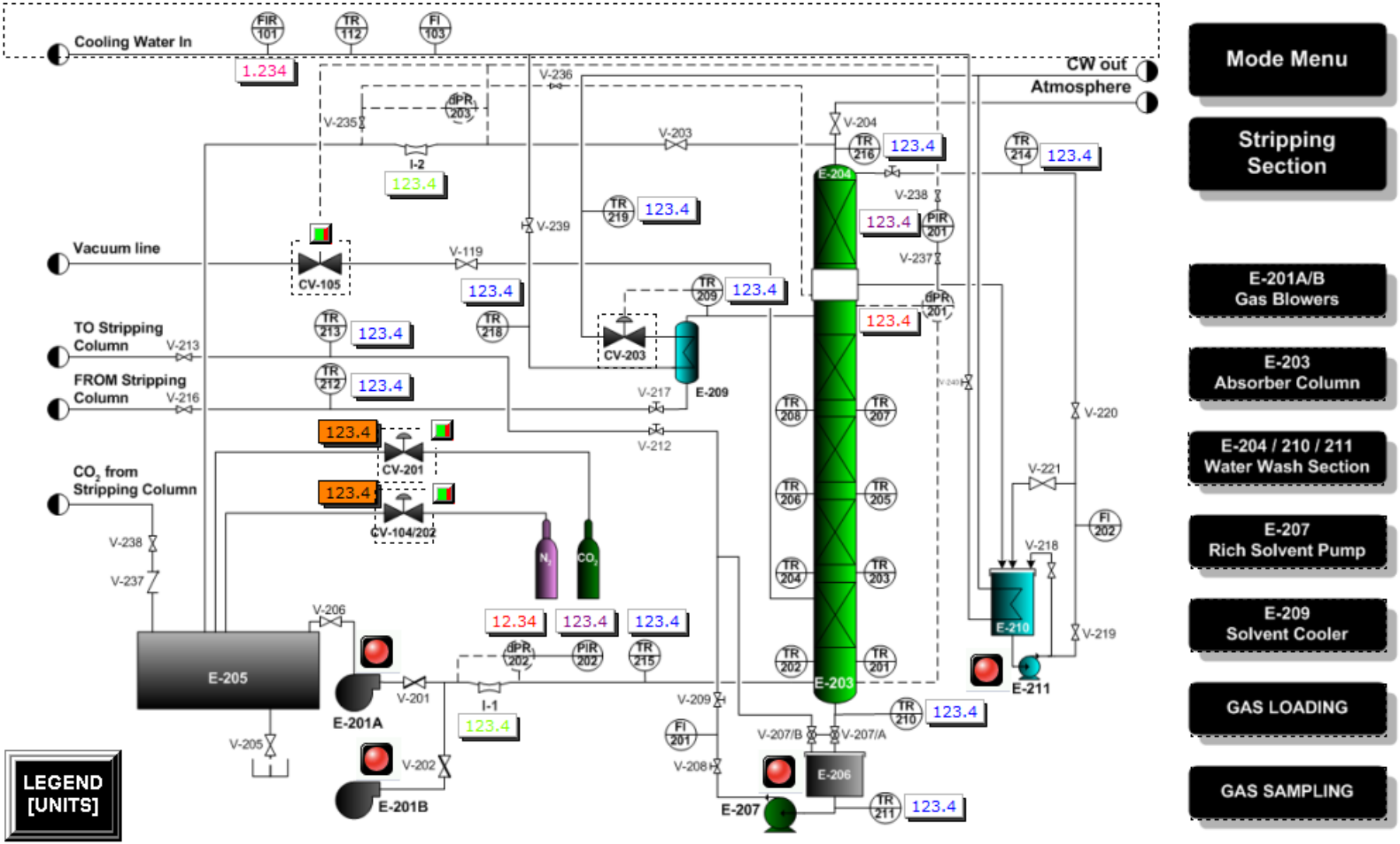

FIGURE 37MAIN SCREEN FOR ABSORPTION SECTION

5.3.1.2. ABSORBER COLUMN TEMPERATURE PROFILES

Figure 38 shows the temperature profile trends for the gas- and the liquid phases in the absorber column (bottom trend). The trend given at the top of the screen gives an indication of the temperature of the feed gas at the bottom of the column (TR-215) and at the top of the column (TR-216). The legends to the various temperatures displayed in the trends can be seen in the coloured blocks below and above the respective trends.

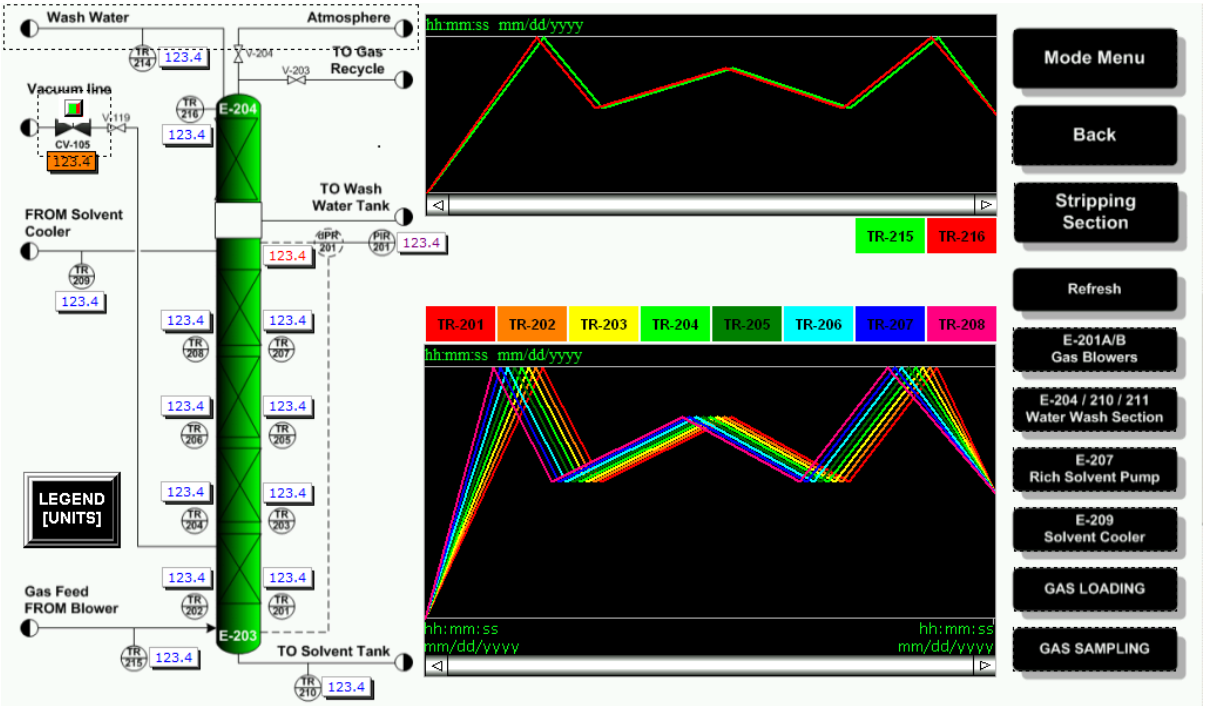

FIGURE 38 TEMPERATURE PROFILES FOR THE ABSORBER COLUMN

A screen displaying the temperature profile trends for the stripping column is also included in the HMI program, but will not be included here. Further trends regarding the gas compositions, gas flow rates and column pressures are also included in the HMI program but will not be discussed in full.

5.3.1.3. GAS BLOWER UNITS

Two gas blowers are available for feeding the bottom of the absorber column. E-201A is a recycle blower that is used to recycle gas from the top of the absorber column, feeding it again from the bottom. E-201B is an air blower unit that can be used whenever airflow is required in the column. **Figure 39** shows the screen for operating the gas blowers.

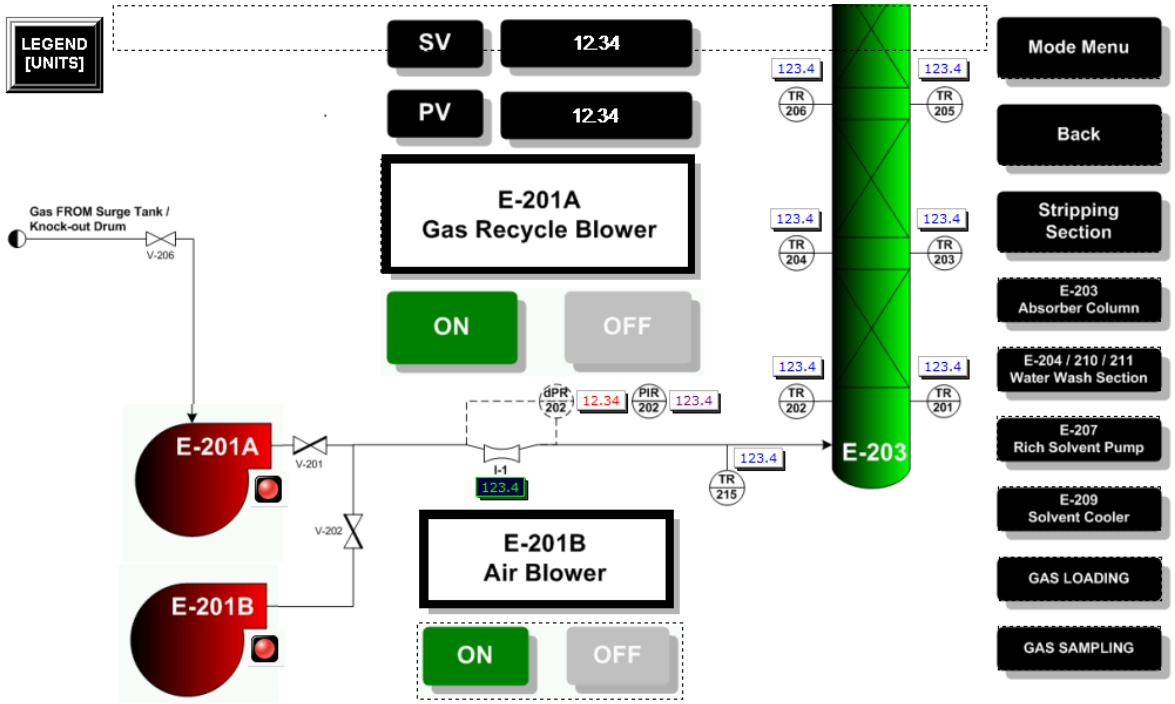

FIGURE 39 PROCESS SCREEN FOR OPERATING THE GAS BLOWER UNITS

E-201A is connected to a variable speed drive (VSD) that allows the user to set the speed of the blower in order to obtain the required mass flow rate of the gas. The mass flow rate of the gas is displayed below the venturi tube (I-1). Details regarding the calculation of the mass flow rate measured by the venturi tubes are given in the Appendix A.

Figure 40 shows the control screen for the variable speed drive of the blower unit. The current drawn by the blower motor, as well as gas temperature, set- and present values are displayed on the screen. The setpoint can be adjusted between 5 and 50 Hz to get mass flow rates within an approximate range of 60 – 1000 kg/h.

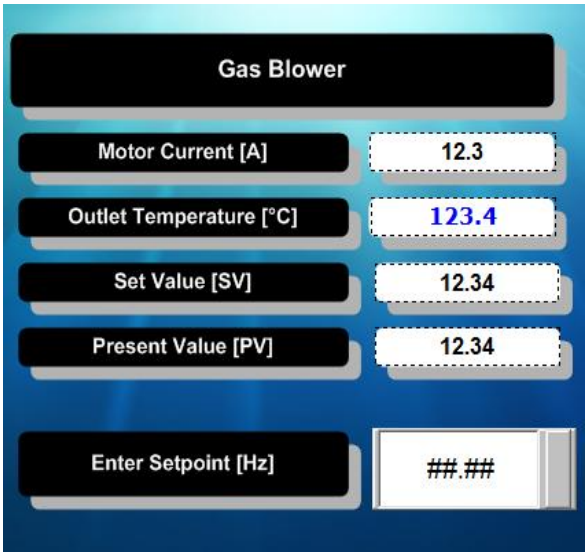

FIGURE 40 CONTROL SCREEN FOR VSD ON BLOWER

5.3.1.4. GAS SAMPLING AND ANALYSIS

Gas samples are drawn from the closed gas loop with a sample pump (E-213). The sample pump can be switched on by pressing the ON button in the screen shown in **Figure 42**. A GREEN light below the sample pump will indicate that it is running. The gas sampling system was set up to allow automated sampling from two different locations in the column. V-225A and V-225B are set up on an alternating timer switch, allowing gas samples from two different locations to be sent alternatively to the online compositions analysers. Both a CO_2 and an O_2 analyser are installed for online gas composition analysis.

The time interval before the valves V-225A and V-225B switch can be set by the pilot plant operator(See **Figure 41**). The time must however be long enough to allow proper stabilization of the gas composition. Enough time should also be allowed for dead volume in the sample tubes to pass through. More information regarding the time required to achieve this is given in Chapter 7.

Valve switching is initiated by the operator pressing the ON button below the valves in **Figure 42**. The valves on screen will flash green and red as they switch between open and closed. The lines indicating the locations from where in the absorber column samples can be drawn are also shown.

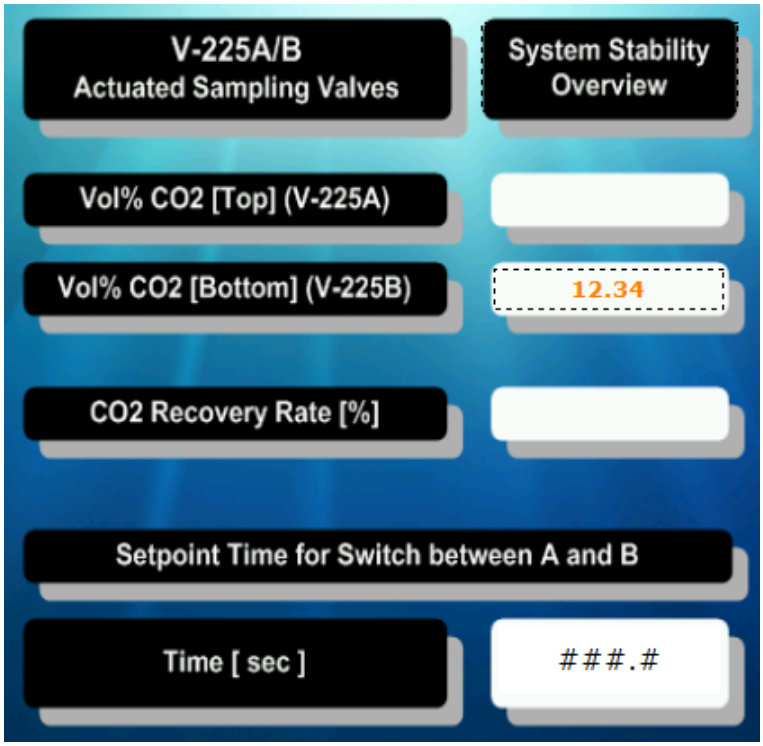

FIGURE 41 TIME INTERVAL FOR VALVE SWITCH

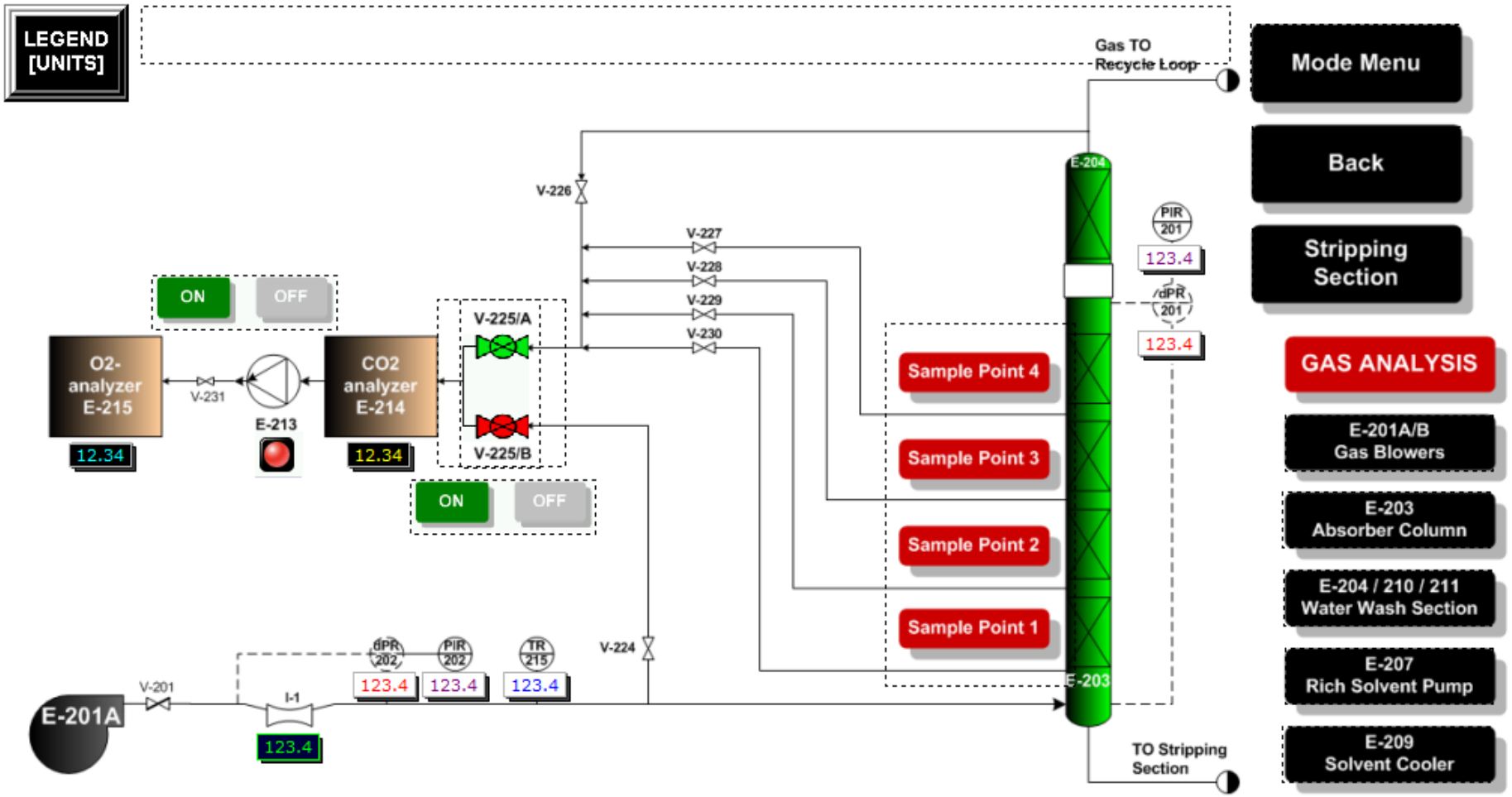

FIGURE 42 PROCESS SCREAN FOR GAS SAMPLING FROM THE ABSORBER COLUMN

5.3.2. STRIPPING SECTION OF MODE 1

The stripping section is discussed mainly to give an example of how the control valves are operated. Specific reference is made to the steam valve supplying the reboiler unit with steam for solvent regeneration.

5.3.2.1. MAIN SCREEN FOR THE STRIPPING SECTION

The main process screen for the stripping section of the CO_2 Capture pilot plant is shown in **Figure 44**. The pumps in this screen can be started and stopped by pressing the red start buttons. RED indicates that the pump is not running, GREEN indicates that the pumps are running. The control valves can also be adjusted from this screen by touching within the dotted area around the valves. Further navigation to a more detailed view of each section within the stripping section can be achieved with the buttons on the right.

5.3.2.2. STEAM REBOILER UNIT

Steam is used for heat addition to the process via CV-101. The steam is fed to the reboiler unit where the solvent is heated for regeneration. The sub-screen for CV-101 can be seen in **Figure 43**. The setpoint of the valve position can be adjusted between 0 – 100.0 %.

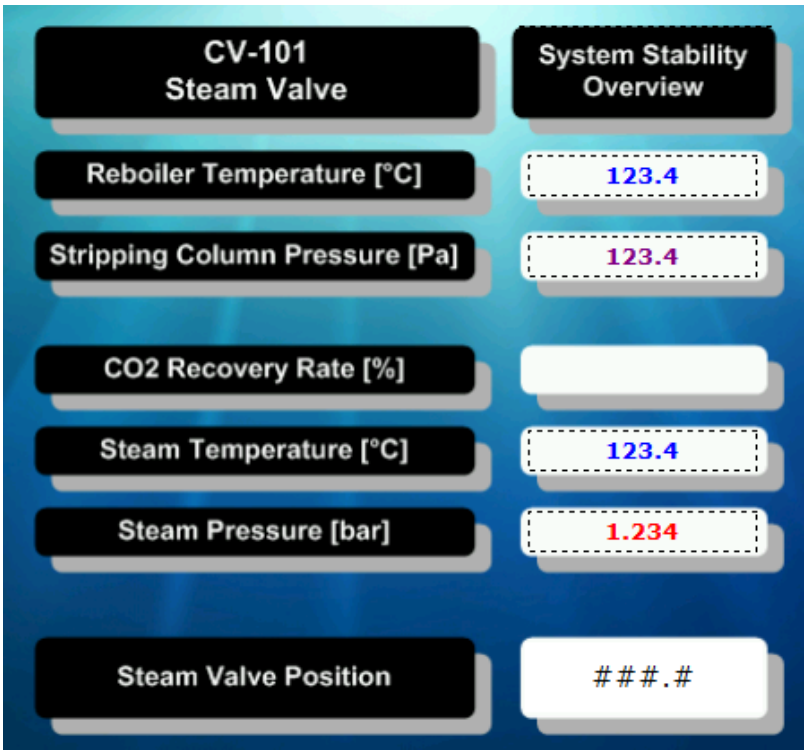

FIGURE 43 CV-101 SETPOINT ADJUSTMENT BETWEEN 0 - 100%

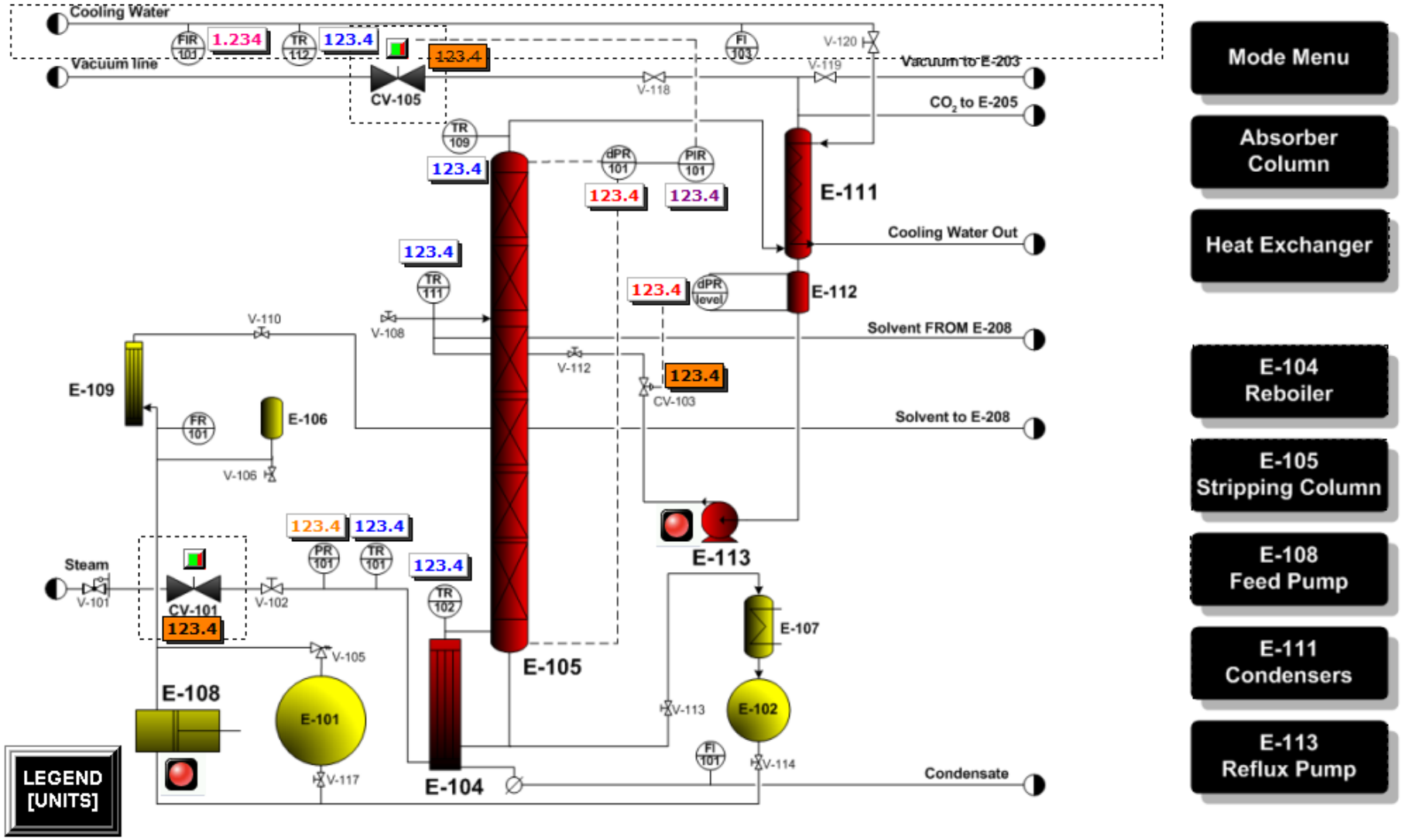

FIGURE 44MAIN SCREEN FOR THE STRIPPING SECTION OF THE CO_2 CAPTURE PLANT

5.4. HAZOP, SAFETY ALARMS- AND SYSTEM INTERLOCK SETUP

A hazard and operability study (HAZOP) was performed before setting up the final control structure for operating the pilot plant. From the HAZOP potential hazards were identified and addressed by implementing a list of alarms and interlocks into the control structure of the pilot plant setup.

5.4.1. HAZOP

The HAZOP study was performed based on the baselines provided by (Turton et al., 2009). All process equipment units used in the pilot plant setup were considered in the study. All the gas and liquid lines feeding to and carrying effluent from the particular process vessels were also included.

The main deviations considered include flow, pressure and temperature. Possible hazardous scenarios were constructed by considering the keywords NO, LESS and MORE of each one of the deviations. The consequences of each one of the deviations were tabulated along with the particular control action that allows safe operation of the pilot plant even when hazardous conditions arise. The HAZOP tables appear in Appendix A.

5.4.2. SYSTEM ALARM SETUP

All system alarms were set up in order to allow the user to specify the alarm setpoint. The user is however limited to enter setpoints within safe operating boundaries. Alarms include the following:

- Temperature HIGH alarms (TAH)
- Pressure HIGH alarms (PAH)
- LOW flow alarms (FAL)
- CO_2 concentration HIGH alarm (CAH)
- O_2 concentration LOW alarm (CAL)

All alarms scroll across the top of the touch panel screen; the alarm screen pops up on the touch panel as soon as any alarm is triggered. The siren can be silenced by acknowledging the particular alarm. All alarms included in the control structure of the pilot plant can be seen in the HAZOP tables in Appendix A.

5.4.3. SYSTEM INTERLOCKS

Some hazardous conditions are out of bounds for continuing to operate the pilot plant setup safely. These conditions were also identified in the HAZOP study and system interlocks were included in the control structure. The user is once again allowed to specify interlocking setpoints for various critical alarm conditions.

All pumps and control valves are automatically interlocked with the critical alarm conditions, protecting both the process equipment as well as the operator against the particular hazardous condition. Once an interlock has been activated, the control structure limits the operator from restarting until all conditions are favourable again for safe operation. The user can then reset all pumps and control valves allowing pilot plant start-up.

The interlocks included in the control structure of the pilot plant can be seen in the HAZOP tables in Appendix A.

5.5. DATA ACQUISITION

Data capturing from the pilot plant setups is done by recording gathered data to a flash drive inserted at the back of the touch panel screen. Data is recorded in CSV-format and can be opened using Microsoft Excel. Twelve different files are generated in an HMI folder on the flash drive. These files have sensor data from different data registries, recorded every second and logged against time and date. The files can be combined into a single spread sheet that will allow an overview of all generated data recorded during a run. The number of sample points to be recorded was set to be 43 200 (10 hours). The number of data points to be recorded can however be adjusted by changing the history buffer setup in the HMI program.

Table 9 gives a summary of all files generated on the flash drive and the data each file contains. The PLC number indicates from which one of the three installed PLC units the data is logged. A summary of all PLC data registers used for storage of various data can be seen in the operating manual of the pilot plant setup. All data registries for storing alarm setpoints, calibration offsets, scaling factors and process parameters are also included in this particular list in the operating manual. The data registry in **Table 9** gives the starting registry for data logging, while the data length indicates the amount of registries recorded in a particular file. Thus, the file 200TEMP.CSV will contain data from 15 different temperature sensors, recorded in the registries ranging from D201 to D215.

TABLE 9 HISTORY BUFFER SETUP FOR DATA GATHERING - FROM HMI PROGRAM

Number	File Name	Description	PLC #	Data Registry	Data Length
1	200TEMP	Logging Temperatures of the Absorber column and AREA 200	2	D201	15
2	100TEMP	Logging Temperatures of the Stripping Column and AREA 100	1	D101	16
3	CO2O2PR3	Logging CO_2/O_2 concentrations and PR-301 (Steam Pressure – Mode 3)	2	D2214	16
4	300PRESS	Logging PIR-101 and dPR-201	3	D101	2
5	200PRESS	Logging PIR201/202; dPR202/203	2	D2201	4
6	100PRESS	Logging FIR101, dPR101/2, PR101	1	D130	14
7	GasMFRs	Logging Gas Flow Rate, Venturi I-1/2	2	D6102	2
8	TR218	Logging TR-218 and TR-219	2	D216	4
9	300TEMP	Logging Total Reflux Column Temperatures and AREA 300	3	D301	7
10	CVALVES	Logging the OUTPUTS from Control Valves	1	D201	14
11	PARAMTRS	Logging Process Parameters – User input. Alternation Sequence, V-225	1	D225	16
12	TR214	Logging Temperature TR-214	2	D115	3

5.6. PILOT PLANT COMMISSIONING

The commissioning of the pilot plant was done in various steps, considering the liquid- and gas recycle loops as well as the steam commissioning. The steps followed are listed below.

1. Liquid circulation – Water was used
2. Gas Recycle Loop Commissioning
3. Steam Commissioning with Water

5.6.1. COMMISSIONING THE LIQUID CYCLE

The liquid cycle was commissioned with water, testing for any leakages and determining how to balance the flows provided by the two different liquid pump units (E-108 and E-207).

The water was pumped from the bottom of the absorber column to the top of the stripping column while simultaneously pumping liquid from the bottom of the stripping column to the top of the absorber column. All leakages were fixed and this gave preliminary information on how the liquid flow rates from the various sections (absorption and desorption) could be balanced during the experimental runs.

5.6.2. COMMISSIONING THE GAS RECYCLE LOOP

The commissioning of the gas recycle loop was divided into various phases. The different phases are summarized below and detailed information and results on the various phases of commissioning can be found in Appendix B.

5.6.2.1. PHASES OF GAS RECYCLE LOOP COMMISSIONING

The main purpose of the gas recycle loop is to limit the amount of CO_2 and N_2 that needs to be added to air in order to simulate process gas that is similar to exhaust gases from power plants. The recycle loop commissioning was thus aimed at determining the amount of CO_2 and N_2 that would be required, by investigating the following:

- Online gas analysers and gas sampling method;
- Time required for gas loading;
- Gas leakage rates into and from the recycle loop;
- Gas loading sequence;
- Effect of gas flow rate on the gas leakage

In order to thoroughly investigate all of the above mentioned process dependent variables, the commissioning were done in four different phases listed below.

Phase 1

Testing of the online gas analysers and gas sampling method with a secondary aim of investigating the gas leakage rates from the system;

Phase 2

Investigation of the optimal sequence for loading the nitrogen (N_2) and the carbon dioxide (CO_2) into the gas recycle loop. The effect of the mass flow rate of the gas on the leakage rates from and into the recycle loop was also investigated.

Phase 3

Preliminary quantification of the leakage rates of CO_2 from and O_2 into the system in terms of volume % per hour. The recycle loop was loaded to obtain concentrations that will typically be used in experimental runs.

Phase 4

Adding fresh CO_2 to the gas recycle loop in order to obtain a constant CO_2 concentration in the process gas.

5.6.2.2. MAIN OUTCOMES FROM GAS CYCLE COMMISSIONING

- The gas sampling method and online CO_2/O_2 analysers worked well. The automated gas sample valves enabled for sampling from different locations in the absorber column and dead volumes in sample tubes did not affect the samples for more than 30 seconds.
- Gas loading should be done by first loading N_2 in order to reduce the O_2 concentration to below 6 volume %. Hereafter the CO_2 can be loaded to the process gas. This reduces the amounts of gas lost from the system.
- The leakage rates of O_2 into the system and CO_2 from the system are directly proportional to the blower speed and thus the process gas flow rate.
- The CO_2 concentration of the process gas can be controlled reasonably well by continuously adding fresh CO_2 to the system.

More detail and results regarding the various phases of gas cycle commissioning are shown in Appendix B.

5.6.3. STEAM COMMISSIONING

The steam commissioning of the pilot plant was also subdivided into various phases. The main goal of each phase will be stated and the main outcomes from the entire steam commissioning process will be given. Detailed information and results on the steam commissioning is given in Appendix B.

5.6.3.1. VARIOUS PHASES OF STEAM COMMISSIONING

Commissioning of the steam supply to the thermosyphon reboiler of the pilot plant was performed using only water in the system. The commissioning was performed in five different phases. The main aims of each phase are summarised below.

Phase 1

The first phase of the steam commissioning was performed in order to investigate the heating effect of the boiling liquid in the thermosyphon reboiler on the rest of the stripping column. The heating and cooling capabilities of the cross heat exchanger (E-208) and the solvent cooler unit (E-209) were also investigated by considering the temperature profiles of the streams entering and exiting the mentioned pieces of equipment.

Phase 2

Phase two of the steam commissioning process was aimed at allowing the system to reach thermal equilibrium while continuously feeding steam to the reboiler. Energy balances for the cross-flow heat exchanger and the solvent cooler were performed at the assumed steady state conditions. The effect of the liquid temperature on the process gas temperature was also investigated as well as the direct cooling effect of circulating the wash water through the water wash section.

Phase 3

This phase was aimed at performing various energy balances over the cross-flow heat exchanger, solvent cooler and the stripping column. This was done in order to estimate the heat loss from the system to the environment. An overall balance for the entire process setup with the exclusion of the absorber column was performed in order to check the % error involved in performing the mass balance.

Phases 4 & 5

Phases 4 and 5 were aimed at performing energy balances with more accurate results by using better ways of determining the mass flow rates of the liquid steams.

5.6.3.2. MAIN OUTCOMES FROM STEAM COMMISSIONING

- The heating and cooling capabilities of the cross-flow heat exchanger and the solvent cooler units are sufficient to allow the system to reach a steady state at reasonable absorber feed temperatures.
- Energy balances over the process equipment can be performed with fair success – predicting energy loss from various process equipment units. An overall energy balance is used in order to verify the calculated heat losses from the system. The overall heat loss from the entire system is estimated to be in the order of between 9 and 10 kW.
- It was found that back-flow into the reflux line was quite significant. Feed from the bottom of the absorber column favoured flowing back into the reflux line rather than to the top of the stripping column. This problem was solved by installing a non-return valve in the reflux line.

The details and results showing the various temperature trends and results from the energy balances that were performed can be seen in Appendix B.

CHAPTER 6

ASPEN PLUS® SIMULATIONS OF THE CAPTURE PROCESS

6.1. PROCESS SIMULATION

6.1.1. PREVIOUS WORK ON SIMULATING THE PROCESS

In a state of the art review Wang et al. (2010), mentioned various authors that have used simulations in order to approach the problem of reducing the energy requirement of the process is. Freguia and Rochelle (2004) made use of the multistage separation model in Aspen Plus® - RateFrac – to simulate the absorber and stripping units. Some of the operating parameters that were investigated include solvent circulation rate, the pressure of the stripping unit as well as inter-stage cooling on the absorber column. In this particular study a reduction of 3.8 % in the reboiler energy requirement, was obtained. Zhang et al. (2009) used Aspen RateSep™ in order to perform a simulation study showing the superiority of using rate based simulations as opposed to the simpler equilibrium stage modelling. Results from the simulation were compared with good success to pilot plant data obtained from a CO_2 capture unit installed at the University of Texas in Austin. The simulation provided accurate predictions of temperature profiles, CO_2 loading and CO_2 removal rates reported in the pilot plant data. Dugas et al. (2009) also set up a simulation for the absorber column using RateSep™ in Aspen Plus® and used pilot plant data from the CASTOR project for validating the model. Predictions of the gas phase temperature and the CO_2 concentration profiles compared well to the pilot plant data.

Other authors have developed and proposed the use of mathematical modelling to set up a dynamic model for the capturing process (Tobiesen et al., 2007), (Lawal et al., 2009). These models take into account fluid hydrodynamics in the column, the mass transfer resistances of liquid- and gas phases as well as the reaction kinetics (Wang et al., 2010).

For the purpose of this study, however, the main focus was on the simulation of steady state conditions and process parameter optimisation. The effect of various column internals on the CO_2 capture process was to be investigated. The results from the simulation were to be used for comparison to results from the established CO_2 capture pilot plant.

6.1.2. MODELLING CO_2 CAPTURE WITH MONO-ETHANOLAMINE USING ASPEN PLUS®

6.1.2.1. METHOD DEVELOPMENT FOR THE ASPEN PLUS® SIMULATION

Wang et al.(2010) refer to numerous modelling studies (Dugas et al., 2009; Freguia and Rochelle, 2004; Lawal et al., 2009; Zhang et al., 2009), and states that these studies were performed by experts in process modelling. Based on this, a concern regarding the simplification of the modelling process for the use the ordinary practicing engineer was stated.

In this study the Aspen Plus® modelling of the CO_2capture process was based on a combination of work published by previous authors. This was done in order to find a way of simplifying the method of simulating the CO_2 capture process. In this section, the methodology of simulating the CO_2 capture process is detailed. Validation results of the simulation are presented in Section 6.2.

FLOWSHEET DECOMPOSITION

Work by Alie et al. (2005) proposed the use of a flowsheet decomposition method in order to simplify the simulation process. A two-step approach to the simulation is recommended. In the first step a stand-alone absorber column is simulated with the solvent and gas inlet conditions of the particular case study. In the second step of the simulating process, a stand-alone stripping column is simulated using the outlet conditions from simulating the absorber column. The RateFrac unit operating model in Aspen Plus® was used for modelling the absorber and stripping columns. An overall conclusion was made that the decomposition method serves as a useful way by which the entire integrated flowsheet could be modelled.

SIMULATING THE ENTIRE PROCESS WITH A TEAR STREAM

Modelling by Freguia and Rochelle (2004) was also performed using the RateFrac operating model in Aspen Plus®. However, the entire flowsheet of the capture process was simulated in a single simulation. The simulation was set up with a tear stream (simulated as an open system as opposed to closing the solvent circulation loop) on the lean MEA feed to the absorber column, allowing the user to specify the inlet conditions of the absorber column as the input to the model. Simulating the process with a tear stream will provide relatively good results, but does not guarantee model convergence when the solvent circulation loop is closed.

SIMULATION METHOD BASED ON COMBINATION OF PREVIOUS WORK

The simulation method for this study was based on a combination of the decomposition method by Alie et al.(2005) and the modelling performed by Freguia and Rochelle (2004). This method

makes use of flowsheet decomposition to deal with convergence problems that is usually related to incorrect specification of the inputs into to the simulation. The decomposed flowsheets are then combined to allow one to simulate the CO_2 capture process with a closed solvent circulation loop. This method of approach to simulate the CO_2 capture process has not been used before and greatly simplifies the simulation process. The method is described in two parts: Part A, which refers to the flowsheet decomposition and Part B, referring to simulating the entire flowsheet with a closed solvent loop.

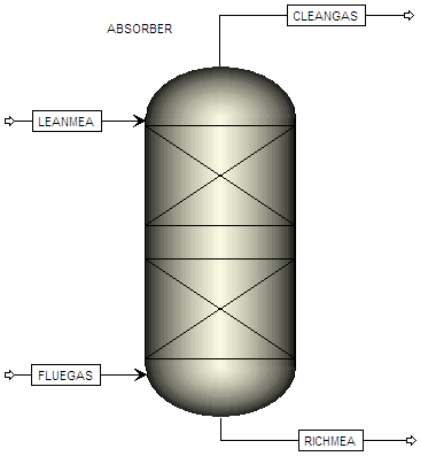

FIGURE 45 STAND-ALONE ABSORBER COLUMN USING ASPEN PLUS®

Simulation method, Part A can be summarised as follows:

- Simulating a stand-alone packed absorber column. Aspen Plus® Rate-based simulation was used for this. See **Figure 45** showing the absorber block.
- In the second step the stripping column was simulated, combining it with the rich-lean heat exchanger and the MEA cooler units. A Radfrac column and a rate-based calculation method were used for simulating the stripping column. A stripping column with a reboiler and no condenser was used for the simulation. Water vapour leaving the top of the stripping column was condensed and separated from the CO_2 in a separate unit, and combined with the lean MEA leaving the bottom of the stripping column: see **Figure 46**.
- The initial simulation of the absorber column was performed with a 30 wt% aqueous MEA solution. The solvent outlet conditions (RICHMEA stream) generated by the simulation were then transferred to the inlet conditions for simulating the stripping column. The results from the stripping column simulation report the lean MEA composition. This was put back into the simulation for the stand-alone absorber column, and this iterative process was followed until the convergence between consecutive iterations was acceptable. Satisfactory convergence was obtained after three iterations.

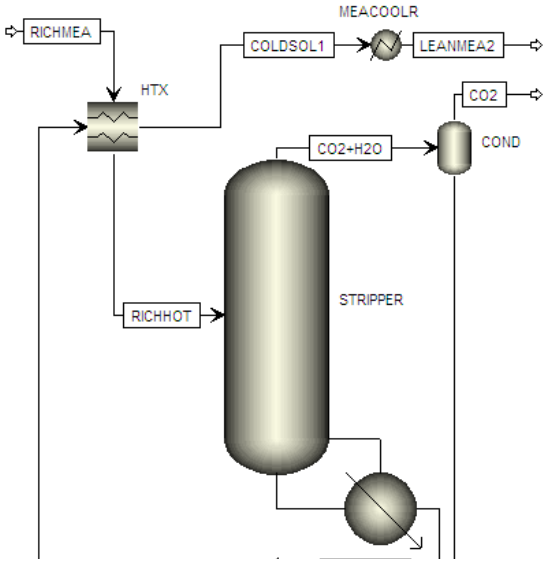

FIGURE 46 SIMULATING STRIPPING COLUMN USING ASPEN PLUS®

Part B of the simulation method involves simulating the entire flowsheet for the CO_2 capture process. Part A of the method deals with most of the convergence problems while part B is focussed on simulating the entire CO_2 capture process by combining the different sections of the simulation.

- The stand-alone absorber column was added to the simulation sheet of the stripping column.
- The lean MEA stream leaving the stripping column was combined with a water make-up stream and replaces the one entering the absorber.
- The simulation was run once with a tear in the RICHMEA stream leaving the bottom of the absorber column.
- Hereafter, the stream entering the heat exchanger was replaced by the one leaving the bottom of the absorber column.
- As the simulation is sensitive to the initial conditions used, it is important that these initial conditions do not deviate too far from the original simulation. With this constraint, it is possible to obtain convergence for the closed solvent loop system.

Figure 47 shows the flowsheet for simulating the CO_2 capture process in Aspen Plus® with a closed solvent loop.

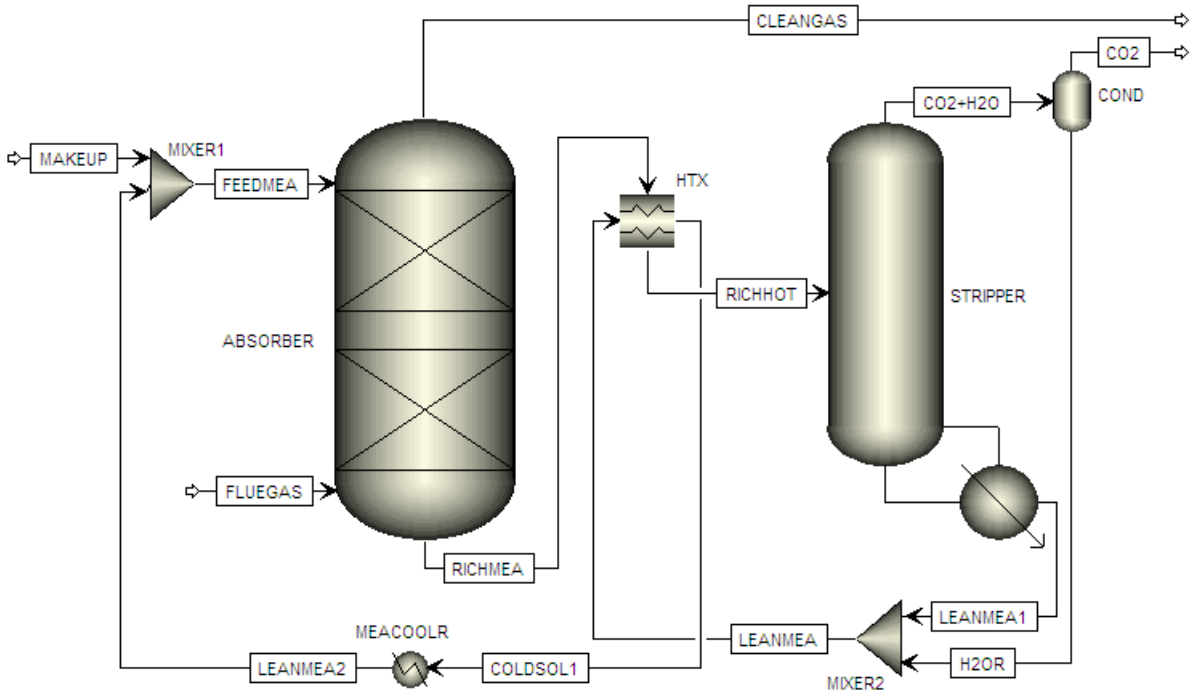

FIGURE 47 FLOWSHEET CREATED IN ASPEN PLUS® FOR SIMULATING THE ENTIRE CAPTURING PROCESS

6.1.2.2. REACTION KINETICS AND THERMODYNAMIC MODEL USED FOR SIMULATING THE PROCESS

Previous studies by Zhang et al. (2009) proved the superiority of using rate-based simulations as opposed to the simpler equilibrium stage modelling. Thus, for the purposes of this study, the focus was on rate-based modelling. The equilibrium reactions (1) – (5) below, were however also included into the model for both the absorber and the stripping columns. In previous studies (Freguia and Rochelle, 2004), only the reaction kinetics of the reactions involving CO_2 were used to described the rate of absorption in the Aspen Plus® model. However, for the stripping column all reactions were set to equilibrium due to the high operating temperature of this column.

The reaction mechanism of CO_2 with MEA in an aqueous solution is given by reactions (1) – (5) (Austgen et al., 1989; Freguia and Rochelle, 2004).

Reaction for ionization of water:

$$2H_2O \leftrightarrow H_3O^+ + OH^- \quad \text{...(Reaction 1)}$$

Reaction representing the dissociation of carbon dioxide:

$$2\,H_2O + \mathbf{CO_2} \leftrightarrow H_3O^+ + HCO_3^- \quad \text{...(Reaction 2)}$$

Bicarbonate dissociation reaction:

$$H_2O + HCO_3^- \leftrightarrow H_3O^+ + CO_3^{2-} \quad \text{...(Reaction 3)}$$

Dissociation of the protonated amine:

$$H_2O + MEAH^+ \leftrightarrow H_3O^+ + \mathbf{MEA} \quad \text{...(Reaction 4)}$$

Bicarbonate formation due to carbamate reversion reaction:

$$H_2O + MEACOO^- \leftrightarrow \mathbf{MEA} + HCO_3^- \quad \text{...(Reaction 5)}$$

Reactions involving both the reactants MEA (monoethanolamine) and CO_2 (carbon dioxide) are given by Reactions (6) and (7).

$$MEA + CO_2 + H_2O \leftrightarrow MEACOO^- + H_3O^+ \quad \text{... Reaction (6)}$$

$$MEA + CO_2 + H_2O \leftrightarrow MEAH^+ + HCO_3^- \quad \text{... Reaction (7)}$$

The equilibrium constants (K_1 – K_5) for the reactions (1) – (5) are temperature dependent. The temperature dependence can be described by Equation (1) and the values of the constants A, B, C and D (along with their references) are given in **Table 10**.

$$lnK_i = A + \frac{B}{T} + ClnT + DT \qquad \text{... Equation (1)}$$

TABLE 10: VALUES OF THE CONSTANTS FROM EQUATION (1)

Equilibrium Constant	A	B	C	D	Temperature Range [K]	Reference
K_1	132.89	-13 445.9	-22.47	0	273 – 498	(Edwards et al., 1978)
K_2	231.46	-12 092.1	-36.78	0	273 – 498	(Edwards et al., 1978)
K_3	216.05	-12 431.7	-35.48	0	273 – 498	(Edwards et al., 1978)
K_4	-3.04	-7 008.3	0	-0.00313	298 -413	(Freguia and Rochelle, 2004)
K_5	-0.52	-2545.53	0	0	298 -413	(Freguia and Rochelle, 2004)

The kinetic reactions that were considered include Reactions (6) and (7). Both these reactions are reversible reactions involving the main reactants, CO_2 and MEA(Freguia and Rochelle, 2004).

Both these reactions are governed by second order rate expressions with temperature dependent rate constants (Freguia and Rochelle, 2004). In work done by Fashami et al.(2007) at the University of Texas in Austin the kinetic expressions for Reactions (6) and (7) were determined. The subscripts "a" and "b" refer to the forward and backward reactions respectively. Equation (2) gives the kinetic expression as it is defined in Aspen Plus®. **Table 11** gives the kinetic parameters as reported by Fashami et al.(2007).

$$r = k \left(\frac{T}{T_0}\right)^n exp\left(-\frac{E}{R}\left(\frac{1}{T} - \frac{1}{T_0}\right)\right) \qquad \text{... Equation (2)}$$

TABLE 11: REACTION KINETIC PARAMETERS FOR REACTIONS (6) AND (7)

Parameter	k	n	E [kJ/kmol]	T_0 [K]
Reaction (6a)	6.0×10^{7}	0.00	2.2×10^{4}	298
Reaction (6b)	8.8×10^{11}	36.8	-5.7×10^{4}	298
Reaction (7a)	1.6×10^{4}	0.00	4.8×10^{4}	298
Reaction (7b)	8.0×10^{-4}	36.8	5.7×10^{3}	298

The Electrolyte-NRTL model was used to describe the thermodynamics and predict the mixed solvent properties of the CO_2-water-monoethanolamine system. Austgen et al.(1989) developed the model and found the predicted results to be in good agreement with the available experimental results. Other authors (Fashami et al., 2007; Freguia and Rochelle, 2004; Zhang et al., 2009) also used the proposed thermodynamic model for their Aspen Plus® simulation studies.

6.1.2.3. DESIGN SPECIFICATIONS USED IN THE SIMULATION

In both the studies mentioned in the two previous sections, the authors made use of an Aspen Plus® Design Specification. A Design Specification can be used when one or more parameters influence the results obtained for another. The one parameter can then be varied within a certain range in order to obtain a desired result in the other parameter. The flow rate of the lean MEA fed to the top of the absorber column was varied in previous studies in order to obtain the desired CO_2 capture efficiency. In setting up this simulation the design specification function in Aspen Plus® was used in three different ways.

VARYING FLUE GAS FLOW RATE

In simulating the standalone absorber column a design specification is imposed on the CO_2 mole fraction of the treated gas stream leaving the top of the column. The CO_2 molar flow in the treated gas stream was set to be only 10% of the CO_2 fed to the bottom of the absorber. This implicates a CO_2 capture efficiency of 90%. The specification is achieved by keeping the solvent flow rate constant and varying the mass flow rate of the flue gas that is fed to the bottom of the absorber column.

After combining the flowsheets for the stripping and the absorption sections the flue gas flow rate was again varied in order to optimise the liquid-to-gas mass flow ratio (L/G-ratio) in the absorber column. The optimisation was performed with regards to the reboiler duty required for sufficient solvent regeneration.

MAKE-UP WATER REQUIREMENT

Once the flowsheets of the stripping- and absorption sections were combined, provision was to be made for water that leaves the system with the CO_2 stream from the top of the stripping column. Make-up water was added to the solvent prior to feeding it to the top of the absorber column. A design specification was set up that calculates the amount of water to be added in order to keep constant the mass flow rate of the solvent fed to the column.

CO_2 CAPTURE RATE

After combining the flowsheets for the stripping- and absorption section, and implementing the solvent recycle loop, a design specification for the CO_2 capture efficiency was set up. This was done by specifying the mole fraction of the CO_2 in the stream leaving the top of the absorber column. The relationship between the mole fraction of CO_2 in this stream ($CO_{2\ mole\ \%\ OUT}$) and the overall CO_2 capture efficiency (α) is given by Equation (3).

$$CO_{2\ mole\ \%\ OUT} = \frac{CO_{2\ mole\ \%\ [IN]} \times (1-\alpha)}{1-\ \alpha \times CO_{2\ mole\ \%\ IN}} \quad \text{...Equation (3)}$$

Seeing that the CO_2 inlet concentration of the flue gas ($CO_{2\ mole\ \%\ [IN]}$) was kept constant for the purpose of the simulation, this relationship can easily be used in order to set up the design specification for the overall CO_2 capture efficiency. Rearranging the equation given in Equation (3) gives the following expression for the CO_2 capture efficiency.

$$\boldsymbol{\alpha = \frac{CO_{2\ vol\ \%\ [IN]} - CO_{2\ vol\ \%\ OUT}}{CO_{2\ vol\ \%\ [IN]} \times\ 1 - CO_{2\ vol\ \%\ OUT}} \times 100} \quad \text{...Equation (4)}$$

When considering the entire capture process, the relationship between the CO_2 capture efficiency and the reboiler duty required for solvent regeneration became apparent. The method of simulation proposed here utilizes this relationship. The design specification was thus set up to achieve the desired CO_2 capture efficiency by varying the reboiler duty of the stripping column.

From understanding and utilizing the relationship between the CO_2 capture efficiency and the stripping columns reboiler duty, the simulation method show potential for further process optimization.

6.1.2.4. PARAMETER OPTIMIZATION

The user input values for various process parameters were one of the keys to obtaining good convergence in process simulations. Literature served as a good source for obtaining realistic starting point values, and was used when simulating the standalone absorber and stripping columns. However, when combining these flowsheets, optimised parameters for the specific flowsheet lead to an increased possibility of simulation convergence.

LEAN LOADING OPTIMISATION

The term loading refers to the molar amount of CO_2 per moles of MEA present in the solvent. The lean loading thus refers to the amount of CO_2 that is still present in the solvent stream after solvent regeneration. A non-linear relationship exists between the amount of energy required for solvent regeneration and the CO_2-loading of the solvent. Thus, the lean solvent loading was one of the parameters that needed to be optimised in order to reduce the amount of energy required for solvent regeneration.

The lean loading of the solvent was optimised just before adding the absorber column to the flowsheet configuration. This was done by varying the reboiler duty of the stripping column and recording the amount of CO_2 that left the top of the column. The energy requirement was then reported as the energy required for solvent regeneration per mass of CO_2 driven off. **Figure 48** shows a plot that was drawn up of the solvent lean loading vs. the energy requirement for solvent regeneration. The previously mentioned non-linear relationship can be observed when considering the data closer to the Y-axis. The plot shows a steep increase in the required energy, from 3.9 – 5.6 MJ/kg CO_2, when reducing the lean loading from 0.3 to 0.2.

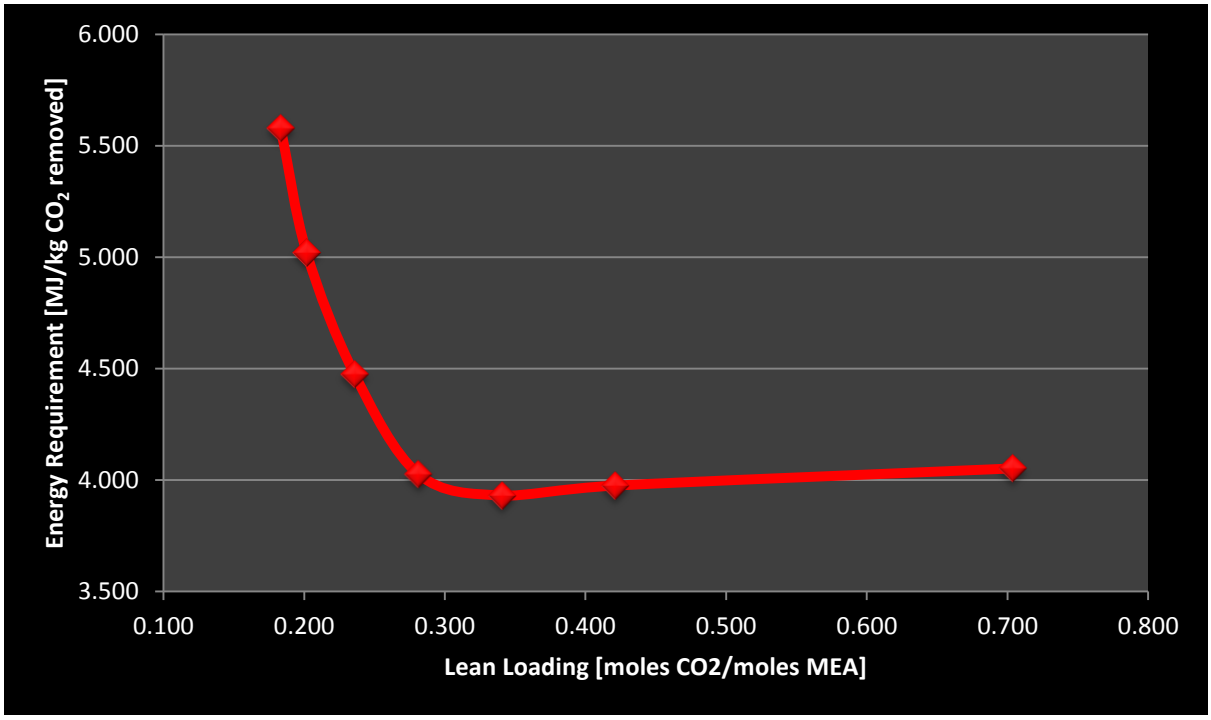

FIGURE 48: OPTIMISATION OF THE LEAN LOADING OF THE 30 WT % MEA (AQ) SOLVENT AT CAPTURE EFFICIENCIES OF 90% AND AN L/G-RATIO OF 2.5; 500X-TYPE PACKING MATERIAL WERE USED.

When considering that the lean solvent is recycled back to the top of the absorber column, it is clear that the lowest possible lean loading would be desired. However, the energy requirement

for solvent regeneration also needs to be considered. The plot given in **Figure 48** can thus be used to optimise the lean loading of the solvent with respect to the regeneration energy requirement. From **Figure 48** the optimum lean loading would be between 0.28 and 0.32 moles of CO_2 per moles of MEA. This corresponds relatively well to optimum lean loadings of 0.25 [moles of CO_2/moles of MEA] reported in literature(Alie et al., 2005).

The reboiler duty obtained from optimising the solvent lean loading was then used as the starting point value when combining the flowsheets and including the solvent recycle stream.

OPTIMISING L/G-RATIO

The L/G-ratio refers to the mass flow rate of the liquid solvent to that of the gas fed to the absorber column. This ratio directly influences the rich solvent loading of the stream leaving the bottom of the absorber column, and thus also the energy requirement for solvent regeneration.

The L/G-ratio is optimised after combining the flowsheets and after closing the solvent recycle stream. All the design specifications, as discussed in the previous section were also included when the optimisation process was commenced. The mass flow rate of the solvent was kept constant while that of the gas was varied. The CO_2 leaving the top of the stripping column and the estimated reboiler duty (from the design specification on the CO_2 capture efficiency) were recorded. These were then used to calculate the energy requirement for solvent regeneration. **Figure 49** shows a plot of the L/G-ratio vs. the energy requirement for solvent regeneration.

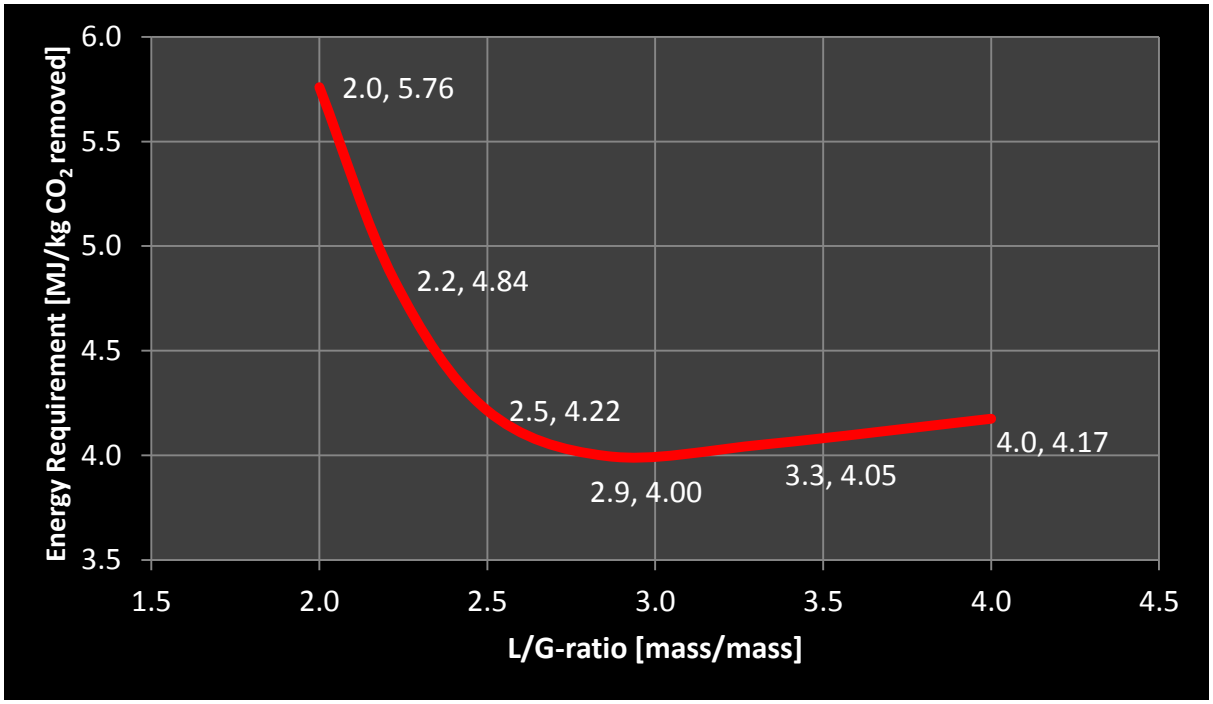

FIGURE 49: OPTIMISATION OF THE L/G-RATIO FOR 500X-TYPE PACKING AT A CO_2 CAPTURE EFFICIENCY OF 90%.

From **Figure 49** a steep increase in the energy requirement when approaching lower L/G-ratios can be observed. This can be explained by an increase in the rich solvent loading, thus requiring more energy for CO_2 stripping. The slight increase in the energy requirement as the L/G-ratio is increased above 3 can be prescribed to the higher solvent circulation rate requiring more energy for solvent heating in the reboiler unit. The specific x- and y-coordinates of the runs that were performed are given on the plot in **Figure 49**.

THE EFFECT OF THE FLUID DYNAMIC LOAD ON THE SOLVENT REGENERATION ENERGY REQUIREMENT

Another parameter that needs to be considered is the fluid dynamic load in the absorber column. This allows one to investigate the effect of the gas- and liquid flow rates on the solvent regeneration energy requirement independently from the L/G-ratio. For these simulations the L/G-ratio was kept at a constant value of 2.5 [kg/kg], operating with a CO_2 capture efficiency of 90%. **Figure 50** shows the results from simulating a variation in the fluid dynamic load of the absorber column.

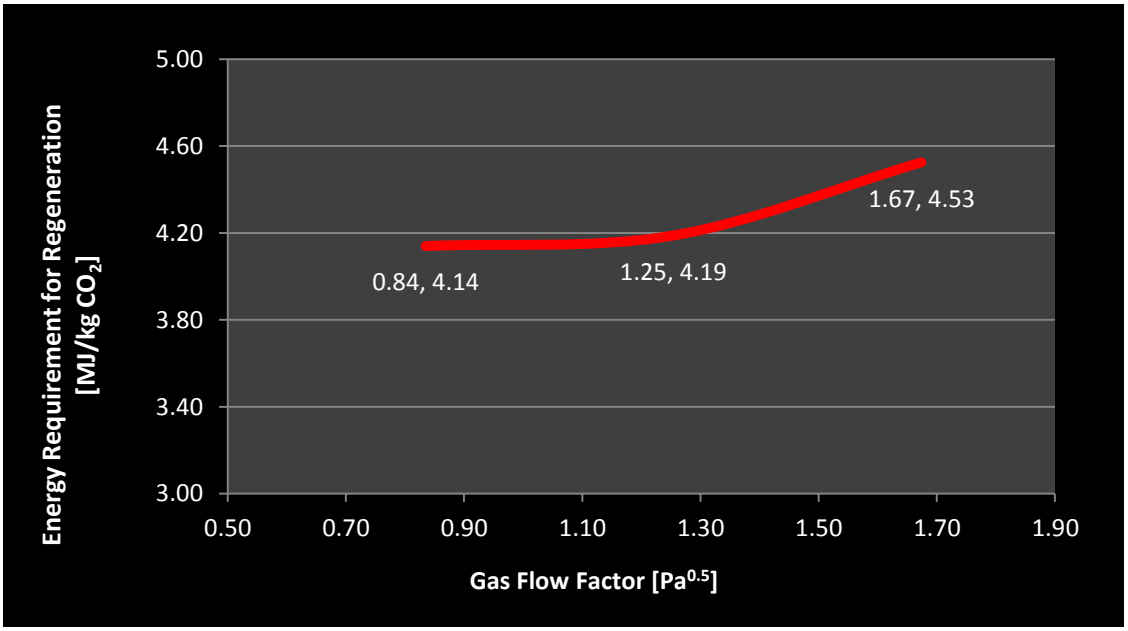

FIGURE 50 EFFECT OF VARYING THE GAS FLOW FACTOR ON THE REGENERATION ENERGY REQUIREMENT FOR 500X TYPE PACKING MATERIAL, WITH L/G-RATIO = 2.5, CAPTURE EFFICIENCY = 90%. PREDICTIONS OF THE ASPEN PLUS® SIMULATION

From **Figure 50** it can be seen that with an increase in the gas flow factor at a constant L/G-ratio, there is an increase in the solvent regeneration energy requirement. A discussion on why this is observed will be given when comparing the simulated results to results obtained by Mangalapally and Hasse, (2011).

6.2. VALIDATION OF THE ASPEN PLUS® PROCESS SIMULATION

In an attempt to validate the method of simulation proposed here, the flowsheet configuration of the Aspen Plus® simulation were adapted to match those of a specific pilot plant setup. The pilot plant used at the University of Kaiserslautern(Mangalapally and Hasse, 2011a; Notz et al., 2012)was chosen for validating the simulation results.

6.2.1. PILOT PLANT CONFIGURATION

The pilot plant consists of an absorber column with an inside diameter of 0.125 meters, and a packed bed height of 4.25 meters. The stripping column also has an internal diameter of 0.125 meters and a packed bed height of 2.5 meters. The flue gas fed to the bottom of the absorber column had an average CO_2mole fraction of 10.1 mole% for the case considered.

Pilot Plant optimisation was done using BX500 type packing material (Mangalapally et al, 2011). The optimisation was focused at optimising the L/G-ratio for the absorber column, with respect to the energy requirement for solvent regeneration. As previously mentioned, this was also done when optimising the operating conditions for the process simulation in Aspen Plus®. **Figure 51** shows a comparison between the results obtained from the pilot plant and the Aspen Plus® simulation optimisation. The x- and the y-coordinates of the reported literature data are indicated next to the data points in **Figure 51**.

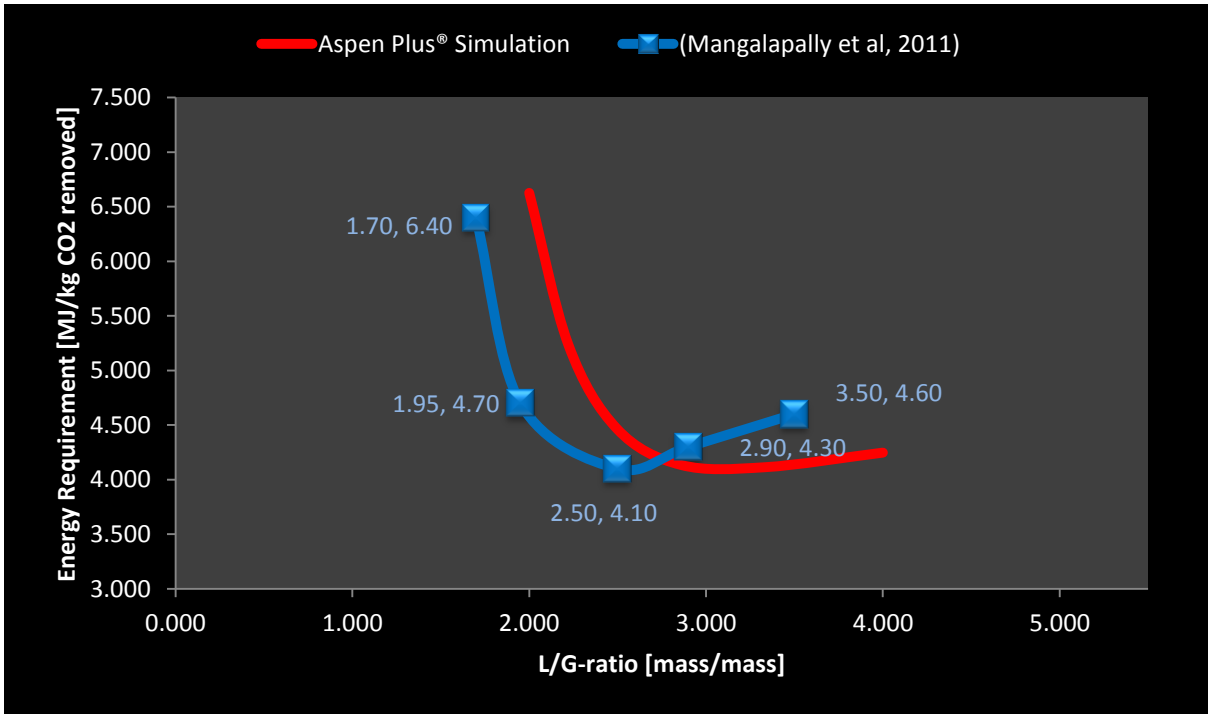

FIGURE 51: COMPARISON OF PILOT PLANT OPTIMISATION RESULTS TO THE SIMULATION OPTIMISATION RESULTS

It can be seen from **Figure 51** that there is a slight discrepancy in the optimum L/G-ratio for the real pilot plant compared to the simulated results. This is however expected seeing that the simulation does not account for factors such as, heat loss to the environment. However it is clear that the trends for both curves in **Figure 51** are very similar and that the energy requirement for solvent regeneration for both cases agrees very well. 4.1 MJ/kg CO_2 removed was reported for the pilot plant after optimisation of the L/G-ratio, while the optimised energy requirement for the simulation was 4.15 MJ/kg CO_2 removed.

6.2.2. FLUID DYNAMIC LOAD IN THE ABSORBER COLUMN

As previously mentioned, it is also important to consider the effect of the gas- and liquid flow rates, independently of L/G-ratio, on the regeneration energy requirement. **Figure 52** shows the comparison of the results from the Aspen Plus® Simulation, to pilot plant results reported by Mangalapally and Hasse (2011). It can be seen that the simulation accurately predicts the trend followed by the pilot plant data. The simulation were performed for an L/G-ratio of 2.5 [kg/kg], the same ratio at which the pilot plant data were gathered. The inaccuracy in the prediction of the exact solvent regeneration energy is similar to what can be observed from **Figure 51** for an L/G-ratio of 2.5 [kg/kg].

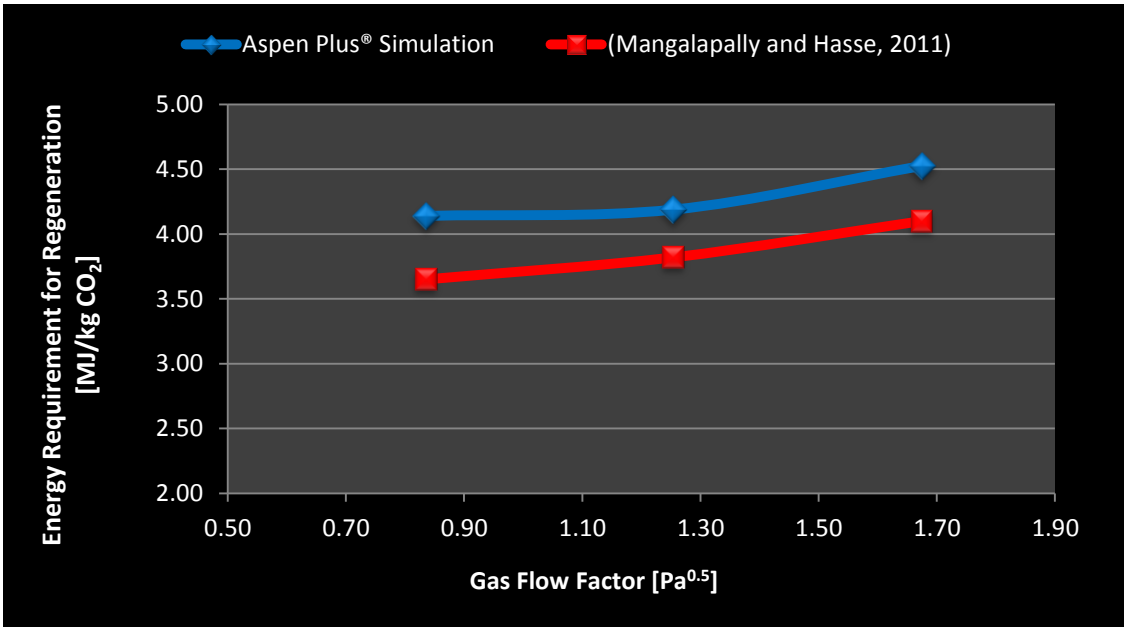

FIGURE 52 COMPARISON SIMULATED AND PILOT PLANT DATA ON THE EFFECT OF VARYING THE GAS FLOW FACTOR ON THE REGENERATION ENERGY REQUIREMENT FOR 500X TYPE PACKING MATERIAL, WITH L/G-RATIO = 2.5, CAPTURE EFFICIENCY = 90%

The Aspen Plus® Simulation results presented in **Figure 52** can be improved by simulating the variation of the fluid dynamic load for the optimum L/G-ratio of the simulation (between 2.8 and 3). Thus, using the optimum L/G-ratio for the simulation and comparing the simulation

results to pilot plant results that have been gathered at the optimum L/G-ratio for the pilot plant. This will yield satisfactory results of the effect of various process parameters on the solvent regeneration energy requirement.

Mangalapally and Hasse (2011) refer to the kinetics of CO_2 mass transfer in the absorber column when explaining the reduction in the regeneration energy requirement at reduced the gas flow factors. When reducing the gas flow rate at a constant CO_2 capture efficiency, the mass of CO_2 that needs to be transferred into the reactive solvent is reduced. Because the CO_2 capture efficiency is kept constant, the reduced amount of CO_2 will require less driving force to be transferred into- and from the reactive solvent, thus the reduced energy requirement for solvent regeneration.

6.2.3. VALIDATION AT VARIOUS CO_2 CAPTURE RATES FOR BX500 PACKING MATERIAL

In order to validate the simulation, energy requirement data reported by Mangalapally and Hasse (2011a) at various CO_2 capture efficiencies were simulated. The simulation was run with CO_2 capture efficiencies of 90%, and downwards in increments of 5%. The data gathered from the simulation were used to generate the curve shown in **Figure 53**.

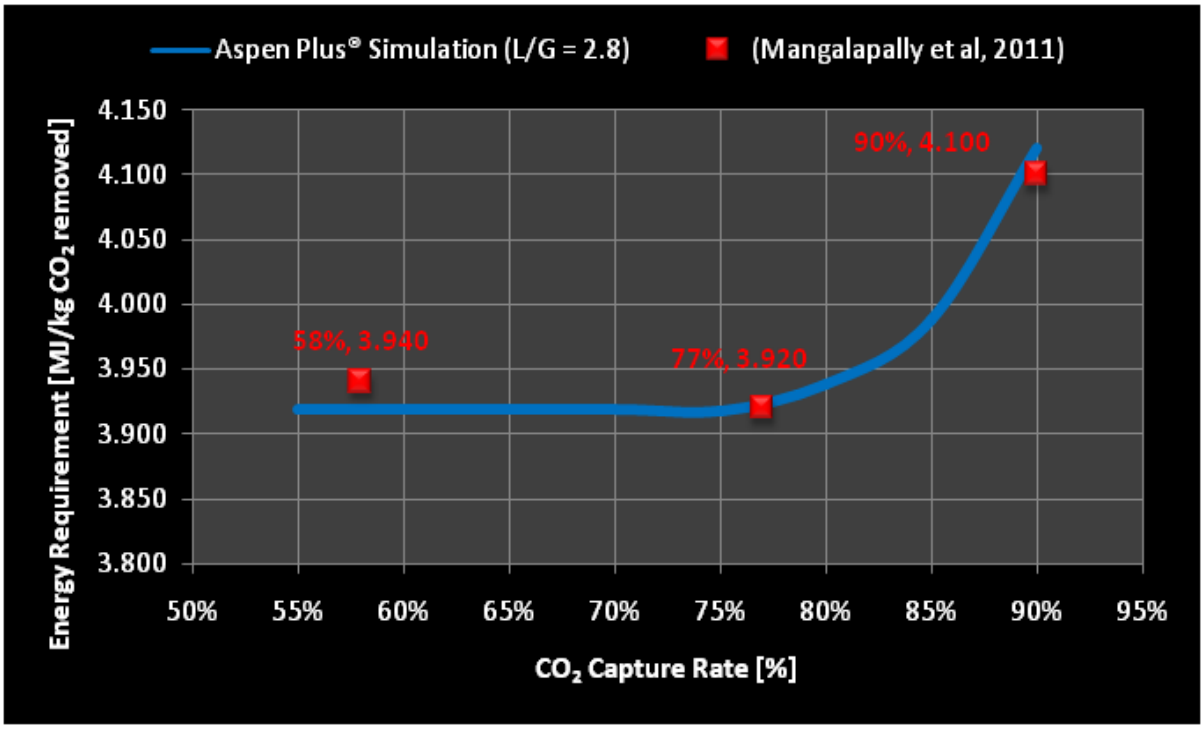

FIGURE 53: SIMULATION VALIDATION BY COMPARISON TO PILOT PLANT DATA

It is clear from **Figure 53** that when considering the optimum L/G-ratios (2.8 [kg/kg] were used for the Aspen Plus® simulation) for both cases, the simulation accurately predicts the energy requirement for solvent regeneration over a range of CO_2 capture efficiencies.

6.2.4. VALIDATION OF SIMULATION AGAINST DATA OBTAINED OVER MELLAPAK 250Y

Notz et al. (2010) made use of the same pilot plant as Mangalapally and Hasse (2011) for CO_2 capture studies using Mellapak 250Y in both columns. The simulation was adapted using Flexipac 250Y for the absorber column and Mellapak 250Y for the stripping column. Flexipac was used in the absorber column, due to proprietary restrictions on simulating absorption with Mellapak packing material.

In the study by Notz et al. (2010) difficulties of reaching a 90% capture efficiency with the 250Y type packing material were encountered. The highest capture efficiency that could be achieved was reported to be 88%. The simulations were once again performed at 90% CO_2 capture efficiency, and downward in 5% increments to a capture efficiency of 50%. The curve generated from the simulated data is shown in **Figure 54**, where it is compared to the recorded pilot plant data.

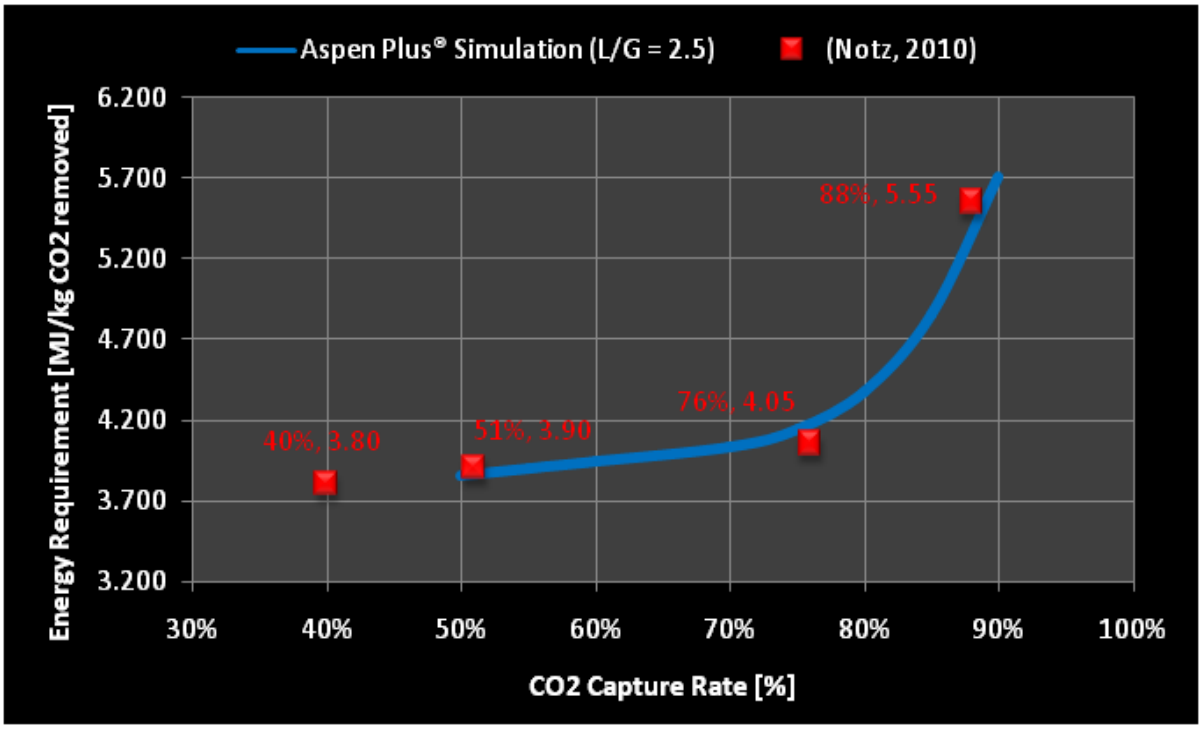

FIGURE 54: VALIDATING THE SIMULATION WITH A DIFFERENT PACKING MATERIAL

Figure 54 shows a very good agreement of the predicted energy requirement at various CO_2 capture efficiency when compared to the actual pilot plant data. The ability of the simulation to

accurately predict the steep increase in energy demand as a capture efficiency of 90% is approached should also be noticed.

The fact that the simulation accurately predicts the energy requirement at different CO_2 capture efficiencies, for different packing materials, is quite significant. This means that the Aspen Plus® simulation can be used to provide a good estimation of what packing material has potential for performing well when used for CO_2 capturing.

6.2.5. USING THE SIMULATION FOR PREDICTION OF TEMPERATURE PROFILES

The ASPEN Plus® Simulation of the pilot plant setup was used to predict the temperature profiles of the absorber- and the stripping columns. The predicted temperature profiles were compared to the pilot plant data reported by Mangalapally and Hasse (2011a). The comparison between the simulated temperature profiles and that obtained from the pilot plant experiments can be seen in **Figure 55**.

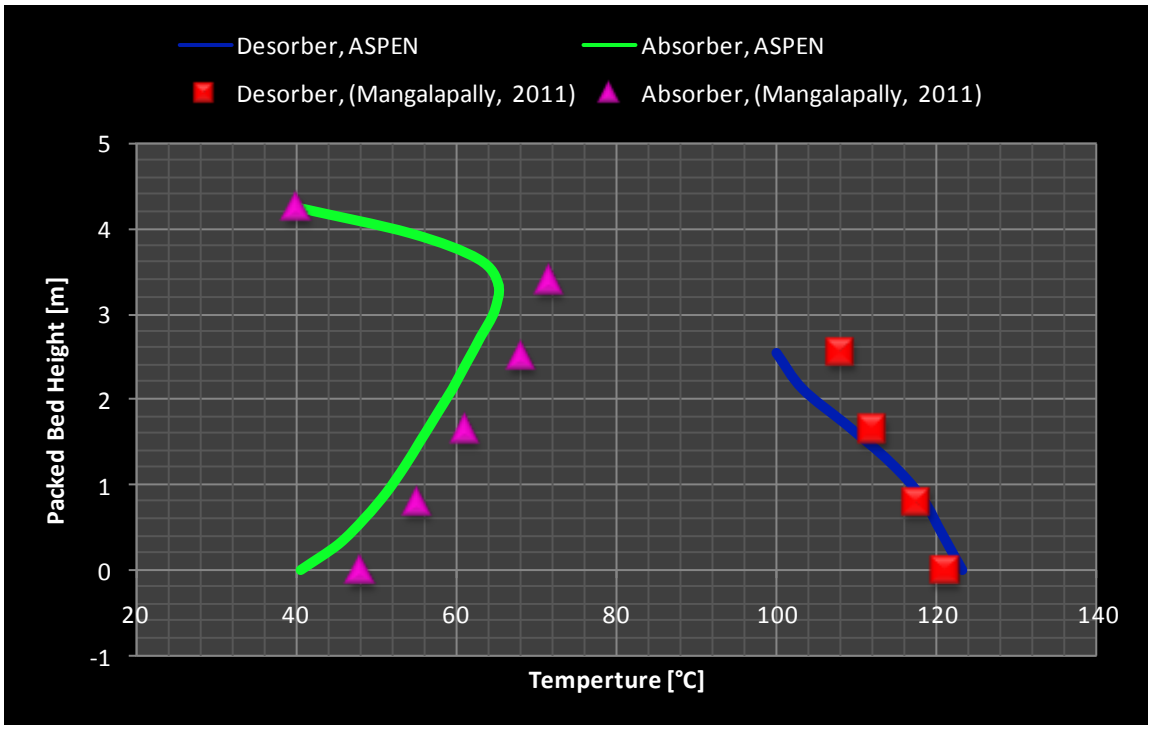

FIGURE 55COMPARISON OF TEMPERATURE PROFILES FROM THE ASPEN PLUS® SIMULATION TO REAL PILOT PLANT DATA

From **Figure 55** it can be seen that the predicted temperature profiles correspond reasonably well to the pilot plant data. This serves as further validation of the proposed method for simulating the CO_2 capture process using ASPEN Plus®.

6.3. APPLICATION OF SIMULATION FOR COMPARISON OF VARIOUS PACKING MATERIALS

The studies by Notz et al. (2012)and Mangalapally and Hasse (2011b) gave insight into the effect of packing material surface area on the CO_2 capture process. The 250Y type packing material (smaller surface area) performed reasonably well at lower capture rates as compared to the BX500 type packing material (larger surface area). However, as the capture efficiency increase above 80% there is a steep increase in the energy requirement for solvent regeneration. When comparing this to only a slight rise in energy requirement when increasing the capture efficiency from 80 to 90% with the BX500 type packing material, it is clear that the larger surface area plays an important role in the efficiency of the capture process.

The simulation was performed with identical conditions, but using a packing material with an even larger surface area, 700Y. This was done in order to test the hypothesis that a larger surface area would lead to energy savings. **Figure 56** gives the results, comparing the energy requirement at different capture efficiencies for the three different packing materials.

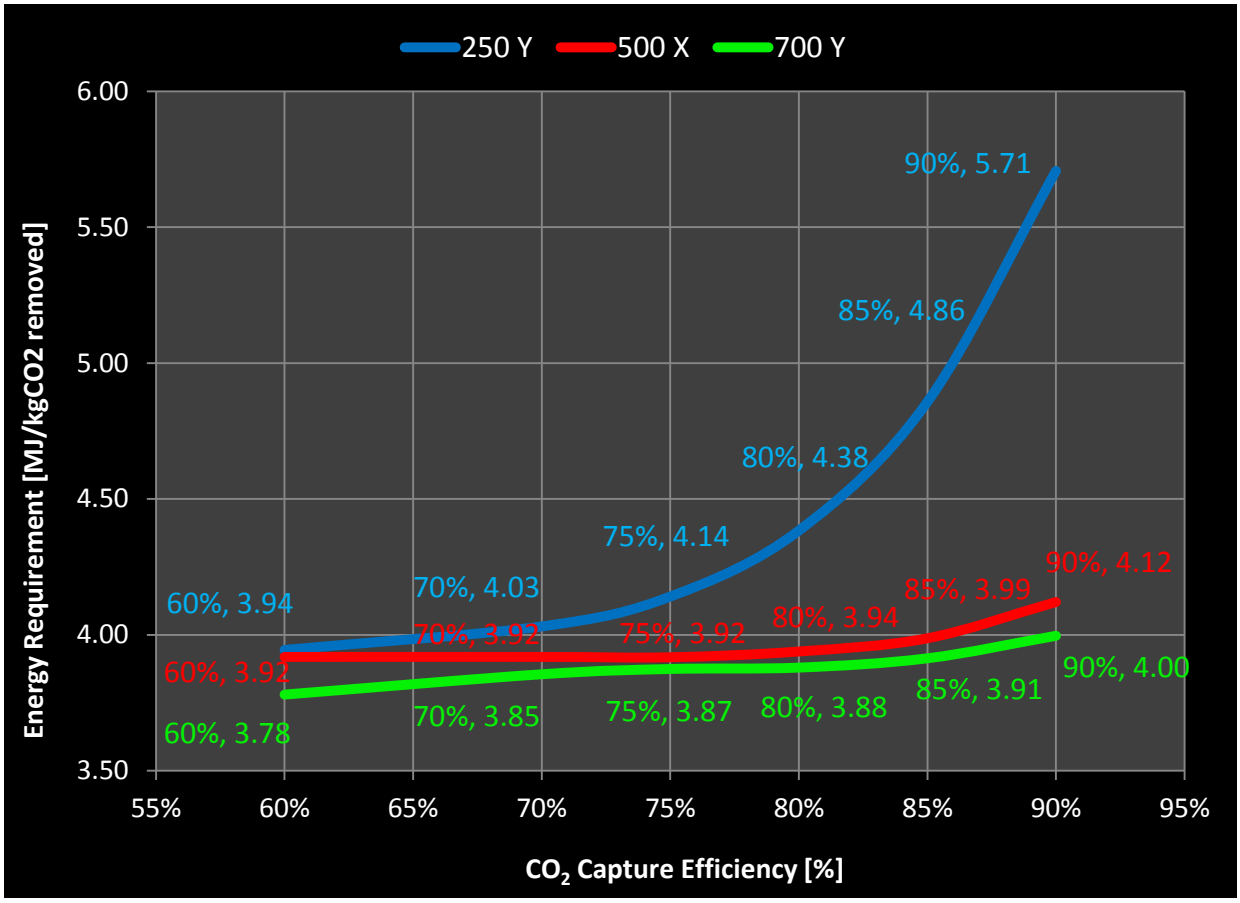

FIGURE 56: COMPARISON OF PREDICTED ENERGY REQUIREMENTS FOR SOLVENT REGENERATION USING DIFFERENT PACKING MATERIALS

It is clear from **Figure 56** that when increasing the surface area of the packing material, the energy requirement for solvent regeneration is reduced. With the use of the simulation the hypothesis was proven to be correct. When considering the decrease in energy requirement between the 250Y and BX500 type packing material and comparing it to the decrease in energy requirement between the BX500 and the 700Y type packing the following is noticed. There is a non-linear relationship between increasing the surface area of the packing material and the decrease in the energy requirement for solvent regeneration.

It should however be kept in mind that the optimal operating conditions for various packing materials will differ. Further investigation on the optimal operating conditions for each packing material will allow one to better compare various packing materials, based on their optimal performance.

In future, simulations might be used to predict whether or not increasing the surface area of the packing material for specific CO_2capture plant configurations would yield the desire reduction in the energy requirement for solvent regeneration.

6.4. CHAPTER CONCLUSIONS

A method for simulating the CO_2 capture process using Aspen Plus® was developed. With the focus being to provide a simplified method of simulating the CO_2 capture process, a new method of simulating the process was developed and detailed in this chapter.

The Aspen Plus® simulation proved to be of great value when performing process optimisation. The simulation was used to optimise with great success the lean solvent loading, liquid-to-gas ratio in the absorber column as well as the fluid dynamic load in the absorber column. The simulation results of the effect of L/G-ratio and the fluid dynamic load on the regeneration energy requirement, showed good agreement to pilot plant data from Mangalapally and Hasse (2011).

The Aspen Plus® simulation was validated by comparing data for various CO_2 capture efficiencies to those reported in Literature. It was found that the optimised simulation accurately predicts the reported energy requirements at various capture efficiencies. This was the case for both 250Y and BX500 type packing materials. The simulation also proves to be valuable in predicting the temperature profiles of both the absorber- and the stripping columns relatively well.

The hypothesis that increasing the surface area of the packing material relates to a decrease in the energy requirement for solvent regeneration was proven correct.

CHAPTER 7

PERFORMANCE OF PROCESS EQUIPMENT AND PILOT PLANT OPERATING PROCEDURE

This chapter reports on the performance of the main pieces of process equipment that were designed and installed during the construction phase of the CO_2 Capture Pilot Plant.

The operating procedure of the pilot plant with reference to the use of the reactive solvent monoethanolamine is also considered. The operating procedure for the pilot plant is summarized briefly with reference to start-up-, operating- and shut-down procedures.

7.1. PERFORMANCE OF PROCESS EQUIPMENT

The performance of various pieces of process equipment will be evaluated in this section. This is done by considering the following:

1. heat recovery in the cross flow heat exchanger;
2. the heat removed in the solvent cooler;
3. gas leakage rates from the gas recycle loop;
4. comparing the similarity of the manufactured venturi mass flow meters;
5. determining dead volumes in sample tubes for online gas analysis;
6. evaluating the differences in gas- and liquid temperatures in the absorber column during the first phase of the reaction.

7.1.1. HEAT EXCHANGER

The cross flow heat exchanger that was installed to allow heat integration between the stripping and the absorption sections, was designed to have a heat duty of 9.1 kW for the investigated flow rate. After evaluation of the performance of the heat exchanger at thermal equilibrium it was found that **8.31 kW** of the energy in the hot steam is transferred to heating the colder stream. The hot stream further loses another **1.62 kW** to the environment, decreasing the energy value of the hot stream with a total of **9.93 kW**. The calculations were performed at a solvent flow rate of 211 kg/h and can be seen in Appendix B, Table B.13.

It was also seen from the experimental runs that the feed stream to the top of the stripping column was heated to temperatures above 70°C, indicating good heat transfer capabilities of the heat exchanger. The heat exchanger was designed with a minimum temperature approach of 10K. This was achieved for most of the experimental runs performed.

7.1.2. SOLVENT COOLER

The solvent cooler was evaluated by calculating the energy removed from the hot solvent stream prior to feeding it to the top of the absorber column. For the case with a solvent flow rate of 211 kg/h, a further **3.03 kW** was removed from the solvent stream before it is fed to the absorber column. This can also be seen in Appendix B, Table B.17.

From the experimental runs it was clear that the solvent cooler performs well, cooling the solvent to temperatures within a range of 38 – 42°C. Thus, it provides sufficient cooling of the solvent stream prior to feeding the absorber column. Literature reports that the temperature of the solvent feed should not exceed 45°C (Mangalapally and Hasse, 2011a; Notz et al., 2012; Wilson et al., 2005).

7.1.3. GAS RECYCLE LOOP

The performance of the gas recycle loop was evaluated by considering the leakage rates of CO_2 from the system, and that of O_2 into the system. The evaluation run was performed at a gas flow rate of about 125 kg/h. The leakage rates are, however, dependent on the mass flow rate of the gas. **Figure 57** shows the leakage rates for both these components. The trendline equations are used to estimate a CO_2 leakage rate of 1.57 volume % per hour and O_2 leakage rates into the system of about 2 volume % per hour.

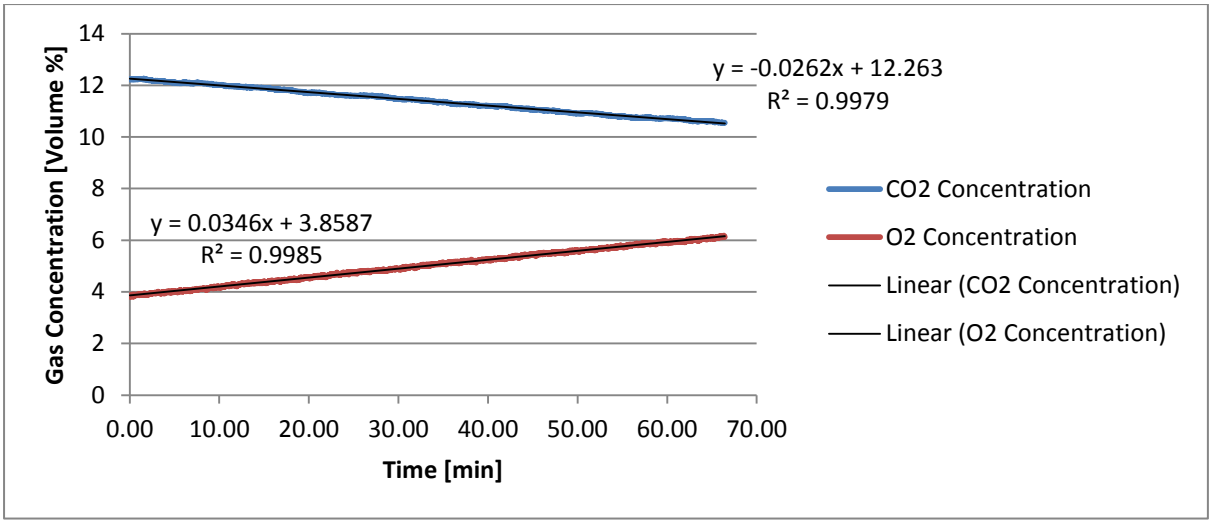

FIGURE 57 LEAKAGE RATES OF CO_2 FROM THE GAS RECYCLE LOOP AND THAT OF O_2 INTO THE GAS RECYCLE LOOP

In performing the experimental runs, it was noted that feeding the make-up CO_2 into the gas recycle loop, reduces the leakage of O_2 into the system. This is due to the positive pressure created by continuously feeding CO_2. Thus, compensating for the CO_2 leakage from the gas cycle has a doubled benefit.

7.1.4. VENTURI MASS FLOW METERS

The similarity of the two venturi mass flow meters installed in the gas recycle loop was considered by comparing the results from each at various blower speeds with a closed loop setup. **Table 12** shows the results obtained at the various variable speed drive (VSD) settings.

TABLE 12 COMPARISON OF RESULTS FROM THE TWO VENTURI MASS FLOW METERS

VSD setting [Hz]	I-1 [kg/h]	I-2 [kg/h]	(I-1)/(I-2)
10	229	231	0.99
15	353	357	0.99
20	477	482	0.99
25	602	609	0.99
30	725	748	0.97

From **Table 12** it can be seen that the venturi flow meters give mass flow rate measurements that are almost identical. The mass flow comparison yields a value of 0.99, except for very high flow rates. The venturi mass flow meters were calibrated with a pitot tube, setting up velocity profiles across the pipe diameter for the various blower speed settings. More information on the calibration procedure can be seen in Appendix A.

7.1.5. ONLINE GAS ANALYSIS SETUP

As previously mentioned the gas sampling system was set up to allow measurements of the CO_2 and O_2 content of the process gas from various locations in the absorber column using only one composition analyser for each gas. The sample pump continuously pumps gas samples from the various locations and the automated sampling valves determine the location of sampling. The automated sampling valves are installed close to the analysers. Thus after switching the sampling location, gas from the previously drawn sample needs to pass through the analysers before the analysed sample is representative of the current process condition.

Figure 58 shows the time period required in order to remove old sample from the longest sampling tube – the top of the column – after a switch in the automated sampling valves have occurred. A time period of about 40 seconds should be allowed in order to remove all gas contained within the dead volume of the sample tube.

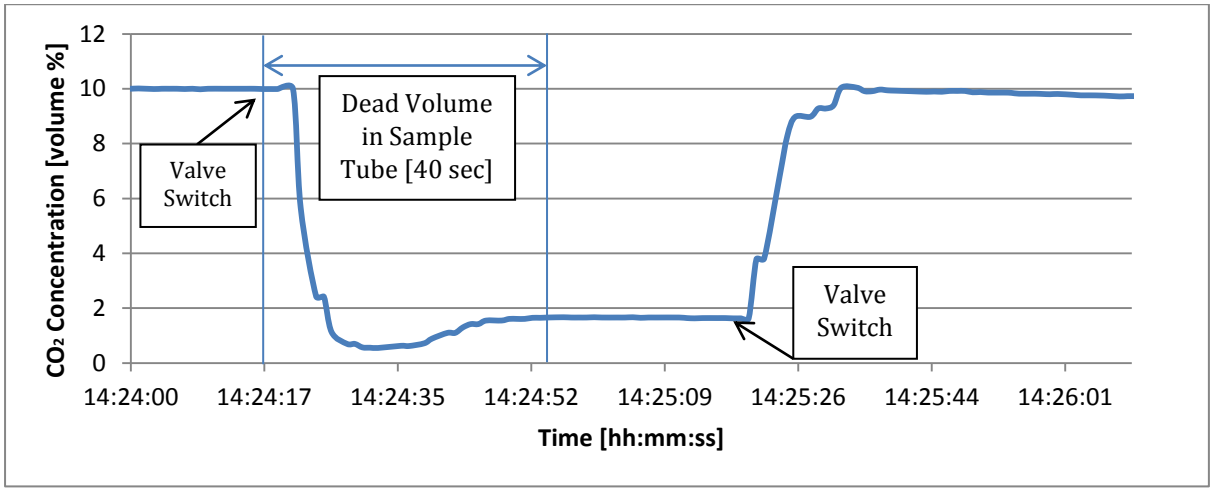

FIGURE 58 ILLUSTRATION OF THE DEAD VOLUME IN THE LONGEST SAMPLE TUBE

From the pilot plant experiments it was seen that the gas sampling method, provides a good way of obtaining gas concentration profiles across the length of the absorber column. The results on the CO_2 concentration profiles are presented and discussed in the next chapter.

7.1.6. TEMPERATURE PROFILES FOR THE ABSORBER COLUMN

The designed and installed Teflon temperature probe separators allows for measuring the gas- and liquid temperatures separately, thus resulting in separate temperature profiles for the gas and the liquid inside the absorber column. The functionality of the probe separators were considered by allowing CO_2 in the process gas to react with the reactive solvent MEA. The reaction is exothermic and will cause a rise in solvent temperature. The results from this experiment can be seen in **Figure 59** to **Figure 61**. In these figures the temperature probes with the odd numbers (TR-201, TR-203, TR-205 and TR-207) are measuring gas temperatures and those with even numbers (TR-202, TR-204, TR-206 and TR-208) are measuring the liquid temperatures.

Figure 59 to **Figure 61** show the temperature trends against time as the reaction takes place in the absorption column. Gas was fed from the bottom and the CO_2 concentration at the bottom of the column was thus the highest and one would expect the majority of the CO_2 to react in this section of the column. It is clear from **Figure 59**(a) and (b) that the recorded liquid temperatures are much higher than the gas temperatures in the bottom section of the column. As the gas moves to the top of the column, most of the CO_2 is depleted and less MEA reacts exothermically. As the gas reaches the top of the column, seen in **Figure 60**, the process gas has been heated by the liquid reacting in the lower parts of the column. This results in the higher gas temperature when compared to the temperature of the solvent.

This short experiment proves that the temperature probe separators work satisfactorily in obtaining two different temperature profiles for the absorber column.

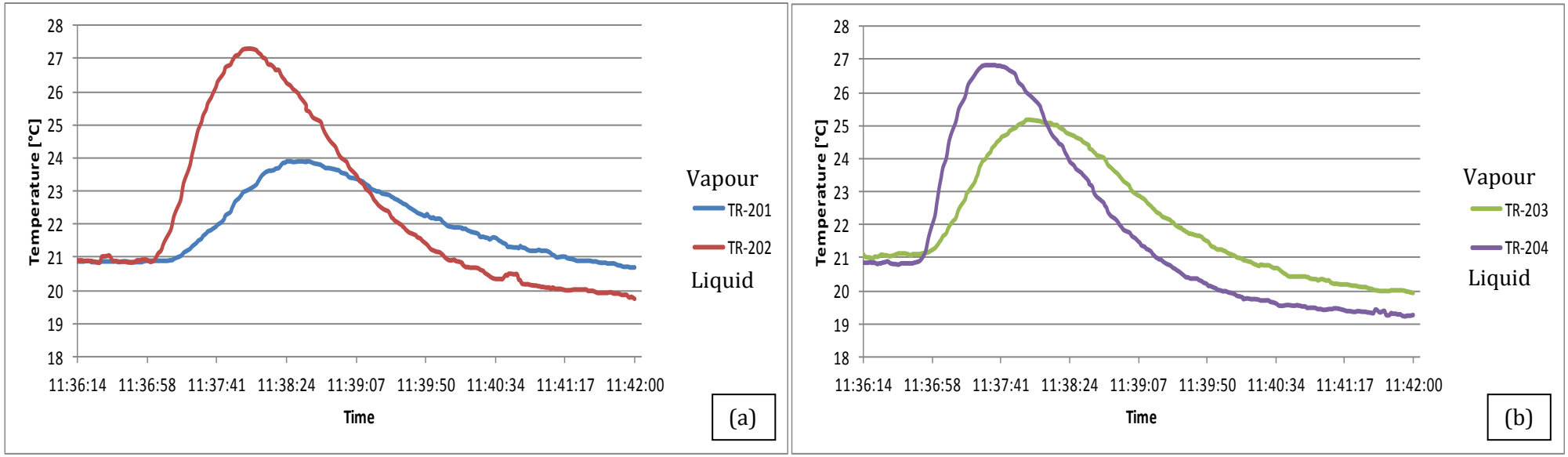

Figure 59BOTTOM TWO SECTIONS OF THE ABSORBER COLUMN, a) 0.54 METERS FROM THE BOTTOM, b) 1.08 METERS FROM THE BOTTOM

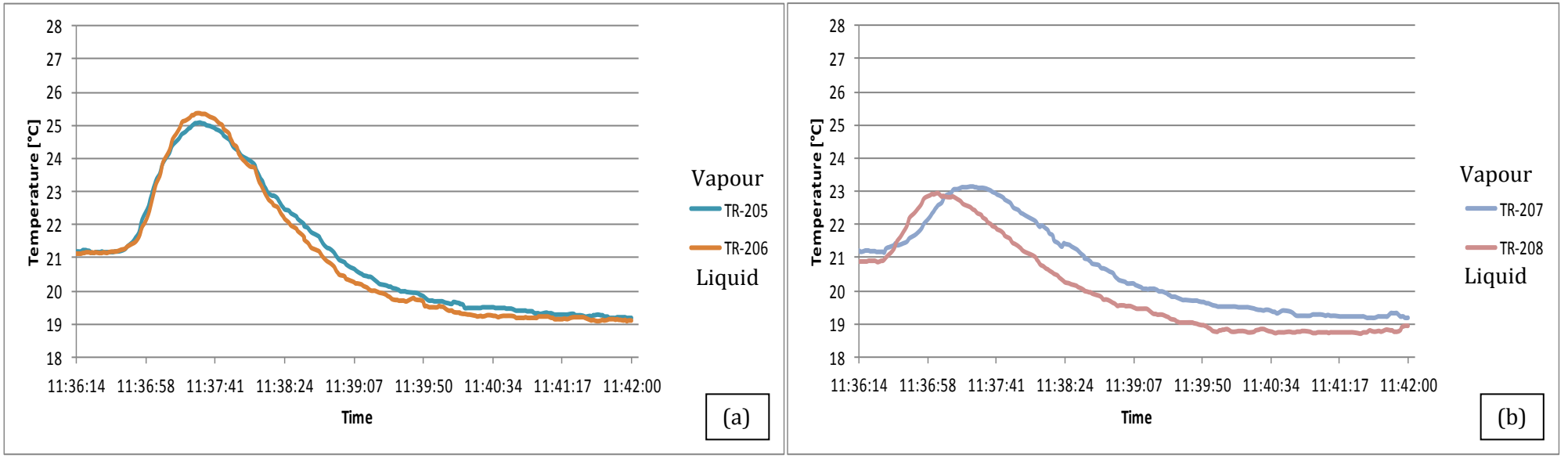

FIGURE 60TOP HALF OF THE ABSORBER COLUMN, (A) 1.62 METERS FROM THE BOTTOM, B) TOP OF THE ABSORBER COLUMN

7.2. OPERATING THE PILOT PLANT FACILITY

The operating procedure for the pilot plant will be discussed in three main steps: The start-up- and shutdown procedures will be detailed in Appendix C, with the main focus of this section being on the operating procedure of the pilot plant in order to obtain steady state conditions.

7.2.1. START-UP AND SHUTDOWN PROCEDURES

The start-up and shutdown procedures for the established pilot plant are given in full in Appendix C. In order to prevent any unsafe conditions and allow for stable operating of the pilot plant facility, these procedures are to be followed very diligently.

7.2.2. OPERATING PROCEDURE FOR THE PILOT PLANT SETUP

The operating procedure for the CO_2 capture pilot plant is discussed with reference to the following:

- Loading the reactive solvent with CO_2,
- Gas composition control;
- Most effective way of balancing the solvent flow rates between the two columns;
- Indication of the desired steady state condition;
- Gas sampling procedure;
- Measuring the steam flow rate

7.2.2.1. LOADING REACTIVE SOLVENT WITH CO_2

Once the system has reached thermal equilibrium, CO_2 can be added to the process gas for reactive absorption in the absorber column. During the first experimental run with aqueous MEA, the first step is to load the solvent with CO_2, up to a certain concentration. As discussed in the literature the solvent has a particular lean loading (normally about 0.2 – 0.25 [moles CO_2 / moles MEA]) which would allow for the lowest amount of solvent regeneration energy requirement.

As the first CO_2 is fed and reacts the solvent CO_2 loading increase, but the energy input to the stripping section is not sufficient to drive off CO_2 at such low concentrations. As the CO_2 loading of the rich solvent stream increases, the amount of energy required to release the first of the CO_2 from the solvent decrease. At a certain rich loading the energy input to the stripping section is sufficient to drive the reverse reaction. From this point onwards, any CO_2 that is captured in the

absorber column will be driven off in the stripping section of the pilot plant. It is only at this point in time that CO_2 from the top of the stripping column flows back into the gas recycle loop for reintroduction into the absorber column feed stream.

7.2.2.2. GAS COMPOSITION CONTROL

CO_2 is fed to the absorber column from a gas cylinder and the concentration is manually controlled to be between 8 – 10 volume percent. Within the time frame indicated in **Figure 61**, the CO_2 content in the process gas increases without any manual increase in the CO_2 fed to the gas recycle loop. This time period is seen as the period when CO_2 from the stripping column returns to the process gas recycle loop. The position of the control valve on the CO_2 feed line can be seen on the secondary axis of **Figure 61**. The CO_2 feed to the gas loop is then adjusted in order to obtain a feed concentration within the required range. The composition of the feed gas is manually controlled for at least one circulation of all solvent in the system. At this point in time there are some fluctuations in the feed gas stream. Further time is allowed for the fluctuations to decrease within a range of 1 volume % around the desired CO_2 concentration. The fluctuations in the CO_2 feed concentration at the assumed steady state can be seen in **Figure 62**.

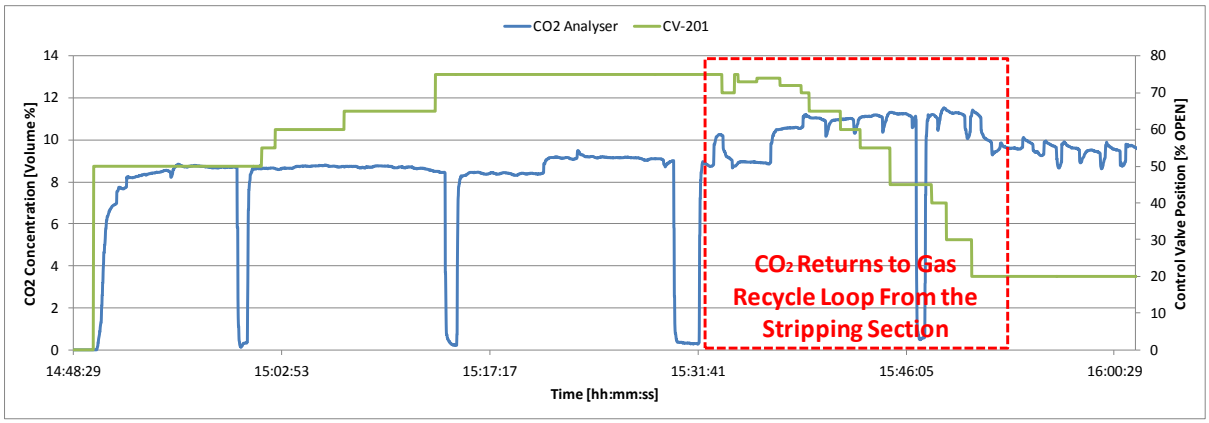

FIGURE 61 THE CO_2 CONCENTRATION PROFILE FOR THE ENTIRE DURATION OF THE RUN

When considering **Figure 61**, the occasional lower CO_2 readings, corresponds to measuring the CO_2 concentration from the top of the absorber column. This can be used to determine the CO_2 capture efficiency.

7.2.2.3. BALANCING THE SOLVENT FLOW RATES BETWEEN THE TWO COLUMNS

Initially the pump flow rate calibration curves can be used to provide flow rates that are similar for both solvent pumps. As the temperature of the lean solvent rises, the density changes leading to a variation in the flow rates delivered by each of the pumps.

The method used to provide a perfect balance in the solvent flow rates between the columns is as follows. The mass flow rate at the bottom of the absorber column (just before the rich solvent pump) was measured manually, and the flow rate delivered by the rich solvent pump was adjusted with a screw-down valve installed in the line downstream from the pump. A calibrated rotameter was used to set the flow rate to exactly the measured mass flow rate. The level indicator on the rich solvent holding tank may also serve as a good indication of balanced flow rates between the two columns.

7.2.2.4. INDICATORS OF THE STEADY STATE CONDITION

There are various indicators of the desired steady state condition. These are either related to temperature or to the composition of the process gas cycle. Those related to temperature will stabilize first, and stabilization of the gas composition will only follow thereafter.

Initially there will be a rise in the absorber column temperature as the exothermic reaction occur. After a while the absorber column temperatures stabilize with the temperature profile displaying a temperature bulge at a certain height in the column. The height of the temperature bulge is related to various process parameters and is discussed in the results section. The temperature of the solvent feed to the top of the absorber column also gives a good indication of when thermal equilibrium has been reached. This temperature should stabilize somewhere between 38 and 42°C, depending on the experimental conditions used.

The second, and also the main indicator of the steady state condition, is the CO_2 concentration in the gas fed to the bottom of the absorber column. As previously explained the gas composition was manually controlled by adjusting the control valve. After compensating for CO_2 that flows back from the stripping column, there is some oscillatory behaviour in the CO_2 concentration of the feed gas steam. This is expected due to the complex behaviour between two columns with a solvent recycle- as well as a gas recycle stream.

However, after allowing sufficient time (at least three solvent circulations) the CO_2 concentration in the feed gas stream displays variations within a 1 volume % range. It is expected that there will be some fluctuations at the steady state condition due to the complex recycling of CO_2 from the absorber- and stripping columns as well as the continuous addition of fresh CO_2 feed to make up for gas leakages from the system. **Figure 62** shows the variations in the feed gas CO_2 concentration at the steady state condition for one of the experimental runs.

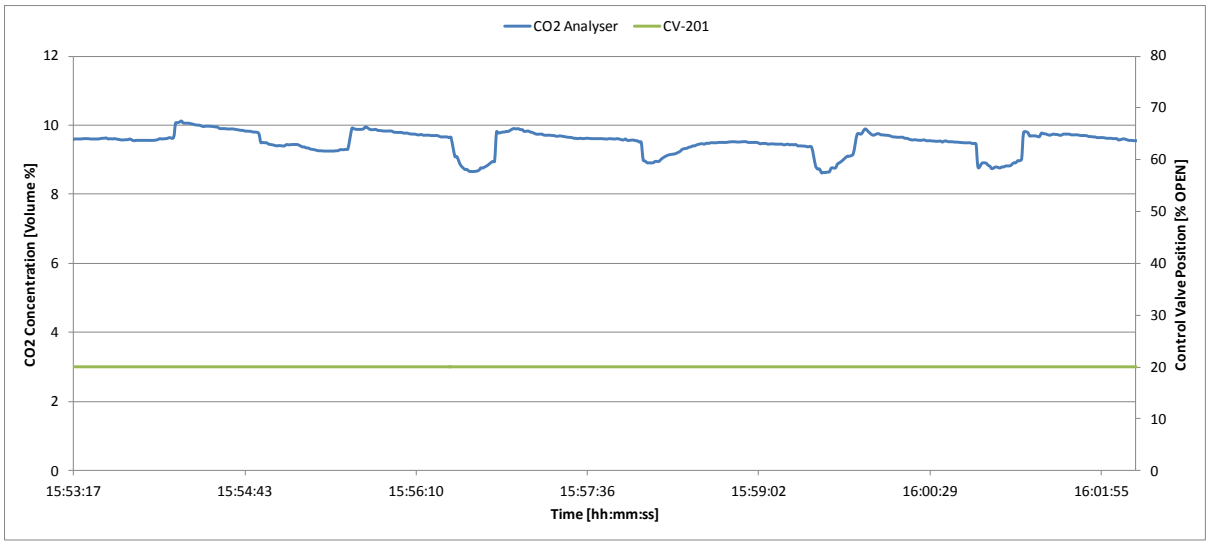

FIGURE 62 FEED GAS CO_2 CONCENTRATION PROFILE AT ASSUMED STEADY STATE CONDITIONS

Notice the variation in the CO_2 concentration even though the control valve position is at a constant value of 20 % OPEN. The plot was created with a data point for every second and no smoothing has been applied.

After reaching the steady state condition, data regarding the operating conditions at the particular steady state were gathered. This included determining the gas concentration profile of the absorber column, measuring the steam flow rate to the reboiler unit and measuring the solvent flow rate. All temperature data at the steady state condition was logged and the time period of the assumed steady state was recorded.

7.2.2.5. GAS SAMPLING PROCEDURE

As previously mentioned the gas sampling is done by pumping sample gas from the column with a sample pump, and two switch valves control whether the sample is drawn from the feed stream or from the gas sampling manifold. The sample manifold is used to select the location from where the gas samples are drawn.

The concentration profile over the height of the absorber column was obtained by adjusting the manual sample valves that change the sample location. **Figure 63** shows the trend of the CO_2 concentration that was the result of determining the CO_2 concentration profile for the absorber column. The four periodic spikes seen in **Figure 63** corresponds to when the gas sample is drawn from the gas feed stream to the bottom of the absorber column. This gives a representation of the CO_2 concentration in the feed stream.

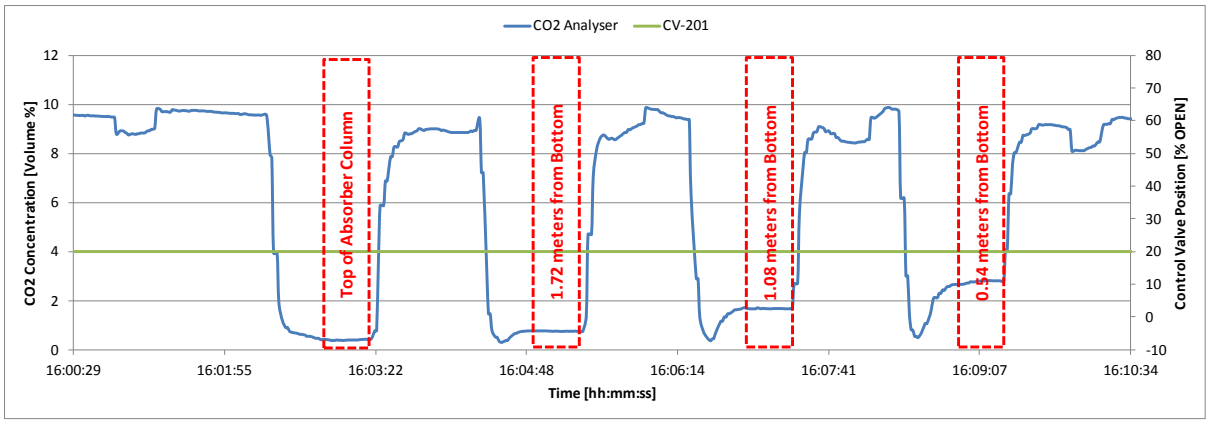

FIGURE 63 ILLUSTRATION OF THE GAS SAMPLING PROCEDURE TO OBTAIN THE CO_2 PROFILE FOR THE ABSORBER COLUMN

From **Figure 63** note the increase in the sample concentration as sampling for this particular case was done from the top to the bottom of the absorber. Also note that most of the CO_2 fed to the column reacts in the bottom half of the absorber.

7.2.2.6. MEASURING THE STEAM FLOW RATE

The steam flow rate was also measured at the steady state condition. This, along with the steam temperature and pressure, gave an indication of the amount of energy input to the reboiler unit for solvent regeneration. The steam flow rate was measured by manually measuring the mass flow rate of the steam condensate. The flow rate measurement was performed downstream from a steam trap unit.

7.3. PROBLEMS ENCOUNTERED IN OPERATION

While operating the pilot plant for the various experimental runs that were performed, some problems were encountered. The problems and actions taken are stated and possible future solutions are suggested.

7.3.1. SOLVENT LEAKAGE FROM THE SYSTEM

During experimental runs it frequently occurred that solvent started leaking from the system. Depending on the rate and the location of solvent leakage a decision can be made on whether or not it would be safe to continue with the particular experimental run.

If the solvent leak is on the third floor, it would not be advisable to continue with the experimental run, as there is a walkway on the second floor and the dripping solvent causes droplets to splash, creating a safety hazard for anyone passing by on the walkway.

When performing an experimental run, make notes on where leakages occur so that it can be fixed after each run. Due to the heating and cooling of the system between runs, the Teflon seals between joint parts may lose the ability to seal properly, and need to be replaced.

7.3.2. COMPOUND FORMATION

After the first experimental run with MEA it was found that in one of the solvent lines where the solvent is stationary while not in operation, a dark blue compound formed. **Figure 64** shows the colour of the compound that formed in the line.

After some inspection it was found that a copper fitting made up part of this section of the solvent line, causing the solvent to degrade with time during the periods when the plant was not in operation. The copper fitting was removed from the line.

Inspection on all the solvent lines containing stationary liquid was carried out, but no other sections were found to reveal any signs of this solvent degradation.

FIGURE 64 BLUE COMPOUND FORMED IN ONE OF THE SOLVENT LINES

7.3.3. SOLVENT DILUTION

Another problem that was encountered during the operation of the pilot plant was the dilution of solvent due to wash water leaking from the water wash section, into the top of the absorber column. This was initially noted by observing an increase in the volume of the solvent in the solvent holding tanks. After some inspection it was found that some of the wash water that is fed to the water wash section creates a splash when landing in the bottom of the section, causing droplets to splash into the gas channels leading to the absorber column.

The solvent dilution in the first experimental run, lead to decreased performance in the runs that followed. The problem was initially addressed by decreasing the flow rate of the wash water to a minimum of 20 litres per minute. This reduced the water leakage into the absorber column considerably.

The problem of solvent dilution was further addressed by removing some of the condensed water in the reflux line of the stripping column. The loss of wash water into the absorber column was thus balanced by removing the condensate (mainly water) from the reflux line of the stripping column. Mangalapally et al.(2009) used the same method of balancing the water in the system.

7.3.4. OVERSHOOTING THE DESIRED CO_2 CONCENTRATION IN THE PROCESS GAS RECYCLE STREAM

In performing an experimental run, one initially starts out with the steam valve in one position, allowing steady state at these experimental conditions. After reaching steady state the steam valve can be adjusted to allow a second steady state condition to be reached at a different CO_2 capture rate. Decreasing the steam flow to the stripping section will result in obtaining a steady state condition at a lower CO_2 capture rate and vice versa.

It was, however, found that increasing the steam flow, and thus the CO_2 capture rate from one steady state condition to the next; results in an overshoot in the CO_2 feed concentration. This can be explained by the higher energy input to the stripping section leading to more CO_2 being stripped from the solvent. For the new steady state condition the solvent fed to the top of the absorber column needs to be leaner than for the previous steady state condition, allowing the higher CO_2 capture rate.

The problem of overshooting the CO_2 concentration for this reason can be avoided by operating the pilot plant at the highest capture rate and decreasing the energy input for every consecutive steady state condition to follow. Thus data is gathered from the highest CO_2 capture rate to the lowest and not the other way round.

CHAPTER 8

PILOT PLANT REPEATABILITY, DATA VERIFICATION, RESULTS AND DISCUSSION

The repeatability of pilot plant data is presented by considering identical experimental runs with both 20 weight % MEA and 30 weight % MEA.

The rest of the chapter is focussed on the results that were obtained from experimental runs with aqueous solutions of MEA as solvent. Reference is made to the performance of the pilot plant setup as a facility for CO_2 capture studies. Data gathered from the pilot plant is compared to literature data in order to verify the results obtained.

8.1. REPEATABILITY

The repeatability of the pilot plant is considered by repeating two experimental runs, one with 20 and one with 30 wt % MEA (aq), using identical operating conditions for each. The pilot plant repeatability is then evaluated by considering the CO_2 concentration profiles for the absorber column as well as the temperature profiles. The solvent regeneration energy added to the thermosyphon reboiler unit is also considered.

8.1.1. EXPERIMENTAL RUNS WITH 20 WEIGHT % MEA [AQ]

8.1.1.1. CO_2 CONCENTRATION PROFILES

The CO_2 concentration profiles that were obtained from the repeatability runs can be seen in **Figure 65**. The error bars indicate the variation in the results from the two experimental runs.

As previously mentioned, a problem regarding wash water leaking into the absorber column occurred during the first experimental runs. The variation in the profiles can thus be explained by the resulting solvent dilution. It is also noted that the biggest variations in the concentration profiles are at the two locations closest to the bottom of the column and that there is only a slight variation in the feed gas CO_2 concentration. This is a further indication that the variation is due to the solvent dilution.

Despite the variation in the CO_2 concentration profile results, the trends obtained for the two runs correspond acceptably well.

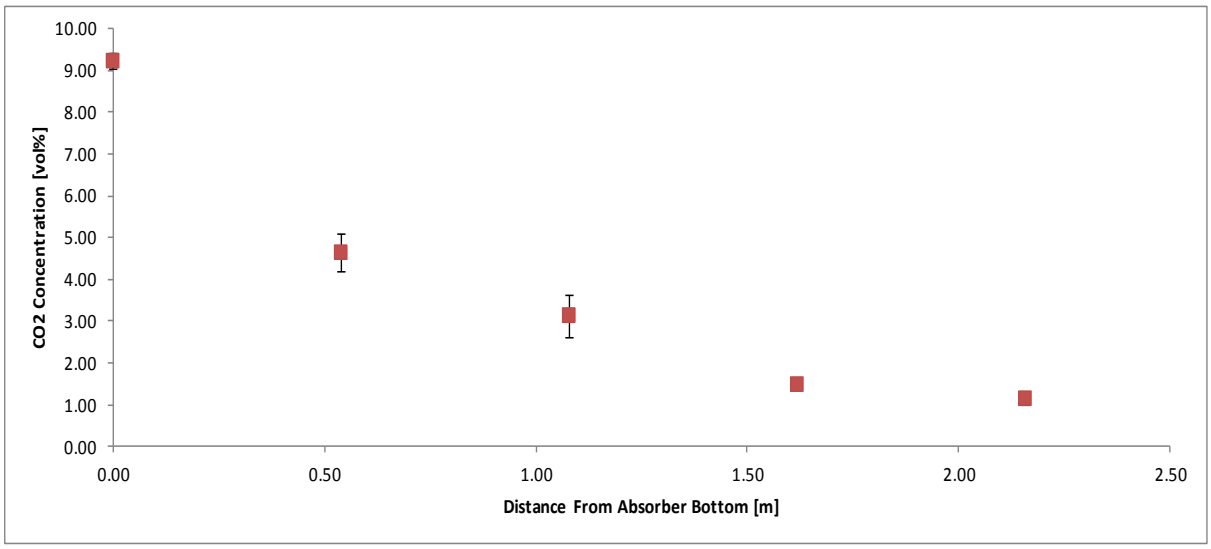

FIGURE 65 CO_2 CONCENTRATION PROFILES IN THE VAPOUR PHASE FOR EXPERIMENTAL RUNS WITH 20 WT% MEA

8.1.1.2. TEMPERATURE PROFILES

The temperature profiles of the absorber column for the two different experimental runs show good repeatability. **Figure 66** shows the vapour- and the liquid temperature profiles and the error bars indicate the variation between results from the two different experimental runs. The shape of the temperature profiles, from the various runs, for both the vapour- and liquid temperatures are in good agreement.

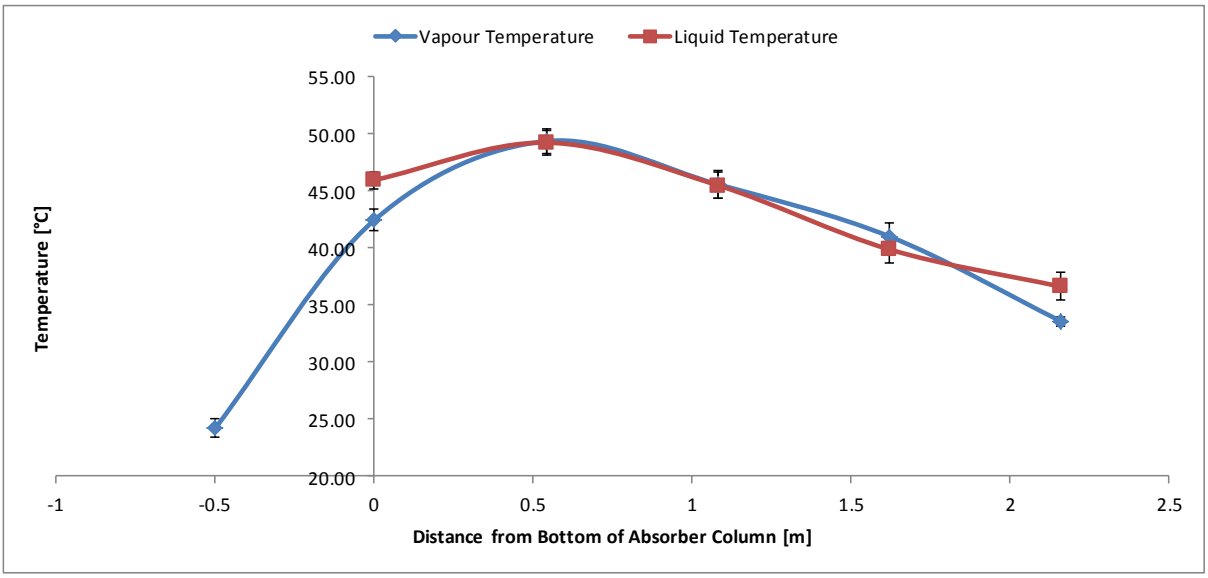

FIGURE 66 TEMPERATURE PROFILES OF THE ABSORBER COLUMN FOR EXPERIMENTAL RUNS WITH 20 WT% MEA

8.1.1.3. SOLVENT REGENERATION ENERGY AND CO_2 CAPURE RATE FOR 20 WT % MEA

The solvent regeneration energy for the two runs performed with 20 wt % MEA showed a variation of only ±0.72% from the mean value for the two experimental runs. The CO_2 capture efficiency showed a variation of ±1.40% from the calculated mean value. These results, as before, show a good repeatability for the two runs performed. However, further investigation was required in order to verify the obtained repeatability. This was done by performing two more experiments with identical operating conditions, using 30 wt % MEA (aq) as the solvent.

8.1.2. EXPERIMENTAL RUNS WITH 30 WEIGHT % MEA [AQ]

For further validation of the repeatability of the pilot plant setup an attempt was made at repeating one of the experimental runs that had a CO_2 capture rate of 92.4%. All operating conditions were kept identical, resulting in a CO_2 capture rate of 91.6%.

8.1.2.1. CO_2 CONCENTRATION PROFILES

The CO_2 concentration profiles for both the experimental runs are shown in **Figure 67**. The gathered concentration profiles once again indicate good repeatability. A maximum deviation of ±3.5% from the mean value was observed. **Table C.1** in Appendix C reports the calculated error percentages.

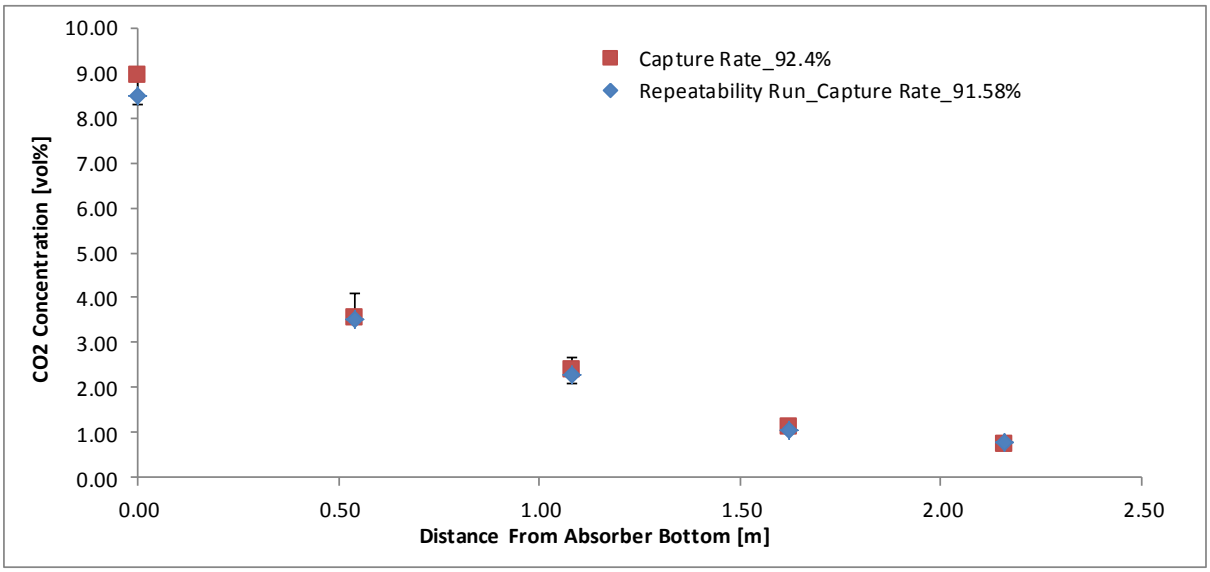

FIGURE 67 CO_2 CONCENTRATION PROFILES FOR REPEATABILITY RUNS WITH 30 WT% MEA

8.1.2.2. SOLVENT REGENERATION ENERGY AND CO_2 CAPTURE RATE

The solvent regeneration energy requirement is one of the key parameters in CO_2 absorption studies. It is thus essential that the pilot plant can also produce repeatable results with respect the mentioned energy requirement.

The solvent regeneration energy requirement is a function of the CO_2 capture rate in the absorption column. **Figure 68** shows the two data points that were the results of the two experimental runs. The results indicate good repeatability with respect to not only the solvent regeneration energy requirement (deviation of ±0.44% from mean value), but also the CO_2 capture efficiency in the absorber column (deviation of ±0.80% from mean value). The fit of the pilot plant data with respect to the curve from the Aspen Plus® simulation, is discussed later in this chapter.

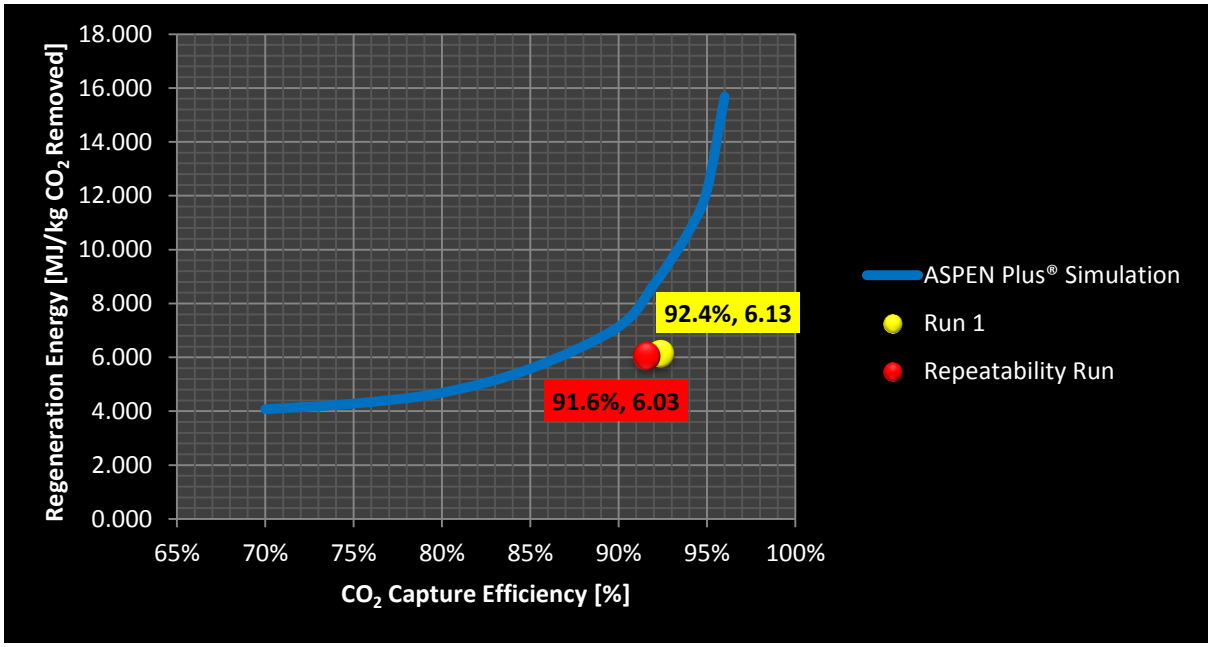

FIGURE 68 RESULTS FROM REPEATABILITY RUNS WITH 30WT% MEA

8.2. PILOT PLANT DATA VERIFICATION AND RESULTS

The pilot plant data verification was performed using aqueous monoethanolamine (MEA) as reactive solvent. Literature data from Mangalapally and Hasse(2011a); Notz et al. (2012) and Wilson et al. (2005, 2003) were used for data verification as their process setups, with regards to column diameter – 0.18 and 0.125 meters respectively – are similar to the pilot plant that was set up in this study. The Aspen Plus® simulation – set up to match the pilot plant configuration and experimental conditions – served as a source of predicted data for further comparison.

8.2.1. PILOT PLANT DATA VERIFICATION EXPERIMENTS

Aqueous MEA (30 wt%) was used for the pilot plant data verification experiments, as this is the most commonly used solvent for CO_2 capture studies. Four experimental runs were performed, gathering a total of 11 steady state data sets. The experimental conditions of all the runs are summarized in **Table 13**.

TABLE 13 EXPERIMENTAL STEADY STATE CONDITIONS OF VERIFICATION EXPERIMENTS

Run #	Steam Valve Position [% OPEN]	Solvent Flow Rate [kg/h]	Gas Flow Rate [kg/h]	L/G-ratio	CO_2 content in Feed Gas [Vol %]
1.1	40.0	228	135 (±4.4)	1.69 (±0.07)	9.18 (±0.33)
1.2	37.5	230	136 (±2.6)	1.69 (±0.04)	8.80 (±0.29)
1.3	35.0	233	139 (±3.1)	1.68 (±0.04)	8.84 (±0.37)
1.4	30.0	231	139 (±3.2)	1.66 (±0.05)	9.22 (±0.56)
2.1	20.0	257	113 (±5.0)	2.28 (±0.11)	8.97 (±0.04)
2.2	15.0	257	117 (±4.3)	2.20 (±0.09)	9.30 (±0.14)
2.3	10.0	266	119 (±3.1)	2.23 (±0.07)	9.33 (±0.12)
3	17.5	267	124 (±4.7)	2.15 (±0.09)	8.64 (± 0.00)
4.1	30.0	250	121 (±4.7)	2.06 (±0.09)	9.48 (±0.12)
4.2	25.0	257	127 (±4.6)	2.03 (±0.08)	9.25 (±0.82)
4.3	20.0	255	130 (±3.6)	1.96 (±0.06)	8.49 (±0.56)

During each run the steam valve position, and thus the energy input for solvent regeneration was varied in order to vary the lean loading of the solvent fed to the top of the absorber column. This in turn has an effect on the CO_2 capture rate in the absorption section of the pilot plant. This method allows data on the solvent regeneration energy and CO_2 capture efficiencies to be gathered at the various steady state conditions.

8.2.2. VERIFICATION OF PILOT PLANT RESULTS WITH LITERATURE DATA

The pilot plant data verification was done by comparing the CO_2 concentration- and temperature profiles of the absorber column to that reported in literature. However, the focus was on reproducing results on the regeneration energy requirement and the CO_2 capture efficiency. This was compared to literature data as well as data from the Aspen Plus® Simulation.

8.2.2.1. CO_2 CONCENTRATION PROFILES

The CO_2 concentration profile for the absorber column varies depending on the lean solvent loading [moles CO_2/moles MEA] and thus also the CO_2 capture rate. One of the experimental runs had a CO_2 capture rate of 92%. **Figure 69** compares the obtained CO_2 concentration profile to that which is reported by Mangalapally and Hasse (2011a).

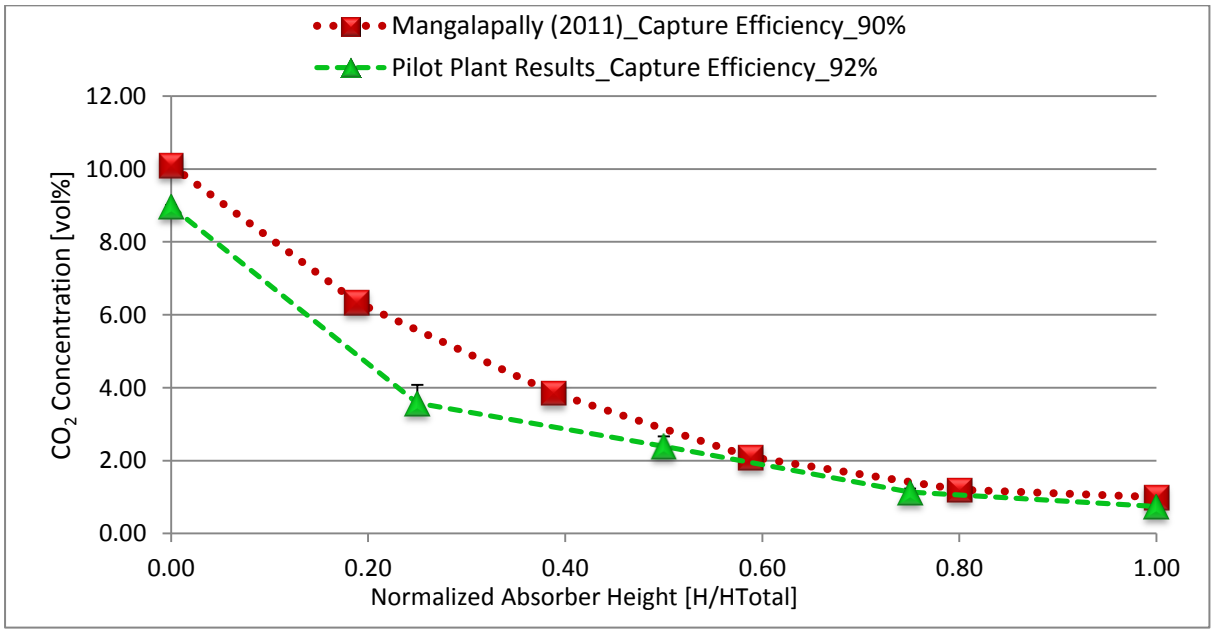

FIGURE 69 COMPARISON OF THE CO_2 CONCENTRATION PROFILES AGAINST A NORMALIZED ABSORBER COLUMN HEIGHT, AT SIMILAR CAPTURE RATES

From **Figure 69** it can be seen that the CO_2 concentration profile follows a similar trend with some deviation at the bottom of the column. The deviation might be explained by a lower CO_2 concentration in the feed gas for the pilot plant experiment performed in this study. Mangalapally and Hasse (2011a) used BX500 packing material compared to the 250Y packing used in these pilot plant studies. Another reason for the observed deviation might be that the preliminary pilot plant experiments were performed at low gas flow rates – in the pre-loading region. A gas flow factor of 1.1 [$Pa^{0.5}$] was used in the pilot plant studies compared to a gas flow factor of 1.6 [$Pa^{0.5}$] used by Mangalapally and Hasse (2011).

The CO_2 gas concentration profiles obtained for lower capture rates deviate from those at higher capture rates. Literature data from Notz et al.(2012) for a capture efficiency of 50% with

the same packing material (250Y-type packing) as what was used in this pilot plant study, is used as validation of the profile obtained from this pilot plant experiment. **Figure 70** shows the comparison between data by Notz et al. (2012) and the pilot plant data.

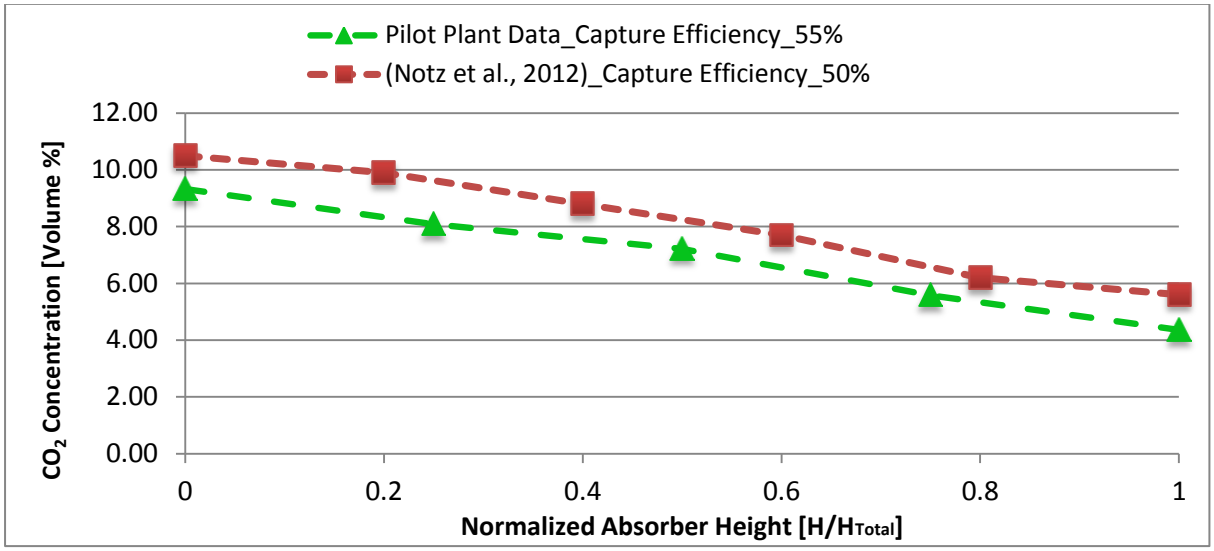

FIGURE 70 COMPARISON OF CO_2 CONCENTRATION PROFILES AT LOW CAPTURE RATES

From **Figure 70** a similar trend for both curves can be observed. However, due to the lower feed concentration in the pilot plant studies it is difficult to directly compare the two curves. **Figure 71** shows the percentage of the captured CO_2 at various normalized column heights. This representation of the data normalizes the effect of the different feed concentrations, allowing for better comparison between the two trends.

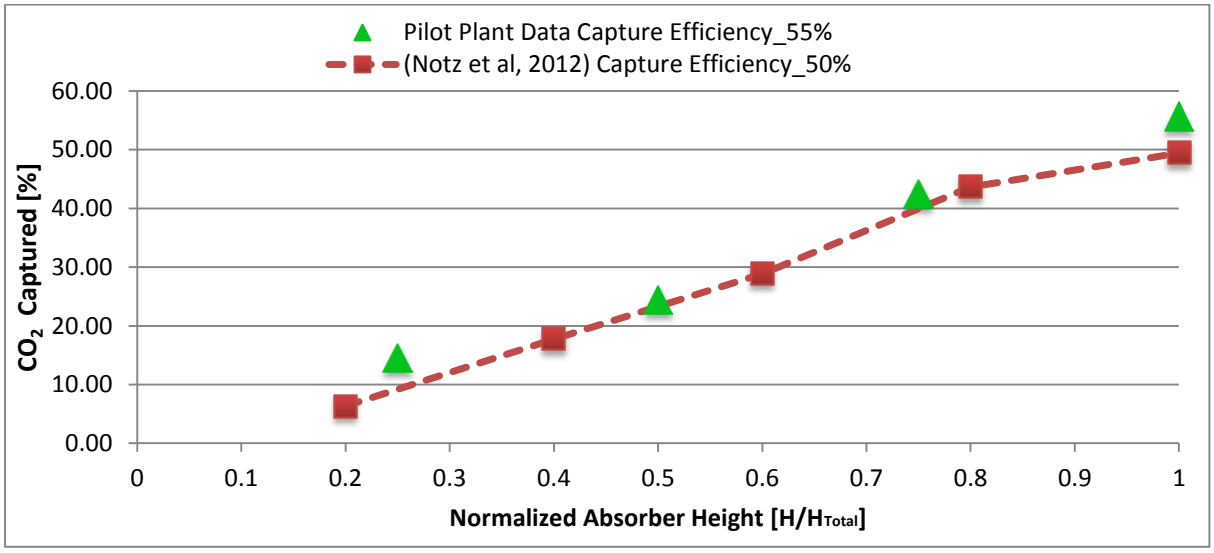

FIGURE 71 COMPARISON OF CO_2 GAS CONCENTRATION PROFILES AT LOW CAPTURE RATES BY CONSIDERING THE AMOUNT OF CO_2 CAPTURED AT VARIOUS HEIGHTS

From **Figure 71** it can be seen that the pilot plant data for the CO_2 gas concentration profiles is in good agreement with what is reported in literature.

8.2.2.2. SOLVENT REGENERATION ENERGY REQUIREMENT

The solvent regeneration energy added to the stripping section is a function of the CO_2 capture rate in the absorber column. Literature reports a drastic increase in the regeneration energy requirement for capture rates above 90% (Wang et al., 2010; Wilson et al., 2005). Even though a 90% capture efficiency is generally aimed for (Mangalapally et al., 2009; Notz et al., 2012), the process specific, steep increase in regeneration energy depicts what would be viable. As shown in work done by Mangalapally and Hasse (2011a) and Notz et al. (2012) the packing material used plays a big part in the capture rate that can be achieved.

Validation runs for the pilot plant were performed using Flexipac 250Y packing material. Notz et al. (2012, 2010) also used 250Y-type packing in an absorber column with an internal diameter of 0.125 meters. Results from the pilot plant experimental runs were compared to the mentioned literature data.

The solvent regeneration energy [MJ/kg CO_2 removed] is calculated from both the reboiler duty [MJ/h] and the amount of captured CO_2 [kg/h]. This gives an indication of the energy required per unit mass of CO_2 for solvent regeneration. **Figure 72** shows the comparison of the pilot plant results to those reported in literature. The pilot plant setup used by Notz et al.(2010) has the constraint of not being able to reach capture rates higher than 88% with 250Y-type packing material.

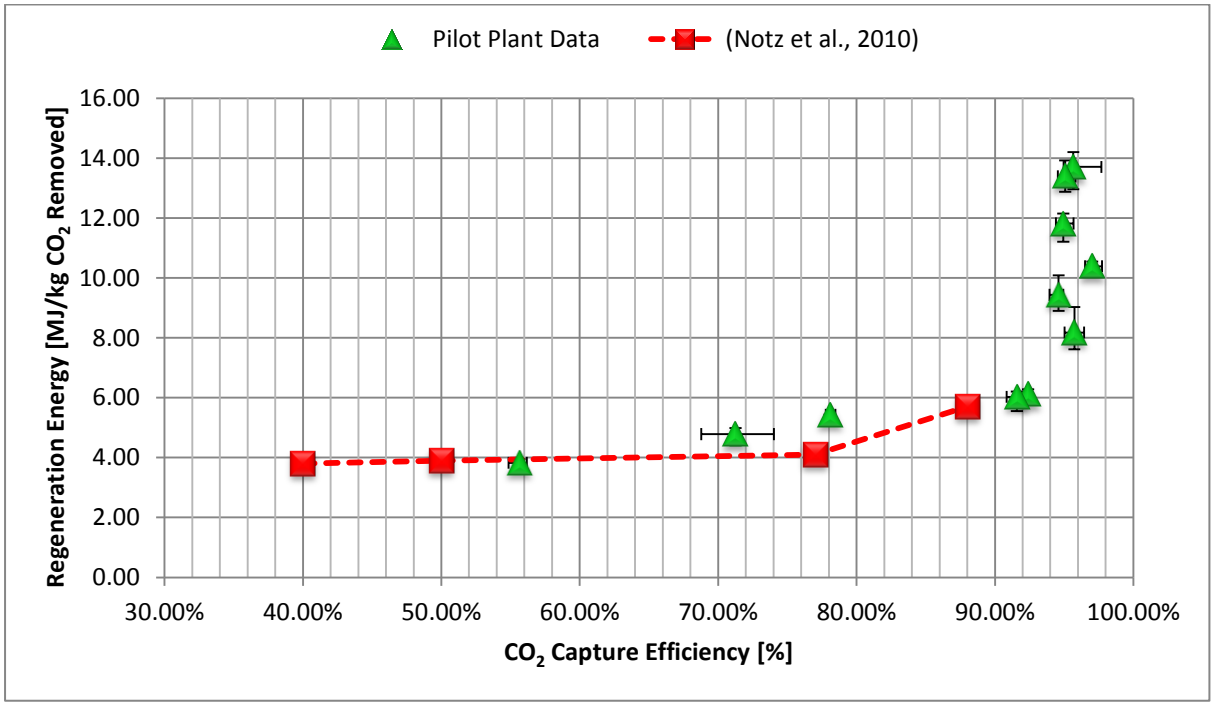

FIGURE 72 COMPARISON OF PILOT PLANT DATA TO PUBLISHED LITERATURE DATA

The pilot plant data corresponds well to the data from literature. Even though for most of the pilot plant experiments the pilot plant achieved higher capture efficiencies than what is reported in literature, it gives a relatively good representation and continuation of the curve reported in literature.

The error bars on the pilot plant data seen in **Figure 72** and **Figure 73** show the possible variation in the data due to fluctuating pilot plant conditions. This will be discussed in detail in Section 8.2.4.2 that follows.

Work by Mangalapally and Hasse(2011a) using the same process equipment as Notz et al.(2010) showed that the use of packing material with a higher surface area – BX500 type packing – not only reduces the energy requirement for solvent regeneration but also allows the reaching of higher capture efficiencies.

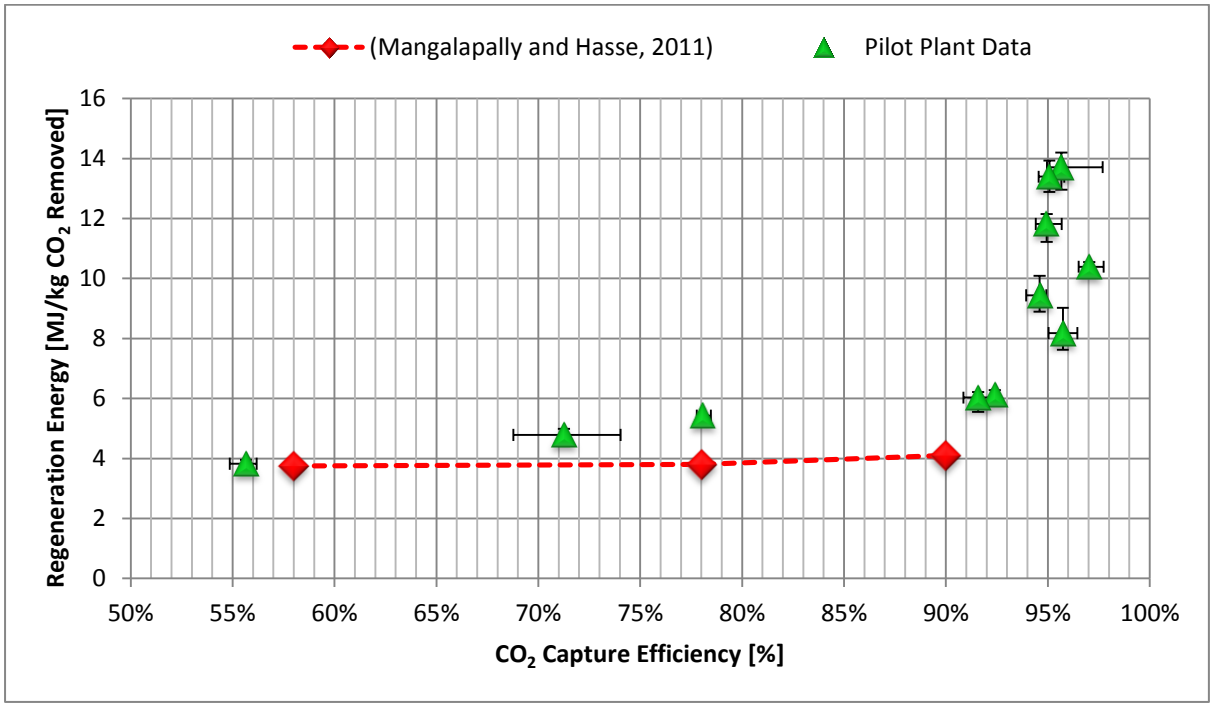

FIGURE 73 COMPARISON OF PILOT PLANT DATA TO PUBLISHED LITERATURE DATA (MANGALAPALLY AND HASSE, 2011)

When comparing the pilot plant results to literature data from Mangalapally and Hasse (2011a), it can be seen the results from the pilot plant show a higher regeneration energy requirement than what is reported. However, this is as expected, seeing that a packing material with a higher surface area would allow capturing more CO_2 with lower solvent regeneration energy requirement.

The considerable increase in steam requirement as observed from the pilot plant results when increasing the CO_2 capture efficiency from 90 to 95 %, agrees with what is reported by Knudsen et al.(2009) for the CASTOR project at the Esbjerg Power Station in Denmark.

8.2.3. VERIFICATION OF PILOT PLANT RESULTS BY COMPARISON TO RESULTS FROM THE ASPEN PLUS® SIMULATION

The Aspen Plus® method of simulation that was developed, discussed and validated in Chapter 6 are used to simulate data to which the pilot plant results at the higher capture rates can be compared.

The simulation was set up to match the pilot plant steady state conditions and an averaged L/G –ratio of 2 was used in simulating the reboiler duties at various CO_2 capture efficiencies. The comparison of the pilot plant data to the simulated data can be seen in **Figure 74**.

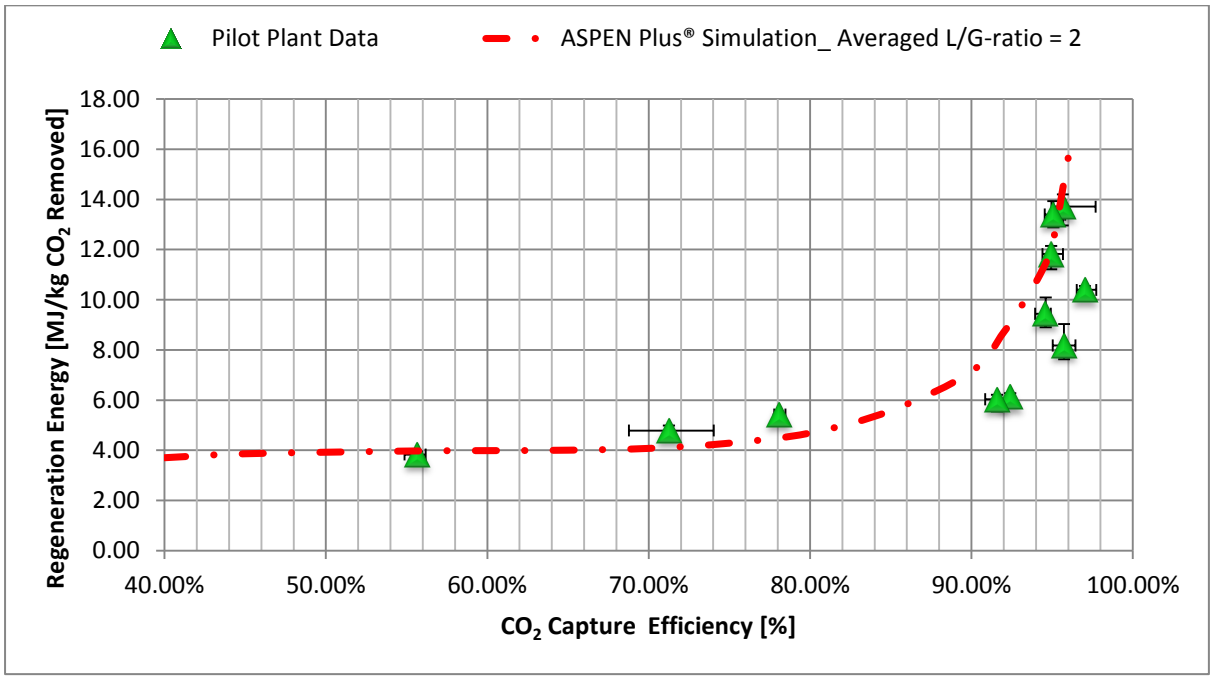

FIGURE 74 COMPARISON OF PILOT PLANT DATA TO RESULTS FROM THE ASPEN PLUS® SIMULATION

From **Figure 74** it can be seen that the pilot plant results and the results from the Aspen Plus® Simulation match relatively well. The Aspen Pus® Simulation also predicts the steep increase in solvent regeneration energy requirement at CO_2 capture rates above 90%.

When considering the plot of regeneration energy vs. L/G-ratio shown in Chapter 6, Section 6.2.1, it can be seen that the optimum L/G-ratio for the simulation is slightly higher than that of the pilot plant setup. One of the reasons for the simulation over predicting some of the data (in **Figure 74**) above a 90% capture rate is the fact that the optimum L/G-ratio for the simulation will be higher than that of the pilot plant setup. Accurate predictions of the optimum L/G-ratio

is one of the limitations of the developed simulating method. Thus a slightly higher L/G-ratio than what was used for the pilot plant experiments would provide better agreement between pilot plant results and results from the simulation.

This can also be seen when considering the results from Run 1 shown in **Figure 75**. An L/G-ratio of 1.7 was used for the first experimental runs. This is slightly lower than what was used for the Aspen Plus® Simulation (L/G-ratio = 2), but the predicted curve from the simulation fits these data points the best.

Figure 75 gives error boundaries on the Aspen Plus® Simulation, the literature data as well as all the pilot plant results. The error boundaries were specified to have a ±10% error in the y-direction (solvent regeneration energy) and a ±3% error in the x-direction (CO_2 capture rate) as this contains most of the pilot plant results for the entire range of capture efficiencies.

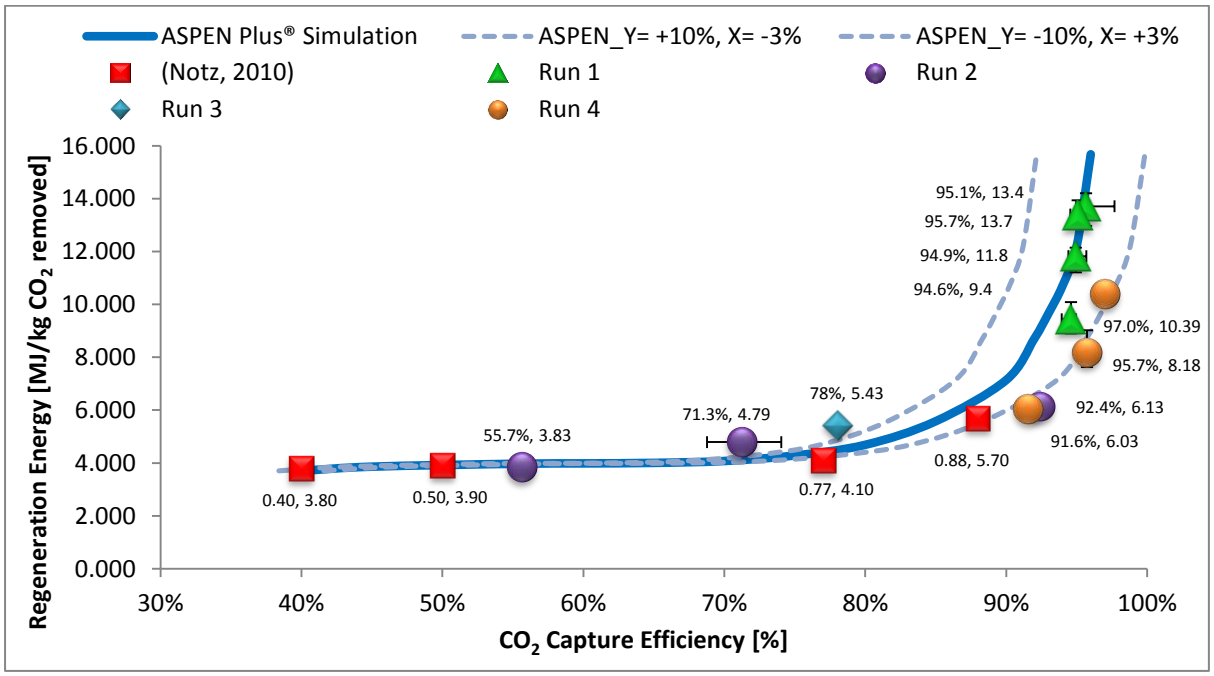

FIGURE 75 ERROR BOUNDARIES ON THE ASPEN SIMULATION CONTAINING ALL GATHERED PILOT PLANT DATA

It can be seen from **Figure 75** that almost all of the pilot plant data falls within the specified error boundaries on the Aspen Plus® Simulation. This serves as preliminary validation for the obtained pilot plant results. With further pilot plant optimization the curve presented here can be refined by properly investigating the lower capture rates. The effect of varying the L/G-ratio in the absorber column on the capture rate and solvent regeneration energy requirement should also be investigated.

A discussion on all the parameters that influence the regeneration energy requirement and the CO_2 Capture rate will be presented in the next section.

8.2.4. PARAMETERS THAT INFLUENCE THE SOLVENT REGENERATION ENERGY REQUIREMENT

There are a few key parameters that influence the final pilot plant results on the regeneration energy and the CO_2 Capture rates. These include the liquid- to-gas (L/G) ratio in the absorber column, variation in the steady state mass flow rate of the feed gas and the variations in the feed gas CO_2 concentration.

8.2.4.1. EFFECT OF L/G-RATIO ON THE REGENERATION ENERGY REQUIREMENT

Finding the optimum L/G-ratio with regards to the energy requirement for solvent regeneration is the key to the optimisation of the pilot plant operating conditions. Mangalapally and Hasse (2011a); Mangalapally et al. (2009) and Notz et al. (2012) used the method of first optimising the L/G-ratio for the specific pilot plant setup, before investigating any other parameters that influence the regeneration energy requirement. This stepwise optimisation procedure aids in finding the optimal operating conditions which require the least amount of energy addition for solvent regeneration.

The method however requires that the CO_2 capture efficiency be set to a predetermined value while the liquid circulation rate between the two columns is adjusted to vary the L/G-ratio. In order to control the CO_2 capture efficiency to a predetermined value one would need to constantly adjust the energy input until the required capture efficiency is achieved. This was done for each investigated L/G-ratio.

In this pilot plant study the experiments were mainly focused on seeing the relationship between the solvent regeneration energy requirement and the CO_2 capture efficiency, with a secondary aim of investigating the effect of L/G-ratio on the regeneration energy requirement. Experiments were set up to allow for 2 different L/G ratios that would provide preliminary results on the effect of L/G –ratio on the energy requirement.

Figure 76 compares the data obtained from pilot plant experiments to those published in literature (Notz et al., 2010). From **Figure 76** it can be seen that the pilot plant data follows the same expected decrease in regeneration energy requirement with an increasing L/G-ratio. Note however that the pilot plant data was gathered at a capture efficiency of 95% while data by Notz et al. (2010) is reported to be at a capture efficiency of 90%. This has resulted in the higher regeneration energy requirement observed.

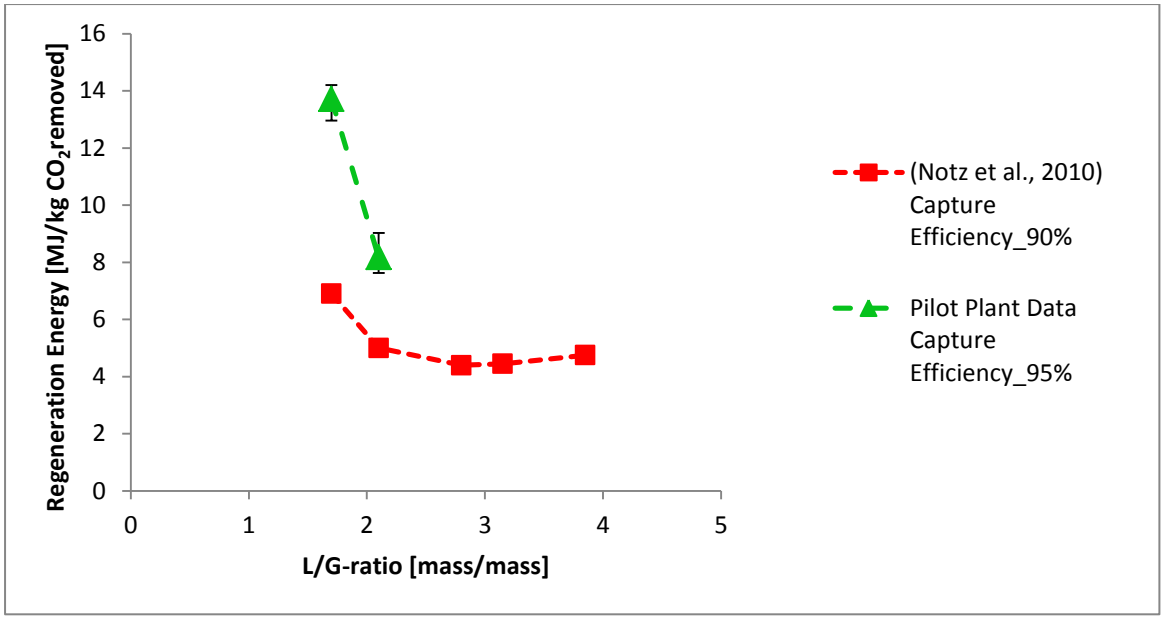

FIGURE 76 EFFECT OF THE L/G-RATIO ON THE REQUIRED SOLVENT REGENERATION ENERGY

The pilot plant results were also compared to results generated using the Aspen Plus® Simulation. **Figure 77** shows the comparison between the pilot plant data and the Aspen Plus® Simulation.

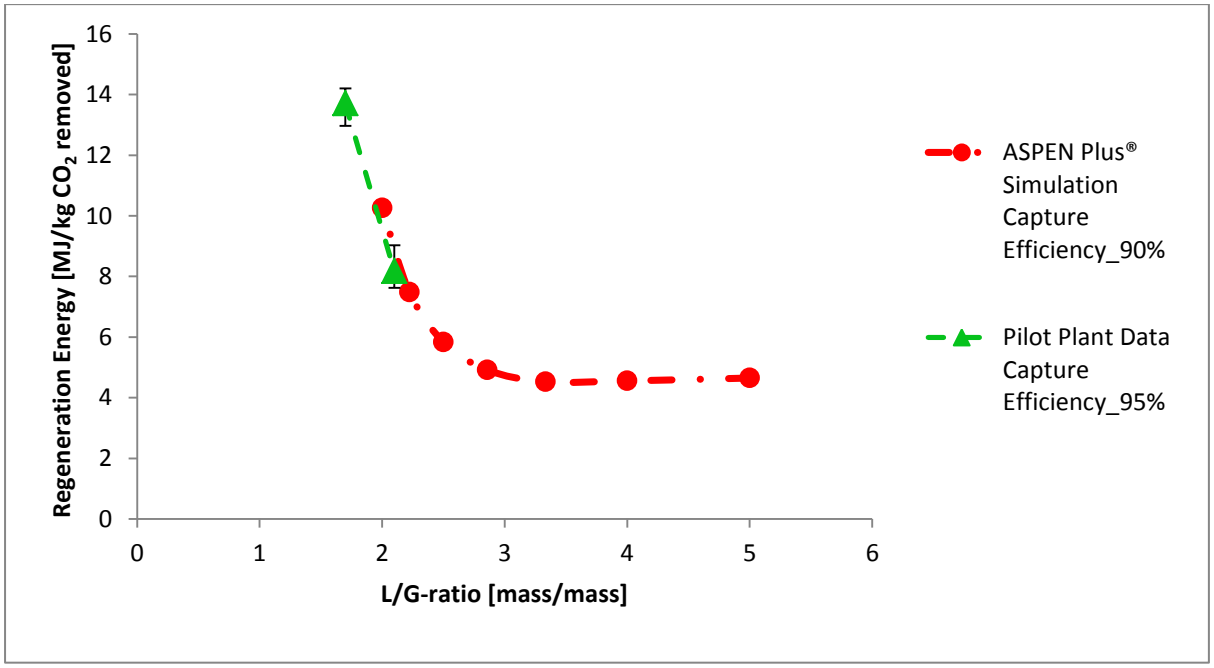

FIGURE 77 COMPARISON OF PILOT PLANT DATA TO RESULTS FROM THE ASPEN PLUS® SIMULATION

Due to the tendency of the ASPEN Plus® Simulation to over predict the regeneration energy at lower L/G-ratios (as seen in Section 6.2.1.) the simulation was set up for a capture rate of 90% rather than 95%. It is clear from **Figure 77** that the pilot plant data corresponds well with the predicted regeneration energy from the Aspen Plus® Simulation.

The observation made from **Figure 77** may prove to be useful once the focus of the pilot plant experiments shift from validation towards optimisation. The ability of the Aspen Plus® Simulation to accurately predict the steady state conditions of the pilot plant setup means that most of the optimisation process can be done using Aspen Plus®. Pilot plant experiments can then only focus on validating the optimisation results as obtained by simulation. This will reduce the time spent and cost related to performing the experiments.

When considering **Table 13**, the variation in the L/G ratio for the various experimental runs can be seen. Due to the shape of the curve seen in **Figure 77** it is evident that at lower L/G-ratios a slight variation in the ratio will lead to a large variation in the regeneration energy requirement. Apart from possible inaccuracies in the Aspen Plus® simulation, this might serve as further explanation for the deviation of the pilot plant results from the curve simulated using Aspen Plus® (**Figure 74** and **Figure 75**).

Figure 78 further supports this theory by representing the results from the eleven pilot plant runs in a three dimensional space. From this plot it is clear that with increasing L/G-ratio there is a reduction in the regeneration energy requirement at similar capture rates. This is most clear when considering the four bars at the highest capture rates.

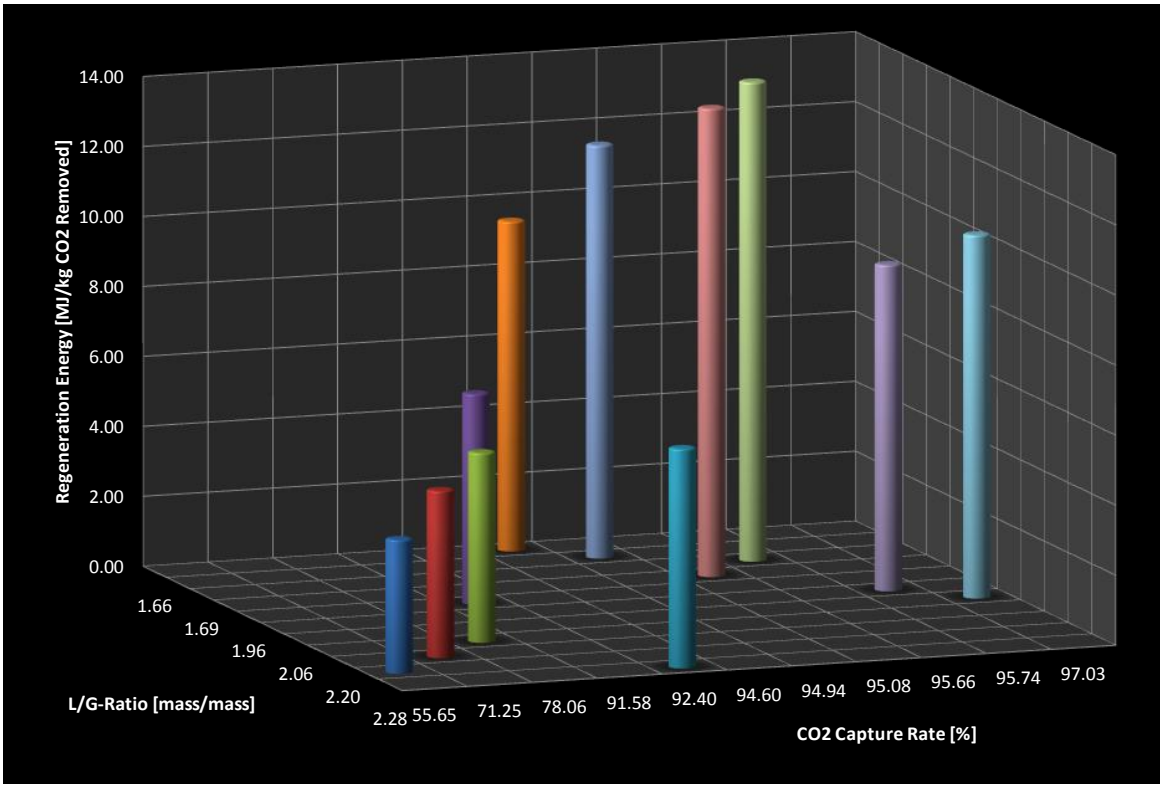

FIGURE 78 3D REPRESENTATION OF THE PILOT PLANT RESULTS SHOWING TEH EFFECT OF VARIATION IN THE L/G-RATIO ON THE REGENERATION ENERGY AND THE CO_2 CAPTURE RATE

Due to the fact that it is problematical to experimentally set up the plot of L/G-ratio vs. the regeneration energy requirement (as seen in **Figure 77**), an alternative approach was followed in obtaining a better fit for the Aspen Plus® model on the experimental data gathered at L/G-ratios close to 2.

The first four runs were performed at L/G-ratios of approximately 1.7. An Aspen Plus® Simulation for a similar L/G-ratio was set up to match the regeneration energy requirement of the pilot plant by varying the CO_2 Capture efficiency in the absorber column. It was found that the simulation yields, on average, capture efficiencies 4% lower than what was gathered from the pilot plant experiments. **Figure 79** shows the results obtained from the Aspen Plus® Simulation.

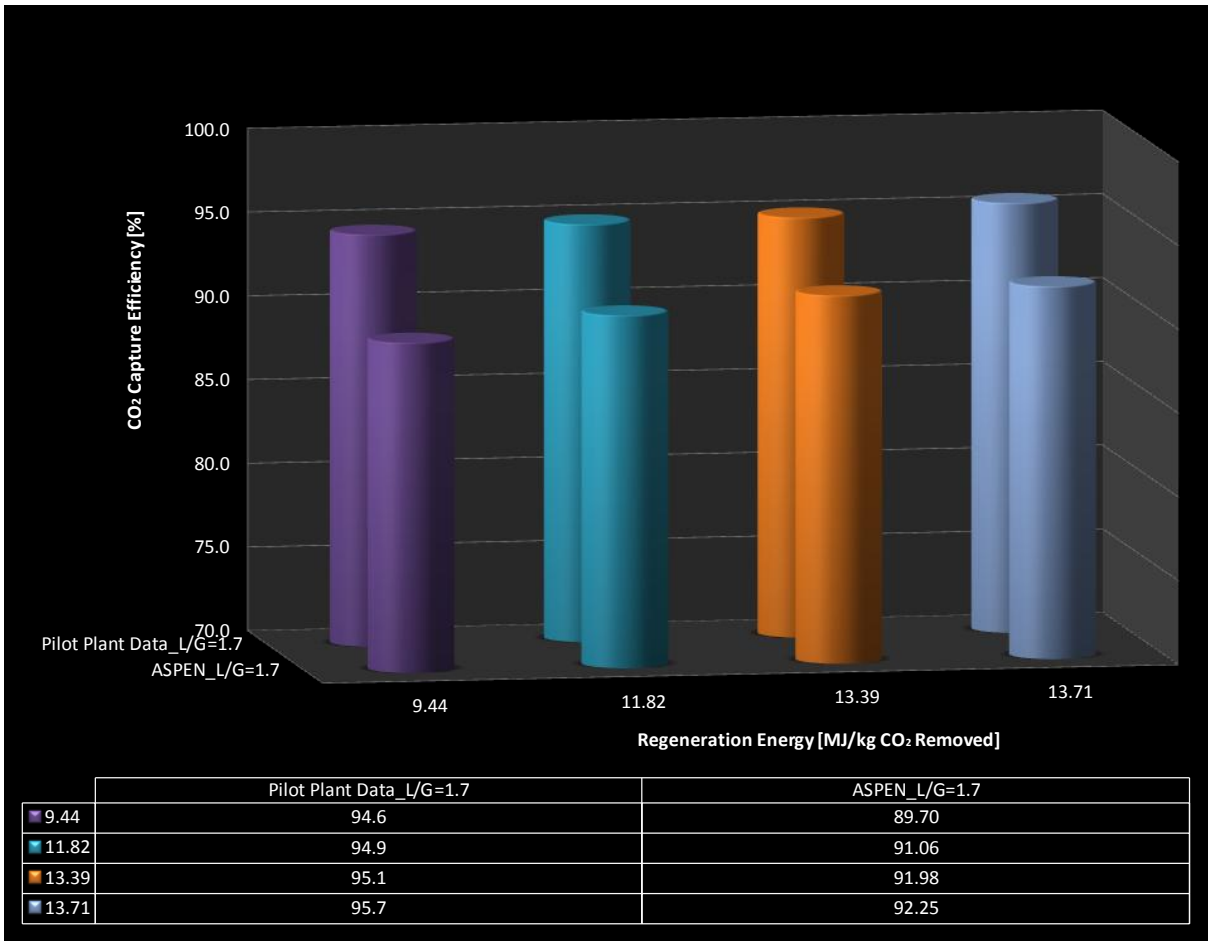

	Pilot Plant Data_L/G=1.7	ASPEN_L/G=1.7
9.44	94.6	89.70
11.82	94.9	91.06
13.39	95.1	91.98
13.71	95.7	92.25

FIGURE 79DETERMINING THE ERROR IN THE ASPEN SIMULATION PREDICTIONS OF CAPTURE EFFICIENCIES WHEN COMPARED TO PILOT PLANT DATA

Based on the assumption that for similar L/G-ratios, and at matched regeneration energy requirements, the Aspen Plus® Simulation will under-predict the CO_2 capture efficiency with about 4 %, the comparison plot between the pilot plant- and simulation results were re-investigated.

Figure 80 shows the results from adding 4% to the predicted CO_2 capture efficiency from the Aspen Plus® Simulation. The adapted model is compared to the experimental runs that had an L/G-ratio close to 2 and a capture rate above 90%. It can be seen that when the simulation is adapted for the error in predicting the CO_2 capture efficiency at removal efficiencies above 90%, it fits the pilot plant data very well. The fit of the corrected Aspen Plus® model can further be described by having an R^2-value of 0.965.

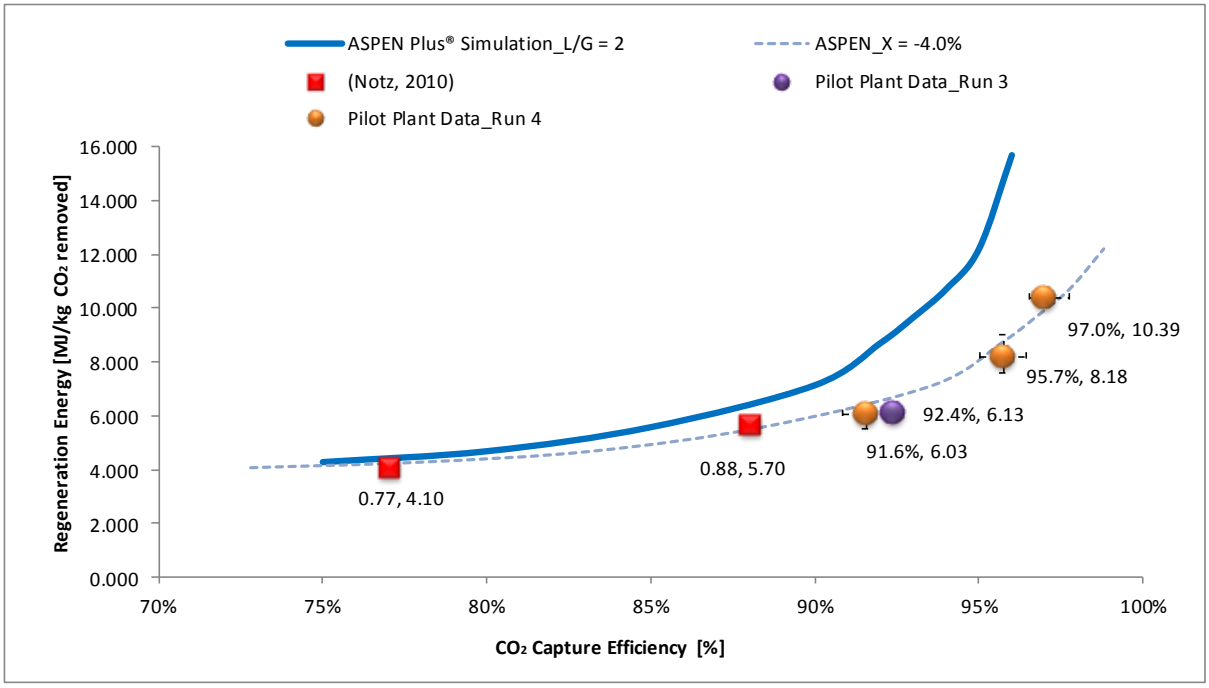

FIGURE 80 COMPARING PILOT PLANT RESULTS TO RESULTS FROM THE ASPEN PLUS® SIMULATION AT L/G-RATIOS OF 2.0 (±0.1)

From this the conclusion can be made that to some extent, the plot of L/G-ratio vs. the regeneration energy requirement for the pilot plant can be generated relatively accurately without having to perform a full range of L/G-ratio experiments. The simulation will also allow one to obtain the curve at various capture rates. This will provide insight into how the plot of L/G-ratio vs. regeneration energy varies with CO_2 Capture efficiency.

Figure 81 gives a three dimensional plot showing the prediction of the corrected Aspen Plus® model at an L/G-ratio of 2. When comparing the results from the simulation to the pilot plant results at other L/G-ratios, it gives a preliminary idea of what the plot of L/G-ratio vs. regeneration energy would be for the various capture efficiencies. The curves shown in **Figure 81** are just a guideline for visualizing the plot of L/G-ratio vs. solvent regeneration energy at the various CO_2 capture efficiencies. By combining simulation results with pilot plant results in the way that it is done in **Figure 81**, the number of experimental runs that would be required for performing a full parametric variation study can be considerably reduced.

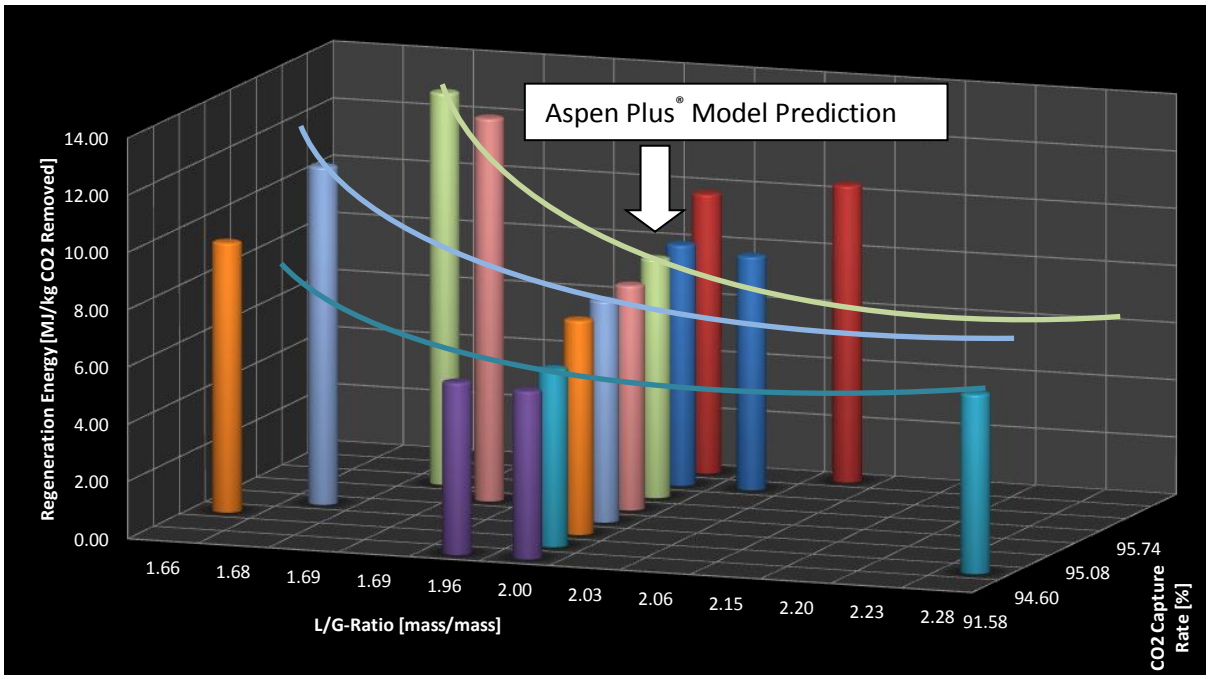

FIGURE 81 COMPARISON OF ASPEN PLUS® CORRECTED MODEL PREDITION TO PILOT PLANT DATA

8.2.4.2. EFFECT THE FLUID DYNAMIC LOAD OF THE ABSORBER COLUMN ON THE SOLVENT REGENERATION ENERGY REQUIREMENT

The concept of what the effect of the fluid dynamic load in the absorber column has on the solvent regeneration energy requirement was introduced in Chapter 6. Variation studies by Mangalapally and Hasse (2011) as well as Notz et al. (2012) considered experimentally the effect of a variation in the fluid dynamic load on the solvent regeneration energy requirement. This was done by performing a number of experiments, keeping the L/G-ratios and the CO_2 capture efficiency of all the experiments at a constant value, but varying the gas- and liquid flow rates in the absorber column.

Figure 82 shows the results that were obtained from both the studies mentioned above; the relationship between the gas flow factor and the solvent regeneration energy requirement is shown. It can be seen that with a decrease in the fluid dynamic load of the absorber column there is a decrease in the energy requirement for solvent regeneration. This is explained by the lower gas flow rate carrying less CO_2 that needs to be transferred from the gas phase to the liquid phase. Due to keeping the CO_2 capture efficiency constant for all experiments, the driving force required for the reduced amount of CO_2 to be transferred, into- and from the liquid, is reduced. This leads to the observed reduction in the amount of steam required for solvent regeneration (Mangalapally and Hasse, 2011).

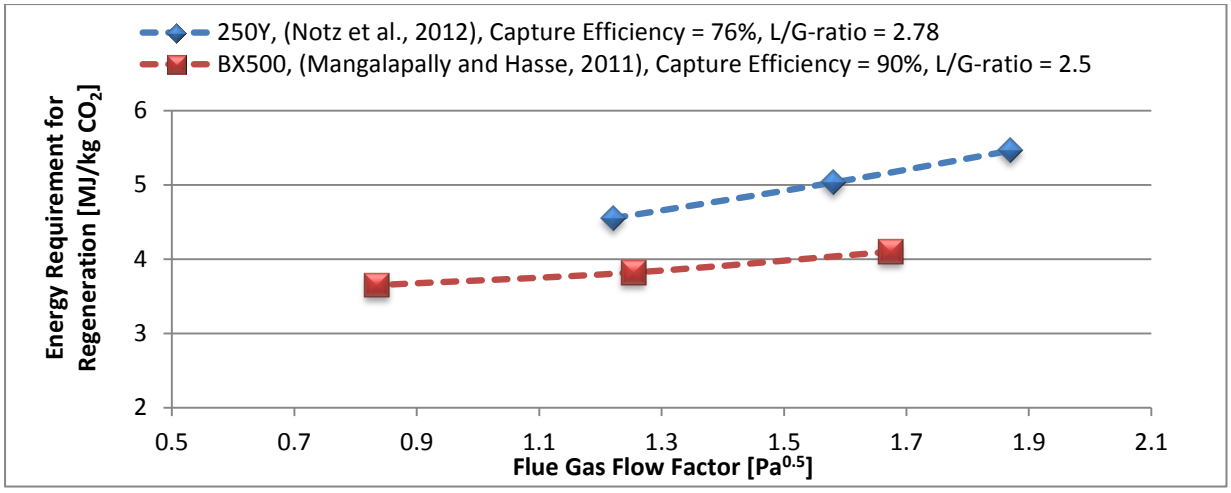

FIGURE 82 EFFECT OF A VARIATION IN THE FLUID DYNAMIC LOAD OF THE COLUMN ON THE SOLVENT REGENERATION ENERGY REQUIREMENT

From **Figure 82** it can be seen that the effect of the fluid dynamic load on the solvent regeneration energy requirement is more prominent for the 250Y-type packing when compared to the BX500-type packing material. However, when the observed effect is compared to the effect of L/G-ratio on the solvent regeneration energy the conclusion can be made that the effect of the L/G-ratio overshadows that of the fluid dynamic load, especially at lower L/G-ratios.

Figure 83 shows the result from one of the pilot plant experiments, compared to the results reported by Notz et al. (2012) with 250Y-type packing material. When comparing the results, the L/G-ratio used in both experiments also needs to be considered. Seeing that the L/G-ratio for the pilot plant experiment was lower (2.15 [kg/kg]) than the 2.78 [kg/kg] used by Notz et al. (2012), an increased solvent regeneration energy requirement is what would be expected. Further pilot plant studies are, however, required to properly investigate the effect of the fluid dynamic load on the solvent regeneration energy requirement.

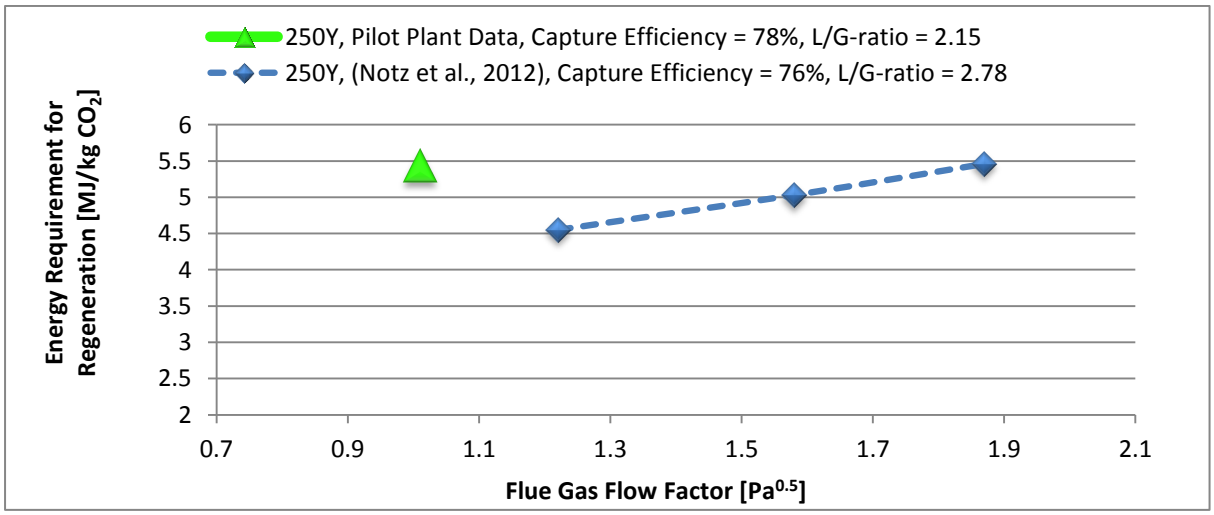

FIGURE 83 DATA POINT GATHERED FROM PILOT PLANT EXPERIMENTS COMPARED TO CONDITIONS USED BY NOTZ ET AL. (2012)

8.2.4.3. INFLUENCE OF STEADY STATE VARIATIONS ON SOLVENT REGENERATION ENERGY REQUIREMENT AND CO_2 CAPTURE EFFICIENCY

Some fluctuations in the steady state conditions have a significant influence on the regeneration energy requirement and the CO_2 capture efficiency. These mainly include fluctuation in the mass flow rate of the gas that is fed to the absorber column, as well as oscillation in the feed gas CO_2 concentration.

The feed gas CO_2 concentration directly influences the CO_2 capture efficiency. If there are major fluctuations in the CO_2 concentration at the assumed steady state condition, the uncertainty of the calculated CO_2 capture efficiencies increase considerably. **Table 14** shows the percentage error for the capture efficiencies of all experimental runs.

TABLE 14 ERRORS IN CALCULATED CO_2 CAPTURE EFFICIENCIES DUE TO FLUCTUATIONS IN THE FEED GAS CO_2 CONCENTRATION

Run #	CO_2 Capture Efficiency [%]			Error [%]	
	Negative	Average	Positive	Negative	Positive
Run 1.1	94.95	95.66	97.69	0.74%	2.11%
Run 1.2	94.54	95.08	95.81	0.56%	0.77%
Run 1.3	94.41	94.94	95.68	0.56%	0.78%
Run 1.4	93.94	94.60	94.93	0.70%	0.35%
Run 2.1	92.27	92.40	92.51	0.15%	0.12%
Run 2.2	68.78	71.25	74.04	3.48%	3.91%
Run 2.3	54.86	55.65	56.18	1.42%	0.95%
Run 3.0	77.78	78.06	78.47	0.36%	0.52%
Run 4.1	96.52	97.03	97.74	0.53%	0.73%
Run 4.2	95.03	95.74	96.45	0.74%	0.74%
Run 4.3	90.85	91.58	92.45	0.80%	0.94%

When considering the calculated confidence intervals in **Table 14**, it can be seen that all intervals are approximately ±1%, with Run 2.2 being an exception. There was some oscillation in the CO_2 feed concentration during the assumed steady state period for Run 2.2 leading to the larger confidence interval.

The influence of fluctuations in the steady state condition on the regeneration energy requirement is even more severe. The reason for this is that the regeneration energy requirement is dependent on all of the following:

- Mass flow rate of the gas;
- L/G-ratio (also dependent on the mass flow rate of the gas);
- CO_2 concentration in the gas feed and gas effluent from the top of the column;

- Lean loading of the solvent;
- Absorber Feed Temperature;
- Stripping column Feed temperature

These parameters are also interdependent on one another, making it challenging to estimate the confidence intervals for the regeneration energy requirement. The effect of variation of L/G-ratio has been discussed in the previous section.

As the most significant contributors to error in regeneration energy calculations, the steady state variation in the mass flow rate of the gas stream and the CO_2 concentration has been used to set up confidence intervals for the regeneration energy requirement. **Table 15** shows these calculated confidence intervals.

TABLE 15 CALCULATED CONFIDENCE INTERVALS BY TAKING INTO ACCOUNT BOTH STEADY STATE VARIATIONS IN MASS FLOW RATE OF THE FEED GAS AS WELL AS THE CO_2 CONCENTRATION OF THE FEED GAS

Run #	Solvent Regeneration Energy [MJ/kgCO_2removed]			Error [%]	
	Negative	Average	Positive	Negative	Positive
Run 1.1	12.96	13.71	14.20	5.4%	3.6%
Run 1.2	12.88	13.39	13.93	3.8%	4.0%
Run 1.3	11.22	11.82	12.15	5.1%	2.8%
Run 1.4	8.90	9.44	10.09	5.7%	6.9%
Run 2.1	5.99	6.13	6.28	2.2%	2.5%
Run 2.2	4.41	4.79	4.99	7.9%	4.3%
Run 2.3	3.59	3.83	3.95	6.2%	3.2%
Run 3.0	5.26	5.43	5.44	3.2%	0.1%
Run 4.1	10.16	10.39	10.55	2.2%	1.5%
Run 4.2	7.62	8.18	9.03	6.8%	10.4%
Run 4.3	5.55	6.03	6.21	8.0%	3.0%

From **Table 15** it can be seen that the confidence intervals are all approximately ±5%, with the exception of Run 4.2. The large confidence interval for Run 4.2 is due to the combined effect of relatively large variations in the CO_2 concentration of the feed gas as well as variation in the mass flow rate of the feed gas.

8.2.5. EFFECT OF SOLVENT LEAN LOADING AND CO_2 CAPTURE RATE ON THE CO_2 CONCENTRATION PROFILES IN THE ABSORBER COLUMN

In this work no liquid samples were analysed for determining the lean solvent loadings at various steady state conditions. However, the effect of lean solvent loading can qualitatively be investigated by considering the CO_2 gas concentration profiles of the absorber column. This is done at various CO_2 capture rates and thus also at different lean solvent loadings.

Wilson et al. (2005) reports the CO_2 gas concentration profiles for the absorber column at various lean solvent loadings. **Figure 84** shows only three of the mentioned curves at three different lean solvent loadings.

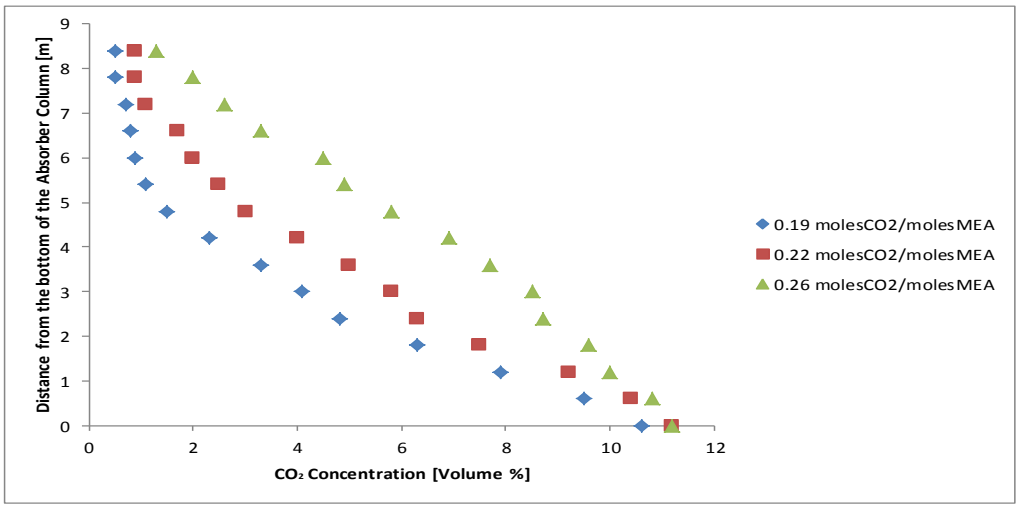

FIGURE 84 CO_2 CONCENTRATION ABSORBER PROFILES AT VARIOUS LEAN SOLVENT LOADINGS (WILSON ET AL., 2005)

Figure 85 shows the CO_2 gas concentration profiles that were obtained in this pilot plant study at various CO_2 capture efficiencies.

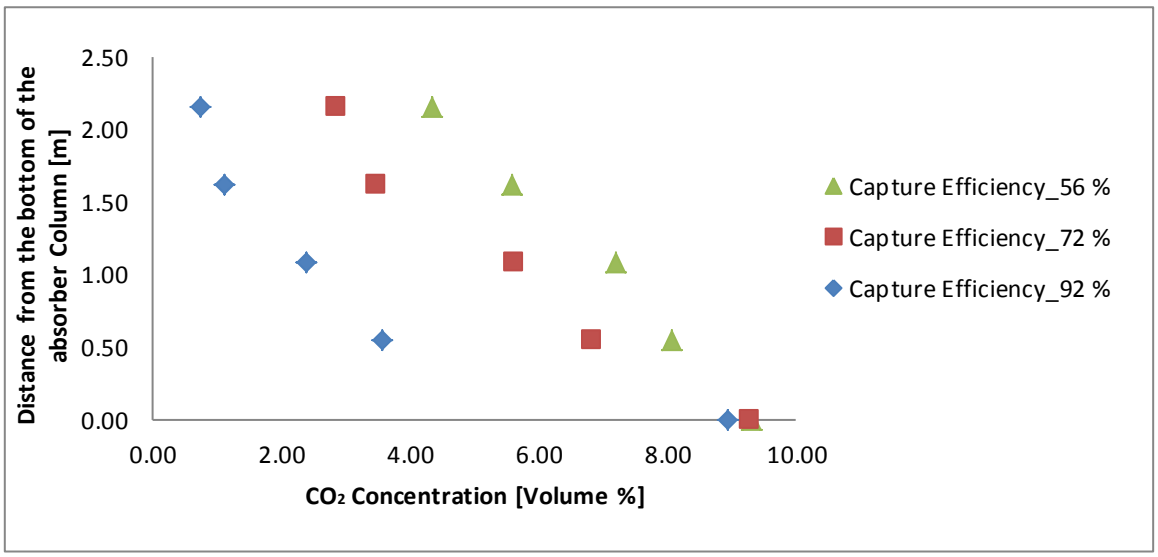

FIGURE 85 CO_2 CONCENTRATION PROFILES FOR THE PILOT PLANT ABSORBER COLUMN AT VARIOUS CO_2 CAPTURE EFFICIENCIES

When considering **Figure 84** it can be seen that as the lean loading increases the CO_2 gas concentration profiles tend to become more linear across the absorber column height. The same trend can be seen in **Figure 85**. With a decreasing CO_2 capture rate the CO_2 gas concentration profile across the absorber height tends to be more linear. This increase in linearity is expected due to the fact that a richer solvent will contain less MEA for reaction with CO_2 in the bottom section of the column. The reaction area will thus be distributed across the entire length of the absorber column, leading to the observed, more linear trend.

By investigating the CO_2 concentration profiles of the process gas in the absorber column, the relationship between the CO_2 capture efficiency and the lean solvent loading can be better understood. Due to the fact that higher capture efficiency requires a lower lean solvent loading, the effect of an increasing lean solvent loading on the CO_2 gas concentration profile in the absorber column, is similar to that of a decreasing CO_2 capture efficiency.

8.2.6. COLUMN TEMPERATURE PROFILES

8.2.6.1. COMPARISON TO LITERATURE DATA

The reaction in the absorber column is exothermic and thus a temperature bulge would be expected along the column height. **Figure 86** shows the temperature trend obtained from one of the pilot plant runs and compares it to literature data by (Wilson et al., 2003).

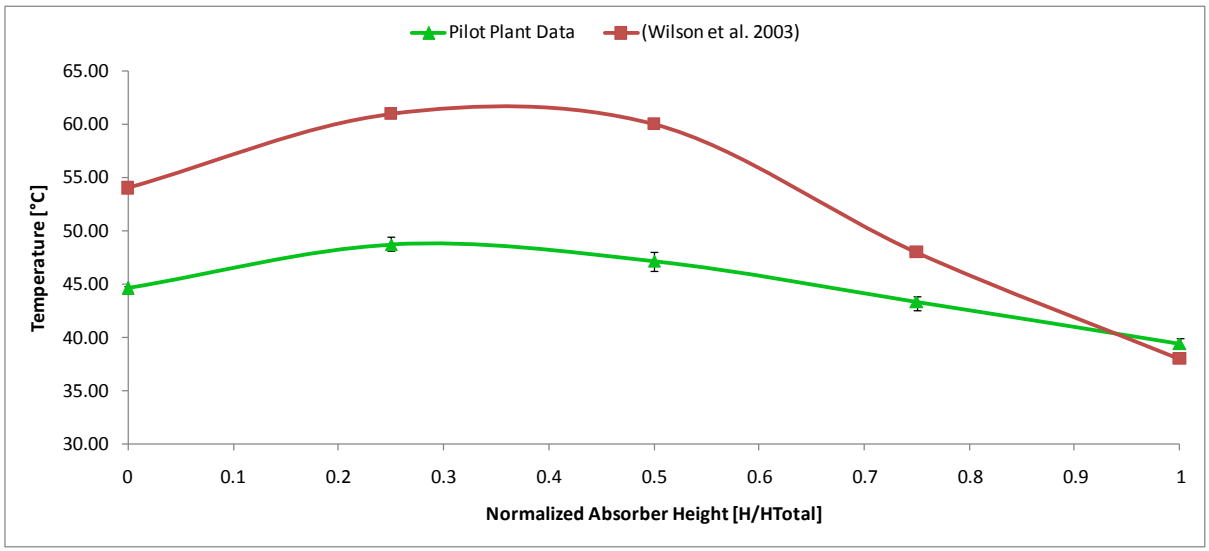

FIGURE 86 ABSORBER TEMPERATURE PROFILE COMPARISON

From **Figure 86** it can be seen that the curve follows a similar trend when compared to data by (Wilson et al., 2003). The higher temperature bulge in the data presented by Wilson et al. (2003), can be explained by the higher solvent feed temperature as well as a higher CO_2 concentration in the feed gas (15 volume %).

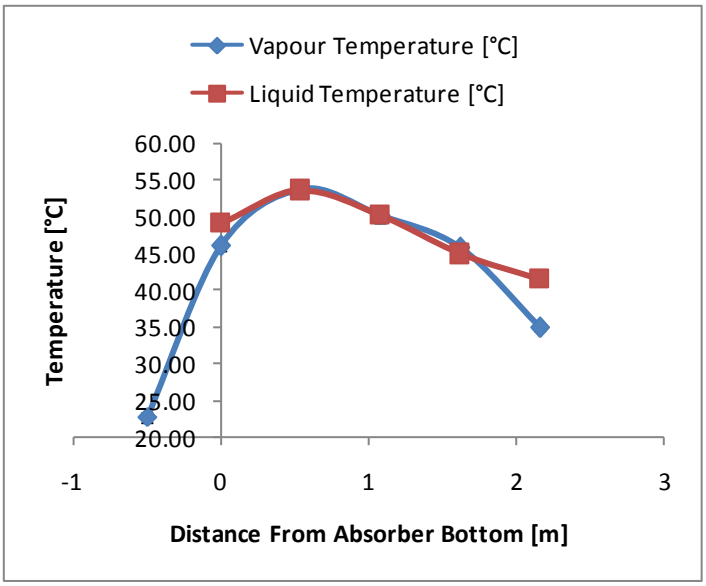

FIGURE 87 VAPOUR- AND LIQUID TEMPERATURE PROFILES FORM THE PILOT PLANT STUDY FOR THE ABSORBER COLUMN

Figure 87 shows an example of the general temperature trends that were obtained from the pilot plant experiments. These temperature profiles display a main temperature bulge at the bottom of the absorber column. Thus, most of the CO_2 that is fed to the column reacts in the bottom section causing the temperature bulge.

In contrast, the majority of the literature (Dugas et al., 2009; Faber et al., 2011; Mangalapally and Hasse, 2011a; Mangalapally et al., 2009; Mejdell et al., 2011; Mores et al., 2010; Notz et al., 2012; Zhang et al., 2009) reports temperature profiles with the main temperature bulge to the top of the absorber column.

With initial water tests in the absorber column it was found that the wall flow towards the bottom of the column was dominant. This was confirmed visually by observing the walls of the glass absorber column. The column was taken down prior to commissioning with MEA and redistribution units were installed every 0.54 meters (after each one of the sample locations). This ensures that the solvent distribution over the packing material is consistent over the entire length of the absorber column. Thus wall flow at the bottom of the column is eliminated and conditions for the liquid phase absorption reaction are favoured, resulting in the temperature bulge at the bottom of the column. This can be one of the reasons for the inconsistency between the profiles from this pilot plant study and those in literature.

Work by (Jockenhövel and Schneider, 2011) on the Siemens Capture Process Pilot Plant uses an absorber column with internal diameter of 200mm, matching the diameter used in this pilot plant study. The experimental absorber temperature profiles from this study also report the temperature bulge in the absorber column to be towards the bottom of the column for capture

efficiencies above 90%. The temperatures are however not reported quantitatively, making a direct comparison to the pilot plant data impossible.

Figure 88 shows a comparison of the temperature profile for the stripping column with published literature data by (Dugas, 2006). Even though the reported literature data regenerates the solvent at higher temperatures the general temperature trend is very similar.

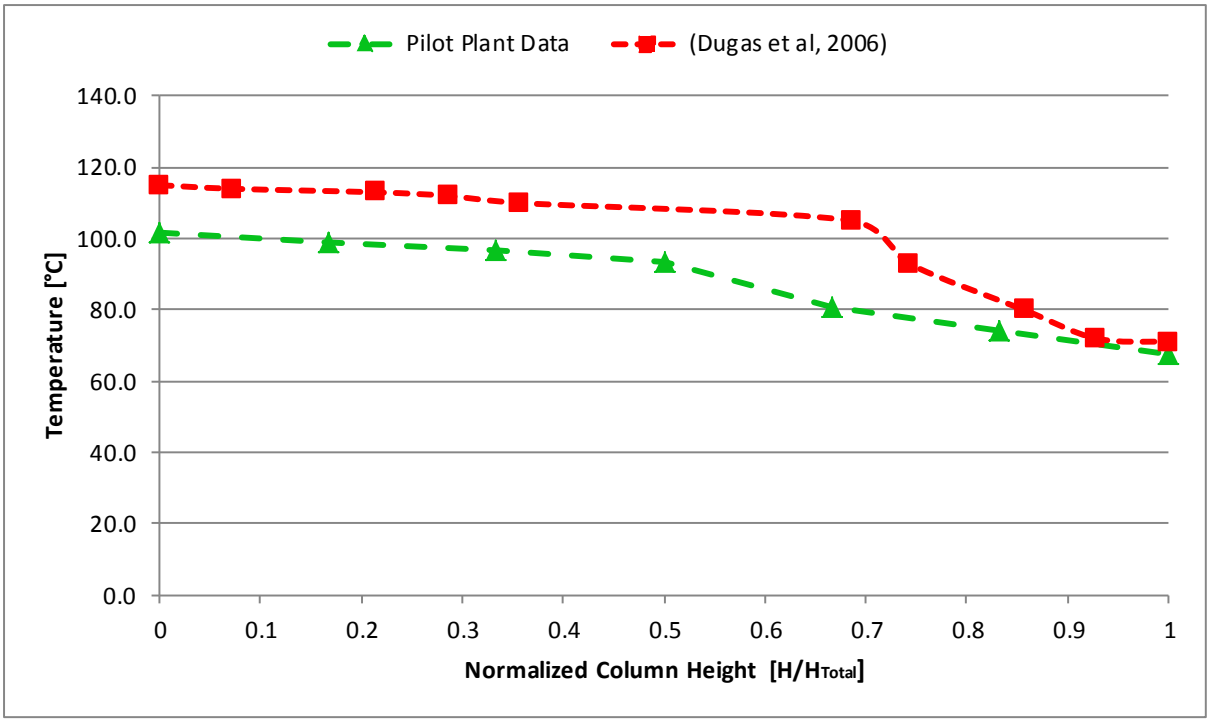

FIGURE 88 COMPARING STRIPPING COLUMN TEMPERATURE PROFILE TO LITERATURE DATA

8.2.6.2. EFFECT OF THE CO_2 CAPTURE RATE ON THE COLUMN TEMPERATURE PROFILES

The effect of the CO2 capture efficiency on the absorber liquid temperature profiles is shown in Figure 89. It can be seen that even though there is a slight increase in the feed temperature for higher capture rates, a larger temperature bulge is displayed. This is in accordance with the fact that at higher capture rates, the steady state lean solvent loading will be less, and thus more solvent will react exothermically with the CO2 that is fed to the bottom of the column. This will result in the display of a higher temperature bulge. The flattening out of the temperature profiles at the lower capture rates can be explained by applying the same logic.

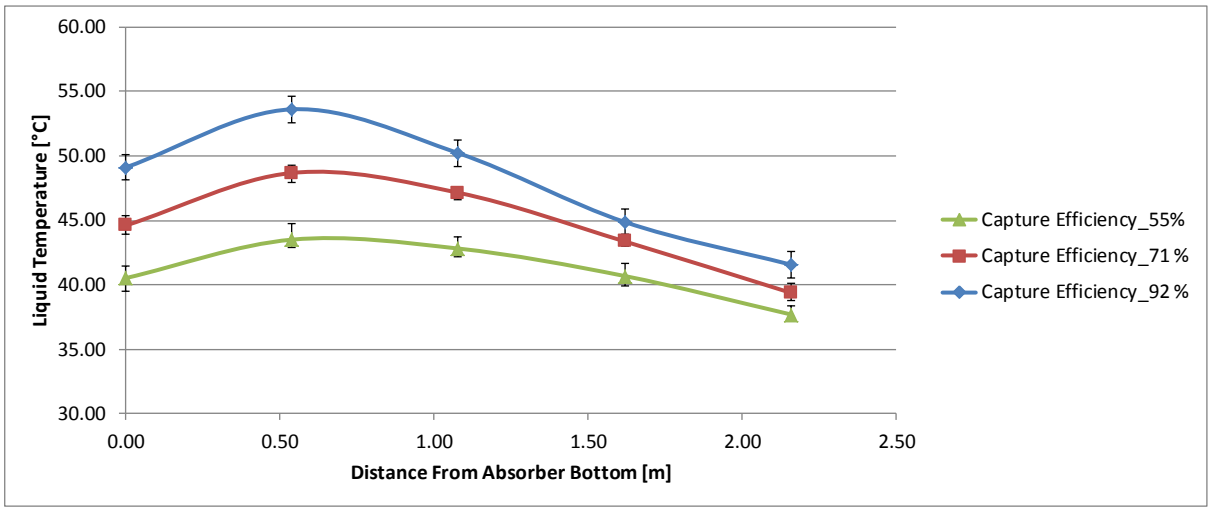

FIGURE 89 EFFECT OF CO_2 CAPTURE RATE ON THE ABSORBER TEMPERATURE PROFILES

Figure 90 shows the effect of capture rate on the stripping column temperature profiles with the feed stage being at 4 meters. At the higher capture rate unnecessary energy is added in order to heat the entire stripping column. At the lower capture rates, most of the energy is applied for reversing the reaction, producing CO_2.

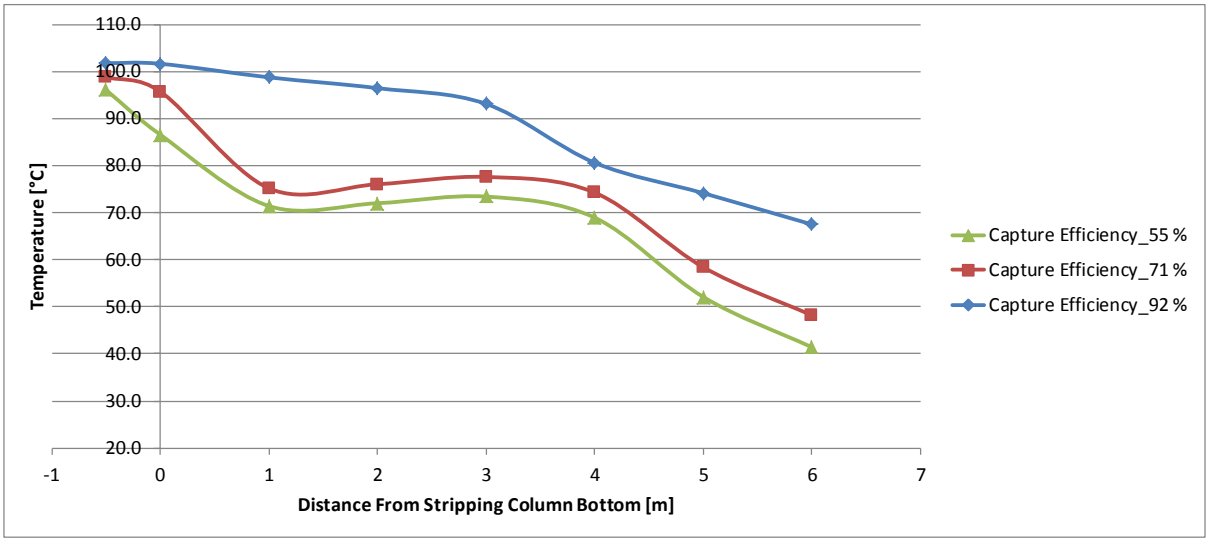

FIGURE 90 EFFECT OF CAPTURE RATE ON THE STRIPPING COLUMN TEMPERATURE PROFILES

8.2.6.3. EFFECT OF L/G-RATIO ON THE ABSORBER TEMPERATURE PROFILES

Figure 91 shows the effect of varying the L/G-ratio on the liquid temperature profiles for the absorber column. It can be seen that with an increasing L/G-ratio the temperature bulge flattens out. This can be explained by the shorter residence time of the solvent in the absorber column, leading to less CO_2 reacting per unit of solvent passing through the column. If less solvent reacts,

the amount of energy given off by the exothermic reaction would decrease resulting in a smaller temperature bulge.

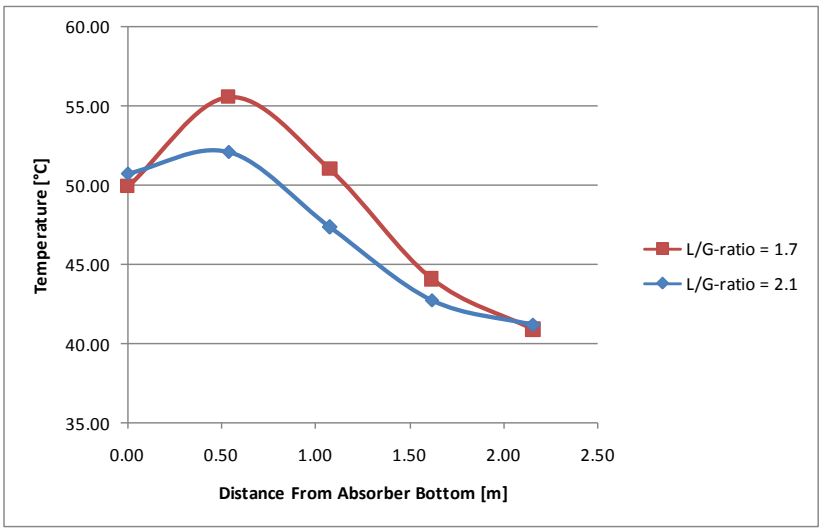

FIGURE 91 EFFECT OF THE L/G-RATIO ON THE ABSORBER TEMPERATURE PROFILES

8.2.6.4. EFFECT OF VARIATION IN THE MEA CONCENTRATION

The effect of variation in the MEA concentration of the solvent used was investigated by performing experimental runs with matched energy input (Steam valve position of 40% OPEN) and at similar liquid-to-gas ratios. The CO_2 concentration profiles in the absorber column are shown in **Figure 92**. From **Figure 92** it can be seen that the rate of absorption in the absorption column is higher for the 30 wt % MEA solution when compared to a 20 wt % MEA (aq) solution. These results reflect what would be expected.

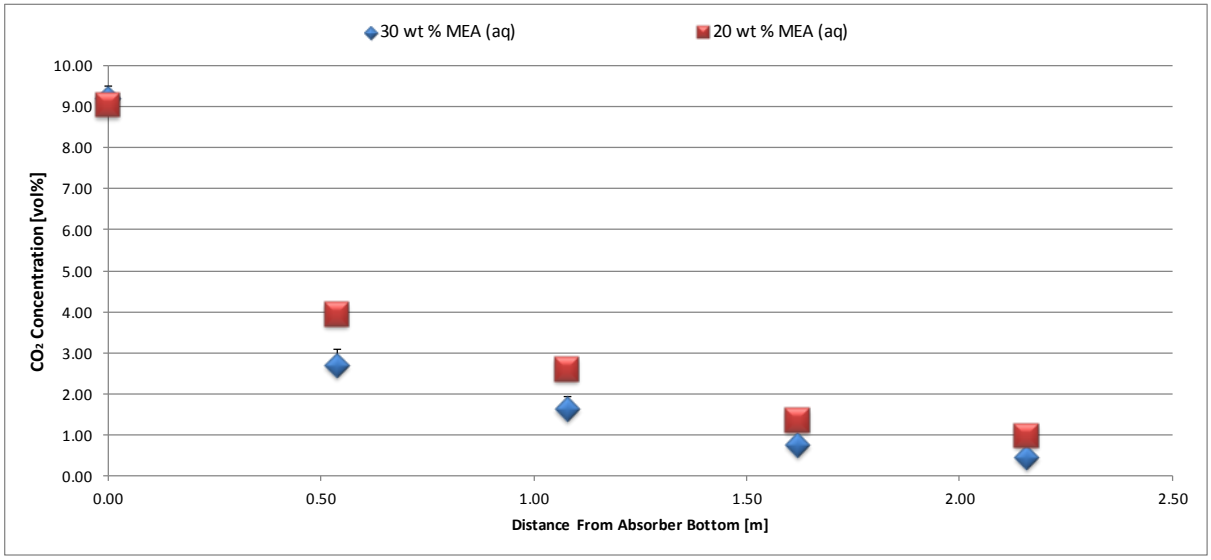

FIGURE 92 CO_2 CONCENTRATION PROFILES IN THE ABSORBER COLUMN FOR VARIOUS MEA SOLVENT CONCENTRATIONS

The temperature trends for the comparison between the 20 wt % and the 30 wt % MEA (aq) experiments are shown in **Figure 93**. From this figure it can be seen that a higher temperature bulge is the result of an increasing MEA concentration. This can be explained by more solvent being available for reacting exothermically in the absorber column, thus causing the higher temperature bulge.

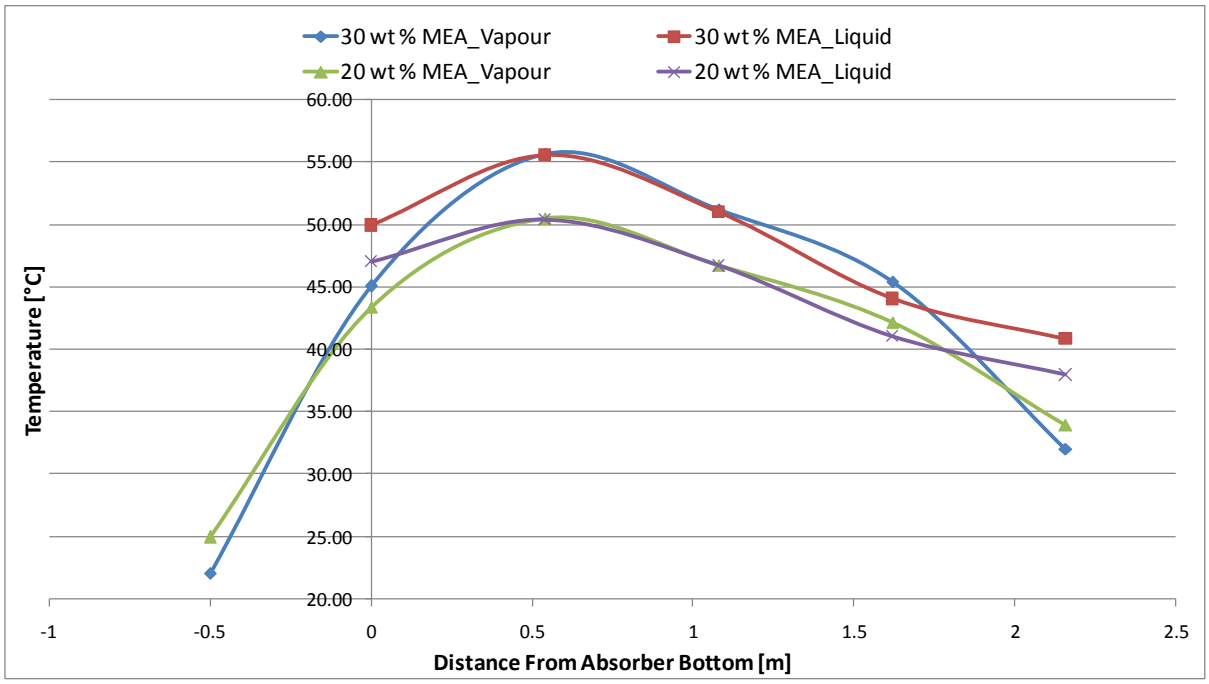

FIGURE 93 ABSORBER TEMPERATURE PROFILES FOR EXPERIMENTAL RUNS WITH BOTH 20WT% AND 30WT% MEA (AQ)

When considering the solvent regeneration energy requirement for both cases it was found that for similar L/G-ratios and regeneration energies (14 [MJ/kg CO_2 removed] for 20wt% MEA (aq) and 13.7 [MJ/kg CO_2 remove] for 30wt% MEA (aq)), the solvent with the higher concentration managed to achieve capture efficiencies of above 95%, while the 20wt% MEA (aq) only managed a capture rate of 90%.

CHAPTER 9

CONCLUSIONS

The conclusions of this study are subdivided into three sections. This first focuses on the establishment of the pilot plant facility and contain conclusions regarding the operation thereof. The focus of the second section shifts toward the conclusions regarding the simulation of the CO_2 capture process using Aspen Plus®. Finally, the main conclusions with regards to the pilot plant repeatability and results are given.

9.1. ESTABLISHING A PILOT PLANT FACILITY

A pilot plant facility for performing CO_2 capture studies was established by adapting already existing process equipment to have a duel function and serve as the main components required for setting up a CO_2 capture plant. A coupled absorption/desorption system was set up and the process equipment that provides the link between these two sections was installed.

From the energy balances that were performed during pilot plant commissioning with water the conclusion can be made that both the heat exchanger and the solvent cooler linking the absorption- and the stripping sections perform well. The heat exchanger heat duty was calculated to be above 9 kW for flow rates similar to those used for the experimental runs. This is in good agreement with the 9.1 kW specified by the supplier.

It was also found that for the experimental runs the solvent cooler unit that further cools the lean solvent before it is fed to the absorption column, sufficiently cooled this stream to temperatures between 38 and 42°C. The conclusion can thus be made that the process equipment installed to provide the link between the absorption and stripping sections has sufficient capacity to allow for the performing of CO_2 capture studies.

The designed absorber column allowed for CO_2 capture efficiencies of up to 95% for the investigated experimental conditions. The liquid distribution in the absorber column was good throughout and the gas sampling from various heights in the column enabled setting up CO_2 gas phase concentration profiles. Temperature profiles for both the liquid- and gas phases were obtained at various column heights. This leads to the conclusion that the absorber column was properly set up for CO_2 absorption studies.

The process gas system has been successfully converted from an open system to a closed gas loop with gas recycling from both the absorber- and the stripping columns. CO_2 from the top of the stripping column is recycled to the designed surge tank where it forms part of the process

gas that is again fed to the bottom of the absorber column. The two designed and manufactured venturi mass flow meters were calibrated to give flow rates that differ by less than 1%.

The online gas sampling method allows one to effectively gather data on the gas composition of the process gas from various locations in the absorber column. The online gas analysis setup can also be used to facilitate controlling the CO_2 concentration of the feed gas and gives a good indication of when the steady state condition is reached.

The control systems for the pilot plant facility were properly set up allowing for effective control in any one of four different modes of operation. Data acquisition is set up to record all sensor information. The alarm structure and system interlocks are also set up to allow safe operation of the pilot plant.

9.2. DEVELOPING A METHOD OF SIMULATION

A simplified method of simulating the CO_2 capture process using Aspen Plus® was successfully developed by combining methods from various sources in literature. This is a new approach of simulating the process and resolves most convergence problems.

The Aspen Plus® Simulation method was validated with published pilot plant data and proven to give valuable and reasonably accurate predictions of the solvent regeneration energy requirement at various CO_2 capture rates. The simulation results were validated with two different types of packing materials, 250Y- and BX500-type of packing. The conclusion was made that the simulation can be used to evaluate the performance of various column internals with respect to their applicability for CO_2 capturing.

The Aspen Plus® Simulation was used to investigate the effect of various process parameters on the solvent regeneration energy of the process. The parameters that were investigated include the lean solvent load, L/G-ratio in the absorber column as well as the fluid dynamic load of the column. It was found that the solvent regeneration energy requirement is most dependent on the L/G-ratio in the absorber column, especially at lower L/G-ratios. The simulation results of L/G-ratio and fluid dynamic load vs. regeneration energy requirement compare reasonably well to reported literature (Mangalapally and Hasse, 2011).

The validated simulation was used to perform a comparative study between packing materials with increasing surface areas. It was found that higher surface area packing materials show improved performance with respect to the solvent regeneration energy requirement of the CO_2 capture process.

The conclusion was made that the developed method of simulating the CO_2 capture process may provide valuable information and results with regards to pilot plant optimisation. This, in future, might reduce the time and costs related to perform complex pilot plant experiments.

9.3. PILOT PLANT REPEATABILITY AND RESULTS

Pilot plant repeatability was investigated with both 20wt% and 30wt% MEA (aq) solutions. In each case identical operating conditions were applied in an attempt to replicate the results obtained. In both cases the results indicated good repeatability with a maximum deviation of ±0.72% for the solvent regeneration energy requirement and ±1.40% for the CO_2 capture rate.

The pilot plant results were verified by comparison to literature data and were found to be in good agreement with published results.

No literature data are available at the capture efficiencies that were obtained with the pilot plant setup. The Aspen Plus® simulation was however used to validate the pilot plant results at the higher CO_2 capture efficiencies (above 90%). The Aspen Plus® simulation was set up for an averaged L/G-ratio and error bands of ±10% in the y-direction (regeneration energy) and ±3% in the x-direction (CO_2 capture rate) contained all the gathered data point from the pilot plant experiments.

Considering the variation in the L/G-ratios between the various experimental runs as well as errors contained within the Aspen Plus® model due to lack of pilot plant data for model optimisation, the model fits the data relatively well. This serves as validation for the pilot plant results at capture efficiencies higher than 90%.

Aspen Plus® Simulations were performed at L/G-ratios of 1.7, and the regeneration energy was matched to that obtained from pilot plant experiments by varying the CO_2 capture efficiency. This gave an indication of the model error with respect to CO_2 capture efficiency, when all other operating conditions are kept constant. The simulation under predicts the capture rate by an average of 4%. When correcting for this error in the model and applying it to the pilot plant results at capture efficiencies above 90% with an L/G-ratio of 2, the corrected model fits the data exceptionally well. The conclusion can thus be made that the Aspen Plus® model can be used, to some extent, to optimise the pilot plant operating conditions. It can also be used to simulate the complex relationship between regeneration energy requirement, CO_2 capture rate and L/G-ratio.

From two experimental runs that were performed at different L/G-ratios, but at similar capture rates, the conclusion could be made that at low L/G-ratios there is a steep increase in the

solvent regeneration energy requirement with a decrease in L/G-ratio. This is in accordance with what is found in literature.

The liquid temperature trends recorded for various capture rates show that at higher capture efficiencies, the height of the temperature bulge for the absorber column increase. From this the conclusion can be made that for an increased capture rate, solvent fed to the top of the absorber column is leaner in CO_2 as is the case for lower capture rates. This theory is supported by data published in literature.

There is some inconsistency in the published literature with regards to the position of the temperature bulge along the height of the absorber column. Most literature reports it to be in the top half of the column. However, this study showed the temperature bulge to be in the bottom half of the column. Other published literature by Jockenhövel and Schneider, (2011) and Wilson et al. (2003) do however report the temperature bulge to be in the bottom half of the column. Another reason for the temperature bulge being closer to the bottom of the absorber column might be the higher capacity of the absorber column used when compared to other pilot plant studies reported in literature. The low flow rates (gas flow factor of 1.1 [$Pa^{0.5}$]) used for preliminary evaluation of the pilot plant might be another reason for the temperature bulge being closer to the bottom of the column.

A comparison between results from experimental runs with 20 wt % MEA and 30 wt % MEA showed that the absorption potential of the 30 wt % MEA solution is superior when compared to the lower concentrations. This is as expected. The same can be said for the observation of the higher temperature bulge in the absorber column. Furthermore, for similar regeneration energy requirements and L/G-ratios the experiments with 20 wt % MEA only managed capture efficiencies of about 90% when compared to capture efficiencies above 95% for the 30 wt % MEA solution. From this the conclusion can be made that 30 wt % MEA requires less regeneration energy for similar capture efficiencies when compared to 20 wt % MEA.

The main conclusion of this study is that a pilot plant facility for CO_2 capture studies has been established, successfully shown to give repeatable results and validated with both literature data and an Aspen Plus® Simulation that was set up to match process configurations and operating conditions used.

CHAPTER 10
RECOMMENDED FUTURE WORK

In setting up a pilot plant for post combustion CO_2 capture studies at the University of Stellenbosch, keeping future work in mind are a necessity. This chapter will give a summary of the possible future work that could be conducted using the Pilot Plant that was set up. Some work concerns the use of the pilot plant as is, but varying various parameters, and acquiring data for each steady state condition. Other opportunities for future work are related to the effect of minor adaptations to the existing setup.

10.1. COMPLETE PARAMETRIC STUDY

In pilot scale research done by Mangalapally and Hasse, (2011a); Notz et al., (2012) systematic parametric studies were performed. Notz et al., (2012) carried out eight different studies for which a single parameter is varied while keeping the other eight parameters constant. The process parameters that were varied include solvent flow rate, solvent composition, solvent temperature and stripping column pressure. For the remaining four variation studies, the following boundary conditions were varied: CO_2 concentration in the flue gas, CO_2 removal rate, flue gas temperature and the fluid dynamic load of the absorber column. These variation studies are all performed in order to access the effect of the various operating and boundary conditions on the energy requirement for solvent regeneration.

The pilot plant setup constructed in this study can be used in order to perform similar systematic variation studies. This will give great insight on what the effect of the various process parameters is on the energy requirement for solvent regeneration. The pilot plant setup allows for varying all parameters that were investigated by (Notz et al., 2012) except for increasing the pressure of the stripping column.

Performing similar variation studies will also allow for proper comparison of pilot plant data, to data published by (Mangalapally and Hasse, 2011a; Notz et al., 2012).

10.2. LIQUID CONCENTRATION PROFILES FOR THE ABSORBER COLUMN

Obtaining CO_2 profiles for the absorber column in the liquid phase did not fall within the scope of the work for this study. However, the liquid sample ports for the absorber column were designed in order to allow for obtaining a diametric profile at four different heights in the absorber column. Liquid samples can thus be gathered from any point along the diameter of the packing material.

These sample ports can primarily be used in order to study the effect of wall flow on the absorption process. It can also be used in order to compare diametric profiles for X- and Y-type structured packing material.

10.3. REACTION KINETIC STUDIES

Accurate predictions of effective interfacial surface area provided by packing material are important to aid in the design of new distillation columns. The reaction of CO_2 with MEA is usually used in order to predict the effective area of column internals. However, the models used for predictions are based on simplified reaction kinetics. Current studies by L.J. du Preez re-evaluate the reaction kinetics of the reaction between CO_2 and MEA, in order to find a model that could more accurately predict the kinetics of the reaction.

Aroonwilas and Tontiwachwuthikul, (2000) developed a mechanistic model based on mass transfer coefficients and the effective interfacial area, in order to predict the performance of structured packing material. The results from the investigation were compared to results obtained from pilot plant studies on the CO_2 capture process.

The pilot plant setup can be used in future to perform effective interfacial area studies of column internals by making use of the improved model for the reaction kinetics.

10.4. IMPLEMENTING INTERSTAGE COOLING FOR ABSORBER COLUMN

Chang and Shih, (2005) made use of Aspen Plus® simulations in order to investigate the effect of inter-stage cooling and split flow configurations to the absorber column. The optimized design, based on the simulations, predicts a cost reduction of between 10 and 26%.

Inter-stage cooling in the absorber column will increase the absorption efficiency and will eventually decrease the energy requirement for solvent regeneration. Inter-stage cooling will also decrease the size of the absorption column that would be required when applying CO_2 capture, on a large scale as retrofitted units, to existing power plants.

The absorber column that is set up in this study has three possible feed ports per meter column height. In total, solvent can be drawn from, or returned to, the column at nine different heights. Provision was made in the design of the column to allow for investigating the effect of inter-stage cooling and split flow configurations in the future.

10.5. USING VARIOUS SOLVENT BLENDS

As already stated the high energy requirement for regenerating MEA is a major drawback. Studies by (Notz et al., 2007) as well as the CASTOR (2004 – 2008) (Knudsen et al., 2009) and CESAR (2008 – 2011) projects (Faber et al., 2011; Mangalapally et al., 2009) investigated novel solvents in an attempt to reduce the regeneration energy requirement.

The pilot plant setup can be used in order to investigate different solvent blends. The effect of the MEA concentration on the solvent circulation rate and regeneration requirement can also be investigated.

10.6. USING VARIOUS PACKING MATERIALS

Pilot plant studies investigating the effect of the type of packing material, has been performed at the University of Stuttgart, Germany (Mangalapally and Hasse, 2011a; Mangalapally et al., 2009; Notz et al., 2012).

The effect of various column internals on the capture process can be thoroughly researched. The columns can also be set up using random packing to see what the benefit of using 4th generation packing material for the absorption process would be.

10.7. SCALE-UP STUDIES

Various pilot plant studies have been performed across the world. All the experimental setups are however set up differently, with column diameters varying from 0.125 meter (Mangalapally and Hasse, 2011a; Notz et al., 2012) to 1.1 meters (Faber et al., 2011). Little has however been reported on what the effect of up-scaling would be on the capture process. When considering that industrial scale plants would be considerably bigger that the pilot plant, the effect of up-scaling should not be neglected.

A packed absorber column with an internal diameter of 0.4 meters are available for performing studies investigating the effect of up-scaling on the capture process. This column can be set up with either random- or structured packing.

10.8. DYNAMIC STUDIES

Pilot plant work on the dynamic behaviour of the CO_2 capture process is limited (Faber et al., 2011). Work on the dynamic behaviour has however been done by Faber et al. (2011), using the setup at the Esbjerg pilot plant. The parameters that were investigated include the steam flow rate to the reboiler unit, flue gas- and solvent flow rates. These parameters were varied one

by one, while keeping the other two parameters constant. The behaviour of the capture plant was recorded.

In order to study the dynamic behaviour of a capture plant, gas recycling needs to be eliminated from the pilot plant setup, as this will render the behaviour of the pilot plant with respect to an actual CO_2 capture plant. A relatively constant flow of CO_2- containing flue gas stream would thus be required. In order to eliminate the cost of synthesizing a flue gas stream, there is a possibility of using off-gas from the steam generating boiler unit as feed gas to the bottom of the absorber. Pre-treatment of the flue gas will involve removal of any sulphur and NO_x components as well as gas cooling would be requirement. However, setting up the process with a continuous supply of flue gas will allow an in depth study of the dynamic behaviour of the process. As is, modelling and predicting the dynamic behaviour of the CO_2 capture process is limited and pilot plant data regarding this would be of great value.

10.9. SIMULATION STUDIES

The method of simulation that was developed in this study has been shown to provide valuable results with respect to pilot plant optimisation. The simulation can in future be used to predict the effects of lean solvent loadings, L/G –ratios in the absorber column as well as the fluid dynamic load in the absorber column on the solvent regeneration energy requirement. The simulation also provides valuable results with regards to the effect of CO_2 capture efficiency on the solvent regeneration energy requirement and this can in future be used to compare the performance of various packing materials.

The simulation also has potential for expanding the simulations with random packing. This will allow one to draw a comparison between the performance of random packing and that of structured packing.

The simulation can also be used to set up various process configurations, simulating elevated stripping column pressure, various split-flow configurations and inter-stage cooling for the absorber column. This applicability of the developed simulation method for performing these studies should however be properly validated.

REFERENCES

Abanades, J.C., Allam, R., Lackner, K.S., Meunier, F., Rubin, E., Sanchez, J.C., Yogo, K., Zevenhoven, R., 2005. Mineral carbonation and industrial uses of carbon dioxide, in: Eliasson, B., Sutamihardja, R.T.M. (Eds.), IPCC Special Report on Carbon Dioxide Capture and Storage, Intergovernmental Panel on Climate Change. Cambridge University Press, pp. 319–338.

Abuzahra, M., Schneiders, L., Niederer, J., Feron, P., Versteeg, G., 2007. CO2 capture from power plantsPartI. A parametric study of the technical performance based on monoethanolamine. International Journal of Greenhouse Gas Control 1, 37–46.

Adams, R.G., Alin, J., Biede, O., Booth, N.J., deMontigny, D., Drew, R., Idem, R., Laursen, M., Peralta-Solorio, D., Sanpasertparnich, T., 2009. CAPRICE project—Engineering study on the integration of post combustion capture technology into the power plant gas path and heat cycle. Energy Procedia 1, 3801–3808.

Alie, C., Backham, L., Croiset, E., Douglas, P.L., 2005. Simulation of CO_2 capture using MEA scrubbing: a flowsheet decomposition method. Energy Conversion and Management 46, 475–487.

Allam, R., Bolland, O., Davison, J., Feron, P., Goede, F., Herrera, A., Iijima, M., Jansen, D., Leites, I., Mathieu, P., Rubin, E., Simbeck, D., Warmuzinski, K., Wilkinson, M., Williams, R., 2005. Capture of CO_2, in: Metz, B., Davidson, O., De Coninck, H., Loos, M., Meyer, L. (Eds.), IPCC Special Report on Carbon Dioxide Capture and Storage, Intergovernmental Panel on Climate Change. Cambridge University Press, pp. 105–178.

Anderson, J., Bachu, S., Bashir Nimir, H., Basu, B., Bradshaw, J., Deguchi, G., Gale, J., Von Goerne, G., Heidug, W., Holloway, S., Kamal, R., Keith, D., Lloyd, P., Rocha, P., Senior, B., Thomson, J., Torp, T., Wildenborg, T., Wilson, M., Zarlenga, F., Zhou, D., 2005. Underground Geological Storage, in: Borm, G., Hawkins, D., Lee, A. (Eds.), IPCC Special Report on Carbon Dioxide Capture and Storage, Intergovernmental Panel on Climate Change. Cambridge University Press, pp. 195–276.

Aronu, U.E., Svendsen, H.F., Hoff, K.A., Juliussen, O., 2009. Solvent selection for carbon dioxide absorption. Energy Procedia 1, 1051–1057.

Aroonwilas, A., Tontiwachwuthikul, P., 2000. Mechanistic model for prediction of structured packing mass transfer performance in CO2 absorption with chemical reactions. Chemical Engineering Science 55, 3651–3663.

Austgen, D.M., Rochelle, G.T., Peng, X., Chen, C.C., 1989. Model of vapor-liquid equilibria for aqueous acid gas-alkanolamine systems using the electrolyte-NRTL equation. Ind. Eng. Chem. Res. 28, 1060–1073.

Bradshaw, J., Chen, Z., Garg, A., Gomez, D., Rogner, H., Simbeck, D., Williams, R., 2005. Sources of CO2, in: Metz, B., Davidson, O., De Coninck, H., Loos, M., Meyer, L. (Eds.), IPCC Special Report on Carbon Dioxide Capture and Storage, Intergovernmental Panel on Climate Change. Cambridge University Press, pp. 75–104.

Brewer, P., Chen, B., Haugan, P., Iwama, T., Johnston, P., Kheshgi, H., Li, Q., Ohsumi, T., Portner, H., Sabine, C., Shirayama, Y., Thomson, J., 2005. Ocean Storage, in: De Young, B., Joos, F. (Eds.), IPCC Special Report on Carbon Dioxide Capture and Storage, Intergovernmental Panel on Climate Change. Cambridge University Press, pp. 277–317.

Cengel, Y.A., Cimbala, J., M., 2006.Fluid Mechanics, Fundamentals and Applications, First Edition in SI Units.ed. McGraw-Hill.

Chakravarti, S., Gupta, A., Hunek, B., 2001.Advanced Technology for the capture of carbon dioxide form flue gases.Presented at the First National Conference on Carbon Sequestration, Washington DC.

Chang, H., Shih, C.-M., 2005. Simulation and optimization for power plant flue gas CO_2 absorption-stripping systems [WWW Document]. URL http://cat.inist.fr/?aModele=afficheN&cpsidt=16592023 (accessed 7.30.12).

Chen, E., Rochelle, G.T., 2005. Pilot plant for CO_2 capture using aqueous piperazine/potassium carbonate, in: Greenhouse Gas Control Technologies 7. Elsevier Science Ltd, Oxford, pp. 1821–1824.

Chen, Freeman, S.A., Rochelle, G.T., 2011. Foaming of aqueous piperazine and monoethanolamine for CO_2 capture. International Journal of Greenhouse Gas Control 5, 381–386.

Cottrell, A.J., McGregor, J.M., Jansen, J., Artanto, Y., Dave, N., Morgan, S., Pearson, P., Attalla, M.I., Wardhaugh, L., Yu, H., 2009. Post-combustion capture R&D and pilot plant operation in Australia. Energy Procedia 1, 1003–1010.

Dugas, R., 2006. Pilot Plant Study of Carbon Dioxide Capture by Aqueous Monoethanolamine (M.S.E. Thesis).

Dugas, R., Alix, P., Lemaire, E., Broutin, P., Rochelle, G., 2009. Absorber model for CO_2 capture by monoethanolamine — application to CASTOR pilot results. Energy Procedia 1, 103–107.

Dugas, R., Rochelle, G., 2009. Absorption and desorption rates of carbon dioxide with monoethanolamine and piperazine. Energy Procedia 1, 1163–1169.

Edwards, T.J., Maurer, G., Newman, J., Prausnitz, J.M., 1978. Vapor-liquid equilibria in multicomponent aqueous solutions of volatile weak electrolytes.AIChE J. 24, 966–976.

Erasmus, A., 2004. Mass Transfer in Structured Packing (PhD Dissertation).

Faber, R., Köpcke, M., Biede, O., Knudsen, J.N., Andersen, J., 2011. Open-loop step responses for the MEA post-combustion capture process: Experimental results from the Esbjerg pilot plant. Energy Procedia 4, 1427–1434.

Fashami, S., Ziaii, Edgar, T.F., Rochelle, G.T., 2007.Modeling and Optimization of CO_2 removal in power plants.

Ferguson, R.C., Nichols, C., Leeuwen, T.V., Kuuskraa, V.A., 2009. Storing CO_2 with enhanced oil recovery. Energy Procedia 1, 1989–1996.

Freguia, S., Rochelle, G.T., 2004.Modeling of CO_2 capture by aqueous monoethanolamine - Freguia - 2004 - AIChE Journal - Wiley Online Library [WWW Document]. URL http://onlinelibrary.wiley.com/doi/10.1002/aic.690490708/pdf (accessed 6.7.12).

Idem, R., Gelowitz, D., Tontiwachwuthikul, P., 2009. Evaluation of the Performance of Various Amine Based Solvents in an Optimized Multipurpose Technology Development Pilot Plant. Energy Procedia 1, 1543–1548.

Jockenhövel, T., Schneider, R., 2011. Towards commercial application of a second-generation post-combustion capture technology — Pilot plant validation of the siemens capture process and implementation of a first demonstration case. Energy Procedia 4, 1451–1458.

Kheshgi, H.S., Archer, D.E., 2004. A nonlinear convolution model for the evasion of CO_2 injected into the deep ocean. J. Geophys. Res. 109, C02007.

Kittel, J., Idem, R., Gelowitz, D., Tontiwachwuthikul, P., Parrain, G., Bonneau, A., 2009. Corrosion in MEA units for CO_2 capture: Pilot plant studies. Energy Procedia 1, 791–797.

Knudsen, J.N., Jensen, J.N., Vilhelmsen, P.-J., Biede, O., 2009. Experience with CO_2 capture from coal flue gas in pilot-scale: Testing of different amine solvents. Energy Procedia 1, 783–790.

Lawal, A., Wang, M., Stephenson, P., Yeung, H., 2009. CERES: Dynamic modelling of CO_2 absorption for post combustion capture in coal-fired power plants [WWW Document]. URL https://dspace.lib.cranfield.ac.uk/handle/1826/3826 (accessed 6.11.12).

Lawal, O., Bello, A., Idem, R., 2005. Pathways and reaction products for the oxidative degradation of CO2 loaded and concentrated aqueous MEA and MEA/MDEA mixtures during CO_2 absorption from flue gases, in: Greenhouse Gas Control Technologies 7. Elsevier Science Ltd, Oxford, pp. 1159–1164.

Liu, F., Lu, P., Zhu, C., Xiao, Y., 2011.Coupled reactive flow and transport modeling of CO_2 sequestration in the Mt. Simon sandstone formation, Midwest U.S.A. International Journal of Greenhouse Gas Control 5, 294–307.

Luo, X., Knudsen, J.N., De Montigny, D., Sanpasertparnich, T., Idem, R., Gelowitz, D., Notz, R., Hoch, S., Hasse, H., Lemaire, E., 2009. Comparison and validation of simulation codes against sixteen sets of data from four different pilot plants. Energy Procedia 1, 1249–1256.

Mangalapally, H.P., Hasse, H., 2011a. Pilot plant study of post-combustion carbon dioxide capture by reactive absorption: Methodology, comparison of different structured packings, and comprehensive results for monoethanolamine. Chemical Engineering Research and Design 89, 1216–1228.

Mangalapally, H.P., Hasse, H., 2011b. Pilot plant experiments for post combustion carbon dioxide capture by reactive absorption with novel solvents. Energy Procedia 4, 1–8.

Mangalapally, H.P., Notz, R., Hoch, S., Asprion, N., Sieder, G., Garcia, H., Hasse, H., 2009. Pilot plant experimental studies of post combustion CO_2 capture by reactive absorption with MEA and new solvents. Energy Procedia 1, 963–970.

Marchetti, C., 1977. On Geoengineering and the CO_2 Problem. Climate Change 1, 59–68.

Mejdell, T., Vassbotn, T., Juliussen, O., Tobiesen, A., Einbu, A., Knuutila, H., Hoff, K.A., Andersson, V., Svendsen, H.F., 2011.Novel full height pilot plant for solvent development and model validation. Energy Procedia 4, 1753–1760.

Metz, B., Davidson, O., De Coninck, H., Loos, M., Meyer, L., 2005.Carbon Dioxide Capture and Storage (IPCC Special Report).Intergovernmental Panel on Climate Change, Cambridge University Press.

Mimura, T., Shimojo, S., Suda, T., Iijima, M., Mitsuoka, S., 1995. Research and development on energy saving technology for flue gas carbon dioxide recovery and steam system in power plant. Energy Conversion and Management 36, 397–400.

Mores, P., Scenna, N., Mussati, S., 2010. Post-combustion CO_2 capture process: Equilibrium stage mathematical model of the chemical absorption of CO_2 into monoethanolamine (MEA) aqueous solution. Chemical Engineering Research and Design.

Notz, R., Asprion, N., Clausen, I., Hasse, H., 2007. Selection and Pilot Plant Tests of New Absorbents for Post-Combustion Carbon Dioxide Capture. Chemical Engineering Research and Design 85, 510–515.

Notz, R., Mangalapally, H.P., Hasse, H., 2012. Post combustion CO_2 capture by reactive absorption: Pilot plant description and results of systematic studies with MEA. International Journal of Greenhouse Gas Control 6, 84–112.

Notz, R., Tönnies, I., Mangalapally, H.P., Hoch, S., Hasse, H., 2010. A short-cut method for assessing absorbents for post-combustion carbon dioxide capture.International Journal of Greenhouse Gas Control.

Oexmann, J., 2008. Evaluation of Post-Combustion CO_2-Capture using Piperazine-Promoted Potassium Carbonate in a Coal Fired Power Station.

Oexmann, J., Kather, A., 2009. Post-combustion CO_2 capture in coal-fired power plants: Comparison of integrated chemical absorption processes with piperazine promoted potassium carbonate and MEA. Energy Procedia 1, 799–806.

Oexmann, J., Kather, A., 2010. Minimising the regeneration heat duty of post-combustion CO_2 capture by wet chemical absorption: The misguided focus on low heat of absorption solvents. International Journal of Greenhouse Gas Control 4, 36–43.

Perry, R., Green, D., 1997. Perry's Chemical Engineers' Handbook, Seventh Edition.ed. McGraw-Hill.

Reddy, S., 2008. Econamine FG PlusSM Technology for Post-Combustion CO_2 Capture.

Retief, F.J.G., 2012. A Novel Approach to Solvent Screening for Post-Combustion Carbon Dioxide Capture with Chemical Absorption (Masters).

Riemer, P.W.F., Ormerod, W.G., 1995. International perspectives and the results of carbon dioxide capture disposal and utilisation studies. Energy Conversion and Management 36, 813–818.

Rochelle, G.T., Chen, E., Freeman, S.A., Van Wagener, D.H., Xu, Q., Voice, A.K., 2011. Aqueous Piperazine as the New Standard for CO_2 Capture Technology. Chemical Engineering Journal In Press, Accepted Manuscript.

Sinnot, R., Towler, G., 2009. Chemical Engineering Design, Fifth.ed. Elsevier.

Takamura, Y., Mori, Y., Noda, H., Narita, S., Saji, A., Uchida, S., 2001. Study on CO_2 removal technology from flue gas on thermal power plant by combined system with pressure swing adsorption and super cold separator, in: Greenhouse Gas Control Technologies: Proceedings of the Fifth International Conference on Greenhouse Gas Control Technologies. CSIRO, Australia, pp. 161–166.

Tobiesen, F.A., Svendsen, H.F., Juliussen, O., 2007. Experimental validation of a rigorous absorber model for CO_2 postcombustion capture.AIChE J. 53, 846–865.

Turton, R., Bailie, R.C., Whiting, W.B., Shaeiwitz, J., 2009. Analysis, Synthesis, and Design of Chemical Processes, Third.ed. Prentice Hall.

Wang, M., Lawal, A., Stephenson, P., Sidders, J., Ramshaw, C., 2010. Post-combustion CO_2 capture with chemical absorption: A state-of-the-art review. Chemical Engineering Research and Design.

Wilson, M., Tontiwachwuthikul, P., Chakma, A., Idem, R., Veawab, A., Aroonwilas, A., Gelowitz, D., Barrie, J., Mariz, C., 2003. Test Results from A CO_2 Extraction Pilot Plant at Boundary Dam Coal-Fired Power Station, in: Greenhouse Gas Control Technologies - 6th International Conference. Pergamon, Oxford, pp. 31–36.

Wilson, M., Tontiwachwuthikul, P., Chakma, A., Idem, R., Veawab, A., Aroonwilas, A., Gelowitz, D., Henni, A., Mahinpey, N., 2005.The International Test Centre for Carbon Dioxide Capture (ITC), in: Greenhouse Gas Control Technologies 7. Elsevier Science Ltd, Oxford, pp. 1807–1810.

Yokoyama, T., 2003.Japanese R&D on CO_2 Capture, in: Greenhouse Gas Control Technologies - 6th International Conference.Pergamon, Oxford, pp. 13–17.

Zhang, Y., Chen, H., Chen, C.-C., Plaza, J.M., Dugas, R., Rochelle, G.T., 2009. Rate-Based Process Modeling Study of CO_2 Capture with Aqueous Monoethanolamine Solution </title>. Ind. Eng. Chem. Res. 48, 9233–9246.

APPENDIX A: DESIGN CALCULATIONS, EQUIPEMENT SPECIFICATION AND HAZOP

SURGE TANK DESIGN CALCULATION

The surge tank design was based on the design method described in Sinnot and Towler (2009). **Table A.16** gives some of the parameters used for calculation of the time required for droplet settling. The formulas for calculating the various parameters are marked by superscripts.

TABLE A.16 SURGE TANK DESIGN – CALCULATED TIME FOR DROPLET SETTLING

Parameters to Consider		Units
Density of the Liquid (Approximation)	1000	[kg/m3]
Density of the Vapour (Approximation)	1.200	[kg/m3]
[1]Settling Velocity, u_t	2.020	[m/s]
No Demister pad, u_s	0.303	[m/s]
Maximum Gas Mass flow Rate	1500	[kg/h]
[2]Vapour Volumetric Flow Rate, Q_v	0.347	[m3/s]
[3]Assume L/D	0.250	
[4]Volume Fraction, f_d	0.195	(Perry and Green, 1997)
[5]Cross-sectional Area for Vapour flow	0.096	
[6]Vapour Velocity, u_V	3.635	[m/s]
[7]Vapour residence time required - droplet settling	0.321	[s]
[8]Actual Residence Time of droplet	0.321	[s]

[1] Settling Velocity (u_t)

$$u_t = 0.07 \times (\rho_L - \rho_v)\ \rho_v^{\ 1\ 2}$$

ρ_L - Liquid Density [kg/m³]

ρ_v - Vapour Density [kg/m³]

[2] Volumetric Flow rate of Vapour (Q_v, [m³/s])

$$Q_v = \frac{m}{3600 \times \rho_v}$$

m - Mass flow Rate of Vapour [kg/h]

[3] Length over diametric Ratio

Sinnot and Towler(2009) propose the use of L_v/D_v = 3 for horisontal vessels with an operating pressure of between 0 – 20 bar.

[4] Volume Fractions for Horisontal Tanks

The horisontal surge tank was designed with a liquid height-to-diameter (H_v/D_v) ratio of 0.25. Perry and Green(1997) were used for calculating the volume fraction for an H_v/D_v-ratio of 0.25.

[5] Cross-sectional Area available for Gas Flow

$$A_c = \frac{\pi {D_v}^2}{4}$$

A_c - Cross-sectional area available for gas flow [m²]

D_v - Diameter of the designed tank [m]

[6] Vapour Velocities (u_v)

$$u_v = \frac{Q_v}{A_c}$$

[7] Residence Time Required for Droplet Settling

$$\frac{H_v}{u_s} = \mathrm{f(D_v)}$$

H_v - Height of the Liquid level in the tank [m]

[8] Actual Droplet Residence Time

$$\frac{L_v}{u_v} = \mathrm{f(D_v)}$$

In order to obtain satisfactory separation the residence time required for droplet settling[7] should be equal to the actual residence time[8]. The required vessel diameter can thus be solved for.

From the design a vessel diameter of 0.389 meters was obtained for the design parameters given in **Table A.16**. A surge tank with an internal diameter of 0.4 meters were constructed and installed.

VENTURI MASS FLOW METER DESIGN AND CALCULATIONS

The venturi mass flow meters for measuring the gas flow rates at various locations in the gas recycle loop were design based on the specifications given by British Standards Institution (BSI) (1981).

The mass flow rates measured by the venturi mass flow meters can be calculated as follows (Cengel and Cimbala, 2006):

$$G\ \frac{kg}{h} = \rho \times C \times E \times \frac{\pi {D_2}^2}{4} \cdot \sqrt{\frac{2.(\boldsymbol{P_1} - \boldsymbol{P_2})}{\rho}} \times 3600$$

Density can be calculated using:

$$\rho = \frac{\boldsymbol{P_1}}{R \times \boldsymbol{T}}$$

With Pressure in [Pa],

R [J/kg.K] and

T in [Kelvin] = T[°C] + 273.15

ALL VALUES THAT WILL BE INPUTS BY THE USER:

C - Coefficient of discharge

[Range: min = 0.2, max = 2; Resolution: 0.000]

R - Gas Constant [J/kg.K]

[Range: min = 0.0, max = 2100; Resolution: 000.0]

ALL CONSTANT VALUES:

D_1 = 0.084 m (inlet)

D_2 = 0.060 m (throat)

$$\boldsymbol{E} = \frac{1}{\sqrt{1 - \left(\frac{0.06}{0.084}\right)^4}} = \frac{1}{\sqrt{1.351914414}}$$

π = 3.141592654

ALL MEASURED VALUES (DISPLAYED IN BOLD):

$P_1 - P_2$ = Pressure difference over venturi, **Sensor: dPR-202/203**

P_1 = Pressure at inlet (Higher Pressure), **Sensor: PIR-201/202**

T = **Kelvin** Temperature downstream from discharge, **Sensor: TR-215/216 (+ 273.15)**

Figure A.94 shows the designed venturi mass flow meter. The pressure taps was installed >0.5×D_1 upstream from where the tapering of the venturi starts. D_2 was installed in the middle of the total length of the throat (D_2/4).

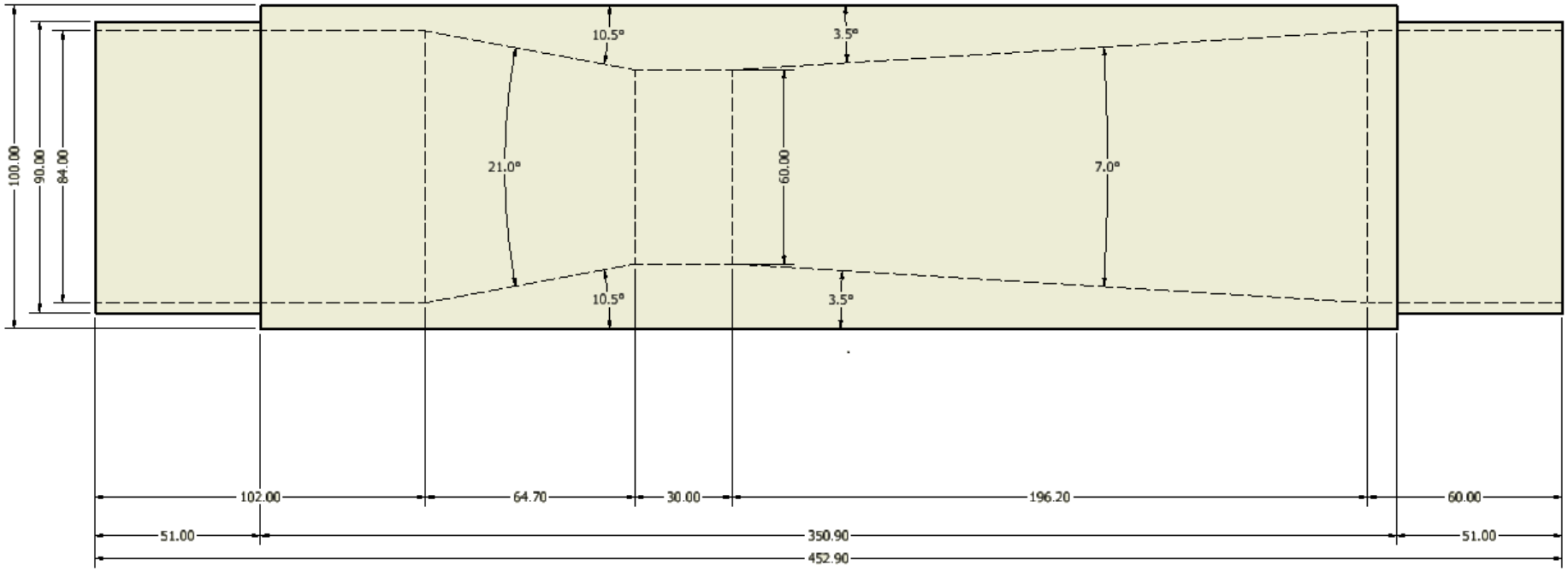

FIGURE A.94 DRAWING OF THE DESIGNED VENTURI MASS FLOW METER

The venturi mass flow meters were calibrated by making use of a pitot tube air flow meter. The pitot tube was used to set up velocity profiles across the diameters of the gas pipe. Half of the velocity profile can be seen in **Figure A.95**

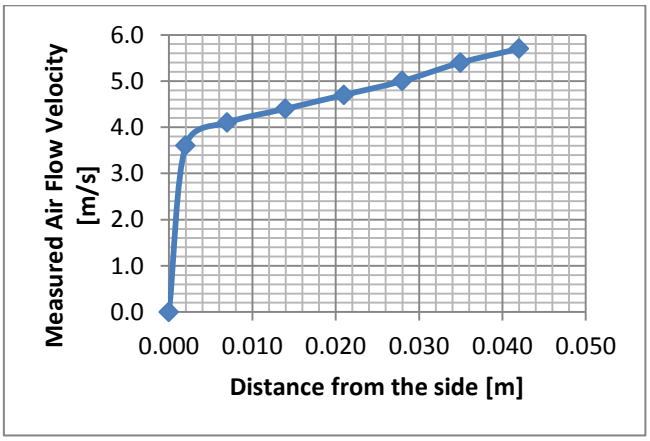

FIGURE A.95 VELOCITY PROFILE SET UP USING THE PITOT TUBE

The velocity profiles were then integrated with respect to the cross-sectional area available for gas flow. This was done according to Equation (A.1). The results from the integration yield the volumetric flow rate of the gas, Q.

$$Q\ \frac{m^3}{s} = \int_{middle\ of\ pipe}^{Side\ of\ pipe} V\ \frac{m}{s}\ .2\pi r\ m\ .dr\ m \qquad \text{...Equation (A.1)}$$

The gas density was further used to calculate the mass flow rate of the gas. **Figure A.96** shows the mass flow rates measured by the different mass flow meters after calibration. It is clear from **Figure A.96** that there is a linear relationship between the VSD setting on the blower unit and the mass flow rate. The recorded flow rates for the various flow meters compare very well.

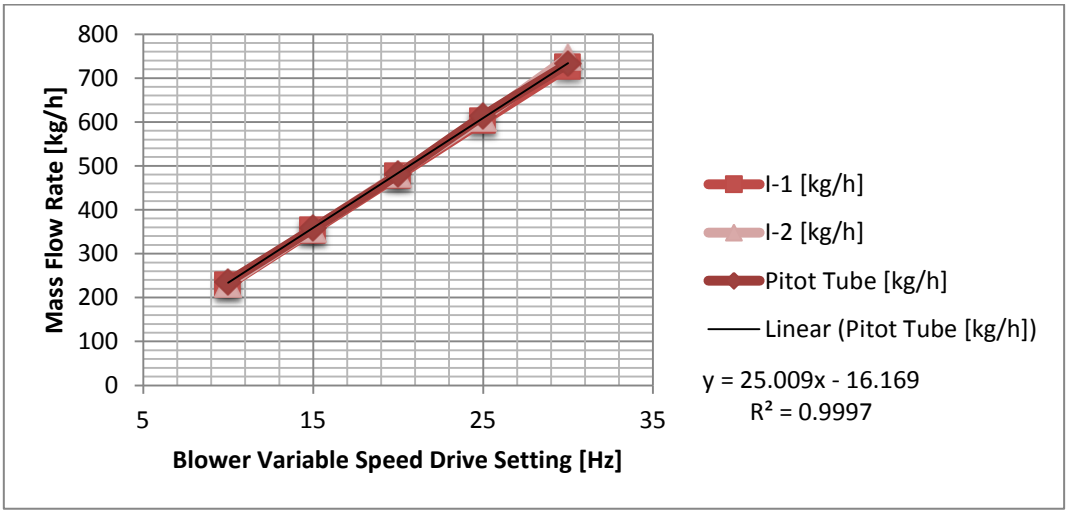

FIGURE A.96 MASS FLOW RATES FOR THE THREE DIFFERENT FLOW MEASUREMENTS AFTER CALIBRATION

BLOWER SPECIFICATIONS

The blower specifications were done to allow a gas flow rate high enough to flood the 200 mm packed column. The blower specifications that were sent to the supplier can be seen in **Table A.17**.

TABLE A.17 BLOWER SPECIFICATIONS AND PRESSURE DROP CALCULATIONS AS PROVIDED TO THE SUPPLIER

Estimation of the Pressure Drop to Overcome by Recycle blower unit		
Maximum Gas Flow Factor	**[Pa^0.5]**	5.5
Maximum Mass Flow Rate for the Gas	**[kg/h]**	700
Maximum packed height allowed by the 200 mm column	**[m]**	3.24
Assuming maximum pressure drop per meter section	**[mbar/m]**	8
Pressure drop over column due to packing material	**[mbar]**	25.92
Number of Distributing units inside the column		4
Estimated pressure drop per distributing unit	**[mbar]**	2
Total pressure drop due to distributing units	**[mbar]**	6
Possible addition of a humidifier with 1 meter packing	**[mbar]**	8
Total estimated pressure drop that to be overcome	**[mbar]**	39.92
Add 25% for pressure drop in the lines to the column	**[mbar]**	49.9
	[bar]	0.0499
Pressure drop to be overcome by the blower unit	**[kPa]**	5.0

CALCULATION OF THE CO_2 CAPTURE EFFICIENCY

The CO_2 Capture efficiency can be calculated using the gas compositions from the bottom (feed stream) and the top of the absorber column. The derivation of the equation for calculating the CO_2 capture efficiency follows.

$$CO_{2\ mole\,\%\ \ OUT} = \frac{CO_{2\ mole\ flow\ \ [IN]} \times (1-\alpha)}{n_{[IN]} - \ \alpha \times CO_{2\ mole\ flow\ \ IN}}$$

Because $CO_{2\ mole\ flow\ \ IN} = n_{[IN]} \times CO_{2\ mole\,\%\ \ [IN]}$, we can write the equation as follows:

$$CO_{2\ mole\,\%\ \ OUT} = \frac{n_{[IN]} \times CO_{2\ mole\,\%\ [IN]} \times (1-\alpha)}{n_{[IN]} - \ \alpha \times n_{[IN]} \times CO_{2\ mole\,\%\ \ IN}}$$

$$CO_{2\ mole\,\%\ \ OUT} = \frac{\cancel{n_{[IN]}} \times CO_{2\ mole\,\%\ [IN]} \times (1-\alpha)}{\cancel{n_{[IN]}}\ 1 - \ \alpha \times CO_{2\ mole\,\%\ \ IN}}$$

$$CO_{2\ mole\,\%\ \ OUT} = \frac{CO_{2\ mole\,\%\ [IN]} \times (1-\alpha)}{1 - \ \alpha \times CO_{2\ mole\,\%\ \ IN}}$$

Now because $CO_{2\ mole\,\%} = CO_{2\ vol\,\%}$, the only unknown in this equation is the CO_2 Capture Efficiency [α]. Rearranging:

$$CO_{2\ vol\,\%\ \ OUT} - \ \alpha \times CO_{2\ vol\,\%\ \ IN} \times CO_{2\ vol\,\%\ \ OUT} = CO_{2\ vol\,\%\ [IN]} \times (1-\alpha)$$

$$\alpha \times CO_{2\ vol\,\%\ [IN]} - \ \alpha \times CO_{2\ vol\,\%\ \ IN} \times CO_{2\ vol\,\%\ \ OUT} = CO_{2\ vol\,\%\ [IN]} - CO_{2\ vol\,\%\ \ OUT}$$

$$\alpha \times \ CO_{2\ vol\,\%\ [IN]} - \ CO_{2\ vol\,\%\ \ IN} \times CO_{2\ vol\,\%\ \ OUT} = CO_{2\ vol\,\%\ [IN]} - CO_{2\ vol\,\%\ \ OUT}$$

$$\alpha = \frac{CO_{2\ vol\,\%\ [IN]} - CO_{2\ vol\,\%\ \ OUT}}{CO_{2\ vol\,\%\ [IN]} - \ CO_{2\ vol\,\%\ \ IN} \times CO_{2\ vol\,\%\ \ OUT}}$$

$$\alpha = \frac{CO_{2\ vol\,\%\ [IN]} - CO_{2\ vol\,\%\ \ OUT}}{CO_{2\ vol\,\%\ [IN]} \times \ 1 - CO_{2\ vol\,\%\ \ OUT}}$$

In order to get a [%]-value:

$$\boldsymbol{\alpha = \frac{CO_{2\ vol\,\%\ [IN]} - CO_{2\ vol\,\%\ \ OUT}}{CO_{2\ vol\,\%\ [IN]} \times \ 1 - CO_{2\ vol\,\%\ \ OUT}} \times 100}$$

CALCULATION OF THE REBOILER CAPABILITIES

The steam requirement were calculated in order to determine if the steam generating boiler unit would be able to provide enough steam for the solvent regeneration required. **Table A.18** shows the steps that were followed in calculating the steam requirements – the blue lines are assumptions that were made.

TABLE A.18 DETERMINING STEAM REQUIREMENT FOR SOLVENT REGENERATION

Calculating Heat Duty of the Stripping Columns Reboiler		Units
Percentage CO2 in the gas stream fed to absorber	12%	[%]
Percentage CO2 removed in absorber column	85%	[%]
Percentage of Remaining CO2 removed in Stripper	98%	[%]
Molecular mass of CO2	44	[g/mol]
Molecular mass of Air	29.00	[g/mol]
Density of CO2 @ 35°C	1.7	[kg/m3]
Density of Air @ 35°C	1.23	[kg/m3]
Mass fraction of CO2 fed to the absorber	17%	[%]
Density of the gas mixture (estimation)	1.31	[kg/m3]
Average molecular weight of the gas mixture	30.80	[g/mol]
Maximum gas flow Factor as per Absorber Design	3	[Pa^0.5]
Column Diameter	0.2	[m]
Maximum gas Velocity through the absorber	2.621	[m/s]
Cross-sectional Area of the column	0.031	[m2]
Volumetric Gas Flow rate	0.082	[m3/s]
Mass flow rate of the Gas Stream	0.108	[kg/s]
Molar flow rate of the gas stream	0.004	[kmol/s]
Molar flow rate of CO2 fed to the Absorber column	1.514	[kmol/h]
Mass flow rate of CO2 fed to the Absorber column	66.594	[kg/h]
Molar flow rate of CO2 removed as stripper top product	1.261	[kmol/h]
Mass flow rate of CO2 removed as stripper top product	55.473	[kg/h]
Converting Mass flow of CO2 to [ton/s]	1.5E-05	[ton/s]
Estimated Regeneration Engergy Required (From Literature)	5500	[MJ/tonCO2]
Energy Requirment in MW	0.085	[MW]
Energy Requirment in kW	84.8	[kW]
Steam Properties		
Steam (8 bar and 180°C) Enthalpy	2777	[kJ/kg]
Condensate (8 bar and 175°C)	741	[kJ/kg]
Energy provide per kg steam	2036	[kJ/kg]
Efficiency of reboiler	75%	[%]
Mass flow rate of Steam Required	0.0555	[kg/s]
Mass flow rate of Steam Required in [kg/h]	**199.8**	**[kg/h]**

The steam generating boiler unit is capable of delivering steam at a flow rate of 400 kg/h and pressure of 8 bars. Thus it satisfies the steam requirements for solvent regeneration.

SENSOR CALIBRATION, RANGES, ACCURACY AND SCALING

TEMPERATURE SENSORS

PT100s are used for measuring the temperatures on the absorption side of the capture process. It was decided to use PT100s in this section seeing that accurate temperatures are required. The accuracy of the PT100s were specified to be ±0.05°C within a range of 0 – 100°C. The sensors will always be used inside this temperature range.

The stripping section of the capture process is fitted with thermocouple temperature sensors. These sensors were calibrated by programming an offset value into the PLC program. The offset value can be set by the user. Calibrations were performed with a mercury thermostat and the accuracy for the thermocouples would be round about ±1°C in the operating range of each. Further calibrations were done by heating the stripping column with boiling water in the thermosyphon reboiler. The offset values can then be adjusted in order to match the boiling point of pure water.

PRESSURE TRANSMITTORS

The pressure transmitters (absolute, differential and steam) were sized according to their specific application in the pilot plant setup. **Table A.19** gives the applications of all the pressure sensors as well as the ranges selected and to which the sensors were scaled.

TABLE A.19 RANGES FOR THE PRESSURE SENSOR AND THEIR VARIOUS APPLICATIONS

Sensor TAG	Application	Range	Units
PIR-101	Absolute Pressure of the Stripping Column	0 – 1.6	Bar (abs)
PIR-201	Absolute Pressure of Absorber Column /Absolute Pressure for Venturi (I-2) Calculations	0.04 – 4	Bar (abs)
PIR-202	Absolute Pressure for Venturi (I-1) Calculations	0.04 – 4	Bar
dPR-101	Pressure Drop over the Stripping Column	1 – 25	Inches H_2O
dPR-102	Level in the T-section storing liquid Reflux	0 – 1	Meter H_2O
dPR-201	Pressure Drop over the Absorber Column	2.5 – 250	mbar
dPR-202	Pressure Drop over Venturi (I-1)	1 – 60	mbar
dPR-203	Pressure Drop over Venturi (I-2)	1 – 60	mbar
PR-101	Steam Pressure on Supply line to E-104	1 – 10	Bar (gauge)

The accuracy of the absolute pressure cells PIR-201 and PIR-202 are specified by the supplier (Siemens) to be ≤0.15% of the measured value.

Accuracies for the differential pressure cells dPR-201, dPR-202 and dPR-203 is specified by the supplier (Siemens) to be ≤ 0.15% of the measured value.

COMPOSITION ANALYSERS

The composition analysers include a CO_2- and an O_2-analyser. The ranges for these two analysers are 0 – 20 volume % and 0 – 25 volume % respectively. The accuracy of the CO_2 sensor is reported to be < ±1.5 % of the measured volume percentage value with a repeatability of ≤ ±0.05 % volume and a long-term drift of < 0.03 % volume over a twelve month period. The reported accuracy for the O_2 analyser is ≤ 0.4 volume %, with a resolution of ≤ 0.1 % volume.

HAZARDOUS AND OPERABILITY STUDY [HAZOP]

The HAZOP was performed by considering each piece of process equipment along with the streams feeding and flowing from them. Possible hazardous scenarios were considered and the consequences and actions were recorded in the form of HAZOP tables. The format given by Turton et al.(2009) was used in setting up the HAZOP tables.

The HAZOP study was divided into three sections. The three different Areas of the pilot plant setup (100, 200 and 300) were considered separately by considering all the process equipment in the specific areas.

Table A.20 gives the HAZOP tables for the stripping section of the pilot plant setup while **Table A.21** gives the HAZOP tables for Area 200 – the absorption section of the pilot plant setup. The HAZOP study was further extended to the total reflux distillation column – Area 300. The HAZOP tables for Area 300 can be seen in **Table A.22**.

TABLE A.20 HAZOP TABLES FOR AREA 100 OF THE PILOT PLANT SETUP

Equipment Steam Reboiler (E-104)
Intention Heating of solvent for regeneration using steam
Line No. 38
Intention Steam supply line to the reboiler unit, via CV-101

Guide Word	Deviation	Cause	Consequences	Action
NO	Flow	Boiler unit offline	No solvent regeneration	Stop CO2 capturing test runs - Inspect Boiler unit
		CV-101 stuck closed	No steam flow to the reboiler unit	Switch off Boiler unit - inspect CV-101
LESS	Flow	CV-101 stuck	Low steam pressure (PR101)	Inspect CV-101
		Faulty Boiler	Low steam pressure (PR101), solvent regeneration incomplete	Stop CO2 capturing test runs - Inspect Boiler unit
		Other Process also using steam	Low steam pressure (PR101), solvent regeneration incomplete	Inspect other online processes using same boiler unit, time scheduling
MORE	Flow	Faulty PRV on steam boiler unit	Steam line pressure high (PR-101)	Close CV-101, Close Isolation valve V-102, Inspect boiler unit
NO	Pressure	Boiler unit offline	No steam supply to reboiler unit	Close CV-101, inspect boiler unit
		CV-101 stuck closed	No steam flow to reboiler unit	Inspect CV-101
LESS	Pressure	CV-101 stuck	Steam flow low, reboiler temperature Low	Inspect CV-101
		Faulty Boiler	Steam flow low, reboiler temperature Low	Stop CO2 capturing test runs - Inspect Boiler unit
		Other Process also using steam	Low reboiler temperature (TR-102)	Inspect other online processes using same boiler unit, time scheduling
MORE	Pressure	Faulty PRV on Boiler unit	Reboiler Temp. HIGH (TR102)	Activate Emergency Stop of the capture process, Critical alarm TR-102 HIGH, CV-101 interlocked with TR-102
		CV-101 stuck open	Reboiler Temp. HIGH (TR102)	Activate Emergency Stop of the capture process, Critical alarm TR-102 HIGH, switch of Boiler unit, Close Isolation valve V-102, CV-101 interlocked with TR-102

(Table A.20 Continues)

NO	Temperature	Boiler unit offline	No steam pressure (PR-101)	Inspected boiler unit
LESS	Temperature	CV-101 stuck closed	No steam pressure (PR-101)	Inspect CV-101
		CV-101 stuck	Low steam pressure (PR-101)	Stop CO2 capturing test runs - Inspect CV-101
		Other processes using same boiler online	Low steam pressure (PR-101)	Inspect other online processes using same boiler unit, time scheduling
MORE	Temperature	CV-101 stuck open	Reboiler Temp. High (TR-102)	Critical alarm Temp. HIGH activates Emergency stop procedure for the Pilot plant setup, CV-101 interlocked with TR-102

Equipment	Stripping Column (E-105)
Intention	Solvent regeneration for recycling back to absorber column
Line No.	17, 18, 28, 38
Intention	Solvent fed to top of column, Stripping column bottoms, column overheads product, steam supply line to reboiler unit (E-104)

Guide Word	Deviation	Cause	Consequences	Action
NO	Flow	Pump (E-207) not switched on	No solvent feed to column, Rising reboiler temp. (TR-102)	Switch on pump (E-207), inspect if broken, Reboiler temp. HIGH alarm, Critical Temp. Alarm activates Emergency Stop
		Blockage in upstream heat exchanger (E208)	No solvent feed to column, Rising reboiler temp. (TR-102)	Inspect heat exchanger lines, Reboiler temp. HIGH alarm, Critical Temp. Alarm activates Emergency Stop
		Manual valve V-213 /214 closed	Rising Level in storage tank (E-206), No solvent feed to E-105, rising reboiler temp (TR-102)	Inspect heat exchanger isolation valves, Reboiler temp. HIGH alarm, Critical Temp. Alarm activates Emergency Stop
		Automated Valves V-207 A/B in wrong position	Solvent from absorber bottom recycled back to storage vessel (E-206)	Switch Valves V-207A/B to allow flow to the top of stripping column (E-105)
LESS	Flow	Pump (E-207) flow not matching flow by Pump (E-108)	Rising level in storage tank (E-206)	Check that the flow rates delivered by the two pumps match according to calibrations that has been done
MORE	Flow	Pump (E-207) flow not matching flow by Pump (E-108)	Rising level in storage tank (E-102)	Check that the flow rates delivered by the two pumps match according to calibrations that has been done

(Table A.20 Continues)

MORE	Pressure	CV-101 stuck open	Reboiler Temp. HIGH (TR102) and rising column pressure (PIR-101)	Activate Emergency Stop of the capture process, Critical alarm TR-102 HIGH, Critical pressure alarm activates Emergency Stop
NO	Temperature	Boiler unit offline	No steam pressure (PR-101)	Inspected boiler unit
		CV-101 stuck closed	No steam pressure (PR-101)	Inspect CV-101
LESS	Temperature	CV-101 stuck	Low steam pressure (PR-101)	Stop CO2 capturing test runs - Inspect CV-101
		Other processes using same boiler online	Low steam pressure (PR-101)	Inspect other online processes using same boiler unit, time scheduling
MORE	Temperature	CV-101 stuck open	Reboiler Temp. High (TR-102), TR-103 column bottom temp high	Critical alarm Temp. HIGH activates Emergency stop procedure for the Pilot plant setup, back-up alarm on TR-103 if TR-102 is faulty

Equipment Pulsation Pump (E-108)
Intention Solvent flow from bottom of stripping column to top of absorber column (E-203), via heat exchanger (E-208) and solvent cooler (E-209)
Line No. 20, 21, 22, 23, 13
Intention Solvent transport from E-102, to E-208 and E-209. Feed to top of absorber column (E-203)

Guide Word	Deviation	Cause	Consequences	Action
NO	Flow	Pump (E-108) faulty	Rising level in storage pot (E-102), no flow indication on rotameter (FI-101)	Stop the process and inspect pump (E-108)
		Upstream line blockage (line 20)	Rising level in storage pot (E-102), no flow indication on rotameter (FI-101)	Stop the process and inspect lines downstream from E-108
		Manual valves V-114 /115 closed	Rising level in storage pot (E-102), no flow indication on rotameter (FI-101)	Check manual valves upstream from pump (E-108)
LESS	Flow	Pump (E-108) on wrong manual setting	Rising level in storage tank (E-206), temp. TR-214 lower than expected	Check manual flow rate setting on the pulsation pump (E-108)
MORE	Flow	Pump (E-108) flow not matching flow by Pump (E-207)	Rising level in storage tank (E-206)	Check that the flow rates delivered by the two pumps match according to calibrations that has been done

(Table A.20 Continues)

Equipment Stripping Column Condensers (E-111)
Intention Condensation of any evaporated solvent from the stripping column
Line No. 28, 32, 33
Intention Carry-over from stripping column for condensation, Cooling water supply to condensers, Cooling water return from condensers

Guide Word	Deviation	Cause	Consequences	Action
NO	Flow	Cooling water pump not switched on	FIR-101 reading registers as 0.000 m3/h. System will not be Started up	Cooling Water LOW FLOW alarm will keep Emergency Stops activated. CV-101 interlocked with FIR-101
		Upstream line blockage (line 32)	No cooling water supply to condensers, rising temperature TR-109	Inspect cooling water lines and upstream manual valves (downstream from FIR-101)
LESS	Flow	Upstream line blockage (line 32)	FIR-101 reading registers below setpoint for LOW FLOW alarm.	LOW FLOW alarm will activated Emergency stops shutting down the process.
MORE	Pressure	Cooling water flow to low	Reboiler Temp. HIGH (TR102) and rising column pressure (PIR-101)	Activate Emergency Stop of the capture process, Critical alarm TR-102 HIGH, Critical pressure alarm activates Emergency Stop, increase Low Flow alarm setpoint
MORE	Temperature	Cooling water flow to low	Reboiler Temp. HIGH (TR102) and rising column pressure (PIR-101)	Activate Emergency Stop of the capture process, Critical alarm TR-102 HIGH, Critical pressure alarm activates Emergency Stop, increase Low Flow alarm setpoint

(Table A.20 Continues)

Equipment T-piece reflux storage unit (E-112)
Intention Creating buffer liquid level for Reflux pump (E-113)
Line No. 29
Intention Ensuring liquid level to prevent reflux pump (E-113) from running dry

Guide Word	Deviation	Cause	Consequences	Action
NO	Flow	Low evaporated solvent flow to condensers, low reboiler temp. (TR102)	Low level in E-112, LOW reading on dPR-102, No reflux to return to top of stripping column (E-105)	Low dPR-102 reading interlocked with reflux pump (E-113).
MORE	Flow	Running Reboiler at capacity	High flow of evaporated solvent to condensers and thus E-112. High reflux flow to top of column required	Reflux pump (E-113) running continuously to return all condensed solvent to the top of the column (E-105)

Equipment Reflux Pump (E-113)
Intention Returning any condensed solvent to the top of the stripping column (E-105)
Line No. 29. 30
Intention Controlling the level in liquid storage T-piece (E-112), Feeding Reflux to the top of the stripping column (E-105)

Guide Word	Deviation	Cause	Consequences	Action
NO	Flow	Low evaporated solvent flow to condensers, low reboiler temp. (TR102)	Low level in E-112, LOW reading on dPR-102, No reflux to return to top of stripping column (E-105)	Low dPR-102 reading interlocked with reflux pump (E-113).
		Blockage in upstream T-piece (E112)	No reflux return to the stripping column (E-105), Reflux will overflow into distillate pot (E-103)	Stop the process, inspect lines and T-piece for possible blockage

TABLE A.21 HAZOP TABLES FOR AREA 200 OF THE PILOT PLANT SETUP

Equipment Recycle Blower unit (E-201A)
Intention Circulation of the Process gas through the absorber colunm, (E-203) and water wash section (E-204) and return to E-205
Line No. 1, 2, 3, 4, 5, 6, 7
Intention Circulation of the Process gas

Guide Word	Deviation	Cause	Consequences	Action
NO	Flow	Manual butterfly valves V-201 /206 or V-203/204 closed	No flow through the absorber column (E203), LOW MFR display on venturi	Switch OFF blower motor, check that all manual butterfly valves are in the required position
		Problem with blower motor	No gas feed to absorber column (E203), LOW MFR display on venturi	Shut down system and inspect blower motor
		Inverter communication failure	No flow through column. Blowe present value stays 0.00	Reset inverter installed for the blower motor.
LESS	Flow	Manual butterfly valves not properly opened	Flow rate recorded by venturi flow meters less than expented.	Stop blower unit and inspect Manual butterfly valves for proper positioning
		Inverter communication failure	Low process gas flow supply to the absorber column (E-203)	Reset inverter and check error messages.
LESS	Pressure	Manual butterfly to atmosheric vent open	Lower Column Pressure (PIR-201) , Loss of loaded gas to the atmosphere	Shut down blower unit and inspect V-204
MORE	Pressure	Blockage at top of column	Low flow through column, pressure build-up, (PIR-201)	Blower interlocked with absorber column pressure (PIR-201), Inspect top section of the column
MORE	Temperature	Gas not sufficiently cooled in Water wash section	Rise in temperature TR-215 and TR-216. Wash water temperature HIGH (TR-214)	Blower interlocked with Temperatures TR-215 and TR-216

(Table A.21 Continues)

Equipment Air blower unit (E-201B)
Intention Feeding Air to the bottom of the absorber column
Line No. 8, 2, 3, 4, 9
Intention Air blower used for studies where the process gas is air, outlet to the atmosphere open

Guide Word	Deviation	Cause	Consequences	Action
NO	Flow	Blower motor failure	No Air flow through the column	Shut down blower, inspect blower motor
		Butterfly valve V-202 closed	No flow through column	Shut down blower, change position of V-202
		Manual valve V-213 /214 closed	Rising Level in storage tank (E-206), No solvent feed to E-105, rising reboiler temp (TR-102)	Inspect heat exchanger isolation valves, Reboiler temp. HIGH alarm, Critical Temp. Alarm activates Emergency Stop
LESS	Flow	Blower air inlet closed	Low air flow through the column	Switch of blower unit, Safely adjust air intake to the air blower
MORE	Flow	Air intake fully open	Air flow higher than required	Switch of blower and adjust blower intake
MORE	Pressure	Vent to the atmosphere closed, V-204	Low flow through the column, pressure increase, PIR-201	Shut down blower unit, inspect valve position (V-204)

(Table A.21 Continues)

Equipment Absorption Column (E-203)
Intention Provides direct contact between reactive solvent and allows absorption of CO2 form the process gas
Line No. 3, 4, 13, 14
Intention Process gas feed from E-201A/B, treated gas outlet from top to E-205, Lean solvent inlet from E-209, Rich solvent outlet to E-206

Guide Word	Deviation	Cause	Consequences	Action
NO	Gas Flow	V-201/202 in closed position	No gas flow to the column	Open V-201/202 depending on the blower unit used
		V-203 and V-204 in closed position	No gas flow through the column	Open either V-203 or V-204 depending of blower used
	Liquid Flow	Upstream manual valve closed	No solvent feed to top of absorber column	Check downstream valves V-110/215/216/217
LESS	Gas Flow	V-201/202 not properly positioned	Low gas flow rate registered by Venturi mass flow meter (I-1)	Check manual butterfly valves (V-201/202)
	Liquid Flow	Upstream obstruction in the solvent line	Low solvent flow to column, depleting liquid level in E-206	Check upstream lines for possible obstructions
MORE	Liquid Flow	Pump (E-108) flow not matching flow by Pump (E-207)	Rising level in storage tank (E-206)	Check that the flow rates delivered by the two pumps match according to calibrations that has been done
LESS	Pressure	Vent valve V-204 to atmosphere open	Loaded gas lost the the atmosphere	Shut down process and close valve V-204 to the atmosphere.
MORE	Pressure	Both V-203 and V-204 closed	No gas outlet, column pressure increase (PIR-201)	Blower unit interlocked with column pressure, PIR-201
	Pressure	Blockage at top of column	Low flow through column, pressure build-up, (PIR-201)	Blower interlocked with absorber column pressure (PIR-201), Inspect top section of the column
MORE	Temperature	Solvent entering column not cooled sufficiently	Absorber column temperature rising, recycled process gas temp. HIGH (TR-215)	Blower interlocked with Process Gas Temp. (TR-215), System interlocked with solvent feed temp. (TR-209)

(Table A.21 Continues)

Equipment Water Wash Section (E-204, E-210, E-211)
Intention Removing any entrained solvent from the process gas before gas is recycled back to surge tank (E-205)
Line No. 4, 24, 25
Intention Gas returned to E-205, Wash water feed to E-204, Wash water return to Wash water tank (E-210)

Guide Word	Deviation	Cause	Consequences	Action
NO	Flow	Faulty Wash water pump	No Water flow to wash water section, Possible solvent carry-over to the gas lines, process gas escape due to liquid seal being absent	Shut down process and inspect wash water pump
		Low level in Wash water tank	No flow to wash water section, possible entrained solvent in process gas lines, process gas escape due to liquid seal being absent	Shut down process, inspect the level of the wash water storage tank, E-210
		Manual ball valves V-219/220/222 closed	All wash water are circulated back to the wash water storage tank (E-210)	Open V-219, V-220, V-222
LESS	Flow	Throttling valve V-219 not sufficiently open	Low flow to wash water section, process gas escape due to liquid seal being absent	Throttle V-219 sufficiently to provide proper flow to the water wash section
MORE	Flow	Throttling valve V-219 fully open	Water flow to wash section to high, Water overflow into absorption column	Throttle V-219 sufficiently to provide proper flow to the water wash section
HIGH	Temperature	Wash Water cooling not sufficient	Increase in wash water temperature (TR-214) and process gas (TR-216)	Blower interlocked with TR-216, Process interlocked with TR-216 for critical temperature

(Table A.21 Continues)

Equipment Surge tank / Knock-out drum (E-205)
Intention Storage for process gas, absorbing pressure spikes due to gas loading, droplet settling from process gas, completes gas recycle loop
Line No. 6, 7, 10, 11, 12
Intention Recycle from E-203, Blower suction line, CO2 line from stripping section (E-105), CO2 and N2 gas feed lines from gas cylinders

Guide Word	Deviation	Cause	Consequences	Action
NO	Flow	V-203 and/or V-206 in closed position	No gas allowed to flow in the gas recycle loop, Venturi flow meters registers no gas flow	Open V-203/206
LESS	Flow	V-204 to atmosphere open	Low gas flow registered by top venturi flow meter (I-2) compared to (I-1)	Close V-204
LESS	Pressure	Leakage from system	Drop in CO2 and N2 compositions in the process gas	Check the system for possible leaks
MORE	Pressure	V-204 to atmosphere open	Loss of pressure in absorber column (PIR-201)	Close V-204
		V-206 closed	Blower suction valve closed, will lead to pressure increase (PIR-201)	Open V-206
	Pressure	CV-201/202 stuck in open Position	Pressure spike in absorber column (PIR-201), PRV installed in surge tank will relieve pressure from tank	Critical column pressure will trigger alarm, system interlock with critical column pressure, Blower interlocked with absorber column pressure (PIR-201), close gas regulators, Inspect control valves
MORE	Temperature	Process gas not sufficiently cooled by Wash Water	Rising process gas temperature (TR-215), absorption less and less efficient	Blower interlocked with Process Gas Temp. (TR-215),

(Table A.21 Continues)

Equipment Rich Solvent Pump (E-207)
Intention Directing rich solvent to the stripping section of the pilot plant
Line No. 15, 16
Intention Solvent from E-206, solvent pumped to top of E-105, via E-208

Guide Word	Deviation	Cause	Consequences	Action
NO	Flow	Inverter malfuntion	No solvent flow to top of stripping column, disturbed balance between E-108 and E-207, E-206 level rises	Reset inverter installed on E-207 motor, check for error messages
		Blockage in upstream solvent storage vessel (E-206)	No solvent flow to top of stripping column, disturbed balance between E-108 and E-207, E-206 level rises	Stop the process, inspect solvent storage vessel (E-206)
			Rising Temperature of TR-111 installed in Feed line to Stripping column	Activate Temperature High Alarm, interlocked with steam valve in order to protect the Reboiler unit (E-104) from going dry
LESS	Flow	V-208/209/212/213 /214 partially closed	Low flow to top of stripping column, disturbed balance between to columns	Open V-208/209/212/213/214
LESS	Temperature	Insufficient absorption in column E-203	Higher reboiler temperature due to rich solvent being lean (TR-102 HIGH)	Alarm for TR-102 high triggered, Steam valve and System interlocked with TR-102 critically high
MORE	Temperature	Insufficient cooling in the solvent cooler (TR-209)	System temperature continue to rise	Temperature Alarms triggered (TR-102/103/208/209/215/216), System emergency stops interlocked with critical temperatures

TABLE A.22 HAZOP TABLES FOR AREA 300 OF THE PILOT PLANT SETUP

Equipment Steam Reboiler (E-301)
Intention Heating the mixture to be separated in the Total Reflux Distillation Column
Line No. 38
Intention Steam supply line to the reboiler unit, via CV-101

Guide Word	Deviation	Cause	Consequences	Action
NO	Flow	Boiler unit offline	No distillation runs can be done	Inspect boiler unit, reasons for boiler being offline
		CV-101 stuck closed	No steam flow to the reboiler unit	Switch off Boiler unit - inspect CV-101
LESS	Flow	CV-101 stuck	Low steam pressure (PR-301)	Inspect CV-101
		Faulty Boiler	Low steam pressure (PR-301), solvent regeneration incomplete	Inspect boiler unit, reasons for boiler being offline
		Other Process also using steam	Low steam pressure (PR-301), solvent regeneration incomplete	Inspect other online processes using same boiler unit, time scheduling
MORE	Flow	Faulty PRV on steam boiler unit	Steam line pressure high (PR-301)	Close CV-101, Close Isolation valve V-V301, Inspect boiler unit
NO	Pressure	Boiler unit offline	No steam supply to reboiler unit	Close CV-101, inspect boiler unit
		CV-101 stuck closed	No steam flow to reboiler unit	Inspect CV-101
LESS	Pressure	CV-101 stuck	Steam flow low, reboiler temperature Low (TR-302)	Inspect CV-101
		Faulty Boiler	Steam flow low, reboiler temperature Low (TR-302)	Inspect Boiler unit for malfunction
		Other Process also using steam	Low reboiler temperature (TR-302)	Inspect other online processes using same boiler unit, time scheduling
MORE	Pressure	Faulty PRV on Boiler unit	Reboiler Temp. HIGH (TR-302)	Activate Emergency Stops, Trigger pressure High alarm, Critical alarm TR-302 HIGH, CV-101 interlocked with TR-302
		CV-101 stuck open	Reboiler Temp. HIGH (TR-302)	Activate Emergency Stop, Critical alarm TR-302 HIGH, switch of Boiler unit, Close Isolation valve V-301, CV-101 interlocked with TR-302

(Table A.22 Continues)

NO	Temperature	Boiler unit offline	No steam pressure (PR-301)	Inspected boiler unit
		CV-101 stuck closed	No steam pressure (PR-301)	Inspect CV-101
LESS	Temperature	CV-101 stuck	Low steam pressure (PR-301)	Stop CO2 capturing test runs - Inspect CV-101
		Other processes using same boiler online	Low steam pressure (PR-301)	Inspect other online processes using same boiler unit, time scheduling
MORE	Temperature	CV-101 stuck open	Reboiler Temp. High (TR-302)	Critical alarm Temp. HIGH activates Emergency stop procedure for the Pilot plant setup, CV-101 interlocked with TR-302

Equipment Total Reflux Column (E-302)
Intention Total Reflux distillation of a mixture of organic components

Guide Word	Deviation	Cause	Consequences	Action
MORE	Pressure	CV-101 stuck open	Reboiler Temp. HIGH (TR302) and rising column pressure (PIR-101)	Activate Emergency Stop, Critical alarm TR-302 HIGH, Critical pressure alarm activates Emergency Stop
NO	Temperature	Boiler unit offline	No steam pressure (PR-301)	Inspected boiler unit
		CV-101 stuck closed	No steam pressure (PR-301)	Inspect CV-101
LESS	Temperature	CV-101 stuck	Low steam pressure (PR-301)	Inspect CV-101
		Other processes using same boiler online	Low steam pressure (PR-301)	Inspect other online processes using same boiler unit, time scheduling
MORE	Temperature	CV-101 stuck open	Reboiler Temp. High (TR-302)	Critical alarm Temp. HIGH activates Emergency stop procedure for the Pilot plant setup

(Table A.22 Continues)

Equipment Total Reflux Column Condensers (E-111)
Intention Total Condensers returning all evaporated organic components to the column
Line No. 36, 37
Intention Cooling water supply line to condensers, Cooling water return line

Guide Word	Deviation	Cause	Consequences	Action
NO	Flow	Cooling water pump not switched on	FIR-101 reading registers as 0.000 m3/h. System will not be Started up	Cooling Water LOW FLOW alarm will keep Emergency Stops activated. CV-101 interlocked with FIR-101
		Upstream line blockage (line 32)	No cooling water supply to condensers, rising temperature TR-109	Inspect cooling water lines and upstream manual valves (downstream from FIR-101)
LESS	Flow	Upstream line blockage (line 32)	FIR-101 reading registers below setpoint for LOW FLOW alarm.	LOW FLOW alarm will activated Emergency stops shutting down the process.
MORE	Temperature	Cooling water flow to low	Reboiler Temp. HIGH (TR-302) and rising column pressure (PIR-101)	Activate Emergency Stop of the capture process, Critical alarm TR-302 HIGH, Critical pressure alarm activates Emergency Stop, increase Low Flow alarm setpoint

APPENDIX B: PILOT PLANT COMMISSIONING

This appendix contains the results from the different phases of the pilot plant commissioning. The commissioning was divided into three different steps and each will be discussed in detail.

1. Liquid circulation – Water was used
2. Gas Recycle Loop Commissioning
3. Steam Commissioning with Water

LIQUID CIRCULATION

This was done in order to check for leaks in the liquid circulation loop. No real results were recorded during this first step of the pilot plant commissioning.

GAS RECYCLE LOOP COMMISSIONING

The gas cycle commissioning was subdivided into three different phases, each investigating a different aspect of the gas recycle loop.

PHASE 1(A)

LOADING GAS CYCLE WITH CARBON DIOXIDE TO DETERMINE GAS LEAKAGE RATES FROM SYSTEM AND TESTING OF THE GAS SAMPLING SYSTEM THAT WAS SET UP

Carbon dioxide was loaded into the gas recycle loop in order to test the gas sampling mechanisms (sample pump, online analysers, switching sample valves and sample valve manifold setup) that were put in place. This also serves as a test in order to determine the rate of gas leakage from the system and the effect of process gas mass flow rate on the leakage rate of the loaded gas from the system.

GAS SAMPLE ANALYSIS

Initially the gas recycle loop was loaded with CO_2 (while purging) to a concentration of about 6 volume % at a gas circulation rate of about 130 kg/h. This can be seen in **Figure B.97**. The sampling switch valves were set on a time sequence of 100 seconds.

After initially only sampling from the feed stream of the column the valve switching were initiated and this can be seen in **Figure B.97** by the sudden drop in CO_2 concentration. At the

first few valve switches the concentration in the sample stream from the top of the column (lower concentration) indicated a leak in this sample line and it could be fixed fairly quickly.

At about 1500 seconds the system CO_2 concentration were again increased to about 4 volume %. From the decreasing CO_2 concentration profile it can be seen that the gas sampling from the top and bottom of the column yields comparable results to that of the sample drawn from the feed line. It can also be seen that the dead volume in the sample lines affects the concentration reading for merely a few seconds.

The gas analysis setup is working well, however the rate of gas leakage from the system are a major concern.

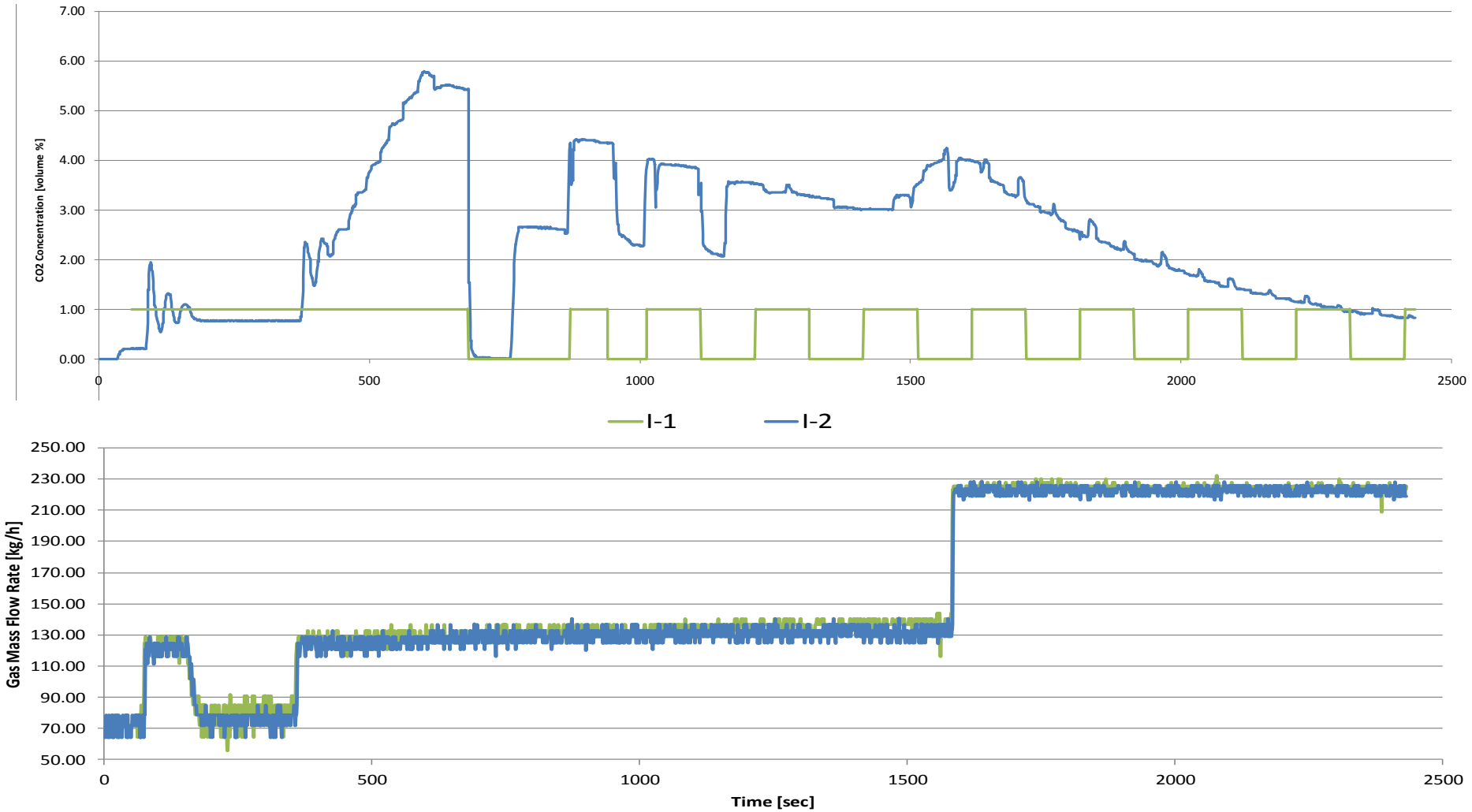

FIGURE B.97PROFILES SHOWING FIRST RUNS FOR GAS COMMISSIONING WITH CO2 GAS, (A) CO_2 CONCENTRATION PROFILE (BLUE), SAMPLING FROM FEED LINE ON/OFF (GREEN) WHEN OFF, SAMPLING FROM TOP OF COLUMN

PHASE 1 (B)

The column was inspected for leaks and all connections where possible gas leakage might occur were checked. **Figure B.98** shows the trends obtained after fixing possible leakages. A low blower speed with a purge to the atmosphere was used in order to load CO_2 into the gas recycle loop (Up to about 500 seconds). After that the purge to atmosphere were closed and the blower speed was increased to about 200 kg/h.

No additional CO_2 were added to the system. In about 10 minutes the concentration decreased with about 1 volume %. Compared to the leakage rates in **Figure B.97** (About 3 volume % in 10 minutes) this is a considerable improvement. In the next phase of the gas cycle commissioning an attempt will be made at quantifying the rate of gas leakage from the system.

The blower speed was increased to about 325 kg/h and this lead to a slightly faster leaking rate, but still around about 2 volume % for 20 minute period. The blower was switched off at about 2400 seconds with a gas concentration of 3.5 volume % CO_2. This concentration dropped from 3.5 to 3.15 over the next hour period.

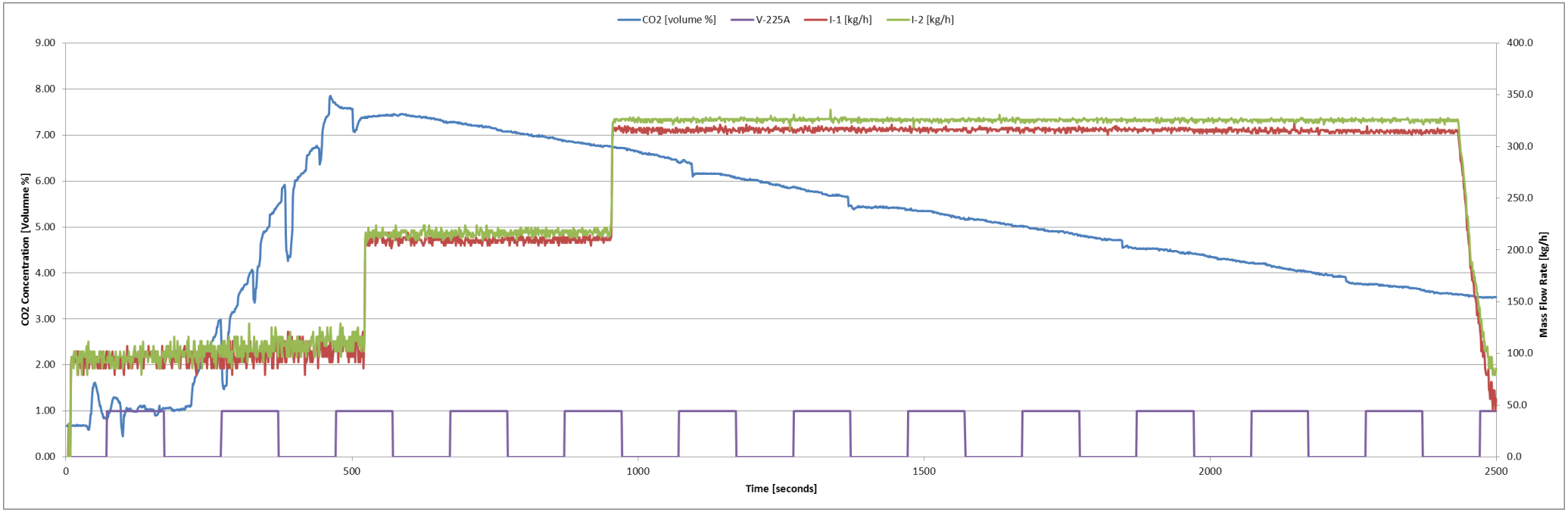

FIGURE B.98 GAS CYCLE COMMISSIONING, LEAKAGE RATE OF THE CO2 GAS OBSERVED FROM THE DECREASING CONCENTRATION

LOADING GAS CYCLE WITH NITROGEN AND CARBON DIOXIDE

The gas cycle is loaded with Nitrogen in order to reduce the oxygen content of the process gas from the normal 20.61 volume % to about 5 volume % prior to starting the experiments. The system is first loaded with nitrogen gas, followed by the CO_2 that will be required for the particular CO_2 capture study run. This is done in order to prevent any loss of CO_2 due to purging required when loading N_2. More detail regarding this is provided in the results of phase 3 of the gas cycle commissioning.

The gas concentrations are also directly related to the blower speed, and this is thus an indication that the leakages from and into the system are mainly situated at the blower shaft. **Figure B.99** shows this clearly when considering the time just after 19h00, when the mass flow rate was increased to about 360 kg/h.

Figure B.100 shows the decrease in the CO_2 concentration for the period when a gas flow rate of 120 kg/h was maintained. This can be further quantified to a decrease of 1 volume % for every 45 minutes.

Figure B.101 shows where nitrogen was added to the system decreasing the O_2 as well as the CO_2 concentration. The mass flow rate was maintained at 120 kg/h. The rates at which the O_2- and CO_2 concentrations increase and decrease respectively are very similar.

Figure B.102 shows the increase in the gas leakage from and into the system when the mass flow rate of the process gas is increased to about 360 kg/h. The equations of the fitted trendlines can be used to quantify the gas leakage from and into the system. The CO_2 loss rate can be calculated to be 3.9 volume % per hour and the O_2 leakage into the system can be calculated to be 3.68 volume % per hour.

The next phase of the gas cycle commissioning will be used in order to load the gas recycle loop to the particular gas concentrations that will be used during experimental runs. The leakage rates at these concentrations will be determined.

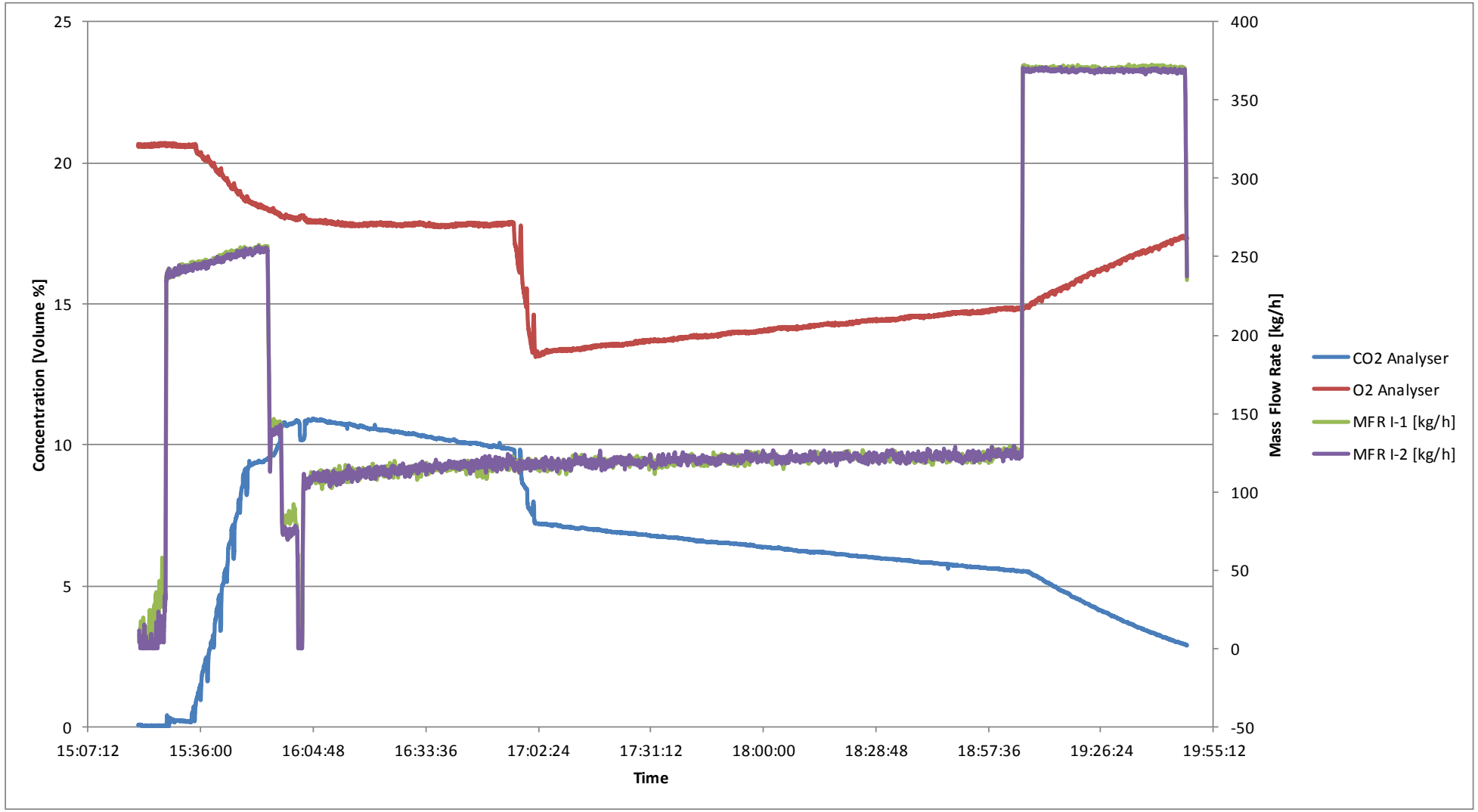

FIGURE B.99 TRENS OF THE GAS CONCENTRATIONS AND MASS FLOW RATES RECORDED DURING THE GAS COMMISSIONING PHASE

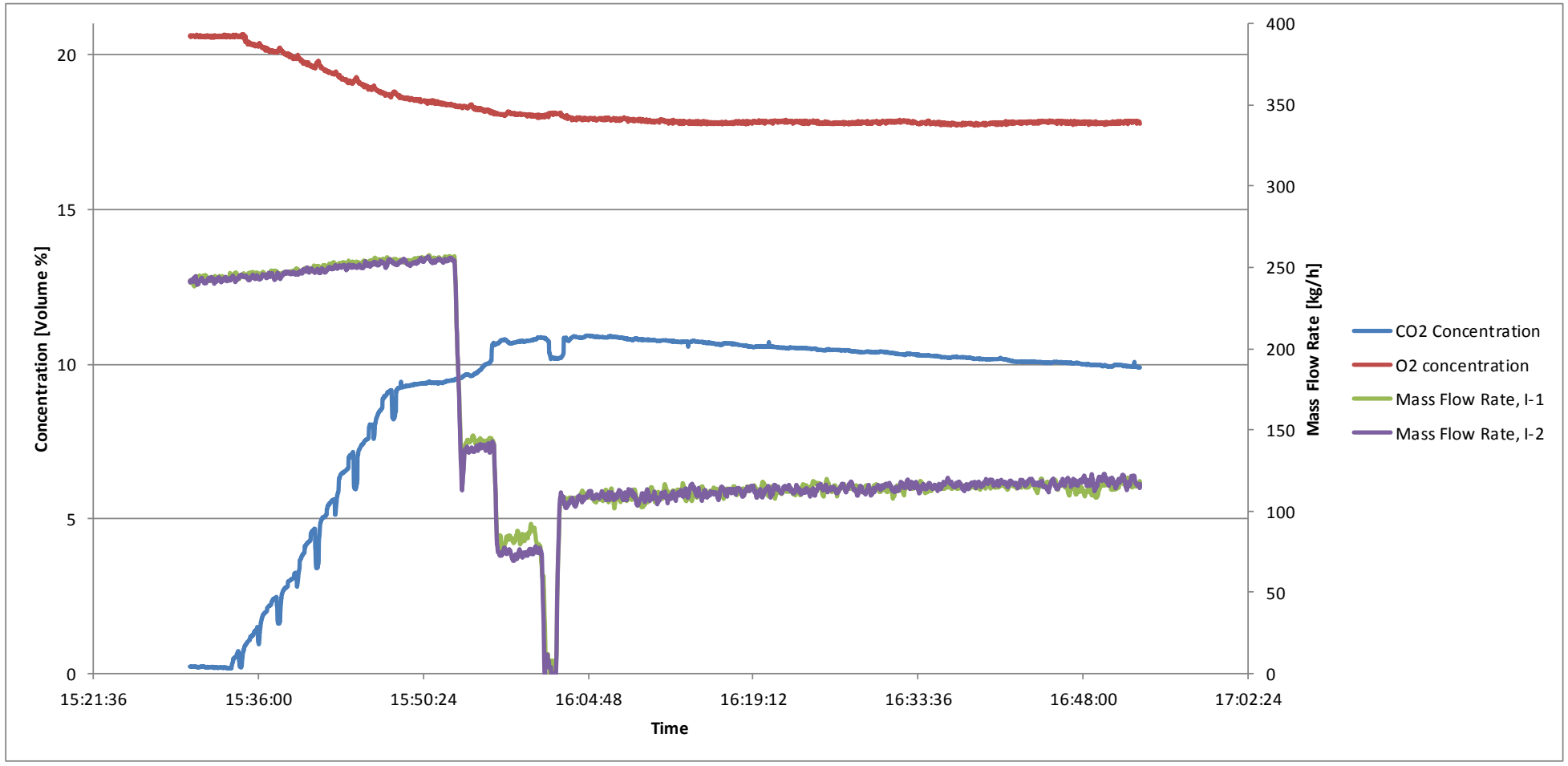

FIGURE B.100 GAS LOADING INTO THE SYSTEM AS WELL AS THE RATE OF LOSS IN CONCENTRATION AT A MASS FLOW RATE OF ABOUT 120 KG/H

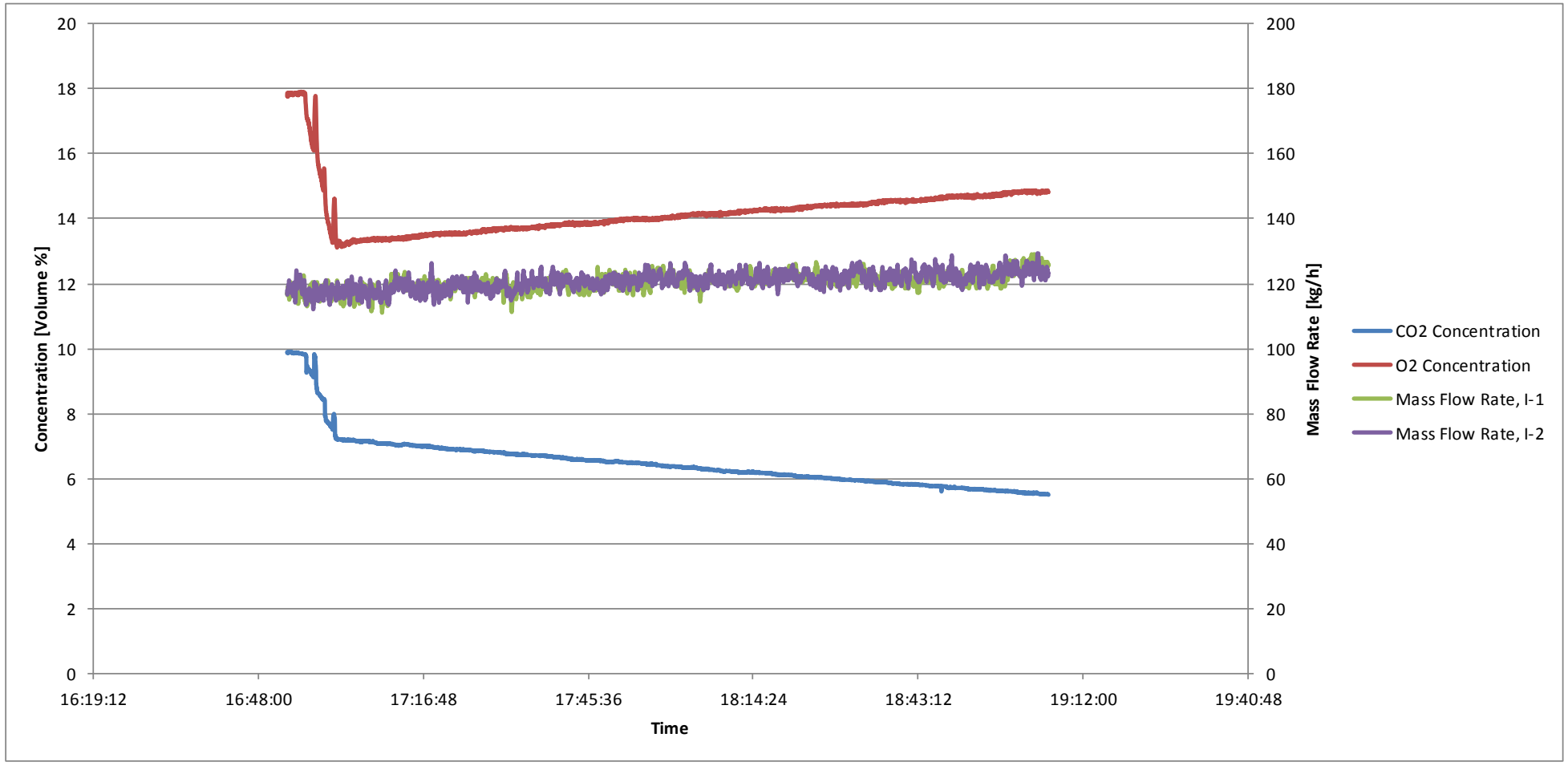

FIGURE B.101 LOADING GAS CYCLE WITH NITROGEN GAS AND THE DECREASING EFFECT IT HAS ON THE CO_2 CONCENTRATION AT MASS FLOW RATES OF 120 KG/H

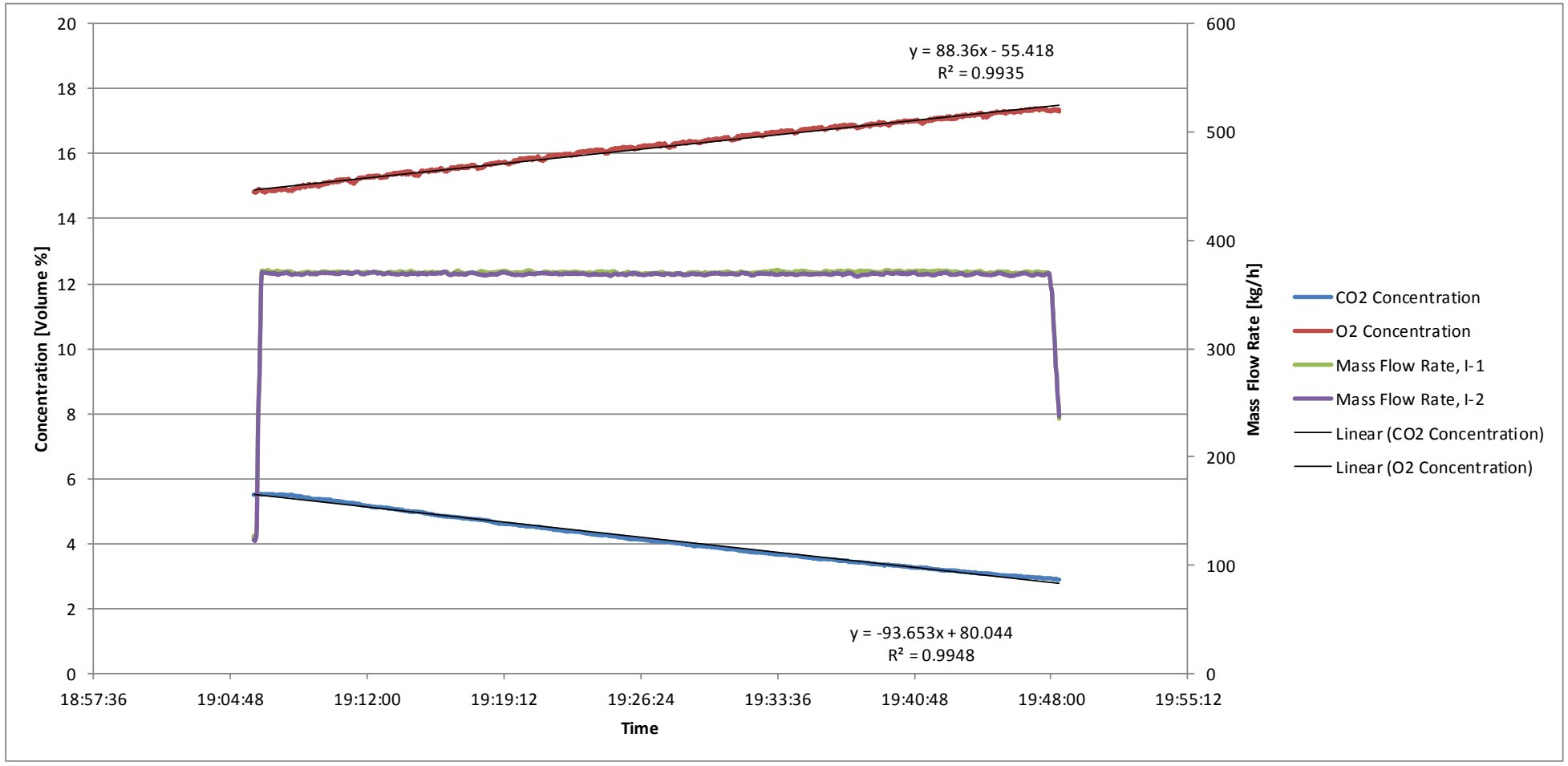

FIGURE B.102 INCREASED GAS LEAKAGE RATES AT HIGHER BLOWER SPEEDS DELIVERING MASS FLOW RATE OF ABOUT 360 KG/H

PHASE 3

LOADING NITROGEN AND OXYGEN TO REQUIRED CONCENTRATIONS – ATTEMPT TO QUANTIFY MAKE-UP GAS REQUIREMENTS

Gas cycle commissioning were continued by loading the gas recycle loop with nitrogen- and carbon dioxide gas to obtain a process gas with the require gas composition. **Figure B.103** shows the gas composition trends that were obtained during this gas cycle commissioning phase.

GAS LOADING METHOD

At first an attempt was made at adding the nitrogen and CO_2 gas simultaneously to the system. This can be seen in **Figure B.103** for the time period 08h30 – 09h00. It was found that in purging the system while loading nitrogen to obtain the required O_2 concentration (about 5 volume %), a considerable amount of CO_2 is also lost from the system. This complicates reaching the required CO_2 concentration and some of the CO_2 is lost to the atmosphere.

An alternative method of gas loading was to load the nitrogen into the gas recycle loop until the required O_2 concentration is reached. This is done prior to loading any CO_2 into the system. After the O_2 concentration is below 6 volume %, CO_2 can be loaded into the system without major losses. This can be seen in **Figure B.103** for the time period 10h00 – 10h25.

MASS FLOW RATE CONTROL

In an attempt to obtain better control on the mass flow rate of the process gas, a throttling valve was installed upstream from the blower inlet. The effect of gas throttling on the gas compositions of the process gas were investigated by comparing the gas leakage from and into the system for both gas circulation with- and without throttling.

The case where gas throttling were employed can be seen for the time period between 09h00 – 10h00, and can be compared to the case with no throttling, 11h30 – 12h00. It can be seen that leakages are less without throttling. This can be explained by the pressure drop caused by the valve upstream from the blower inlet, leading to a lower pressure at the blower intake and thus a higher rate of air leakage into the system.

Reduced leakage rates can be seen in **Figure B.104**. Leakage rates can be quantified, with the use of fitted trendlines, to be 1.57 and 2.01 volume % per hour for CO_2 (from system) and O_2 (into system) respectively. This is for a process gas mass flow rate of 125 kg/h.

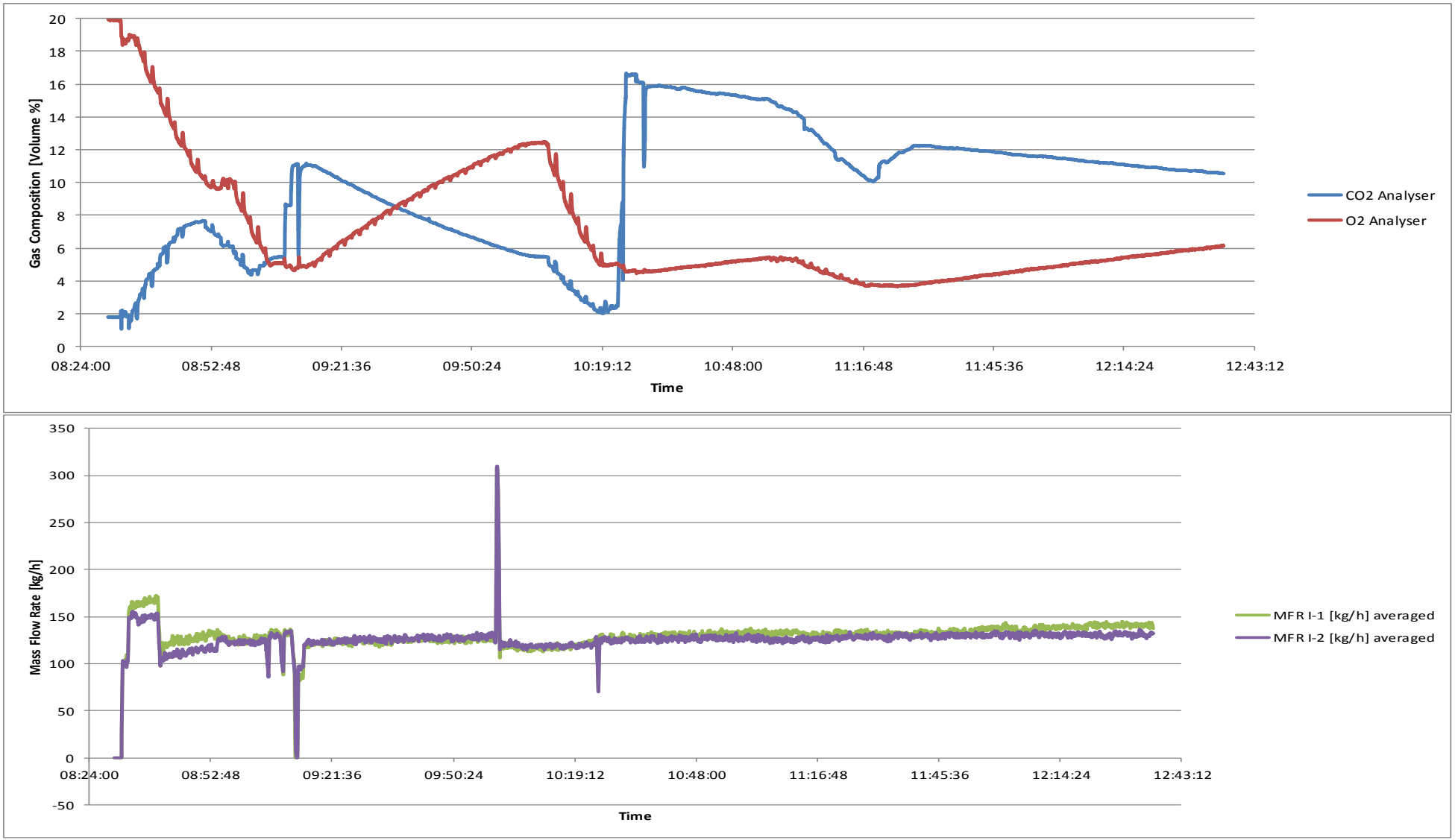

FIGURE B.103A) GAS COMPOSITIONS FOR THE GAS CYCLE COMMISSIONING PHASE (TOP); **B)** MASS FLOW RATE OF THE PROCESS GAS STREAM (BOTTOM)

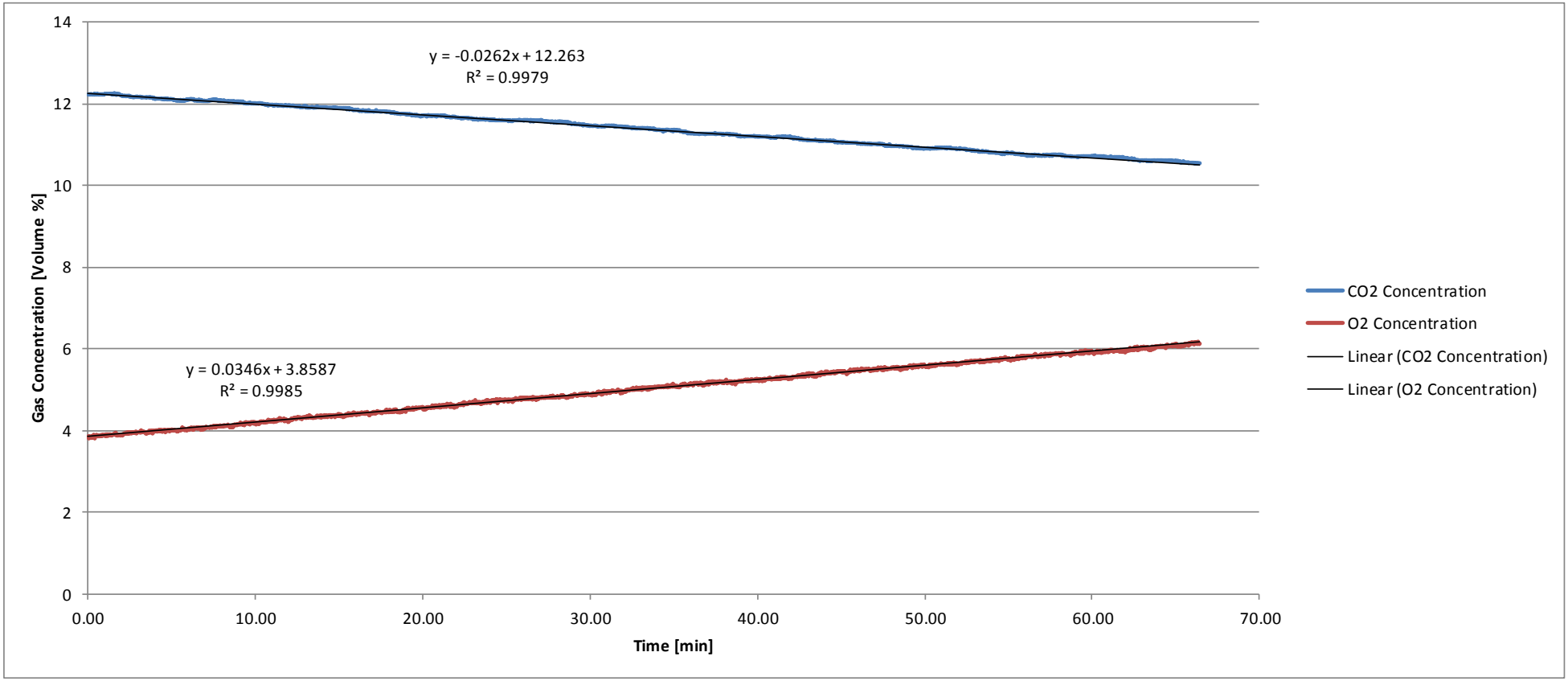

FIGURE B.104 QUANTIFICATION OF THE GAS LEAKAGE FROM THE SYSTEM

The steam commissioning to the pilot plant setup was done in five different phases which covers the heating and cooling capabilities of the cross heat exchanger and the solvent cooler, allowing the pilot plant to reach thermal equilibrium and performing energy balances at different liquid flow rate and steam flow rates. This was used to estimate the heat loss from the pilot plant to the environment.

PHASE 1

STEAM COMMISSIONING AND LIQUID CIRCULATION FOR TESTING HEATING AND COOLING CAPABILITIES OF THE HEAT EXCHANGER AND COOLER UNITS

The steam commissioning was done with water instead of reactive solvent. The steam valve was set to 30 % OPEN and the stripping column was heated gradually. The temperature profiles of the stripping column were recorded and plotted against time. An attempt was also made at testing the heating and cooling capabilities of the heat exchanger and the solvent cooler units, by circulating the liquid throughout the entire system. The liquid flow rates between the stripping- and absorber columns were balanced by adjusting the setpoints on pumps E-108 and E-207.

Figure B.105 shows the temperature profile for the steam during the commissioning period. The steam valve was closed at round about 16h20.

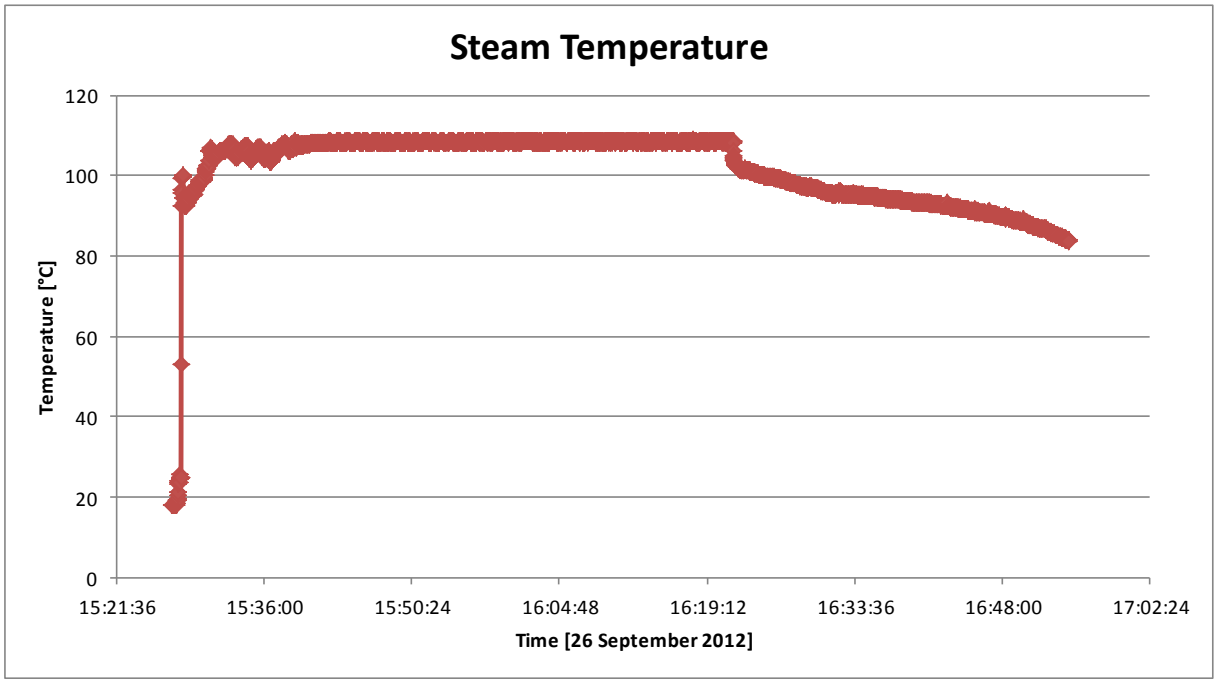

FIGURE B.105 STEAM TEMPERATURE RECORDED FOR THE COMMISSIONING PERIOD

Figure B.106 shows the temperature profiles for the stripping column as it was heated from the bottom to the top. The locations for the various temperature tags showed in the plots (**Figure B.106**, **Figure B.107** and **Figure B.108**) can be seen in the P&ID presented in **Figure 28**.

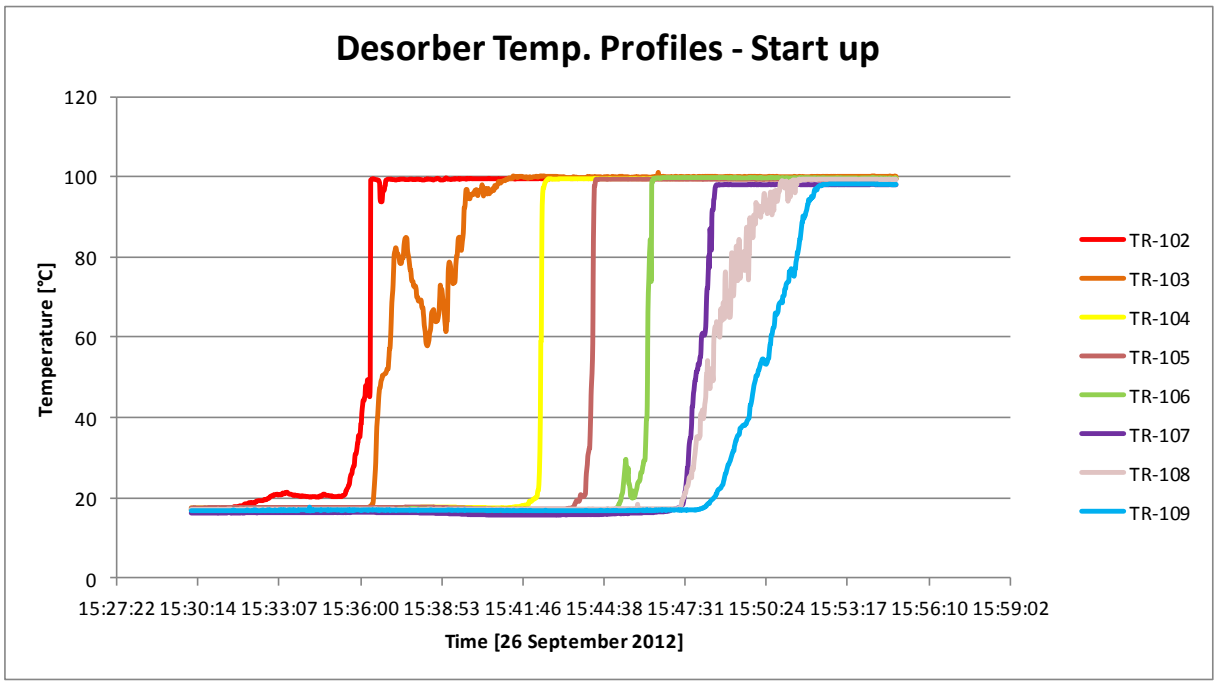

FIGURE B.106 STRIPPING COLUMN TEMPERATURE PROFILES FOR COMMISSIONING PERIOD

The heating and cooling capabilities of the cross heat exchanger (E-208) were investigated by logging the temperatures of the various streams entering (TR-110 and TR-213) and leaving (TR-212 and TR-111) the exchanger. The temperature trends can be seen in **Figure B.107**. The mass flow rate of the liquid in both streams were set to be 140 kg/h for the period up to 16h30 after with it was increased to 295 kg/h.

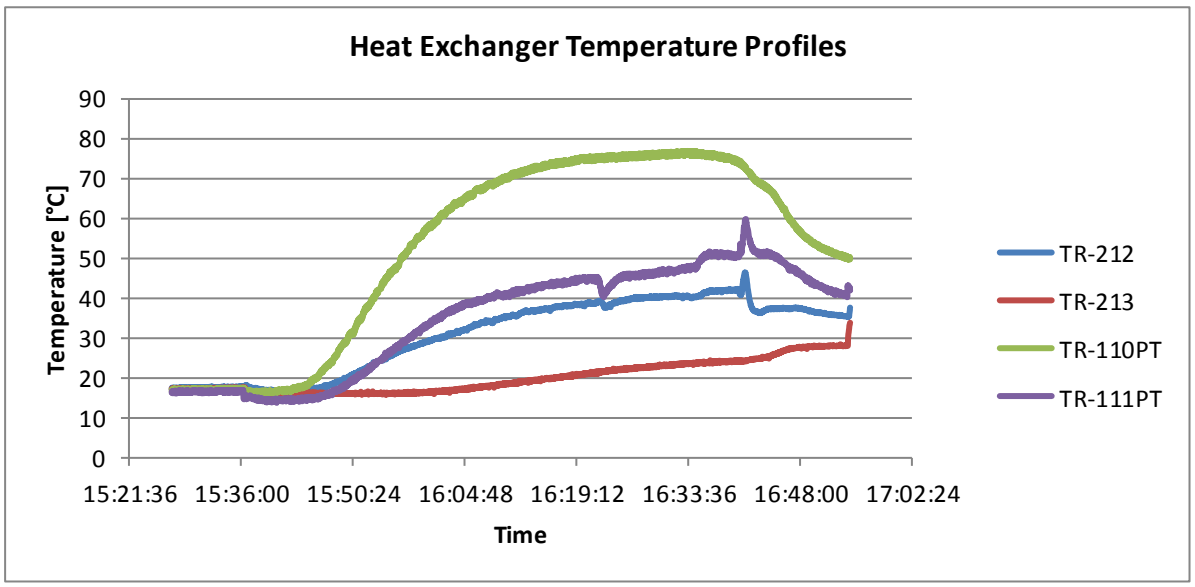

FIGURE B.107 HEAT EXCHANGER FEED AND OUTLET TEMPERATURE PROFILES

The heating and cooling capabilities of the exchanger will further be quantified in the next phase of the steam commissioning by performing an energy balance over the unit.

The cooling capabilities of the solvent cooler unit (E-209) were also investigated by logging the solvent temperature entering (TR-212) and leaving (TR-209) the cooler. The cooling water temperatures (IN – TR-218 and OUT – TR-219) are also recorded. The flow rate of the hot water to be cooled was 140 kg/h up to 16h30, and was increased to 295 at about 16h40.

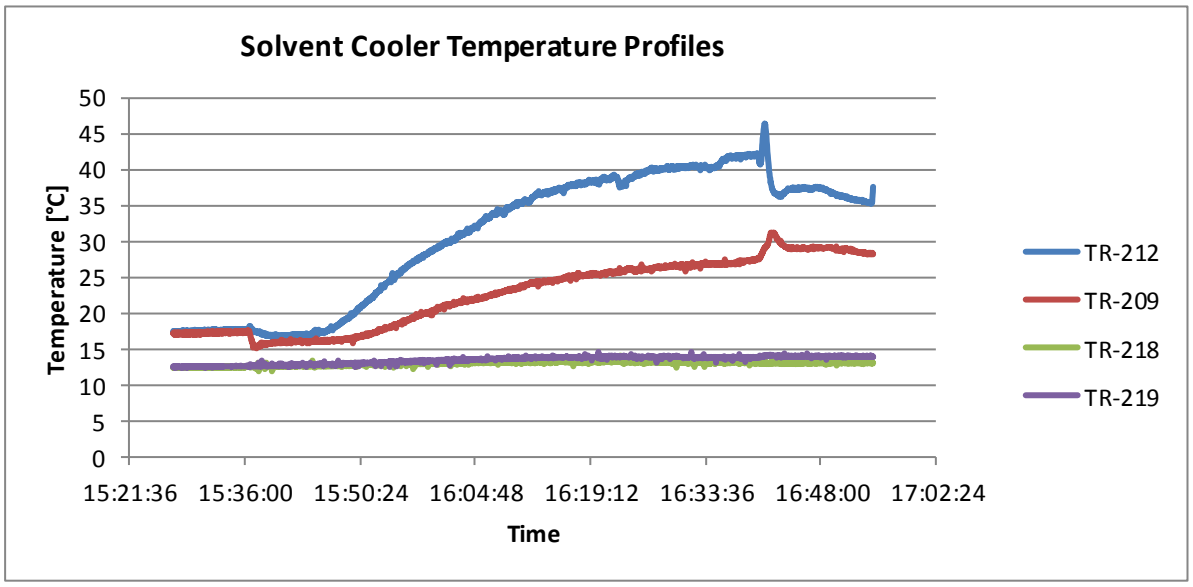

FIGURE B.108 SOLVENT COOLER INLET AND OUTLET TEMPERATURE PROFILES

Stripping column is heated from the bottom to the top after which liquid circulation is commenced until the temperatures of the streams stabilize. Temperature trends of the stripping column are shown in **Figure B.109**.

The final position of the steam valve CV-101 was set to 40 %OPEN. Heat was added continuously by feeding steam to the thermosyphon reboiler. This was done until stabilization in the temperatures of the streams flowing from the one column to the other started to set in.

Mass flow rate of the liquid steams from the both columns to the other were measured to be 183 kg/h. This was used in order to perform the energy balances on the heat exchanger and the cooler units.

Heat duty of the HOT and COLD sides of the heat exchanger was calculated at the stabilized temperatures and the heat loss from the exchanger were estimated to be about 2.16 kW. This can be seen in **Table B.23** and the temperature trends in **Figure B.110**.

TABLE B.23 HEAT EXCHANGER (E-208) HEAT DUTY CALCULATIONS

Measured Mass Flow Rate	**186**	**[kg/h]**
Heat Capacity	4.18	[kJ/kg.K]
Temp[HOT] IN	83	[°C]
Temp[HOT] OUT	43	[°C]
Temp[COLD] IN	26	[°C]
Temp[COLD] OUT	56	[°C]
deltaT [HOT]	40	[°C]
deltaT [COLD]	30	[°C]
Q = m.c.ΔT [HOT]	**8.64**	**[kW]**
Q = m.c.ΔT [COLD]	**6.48**	**[kW]**
HEAT LOSS in lines	**2.16**	**[kW]**

Cooling capabilities of the Cooler Unit E-209 were investigated by recording the inlet and outlet temperatures and calculating the heat removed from the hot liquid steam. See calculations in **Table B.24** and the temperature trends in **Figure B.111**.

TABLE B.24 COOLING DUTY CALCULATION FOR COOLER E-209

Measured Mass Flow Rate	**186**	**[kg/h]**
Heat Capacity	4.18	[kJ/kg.K]
Temp[HOT] IN	43	[°C]
Temp[HOT] OUT	31	[°C]
deltaT	12	[°C]
Q = m.c.ΔT [HOT]	**2.59**	**[kW]**

Air was circulated through the absorber column to see the effect of the feed liquid temperature on the gas temperature. After some time (at 15h25) the wash water feed to the water wash section was switched on to investigate the direct contact cooling effect thereof on the gas temperature. The temperature trends for this investigation can be seen in **Figure B.112**. It can be seen that the gas temperature increases as the liquid feed temperature increases. It continues to increase until the wash water is fed to the wash section. Thereafter the wash water cools the gas temperature, after which both these temperatures increase slightly. The temperature of the gas fed to the bottom of the absorber column shows a slight increase over time, but not as severe as the increase in the outlet from the top of the absorber column.

In the next phase of the pilot plant steam commissioning an attempt will be made at performing an energy balance over the stripping column, stripping column condensers, heat exchanger, cooler and a combination of all these process equipment.

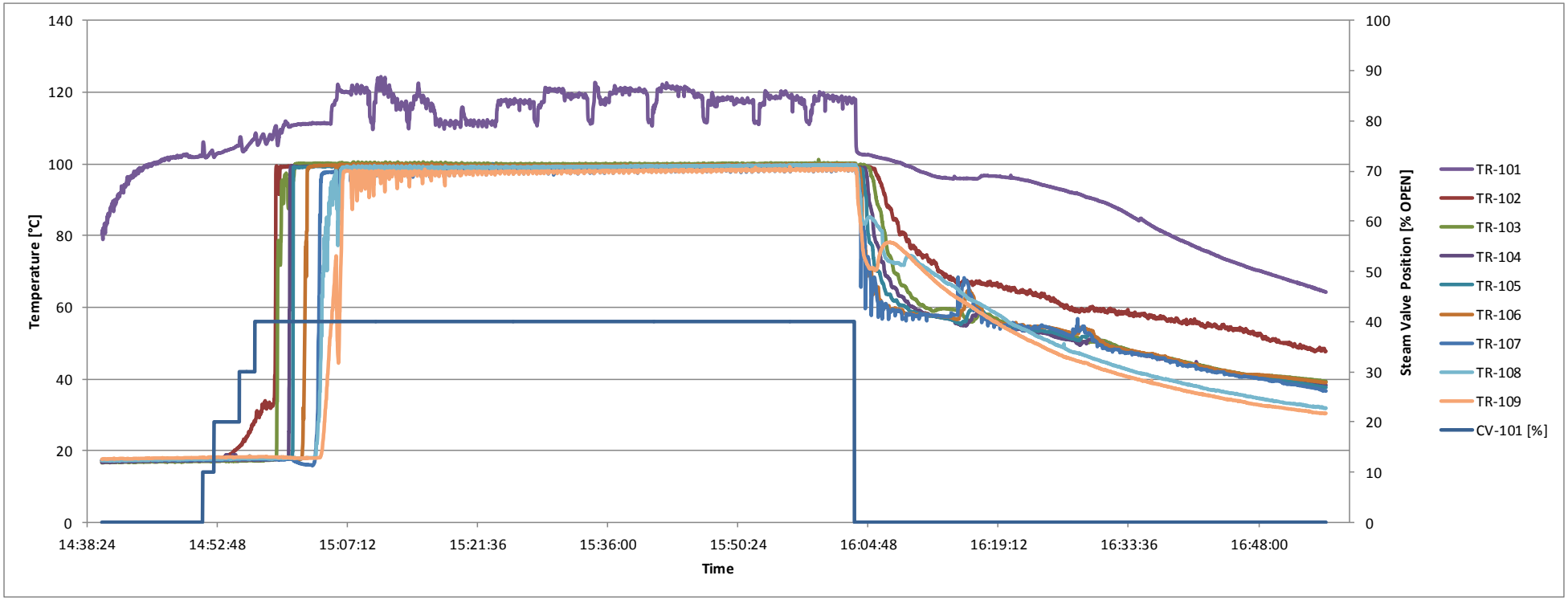

FIGURE B.109 HEATING OF THE STRIPPING COLUMN FROM THE BOTTOM (TR-102) TO THE TOP (TR-109) AND THE COOL DOWN PERIOD AFTER THE STEAM VALVE HAS BEEN CLOSED

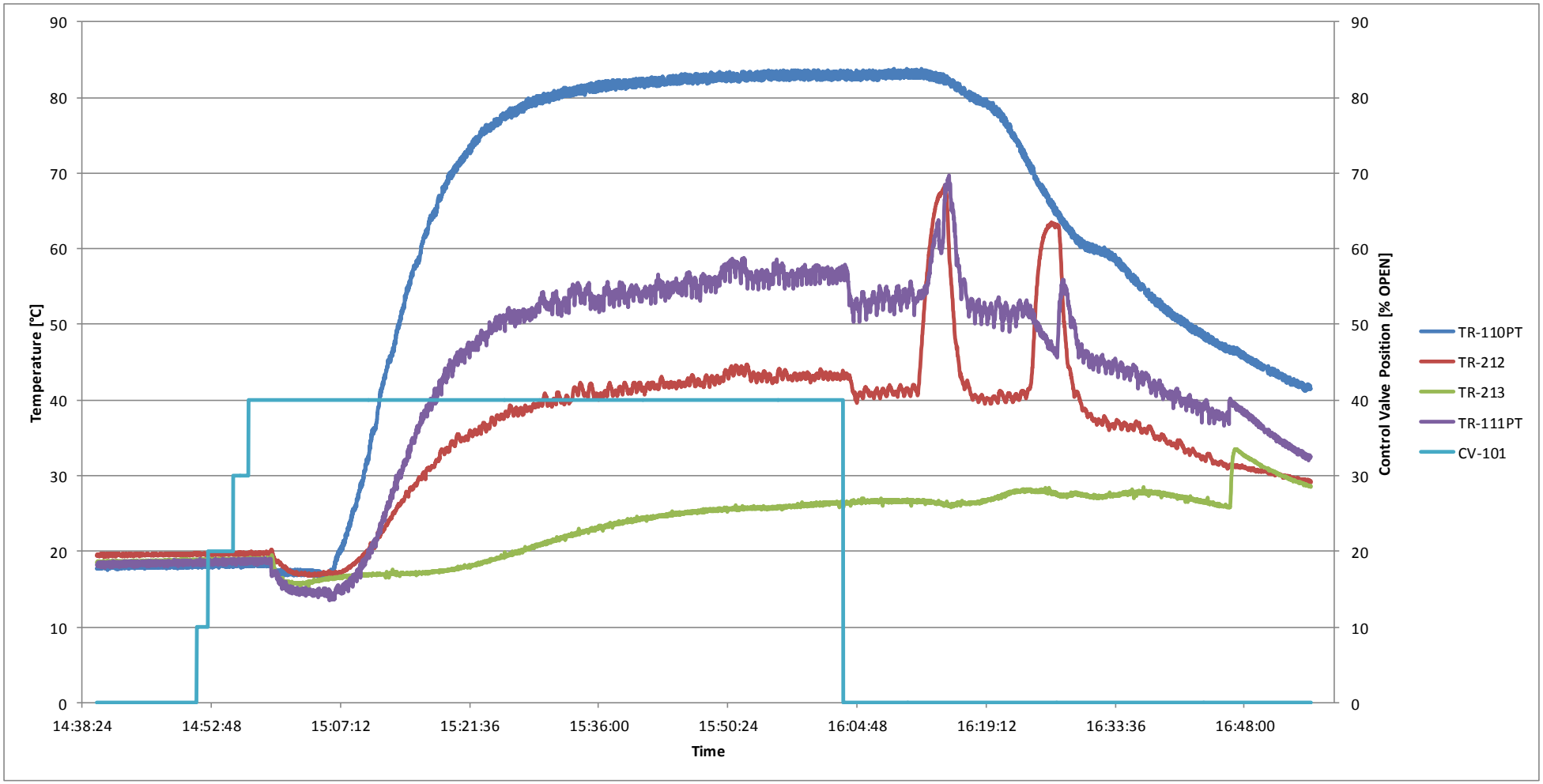

FIGURE B.110 TEMPERATURE PROFILES OF THE STREAMS ENTERING (TR-110[HOT], TR-213[COLD]) AND LEAVING (TR-111[COLD], TR-212[HOT]) THE HEAT EXCHANGER E-208. THE BUMPS IN THE TEMPERATURE PROFILES AT 16H15 AND 16H25 REPRESENT A PERIOD WHEN THE FLOW FROM THE ABSORBER TO THE STRIPPING COLUMN WERE REDUCED TO ZERO

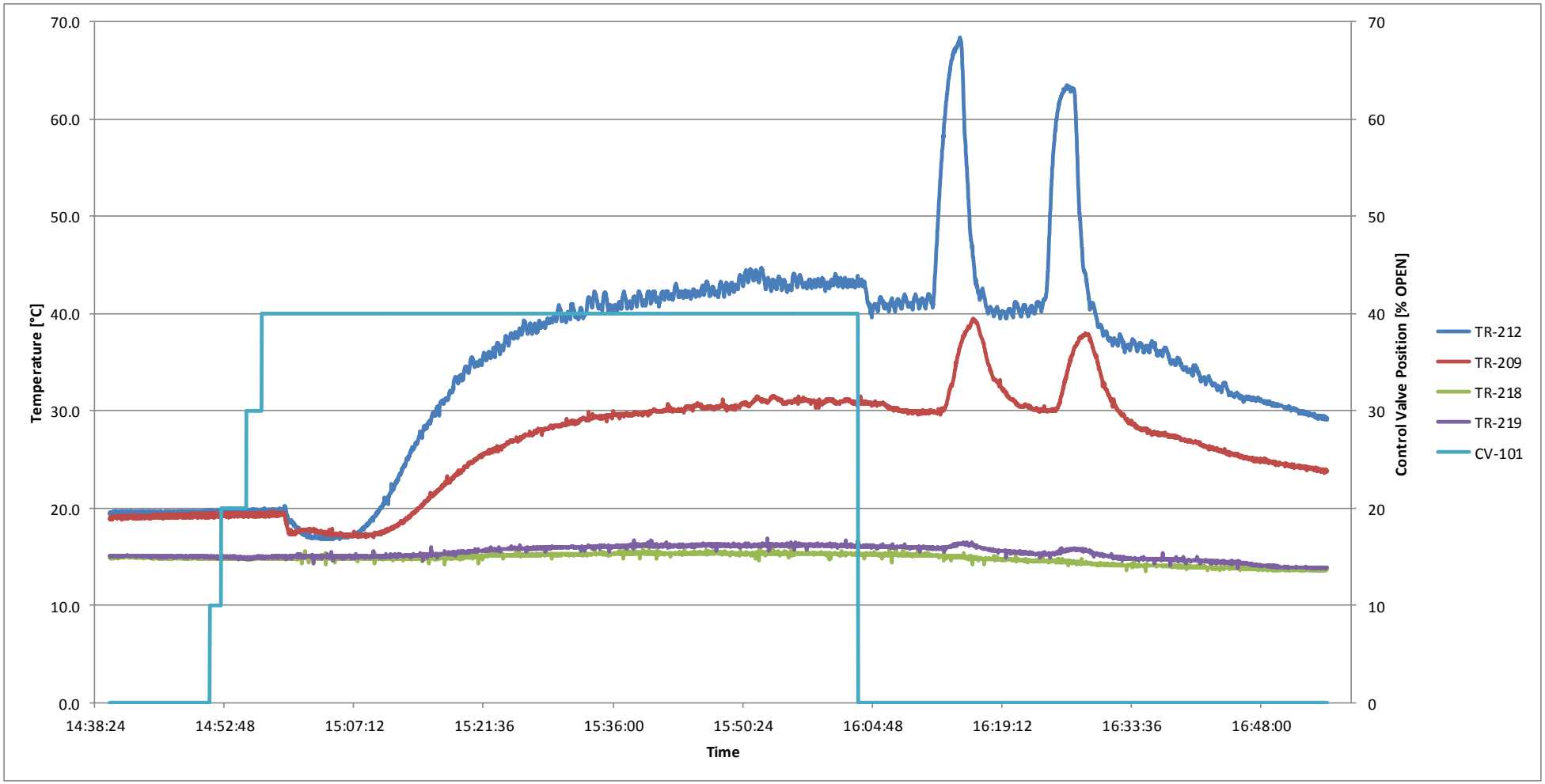

FIGURE B.111 TEMPERATURE PROFILES OF THE STREAMS ENTERING AND LEAVING THE SOLVENT COOLER UNIT E-209. THE BUMPS IN THE TEMPERATURE PROFILES AT 16H15 AND 16H25 REPRESENT A PERIOD WHEN THE FLOW FROM THE ABSORBER TO THE STRIPPING COLUMN WERE REDUCED TO ZERO

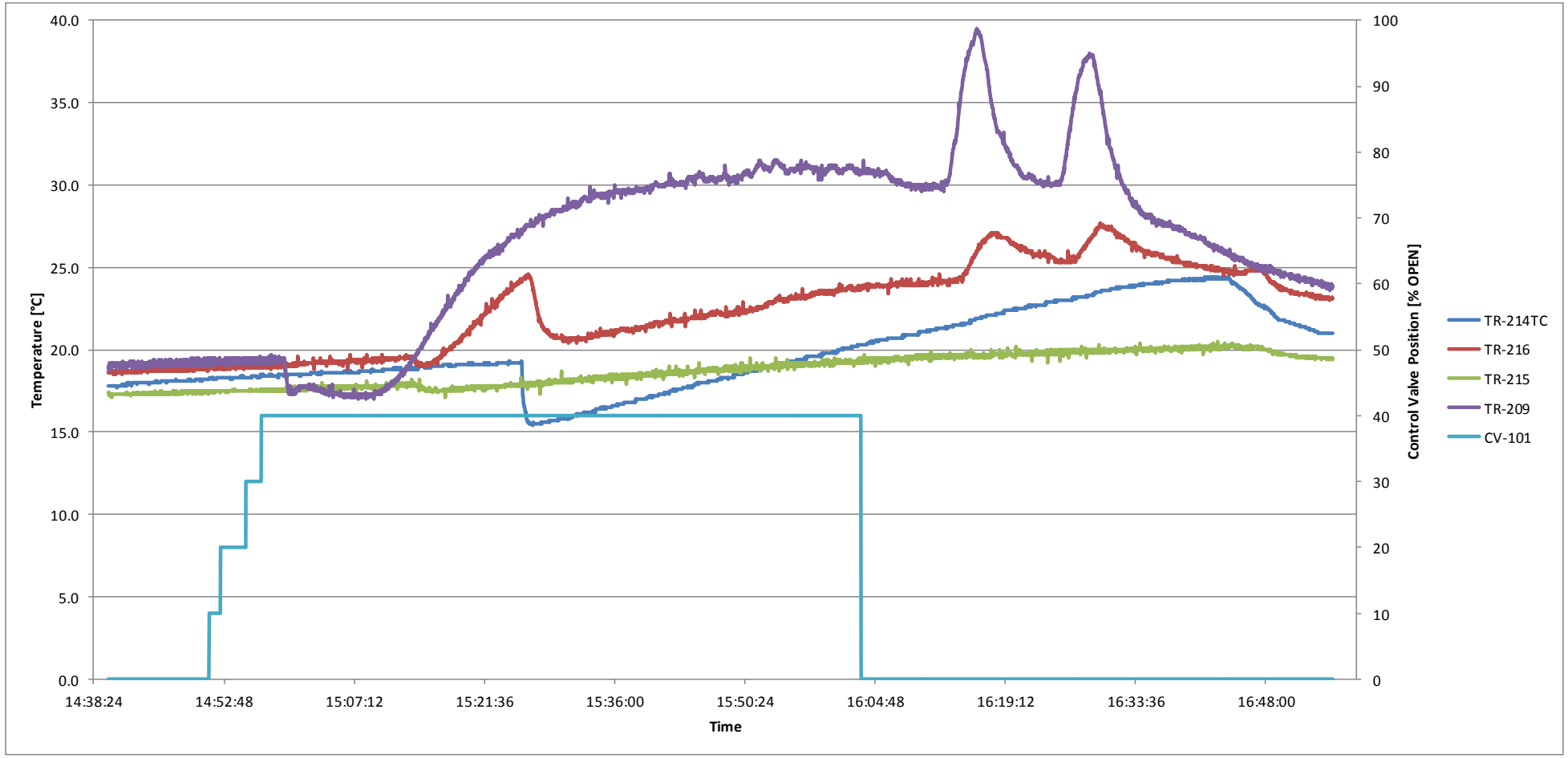

FIGURE B.112 EFFECT OF LIQUID FEED TEMPERATURE (TR-209) ON THE GAS INLET- (TR-215) AND OUTLET (TR-216) TEMPERATURES. WASH WATER (TR-214TC) CIRCULATION COMMENCED AT ABOUT 15H25.

Steam was supplied to the thermosyphon reboiler by opening the steam valve to 40 % OPEN. The stripping column was once again heated from the bottom to the top before liquid circulation between the two columns was commenced. After the first attempt at commissioning the steam valve was closed again in order to fix a leak in one of the liquid lines. The valve was opened again in order to heat the column again. This can be observed from the temperature plots shown in **Figure B.113**.

Liquid was circulated between the two columns at a measured mass flow rate of 189 kg/h. The liquid circulation continued until stabilization in the temperatures was observed. At this time steady state were assumed and an average temperature over 5 minutes were taken to perform the energy balance (16h00 – 16h05). The temperature stabilization can be seen in **Figure B.110** and **Figure B.111** showing the temperature trends for the heat exchanger and cooler units respectively.

The temperature trends for the absorber liquid- and gas feed, gas outlet and wash water temperature are shown in **Figure B.112**. Once again there is a minimal rise in the absorber feed temperature which is a desired.

The energy balance was performed in five different steps. The steps and the various balances performed are summarized in **Table B.26**. **Figure B.117** also shows the sections on the P&ID over which energy balances were performed. The energy balance and heat loss estimation for the heat exchanger is shown in **Table B.23**.

TABLE B.25 HEAT EXCHANGER (E-208) HEAT DUTY CALCULATIONS

Measured Mass Flow Rate	189	[kg/h]
Heat Capacity	4.18	[kJ/kg.K]
Temp[HOT] IN	83.1	[°C]
Temp[HOT] OUT	41.8	[°C]
Temp[COLD] IN	25.1	[°C]
Temp[COLD] OUT	59.2	[°C]
deltaT [HOT]	41.23	[°C]
deltaT [COLD]	34.08	[°C]
Q = m.c.ΔT [HOT]	**9.05**	**[kW]**
Q = m.c.ΔT [COLD]	**7.48**	**[kW]**
HEAT LOSS in lines	**1.57**	**[kW]**

Figure B.113 Heating of the Stripping column from the bottom (TR-102) to the top (TR-109) and the cool down period after the steam valve has been closed

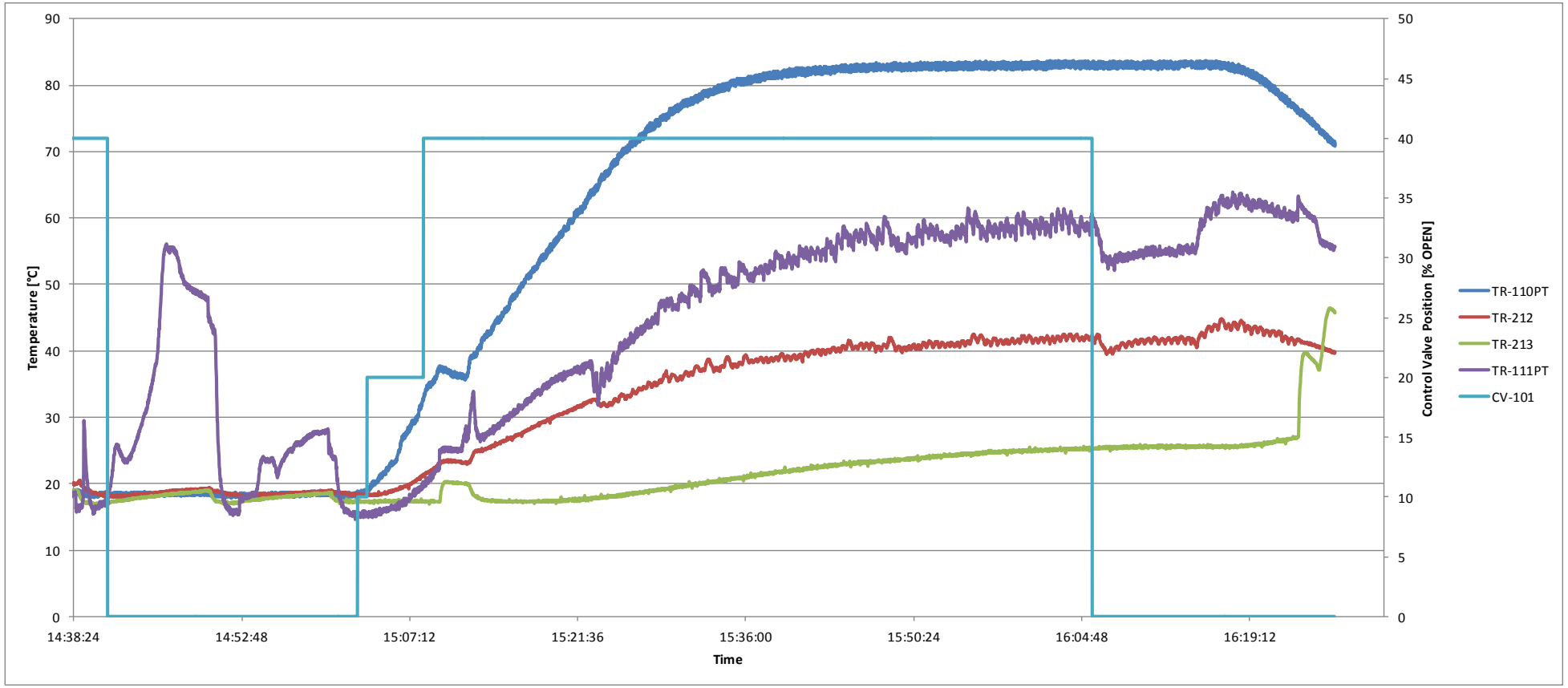

FIGURE B.114 TEMPERATURE PROFILES OF THE STREAMS ENTERING (TR-110[HOT], TR-213[COLD]) AND LEAVING (TR-111[COLD], TR-212[HOT]) THE HEAT EXCHANGER E-208. THE BUMPS IN THE TEMPERATURE PROFILES AT 16H15 AND 16H25 REPRESENT A PERIOD WHEN THE FLOW FROM THE ABSORBER TO THE STRIPPING COLUMN WERE REDUCED TO ZERO

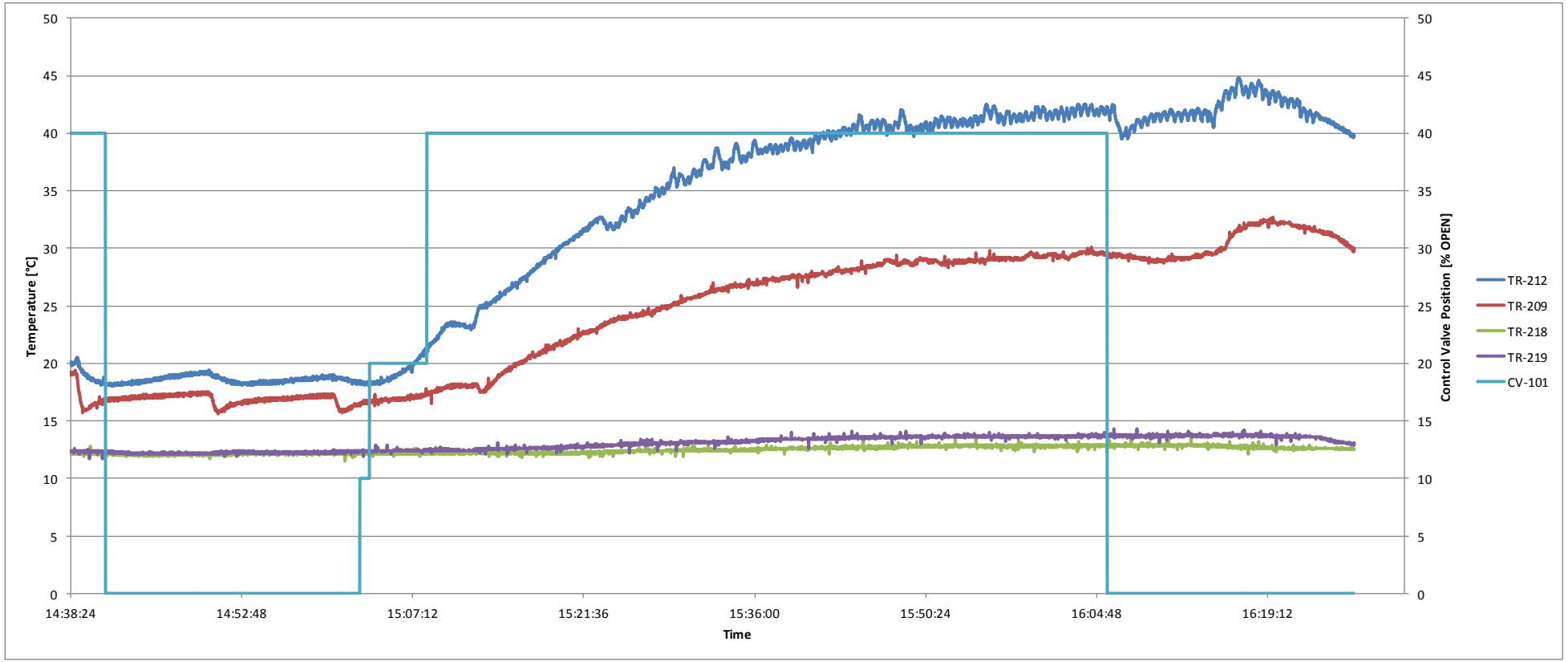

FIGURE B.115 TEMPERATURE PROFILES OF THE STREAMS ENTERING AND LEAVING THE SOLVENT COOLER UNIT E-209. THE BUMPS IN THE TEMPERATURE PROFILES AT 16H15 AND 16H25 REPRESENT A PERIOD WHEN THE FLOW FROM THE ABSORBER TO THE STRIPPING COLUMN WERE REDUCED TO ZERO

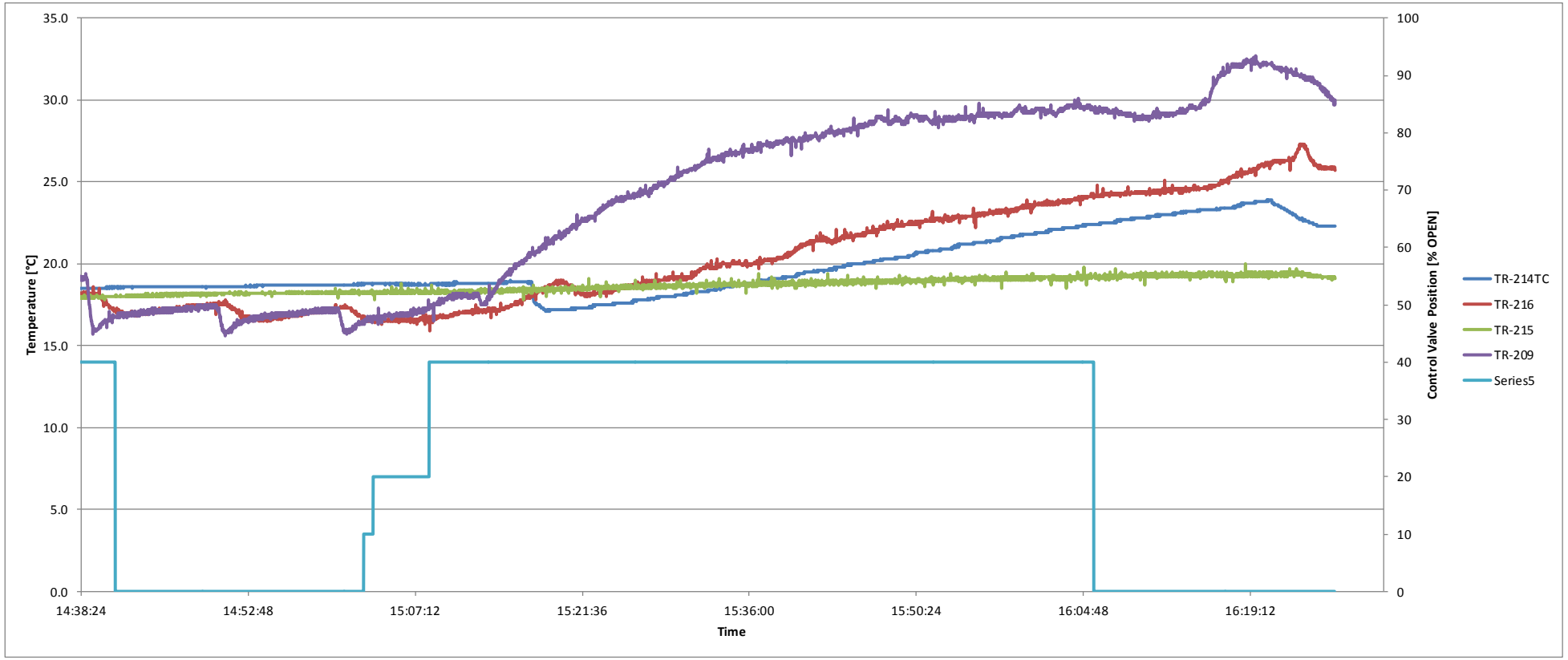

FIGURE B.116 EFFECT OF LIQUID FEED TEMPERATURE (TR-209) ON THE GAS INLET- (TR-215) AND OUTLET (TR-216) TEMPERATURES. WASH WATER (TR-214TC) CICULATIOIN COMMENCED AT ABOUT 15H25.

TABLE B.26 REFERENCE TO THE FIVE ENERGY BALANCES THER WERE PERFORMED

Five separate energy balances were performed different energy balances were performed
1. Over the heat exchanger estimating the heat transfer from the hot stream, heat absorbed by the cold stream and evidently the heat loss in the exchanger
2. Over the Cooler unit in order to estimate the cooling water split ratio to the cooler and the stripping column condensers
3. Over stripping column condensers and column separately in order to estimate HEAT LOSS from column (heat loss factor incorporated into condensers)
4. Over all process equipment except the Absorber column - Absorber in-/outlets used as the in- and outputs for the enery balance (% ERROR = 2%)
5. Over the stripping column with the condensers (% ERROR = 4.9%)

TABLE B.27 ENERGY BALANCES OVER THE COOLER UNIT, COOLING WATER SPLIT RATION ESTIMATION;

HEAT LOSS ESTIMATION AND ENERGY BALANCE OVER STRIPPING COLUMN

COOLING DUTY of SOLVENT COOLER Calculations			**MASS FLOW RATE to CONDENSERS Calculations**			**ENERGY BALANCE OVER STRIPPER without CONDENSERS**		
Measured Mass Flow Rate	189.00	[kg/h]	Total volumetric flow rate	5.27	[m3/h]	**IN:** Feed stream entering top of stripper	13.02	[kW]
Heat Capacity	4.18	[kJ/kg.K]	Total Mass flow rate [MEASURED]	5267.71	[kg/h]	**IN:** Condensate Return in Reflux Line	8.22	[kW]
Temp[HOT] IN	41.83	[°C]	**MFR OF COOLING WATER to CONDENSERS**	**2520.31**	**[KG/H]**	**IN:** ***HEAT ADDITION BY STEAM***	**49.75**	**[kW]**
Temp[HOT] OUT	29.42	[°C]	Temperature of Cooling water return	29.19	[°C]	**OUT:** Stream from bottom of Stripping column	18.27	[kW]
deltaT	12.41	[°C]	deltaT	16.37	[°C]	**OUT:** Vapour stream from top of Stripping column	52.71	[kW]
Q = m.c. ΔT [HOT]	**2.68**	**[kW]**	***ENERGY REMOVED IN CONDENSERS***	**47.33**	**[kW]**	*Estemated* HEAT LOSS from process equip	2.84	[kW]
	2.68							
MASS FLOW RATE of COOLING WATER Calculations			**MASS FLOW RATE OF CONDENSATE Calculations**			**STEAM FLOW RATE Calculations**		
Assumed [%] of energy transfer	100%	[%]	*Assumed* [%] of energy to condensation	94%	[%]	Average Steam temperature	116.18	[°C]
Energy change in Cooling Water	2.68	[kW]	Heat of Condensation for Water	2257.40	[kJ/kg]	Energy given of by the condensing steam	2282.50	[kJ/kg]
INLET Temperature	12.81	[°C]	Total energy removed in condensers	47.33	[kW]	Calculated heat addition by steam	49.75	[kW]
OUTLET Temperature	13.65	[°C]	***MASS FLOW RATE OF CONDENSATE***	**70.94**	**[KG/H]**	***Calculated STEAM FLOW RATE***	**78.46**	**[KG/H]**
deltaT	0.84	[°C]	Heat loss in the stripping column	2.84	[kW]	***Measured STEAM FLOW RATE***	78.46	[KG/H]
MFR OF COOLING WATER TO COOLER	**2747.40**	**[KG/H]**				*Set to ZERO to calculate HEAT LOSS*	0.00	

TABLE B.28 ENERGY BALANCE OVER THE ENTIRE SYSTEM WITH THE EXCLUSION OF THE ABSORBER COLUMN

ENERGY BALANCE OVER STRIPPING COLUMN + CONDENSERS + HTX + COOLER			
Feed stream entering top of ABSORBER	6.46 [kW]	*IN*	135.00
Feed stream to HTX from ABSORBER	**5.51 [kW]**	*OUT*	138.31
Heat addition by STEAM	**49.74 [kW]**	*Balance*	3.31
Cooling water into the system	**79.75 [kW]**	**% ERROR**	**2%**
Cooling Water OUT form COOLER	42.74 [kW]		
Cooling Water OUT from CONDENSERS	84.71 [kW]		
Heat LOSS from the system	4.41 [kW]		
Cooling water Flow rate Calculations			
Cooling water to the cooler unit	2747.40 [°C]	**COOLING WATER SPLIT**	
Cooling water to the condenser units	2520.31 [kJ/kg]	x	0.5216

TABLE B.29 ENERGY BALANCE OVER THE STRIPPING COLUMN AND THE CONDENSERS

ENERGY BALANCE STRIPPING COLUMN with CONDENSERS	
Feed stream entering top of stripper	13.02 [kW]
Cooling Water into condensers	38.15 [kW]
HEAT ADDITION BY STEAM	**49.74 [kW]**
Stream from bottom of Stripping column	18.27 [kW]
Cooling Water from the condensers	84.71 [kW]
Estemated HEAT LOSS from process equip	2.84 [kW]
IN	100.92 [kW]
OUT	105.82 [kW]
BALANCE	4.90 [kW]
% ERROR	**4.9%** [%]

Table B.27 shows the energy balances that were performed for the cooler unit. The cooler duty was first estimated by using the heat removed from the hot stream. The assumption was made that the gain in the cooling water temperature is solely due to heat absorbed from the hot liquid to be cooled. This assumption would be valid, seeing that the temperature sensors in the cooling water lines are installed directly before water enters and exits the cooler unit. Based on this assumption the cooling water flow rate to the cooler was estimated and thus also the split ratio of cooling water going to condensers and the cooler. The ratio calculated shows that 52.2 % of all cooling water fed to the pilot plant is directed to cooler unit.

In knowing the mass flow rate of cooling water to the stripping column condensers as well as the in and outlet temperatures, the heat removed in the condensers can be estimated. Furthermore the mass flow rate of the condensate from the condensers was estimated,

incorporating a factor (assumed energy to condensation of vapour) that allows for the estimation of the heat loss in the stripping column (the remaining energy).

An energy balance over the stripping column alone was performed by taking all in- and outlet streams as well as the utility in- and outlets into account. The calculated steam flow rate was matched to the measured steam flow rate by varying the factor for estimating the heat loss in the stripping column (incorporated in the condenser energy balance). **Table B.27**show these energy balances and the estimated heat loss from the stripping section of about 2.84 kW.

For the fourth energy balance (See **Figure B.117**) the entire process with the exception of the absorber column were considered. The estimated heat losses for the stripping section, as well as the heat exchanger were included in this energy balance. **Table B.28** shows the energy balance for this section of the process and also reports the % error between energy IN and energy OUT to be only 2%.

The fifth energy balance was performed over the stripping column and the condensers (See **Figure B.117**). **Table B.29** shows the energy balance for this particular section. The estimated heat loss for the stripping section was included in the balance. The % error between the energy into and energy flow from the system were calculated to be 4.9%.

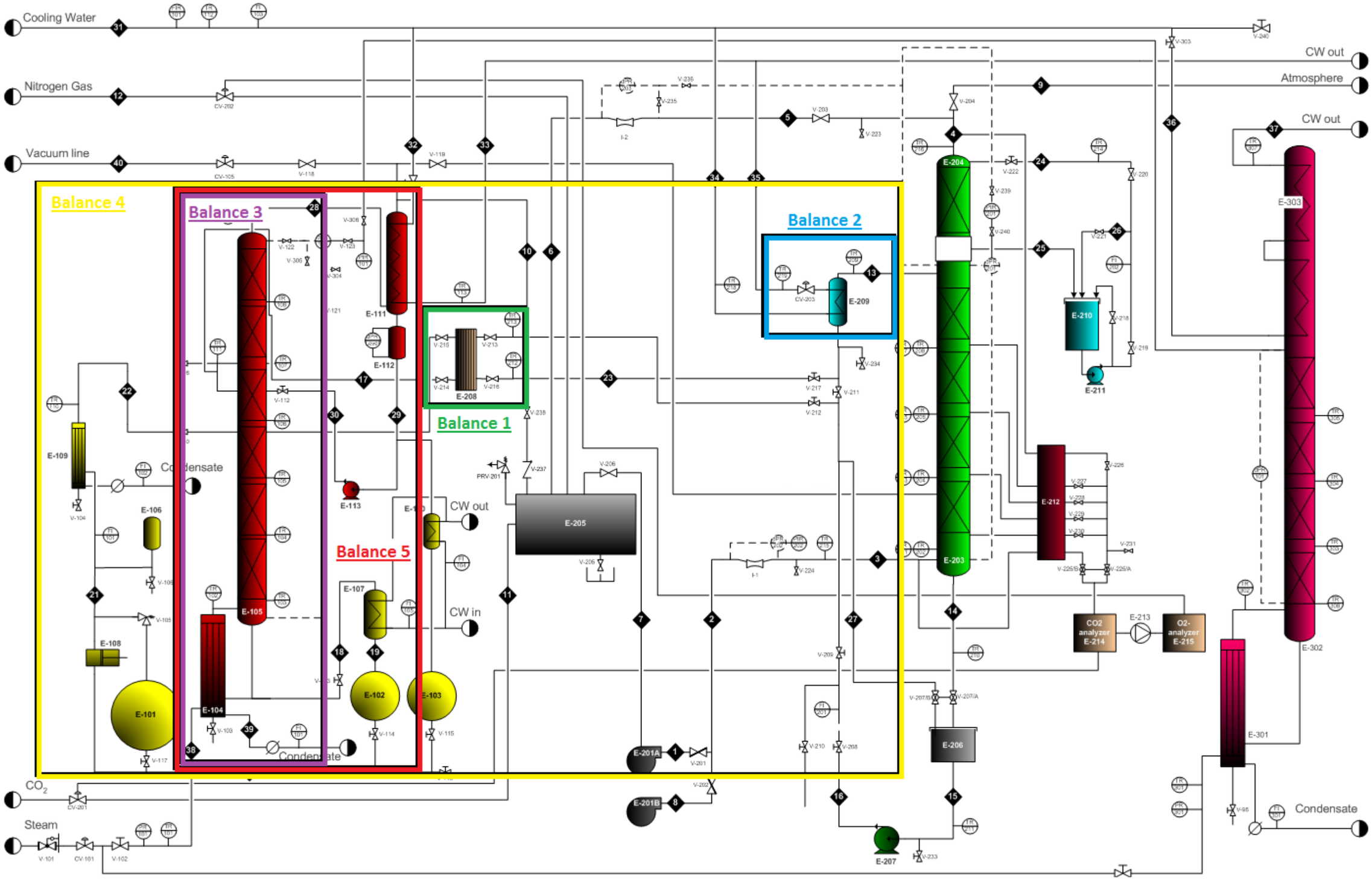

FIGURE B.117 ZONED OFF ENERGY BALANCES DONE ON THE VARIOUS PROCESS EQUIPMENT

TABLE B.30 LIST OF PROCESS EQUIPMENT

Area 100

E-101	Spherical Storage Tank
E-102	Bottoms Holding Tank
E-103	Distillate Holding Tank
E-104	Thermosyphon Reboiler
E-105	Stripping/Continuous Distillation Column
E-106	Pulse Reduction Pot
E-107	Bottom Cooler
E-108	Pulsation Feed Pump
E-109	Pre-heater
E-110	Distillate Cooler
E-111	Total Condenser Units
E-112	T-piece Reflux Holding vessel
E-113	Reflux Pump

Area 200

E-201	Gas Recycle Blower
E-202	Air Blower
E-203	Absorber Column
E-204	Water Wash Section
E-205	Gas Surge Tank/Knock-out Drum
E-206	Solvent Storage Vessel
E-207	Liquid Feed Pump
E-208	Cross flow Heat Exchanger
E-209	Solvent Cooler
E-210	Wash Water Storage Tank
E-211	Wash Water Pump
E-212	Cold Trap
E-213	Sample Pump
E-214	CO2 Analyser
E-215	O2 Analyser

Area 300

E-301	Total Reflux Column ThermosyphonReboiler
E-302	Total Reflux Distillation Column
E-303	Total Reflux Column Condenser Units

In this list indicating the placement of each one of the installed temperature sensors, an indication will be given as to which sensors are thermocouples (TC) and which are PT100s (PT).

Area 100

TR-101TC - Steam supply line to stripping column reboiler unit (Stream 38)

TR-102TC - Stripping column reboiler (E-104)

TR-103TC - Bottom of stripping column (E-105)

TR-104^{TC} - 1 meter from stripping column bottom (E-105)

TR-105^{TC} - 2 meters from stripping column bottom (E-105)

TR-106^{TC} - 3 meters from stripping column bottom (E-105)

TR-107^{TC} - 4 meters from stripping column bottom (E-105)

TR-108^{TC} - 5 meters from stripping column bottom (E-105) (Section not packed)

TR-109^{TC} - Top of the stripping column unit (Stream 28)

TR-110^{PT} - After pre-heating unit (Stream 22)

TR-111^{PT} - Stripping Column liquid feed (Stream 17)

TR-112^{TC} - Cooling Water supply line (Stream 31)

TR-113^{TC} - Cooling water return line (Stream 33)

Area 200

TR-201^{PT} - 1st sample point, absorber column, process gas (E-203)

TR-202^{PT} - 1st sample point, absorber column, solvent (E-203)

TR-203^{PT} - 2nd sample point, absorber column, process gas (E-203)

TR-204^{PT} - 2nd sample point, absorber column, solvent (E-203)

TR-205^{PT} - 3rd sample point, absorber column, process gas (E-203)

TR-206^{PT} - 3rd sample point, absorber column, solvent (E-203)

TR-207^{PT} - 4th sample point, absorber column, process gas (E-203)

TR-208^{PT} - 4th sample point, absorber column, solvent (E-203)

TR-209^{PT} - Absorber column solvent feed line (Stream 13)

TR-210^{PT} - Solvent leaving bottom of absorber column (Stream 14)

TR-211^{PT} - Solvent leaving solvent storage tank (Stream 15)

TR-212^{PT} - Lean solvent return from stripping column after exchanger (Stream 23)

TR-213^{PT} - Rich solvent feed line to heat exchanger (Stream 16)

TR-214^{TC} - Wash water temperature (Stream 24)

TR-215^{PT} - Process feed gas (Stream 3)

TR-216^{PT} - Process gas leaving top of absorber column (Stream 4)

TR-217^{PT} - CO_2 return line from top of stripping column (Not installed)

TR-218^{PT} - Cooling water supply line (Stream 34)

TR-219^{PT} - Cooling water return line (Stream 35)

Area 300

TR-301^{TC}	-	Steam temperature (Stream 38)
TR-302^{TC}	-	Reboiler of the total reflux column (E-301)
TR-303^{TC}	-	1 meter from the bottom of the total reflux column (E-302)
TR-304^{TC}	-	2 meters from the bottom of the total reflux column (E-302)
TR-305^{TC}	-	3 meters from the bottom of the total reflux column (E-302)
TR-307^{TC}	-	Cooling water return (Stream 37)
TR-308^{TC}	-	Sump temperature of the total reflux column (E-302)

PHASE 4

ENERGY BALANCE WITH MORE ACCURATE MASS FLOW RATES

This phase of the steam commissioning was aimed at obtaining more accurate information on the mass flow rates of all the steams in order to allow for a proper energy balance. A rotameter were installed in the line feeding the colder liquid to the heat exchanger and stripping column. The rotameter were properly calibrated prior to starting the steam commissioning process.

INTERLOCK REQUIRED – OUTPUT IDENTIFIED

Steam commissioning was commenced by heating the stripping column with a steam valve position of 30 % OPEN, after which liquid circulation between the two columns was set at a mass flow rate of 100 kg/h. However, a problem with the rotameter installed in the liquid line from the bottom of the absorber column caused a blockage in the line, leading to a decrease in the water in the reboiler unit and the process had to be stopped. See **Figure B.109** for the steam valve position trend – closing at 14h45.

This necessitates the use of an interlock build into the controls of the pilot plant in order to prevent the boiler unit from going dry, possible damage to the equipment as well as a hazardous working environment. **Figure B.110** shows the output that can be used in order to interlock the steam valve. The temperature of the liquid feed line to the top of the stripping column shoots up to above 90°C. Temperature can thus be used in order to create an interlock for the steam valve that will prevent this from happening again.

ENERGY BALANCE

For the second run, an attempt was made at balancing the liquid flow rates at 150kg/h. However, as can be seen from the trend of TR-111 in **Figure B.110**, this was a difficult task. For the rest of the experiment, the liquid flow rates were kept above 300 kg/h to be safe.

Five minutes prior to closing the steam valve the mass flow rates of the circulated liquid and the steam flow to the reboiler were measured for performing the energy balance. All temperatures

and flow rates used in the energy balance were averaged for an assumed steady state period of 5 minutes prior to closing the steam valve.

The energy balance over the heat exchanger can be seen in **Table B.23**. The heat loss in the heat exchanger was estimated to be 1.49 kW. The energy balances for the cooler unit, stripping column condensers and the stripping column is shown in **Table B.32**. The heat loss from the stripping column was estimated to be 3.01 kW.

Table B.34 and **Table B.33** shows the energy balances for the entire system (exclusion of absorber) and the stripping column with condenser units respectively. The % errors for these to energy balances were calculated to be -0.3 and -0.4%.

TABLE B.31 HEAT EXCHANGER (E-208) HEAT DUTY CALCULATIONS

Measured Mass Flow Rate	**348**	**[kg/h]**
Heat Capacity	4.18	[kJ/kg.K]
Temp[HOT] IN	87.0	[°C]
Temp[HOT] OUT	45.8	[°C]
Temp[COLD] IN	28.4	[°C]
Temp[COLD] OUT	65.9	[°C]
deltaT [HOT]	41.22	[°C]
deltaT [COLD]	37.52	[°C]
Q = m.c.ΔT [HOT]	**16.65**	**[kW]**
Q = m.c.ΔT [COLD]	**15.16**	**[kW]**
HEAT LOSS in lines	**1.49**	**[kW]**

OTHER PROBLEMS ENCOUNTERED

Another problem that was encountered during this phase of steam commissioning is related to back flow of condensed liquid into the reflux line after feeding it to the top of the stripping column. The ON/OFF control on the reflux pump creates a scenario where the decreasing level in the reflux feed line creates a vacuum. This then leads to the upward flow of liquid fed from the absorber – into the reflux line, rather than into the top of the stripping column.

A further problem regarding balancing the flow rates of liquids with different densities (due to their different temperatures) were noticed.

The next phase of commissioning will aim at solving the problems encountered in this phase of the pilot plant commissioning.

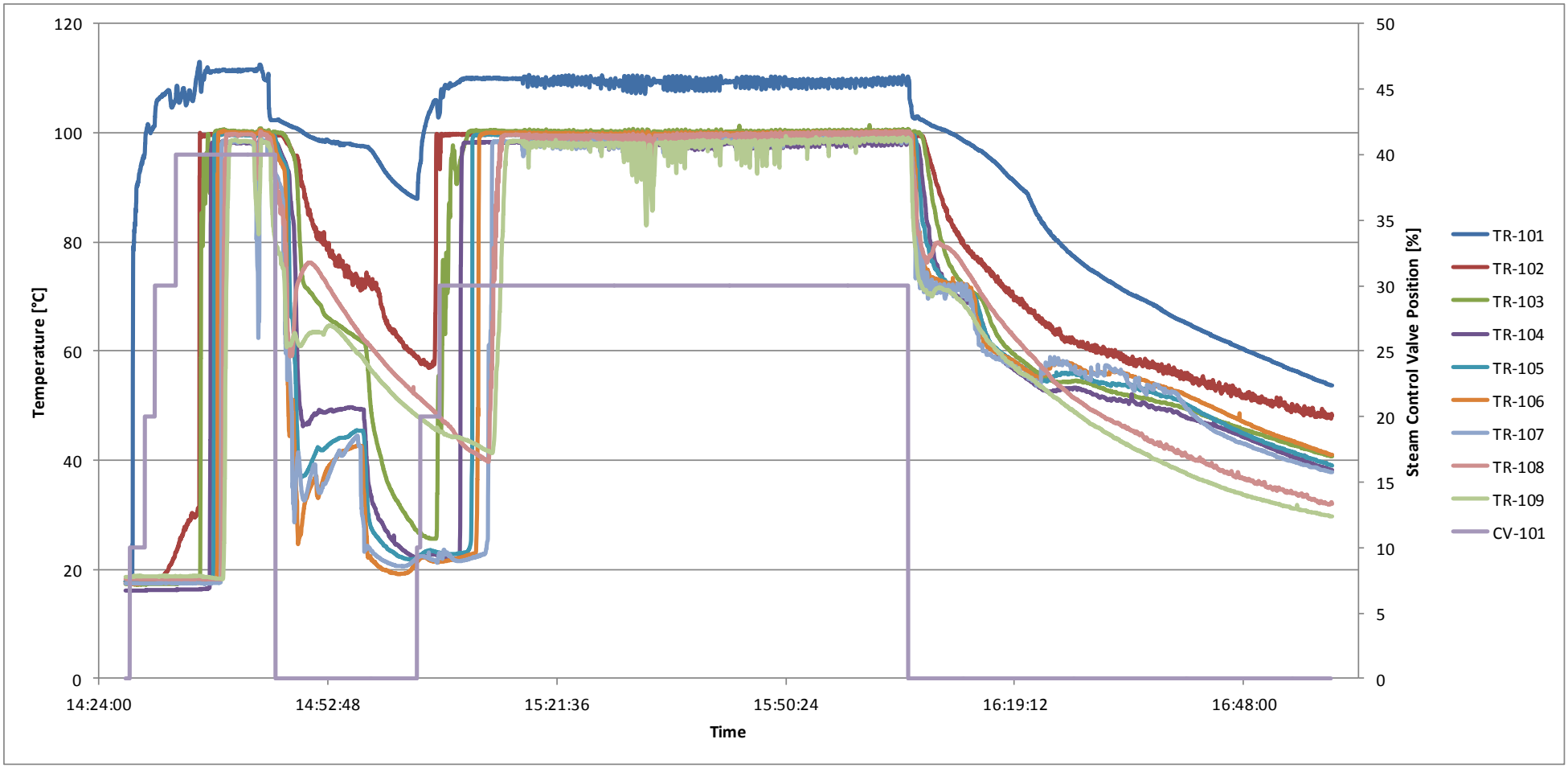

FIGURE B.118 HEATING OF THE STRIPPING COLUMN FROM THE BOTTOM (TR-102) TO THE TOP (TR-109) AND THE COOL DOWN PERIOD AFTER THE STEAM VALVE HAS BEEN CLOSED

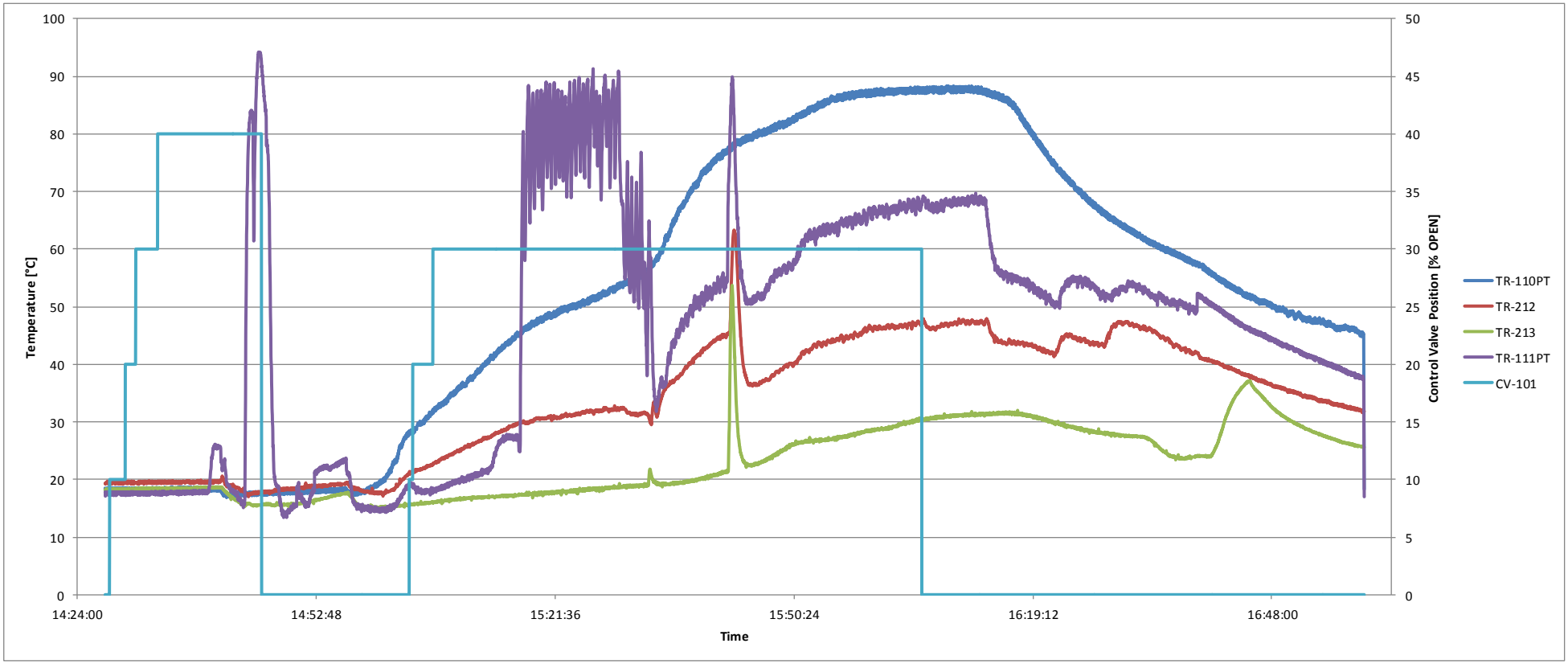

FIGURE B.119 TEMPERATURE PROFILES OF THE STREAMS ENTERING (TR-110[HOT], TR-213[COLD]) AND LEAVING (TR-111[COLD], TR-212[HOT]) THE HEAT EXCHANGER E-208. THE PEAK DISPLAYED IN TREND OF TR-111 INDICATES LOSS IN FLOW FROM THE BOTTOM OF THE STRIPPING COLUMN. THIS WILL BE USED AS THE OUTPUT TO EMPLOY AN INTERLOCK ON THE STEAM VALVE.

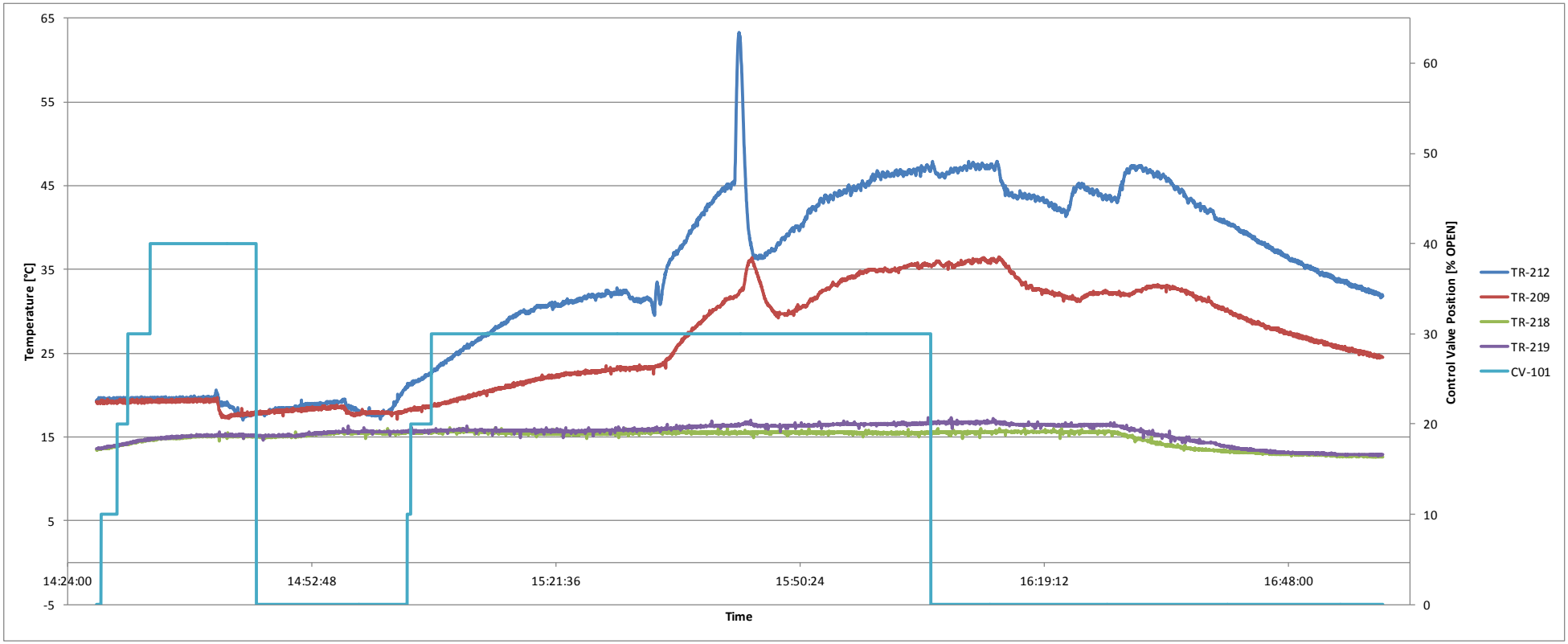

FIGURE B.120 TEMPERATURE PROFILES OF THE STREAMS ENTERING AND LEAVING THE SOLVENT COOLER UNIT E-209. THE BUMPS IN THE TEMPERATURE PROFILES AT 16H40 REPRESENTS A PERIOD WHEN THE FLOW FROM THE ABSORBER TO THE STRIPPING COLUMN WERE REDUCED TO ZERO

TABLE B.32 ENERGY BALANCES OVER THE COOLER UNIT, STRIPPING COLUMN CONDENSERS AND STRIPPING COLUMN

COOLING DUTY of SOLVENT COOLER Calculations			**MASS FLOW RATE to CONDENSERS Calculations**			**ENERGY BALANCE OVER STRIPPER without CONDENSERS**	
Measured Mass Flow Rate	348.00	[kg/h]	Total volumetric flow rate	5.25	[m3/h]	**IN:** Feed stream entering top of stripper	26.71 [kW]
Heat Capacity	4.18	[kJ/kg.K]	Total Mass flow rate [MEASURED]	5239.76	[kg/h]	**IN:** Condensate Return in Reflux Line	2.49 [kW]
Temp[HOT] IN	45.83	[°C]	**MFR OF COOLING WATER to CONDENSERS**	**1672.70**	**[KG/H]**	**IN:** ***HEAT ADDITION BY STEAM***	**27.33 [kW]**
Temp[HOT] OUT	34.82	[°C]	Temperature of Cooling water return	23.38	[°C]	**OUT:** Stream from bottom of Stripping column	35.24 [kW]
deltaT	11.01	[°C]	deltaT	7.92	[°C]	**OUT:** Vapour stream from top of Stripping column	18.26 [kW]
Q = m.c.ΔT [HOT]	**4.45**	**[kW]**	***ENERGY REMOVED IN CONDENSERS***	**15.41**	**[kW]**	*Estemated* HEAT LOSS from process equip	3.01 [kW]
MASS FLOW RATE of COOLING WATER Calculations			**MASS FLOW RATE OF CONDENSATE Calculations**			**STEAM FLOW RATE Calculations**	
Assumed [%] of energy transfer	100%	[%]	*Assumed* [%] of energy to condensation	100%	[%]	Average Steam temperature	109.36 [°C]
Energy change in Cooling Water	4.45	[kW]	Heat of Condensation for Water	2257.40	[kJ/kg]	Energy given of by the condensing steam	2282.50 [kJ/kg]
INLET Temperature	15.46	[°C]	Total energy removed in condensers	15.41	[kW]	Calculated heat addition by steam	27.33 [kW]
OUTLET Temperature	16.53	[°C]	***MASS FLOW RATE OF CONDENSATE***	**24.58**	**[KG/H]**	***Measured STEAM FLOW RATE***	43.10 [KG/H]
deltaT	1.07	[°C]					
MFR OF COOLING WATER TO COOLER	**3567.05**	**[KG/H]**					

TABLE B.34 ENERGY BALANCE OVER ENTIRE SYSTEM (EXCLUSION OF ABSORBER)

ENERGY BALANCE OVER STRIPPING COLUMN + CONDENSERS + HTX + COOLER				
Feed stream entering top of ABSORBER	14.11	[kW]	*IN*	133.32
Feed stream to HTX from ABSORBER	**11.52**	**[kW]**	*OUT*	132.95
Heat addition by STEAM	**27.33**	**[kW]**	*Balance*	-0.36
Cooling water into the system	**94.47**	**[kW]**	**% ERROR**	**-0.3%**
Cooling Water OUT form COOLER	68.77	[kW]		
Cooling Water OUT from CONDENSERS	45.57	[kW]		
Heat LOSS from the system	4.51	[kW]		
Cooling water Flow rate Calculations				
Cooling water to the cooler unit	3567.05	[°C]	**COOLING WATER SPLIT**	
Cooling water to the condenser units	1672.70	[kJ/kg]	x	0.6808

TABLE B.33 ENERGY BALANCE OVER STRIPPING COLUMN + CONDENSERS

ENERGY BALANCE STRIPPING COLUMN with CONDENSERS	
Feed stream entering top of stripper	26.71 [kW]
Cooling Water into condensers	30.16 [kW]
HEAT ADDITION BY STEAM	**27.33 [kW]**
Stream from bottom of Stripping column	35.24 [kW]
Cooling Water from the condensers	45.57 [kW]
Estemated HEAT LOSS from process equip	3.01 [kW]
IN	84.19 [kW]
OUT	83.83 [kW]
BALANCE	-0.36 [kW]
% ERROR	**-0.4%** [%]

PHASE 5

FINAL PILOT PLANT STEAM COMMISSIONING PHASE WITH WATER

This phase of the pilot plant commissioning was aimed at verifying that the changes made after Phase 4 work properly. The effect of a step change in the liquid flow rate was also investigated.

SOLUTIONS TO THE PROBLEMS ENCOUNTERD DURING PHASE 4

For the sake of being complete the problems encountered during Phase 4 of the pilot plant steam commissioning are listed below.

1. Faulty rotameter leading to a line blockage; no flow to top of stripping column causing low liquid level in steam reboiler unit;
2. Necessity of implementing an interlock setup on the steam valve when there is no flow to the top of the stripping column.
3. Back flow of liquid fed from absorber into the reflux feed line – rather than to the top of the stripping column.
4. Balancing the mass flow rates of the liquid with different densities due to their different temperatures.

In an attempt to be concise the solutions to the problems encountered will be given with reference to the relevant number in the list above.

1. Rotameter was fixed to prevent any possibility of blocking the line (will be recalibrated with the solvent used for experiments).
2. An alarm and interlock was programmed into the PLC program that monitors the temperature of the feed stream to the top of the stripping column. Should this temperature increase above 75°C the alarm will alert the operator of the low liquid flow and at temperatures above 80°C, the interlock on the steam valve will be set, closing the steam valve. This will prevent the level in the reboiler unit from dropping to low.
3. A non-return valve were made and installed in the reflux line to prevent any possibility of back-flow into this line. The non-return valve works well.
4. The mass flow rate of the stream from the stripping column is measured just prior to the inlet of the pump that should balance this flow. The temperature corrected calibrations for the rotameter are then used to adjust the flow rate delivered by the pump feeding liquid back to the top of the stripping column. This method of balancing the mass flow rates are working quite well.

The energy balances were performed based on the cooling water split ratio that was calculated in the energy balances of Phase 4 of the steam commissioning procedure. **Table B.35** and **Table B.36** give the energy balances over the heat exchanger for liquid mass flow rates of 100 kg/h and 211 kg/h. The effect of the step change in the mass flow rate on the temperature profiles can be seen in **Figure B.122** and **Figure B.123**.

TABLE B.35 HEAT EXCHANGER (E-208) HEAT DUTY CALCULATIONS FOR MASS FLOW RATES OF 100KG/H

Measured Mass Flow Rate	**100**	**[kg/h]**
Heat Capacity	4.18	[kJ/kg.K]
Temp[HOT] IN	73.5	[°C]
Temp[HOT] OUT	37.9	[°C]
Temp[COLD] IN	20.0	[°C]
Temp[COLD] OUT	51.0	[°C]
deltaT [HOT]	35.57	[°C]
deltaT [COLD]	31.01	[°C]
Q = m.c.ΔT [HOT]	**4.13**	**[kW]**
Q = m.c.ΔT [COLD]	**3.60**	**[kW]**
HEAT LOSS in lines	**0.53**	**[kW]**

TABLE B.36 ENERGY BALANCE FOR HEAT EXCHANGER WITH MASS FLOW RATES OF 211 KG/H

Measured Mass Flow Rate	**211**	**[kg/h]**
Heat Capacity	4.18	[kJ/kg.K]
Temp[HOT] IN	84.0	[°C]
Temp[HOT] OUT	43.5	[°C]
Temp[COLD] IN	26.1	[°C]
Temp[COLD] OUT	60.0	[°C]
deltaT [HOT]	40.51	[°C]
deltaT [COLD]	33.90	[°C]
Q = m.c.ΔT [HOT]	**9.93**	**[kW]**
Q = m.c.ΔT [COLD]	**8.31**	**[kW]**
HEAT LOSS in lines	**1.62**	**[kW]**

The results from the energy balances for the two cases (liquid mass flow rates of 100 and 211 kg/h) can be seen in **Table B.37** to Table B.41. It can be seen that the % errors reported in the energy balances are relatively small.

Calculated heat losses from the system are similar for the two runs.

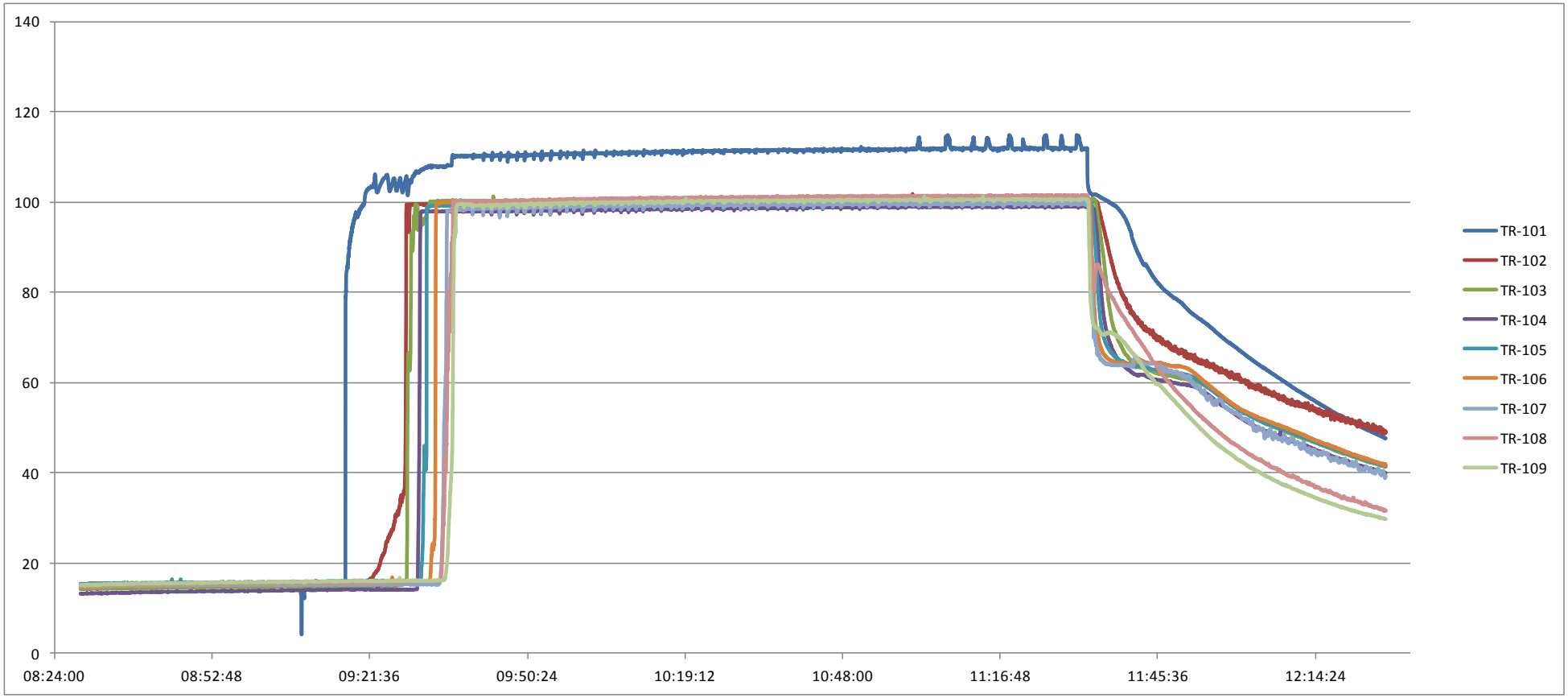

FIGURE B.121 HEATING OF THE STRIPPING COLUMN FROM THE BOTTOM (TR-102) TO THE TOP (TR-109) AND THE COOL DOWN PERIOD AFTER THE STEAM VALVE HAS BEEN CLOSED

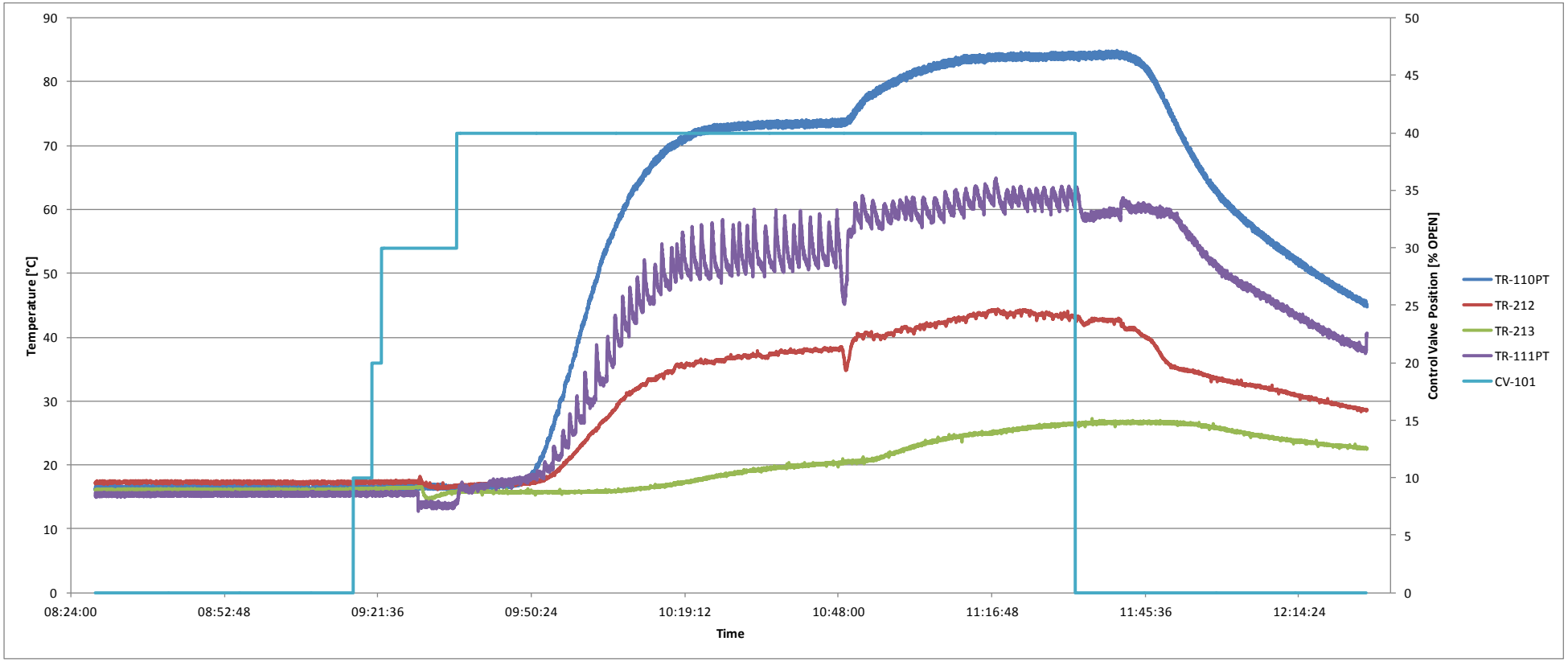

FIGURE B.122 TEMPERATURE PROFILES OF THE STREAMS ENTERING (TR-110[HOT], TR-213[COLD]) AND LEAVING (TR-111[COLD], TR-212[HOT]) THE HEAT EXCHANGER E-208. THE EFFECT OF THE STEP CHANGE IN THE LIQUID FLOW RATE (FROM 100 – 211 KG/H) CAN BE SEEN AT 10H50

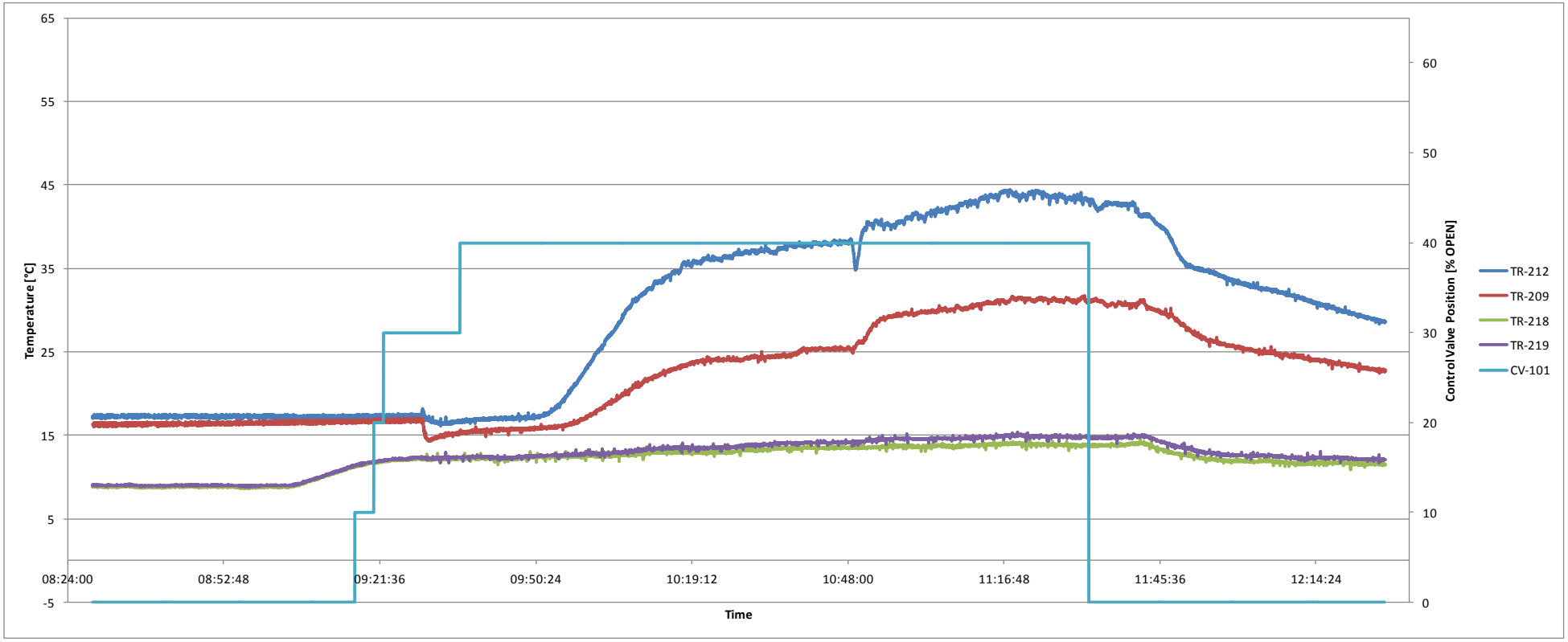

FIGURE B.123 TEMPERATURE PROFILES OF THE STREAMS ENTERING AND LEAVING THE SOLVENT COOLER UNIT E-209, THE STEP CHANGE IN THE LIQUID FLOW RATE CAN BE SEEN AT A TIME OF 10H50

TABLE B.37 ENERGY BALANCES OVER THE COOLER UNIT, STRIPPING COLUMN CONDENSERS AND STRIPPING COLUMN

COOLING DUTY of SOLVENT COOLER Calculations		**MASS FLOW RATE to CONDENSERS Calculations**		**ENERGY BALANCE OVER STRIPPER without CONDENSERS**	
Measured Mass Flow Rate	100.00 [kg/h]	Total volumetric flow rate	5.26 [m3/h]	**IN:** Feed stream entering top of stripper	5.94 [kW]
Heat Capacity	4.18 [kJ/kg.K]	Total Mass flow rate [MEASURED]	5255.51 [kg/h]	**IN:** Condensate Return in Reflux Line	4.69 [kW]
Temp[HOT] IN	37.89 [°C]	**MFR OF COOLING WATER to CONDENSERS**	**1681.76 [KG/H]**	**IN:** ***HEAT ADDITION BY STEAM***	**47.32 [kW]**
Temp[HOT] OUT	25.27 [°C]	Temperature of Cooling water return	31.15 [°C]	**OUT:** Stream from bottom of Stripping column	8.55 [kW]
deltaT	12.61 [°C]	deltaT	17.58 [°C]	**OUT:** Vapour stream from top of Stripping column	40.74 [kW]
Q = m.c.ΔT [HOT]	**1.47 [kW]**	***ENERGY REMOVED IN CONDENSERS***	**34.38 [kW]**	*Estemated* HEAT LOSS from process equip	8.66 [kW]
COOLING WATER temperatures		**MASS FLOW RATE OF CONDENSATE Calculations**		**STEAM FLOW RATE Calculations**	
INLET Temperature	13.57 [°C]	*Assumed* [%] of energy to condensation	100% [%]	Average Steam temperature	111.63 [°C]
OUTLET Temperature	14.10 [°C]	Heat of Condensation for Water	2257.40 [kJ/kg]	Energy given of by the condensing steam	2282.50 [kJ/kg]
		Total energy removed in condensers	34.38 [kW]	Calculated heat addition by steam	47.32 [kW]
		MASS FLOW RATE OF CONDENSATE	**54.83 [KG/H]**	***Measured STEAM FLOW RATE***	74.64 [KG/H]

Table B.39 Energy balance over Entire system (exclusion of absorber)

ENERGY BALANCE OVER STRIPPING COLUMN + CONDENSERS + HTX + COOLER			
Feed stream entering top of ABSORBER	2.94 [kW]	*IN*	132.85
Feed stream to HTX from ABSORBER	**2.33 [kW]**	*OUT*	131.94
Heat addition by STEAM	**47.32 [kW]**	*Balance*	-0.90
Cooling water into the system	**83.19 [kW]**	**% ERROR**	**-0.7%**
Cooling Water OUT form COOLER	58.81 [kW]		
Cooling Water OUT from CONDENSERS	61.00 [kW]		
Heat LOSS from the system	9.19 [kW]		
Cooling water Flow rate Calculations			
Cooling water to the cooler unit	3573.74 [°C]	**COOLING WATER SPLIT**	
Cooling water to the condenser units	1681.76 [kJ/kg]	x	0.6800

TABLE B.38 ENERGY BALANCE OVER STRIPPING COLUMN + CONDENSERS

ENERGY BALANCE STRIPPING COLUMN with CONDENSERS	
Feed stream entering top of stripper	5.94 [kW]
Cooling Water into condensers	26.62 [kW]
HEAT ADDITION BY STEAM	**47.32 [kW]**
Stream from bottom of Stripping column	8.55 [kW]
Cooling Water from the condensers	61.00 [kW]
Estemated HEAT LOSS from process equip	8.66 [kW]
IN	79.88 [kW]
OUT	78.21 [kW]
BALANCE	-1.67 [kW]
% ERROR	**-2.1%** [%]

TABLE B.40 ENERGY BALANCES FOR LIQUID MASS FLOW RATES OF 211 KG/H

COOLING DUTY of SOLVENT COOLER Calculations		**MASS FLOW RATE to CONDENSERS Calculations**		**ENERGY BALANCE OVER STRIPPER without CONDENSERS**	
Measured Mass Flow Rate	211.00 [kg/h]	Total volumetric flow rate	5.26 [m3/h]	**IN:** Feed stream entering top of stripper	14.73 [kW]
Heat Capacity	4.18 [kJ/kg.K]	Total Mass flow rate [MEASURED]	5254.34 [kg/h]	**IN:** Condensate Return in Reflux Line	4.97 [kW]
Temp[HOT] IN	43.52 [°C]	**MFR OF COOLING WATER to CONDENSERS**	**1681.39 [KG/H]**	**IN:** ***HEAT ADDITION BY STEAM***	**46.94 [kW]**
Temp[HOT] OUT	31.17 [°C]	Temperature of Cooling water return	30.21 [°C]	**OUT:** Stream from bottom of Stripping column	20.63 [kW]
deltaT	12.35 [°C]	deltaT	16.29 [°C]	**OUT:** Vapour stream from top of Stripping column	37.75 [kW]
Q = m.c. ΔT [HOT]	**3.03 [kW]**	***ENERGY REMOVED IN CONDENSERS***	**31.86 [kW]**	*Estemated* HEAT LOSS from process equip	8.27 [kW]
MASS FLOW RATE of COOLING WATER Calculations		**MASS FLOW RATE OF CONDENSATE Calculations**		**STEAM FLOW RATE Calculations**	
INLET Temperature	13.91 [°C]	*Assumed* [%] of energy to condensation	100% [%]	Average Steam temperature	112.38 [°C]
OUTLET Temperature	14.82 [°C]	Heat of Condensation for Water	2257.40 [kJ/kg]	Energy given of by the condensing steam	2282.50 [kJ/kg]
		Total energy removed in condensers	31.86 [kW]	Calculated heat addition by steam	46.94 [kW]
		MASS FLOW RATE OF CONDENSATE	**50.80 [KG/H]**	***Measured STEAM FLOW RATE***	74.04 [KG/H]

TABLE B.42 ENERGY BALANCE FOR ENTIRE SYSTEM EXCLUDING ABSORBER

ENERGY BALANCE OVER STRIPPING COLUMN + CONDENSERS + HTX + COOLER			
Feed stream entering top of ABSORBER	7.66 [kW]	*IN*	138.67
Feed stream to HTX from ABSORBER	**6.42 [kW]**	*OUT*	138.49
Heat addition by STEAM	**46.94 [kW]**	*Balance*	-0.18
Cooling water into the system	**85.31 [kW]**	**% ERROR**	**-0.1%**
Cooling Water OUT form COOLER	61.79 [kW]		
Cooling Water OUT from CONDENSERS	59.16 [kW]		
Heat LOSS from the system	9.89 [kW]		
Cooling water Flow rate Calculations			
Cooling water to the cooler unit	3572.95 [°C]	**COOLING WATER SPLIT**	
Cooling water to the condenser units	1681.39 [kJ/kg]	x	0.6800

TABLE B.41 ENERGY BALANCE FOR THE STRIPPER + CONDENSERS

ENERGY BALANCE STRIPPING COLUMN with CONDENSERS	
Feed stream entering top of stripper	14.73 [kW]
Cooling Water into condensers	27.30 [kW]
HEAT ADDITION BY STEAM	**46.94 [kW]**
Stream from bottom of Stripping column	20.63 [kW]
Cooling Water from the condensers	59.16 [kW]
Estemated HEAT LOSS from process equip	8.27 [kW]
IN	88.98 [kW]
OUT	88.05 [kW]
BALANCE	-0.92 [kW]
% ERROR	**-1.0%** [%]

APPENDIX C: PILOT PLANT RESULTS

REPEATABILITY RESULTS

TABLE C.43 ERRORS IN CO_2 CONCENTRATION PROFILES FOR REPEATABILITY RUNS WITH 20 WT % MEA - LARGE ERRORS DUE TO SOLVENT DILUTION AFTER FIRST RUN

Sample Point	Run 1_CO2 Concentration [Vol %]	Run 2_CO2 Concentration [Vol %]	Average [vol %]	Error [%]
Feed	9.05	9.40	9.22	± 1.9%
SP 1	3.94	5.07	4.50	± 12.5%
SP 2	2.6	3.63	3.11	± 16.5%
SP 3	1.34	1.63	1.49	± 9.8%
TOP	0.97	1.26	1.12	± 13.1%

TABLE C.44 ERRORS IN THE REGENERATION ENERGY AND CAPTURE RATES FOR REPEATABILITY RUNS WITH 20 WT % MEA

	Run 1	Run 2	Average	Error [%]
Regeneration Energy [MJ/kgCO2 removed]	90.16	87.66	88.91	± 1.4%
CO2 Capture Rate [%]	17.24	17.00	17.12	± 0.7%

TABLE C.45 ERRORS IN THE CO_2 CONCENTRATION PROFILES FROM REPEATABILITY RUNS WITH 30WT% MEA

Sample Point	Run 1_CO2 Concentration [Vol %]	Run 2_CO2 Concentration [Vol %]	Average [Vol %]	Error [%]
Feed	8.49	8.97	8.73	± 2.7%
SP 1	3.53	3.57	3.55	± 0.7%
SP 2	2.27	2.39	2.33	± 2.6%
SP 3	1.06	1.14	1.10	± 3.5%
TOP	0.77	0.74	0.76	± 2.1%

TABLE C.46 ERRORS IN THE REGENERATION ENERGY AND CO_2 CAPTURE RATES FOR REPEATABILITY RUNS WITH 30 WT% MEA

	Run 1	Run 2	Average	Error [%]
Regeneration Energy [MJ/kgCO2 removed]	6.13	6.03	6.08	± 0.80%
CO2 Capture Rate [%]	92.4	91.6	90.0	± 0.44%

START-UP PROCEDURE

The start-up procedure is commenced by running a series of checks that ensures all valves are set for operating the process equipment in Mode 1 – The post-combustion CO_2 capture pilot plant. The list of checks is briefly summarized below.

1. Check that the screw-down valves installed in the glass lines are open to guide liquid flow from the stripping section to the absorption section and vice versa.
2. Check that all the isolation valves to the heat exchanger are fully open.
3. Check that all manual valves providing cooling water to the stripping column condensers and the solvent cooler unit are fully open.
4. Check that the isolation valve on the steam supply line to the reboiler unit is fully open.
5. Check that the butterfly valves in the gas circulation loop are set for the use of the recycle blower unit.

Starting up the pilot plant will be summarized in point form and reference will be made to all the important things that should be considered.

1. Switch on the cooling water pump providing the pilot plant setup with cooling water.
2. Switch on the boiler unit that provides the pilot plant with steam for solvent regeneration.
3. Check that there are no indicated alarms on the screen of the control panel.
4. Start-up can be commenced by opening the steam valve (CV-101) to about 20 % OPEN. After about 3 minutes this can be increased to 30 % OPEN (depending on the operating conditions for the particular run).
5. While heating the stripping column, start circulating the gas in the gas recycle stream.
6. Start the sample pump allowing gas sampling from the feed stream.
7. While purging, add nitrogen to the process gas by opening the control valve, CV-202. Continuously add nitrogen to the system until the O_2 concentration of the feed gas is sufficiently reduced.
8. Keep checking the temperature trends of the stripping column and observe as it is heated from the bottom to the top.
9. When the bottom 3 meters of the stripping column is heated to the boiling temperature of the solvent, start feeding solvent to the top of the absorber column by starting the rich solvent feed pump, E-207.
10. Start the wash water feed pump (E-211), setting the wash water flow rate to about 20 [liters/hour]
11. Start the lean solvent pulsation pump (E-108) feeding solvent from the bottom of the stripping column to the top of the absorber column.

12. Start the reflux pump that is used to control the level of the reflux in a small holding vessel. The setpoint value for the height of the liquid can be adjusted [Units in cm].
13. Use the calibration charts for the pumps in order to roughly balance the flow rates between the columns by adjusting the screw-down valve downstream from the rich solvent pump.
14. Keep checking the levels in the solvent buffer tanks in order to continuously balance the solvent flow rate. As the temperature of the pumped fluids changes, the density will change and the flow rate will have to be adjusted.
15. Allow sufficient time for stabilization of two key temperatures: The lean solvent feed to the top of the absorber column, and the rich solvent feed to the top of the stripping column.
16. Once the system has reach thermal equilibrium, the operating procedure for the experimental runs can be commenced.

SHUTDOWN PROCEDURE

The shutdown procedure is fairly simple and mainly sufficient time should be allowed for the cool down of the heated liquid solvent. The procedure is summarized below.

1. Close the control valve feeding steam to the reboiler unit – CV-101.
2. Close the control valve feeding CO_2 to the gas recycle loop – CV-201.
3. Stop the blower unit (E-201) from circulating gas through the solvent, as MEA is prone to oxidative degradation and without CO_2 fed to the recycle loop the concentration of the O_2 rises fairly quickly.
4. Stop the sample pump and the switch valves – V-225A/B.
5. Stop the wash water circulation pump – E-211.
6. Switch off the boiler unit as no further steam is required.
7. Keep circulating the solvent through the systems unit sufficiently cooled.
8. After the solvent has reached an acceptable temperature, switch of the solvent pumps – E-108 and E-207.
9. Switch off the reflux pump if there is no condensate flowing into the small holding vessel – E-113.
10. Allow the cooling water to run for at least another hour.
11. Switch off the cooling water supply pump.

Close the isolation valve on the steam supply line to the reboiler unit.

Due to the size of the spread sheets containing the data of each experimental run, the most important steady state results were gathered and are reported in **Table C.43** to **Table C.57**. The absorber column CO_2 concentration profiles, gas- and liquid temperature profiles as well as the steady state deviations from the mean values are reported in these tables. All the steady state conditions, measured and calculated is given in the tables along with their minimum and maximum values for the steady state period.

TABLEC.47 EXPERIMENTAL RESULT FROM RUN 1.1

1.1

Profiles for Absorber Column

	Distance from Bottom [m]	*CO2 Concentration [Volume %]*	[%] Captured	*Vapour Temperature [°C]*	*Liquid Temperature [°C]*
Feed/Sump	-0.5			22.12	48.35
	0.00	9.18	0.00	45.09	49.95
	0.54	2.69	72.70	55.72	55.58
	1.08	1.63	83.56	51.25	51.04
	1.62	0.76	92.45	45.43	44.08
	2.16	0.44	95.66	32.04	40.89

Deviations in CO2 concentration Profile [Vol %]

Negative	*Positive*
0.244	0.331
0.125	0.385
0.075	0.305
0.012	0.048
0.194	0.056

Various Steady State Conditions

Steady State Period	16h00 - 16h10	
Steam Flow Rate	73.464	**[kg/h]**
Solvent Flow rate	227.7	**[kg/h]**
Gas Feed Rate	135.0	**[kg/h]**
L/G-ratio	1.7	**[mass/mass]**
Cleaned Gas Flow Rate	119.4	**[kg/h]**
CO2 absorbed	11.9	**[kg/h]**
CO2 Capture Rate [%]	95.66	**[%]**
Regeneration Energy	13.7106	**[MJ/kgCO2]**

Deviations in Various Parameters

	Negative	*Positive*
CO2 Capture Rate [%]	95.0	97.7
Feed Gas Flow Rate [kg/h]	130.6	138.2
Cleaned Gas Flow Rate [kg/h]	117.0	122.2
CO2 Absorbed [kg/h]	11.5	12.6
Regeneration Energy [MJ/kgCO2]	13.0	14.2

TABLE C.48 EXPERIMENTAL RESULTS FROM RUN 1.2

1.2

Profiles for Absorber Column

	Distance from Bottom [m]	*CO2 Concentration [Volume %]*	**[%] Captured**	*Vapour Temperature [°C]*	*Liquid Temperature [°C]*
Feed/Sump	-0.5			22.58	46.24
	0.00	8.80	0.00	43.47	47.76
	0.54	2.73	70.88	50.88	50.58
	1.08	1.65	82.64	46.25	46.02
	1.62	0.77	91.96	41.57	40.58
	2.16	0.47	95.08	31.94	38.28

Deviations in CO2 concentration Profile [Vol %]

Negative	***Positive***
0.292	0.252
0.039	0.071
0.023	0.037
0.021	0.029
0.058	0.032

Various Steady State Conditions

Steady State Period	16h40 - 16h50	
Steam Flow Rate	68.484	**[kg/h]**
Solvent Flow rate	229.6	**[kg/h]**
Gas Feed Rate	135.6	**[kg/h]**
L/G-ratio	1.7	**[mass/mass]**
Cleaned Gas Flow Rate	121.9	**[kg/h]**
CO2 absorbed	11.4	**[kg/h]**
CO2 Capture Rate [%]	95.08	**[%]**
Regeneration Energy	13.39	**[MJ/kgCO2]**

Deviations in Various Parameters	***Negative***	***Positive***
CO2 Capture Rate [%]	94.5	95.8
Feed Gas Flow Rate [kg/h]	133.4	138.7
Cleaned Gas Flow Rate [kg/h]	118.1	126.4
CO2 Absorbed [kg/h]	10.9	11.8
Regeneration Energy [MJ/kgCO2]	12.9	13.9

TABLE C.49 EXPERIMENTAL RESULTS FROM RUN 1.3

1.3

Profiles for Absorber Column

	Distance from Bottom [m]	CO2 Concentration [Volume %]	[%] Captured	Vapour Temperature [°C]	Liquid Temperature [°C]
Feed/Sump	-0.5			22.98	45.50
	0.00	8.84	0.00	42.80	46.96
	0.54	2.85	69.72	48.80	48.51
	1.08	1.74	81.69	44.31	44.15
	1.62	0.79	91.79	39.89	39.01
	2.16	0.49	94.94	30.44	37.06

Various Steady State Conditions

Steady State Period	17h30 - 17h40	
Steam Flow Rate	62.034	**[kg/h]**
Solvent Flow rate	233.2	**[kg/h]**
Gas Feed Rate	138.6	**[kg/h]**
L/G-ratio	1.7	**[mass/mass]**
Cleaned Gas Flow Rate	123.1	**[kg/h]**
CO2 absorbed	11.7	**[kg/h]**
CO2 Capture Rate [%]	94.94	**[%]**
Regeneration Energy	11.82	**[MJ/kgCO2]**

Deviations in CO2

Negative	*Positive*
0.194	0.378
0.077	0.163
0.055	0.075
0.160	0.020
0.052	0.038

Deviations in Various Parameters	*Negative*	*Positive*
CO2 Capture Rate [%]	94.4	95.7
Feed Gas Flow Rate [kg/h]	136.1	142.2
Cleaned Gas Flow Rate [kg/h]	118.9	126.8
CO2 Absorbed [kg/h]	11.3	12.3
Regeneration Energy [MJ/kgCO2]	11.2	12.1

TABLE C.50 EXPERIMENTAL RESULTS FROM RUN 1.4

1.4

Profiles for Absorber Column

	Distance from Bottom [m]	*CO2 Concentration [Volume %]*	**[%] Captured**	*Vapour Temperature [°C]*	*Liquid Temperature [°C]*
Feed/Sump	-0.5			23.23	45.66
	0.00	9.22	0.00	42.91	47.19
	0.54	3.11	68.39	49.12	48.93
	1.08	2.03	79.60	44.52	44.34
	1.62	0.93	90.74	39.78	38.87
	2.16	0.55	94.60	29.30	36.74

Deviations in CO2

Negative	***Positive***
0.561	0.471
0.039	0.081
0.071	0.139
0.019	0.021
0.004	0.026

Various Steady State Conditions

Steady State Period	18h20 - 18h30	
Steam Flow Rate	51.432	**[kg/h]**
Solvent Flow rate	231	**[kg/h]**
Gas Feed Rate	138.9	**[kg/h]**
L/G-ratio	1.7	**[mass/mass]**
Cleaned Gas Flow Rate	124.9	**[kg/h]**
CO2 absorbed	12.1	**[kg/h]**
CO2 Capture Rate [%]	94.60	**[%]**
Regeneration Energy	9.44	**[MJ/kgCO2]**

Deviations in Various Parameters	***Negative***	***Positive***
CO2 Capture Rate [%]	93.9	94.9
Feed Gas Flow Rate [kg/h]	135.8	141.5
Cleaned Gas Flow Rate [kg/h]	121.4	128.2
CO2 Absorbed [kg/h]	11.3	12.8
Regeneration Energy [MJ/kgCO2]	8.9	10.1

TABLE C.51 EXPERIMENTAL RESULTS FROM RUN 2.1

2.1

Profiles for Absorber Column

	Distance from Bottom [m]	CO2 Concentration [Volume %]	[%] Captured	Vapour Temperature [°C]	Liquid Temperature [°C]
Feed/Sump	-0.5			22.78	47.16
	0.00	8.97	0.00	45.98	49.11
	0.54	3.57	62.36	53.75	53.62
	1.08	2.39	75.12	50.28	50.22
	1.62	1.14	88.34	45.75	44.88
	2.16	0.74	92.40	34.84	41.56

Deviations in CO2 concentration			Error on [%] Captured	
Negative	Positive	[%] Captured	Negative	Positive
0.00	0.05	0%	0.00	0.00
0.12	0.50	62%	0.09	0.02
0.05	0.27	75%	0.09	0.02
0.02	0.10	88%	0.07	0.01
0.01	0.01	92%	0.02	0.01

Stripper Temp Profiles	Distance from Bottom [m]	Temperature [°C]	Normalized Heigh
Sump	-0.5	101.8	
	0	101.7	0.00
	1	98.8	0.17
	2	96.5	0.33
	3	93.2	0.50
	4	80.7	0.67
	5	74.2	0.83
	6	67.5	1.00

Various Steady State Conditions	1	[steam quality]
Steady State Period	12h00 - 12h10	
Steam Flow Rate	25.755	[kg/h]
Solvent Flow rate	257.1	[kg/h]
Gas Feed Rate	113.3	[kg/h]
L/G-ratio	2.3	[mass/mass]
Cleaned Gas Flow Rate	98.6	[kg/h]
CO2 absorbed	9.4	[kg/h]
CO2 Capture Rate [%]	92.40	[%]
Regeneration Energy	6.13	[MJ/kgCO2]

Deviations in Various Parameters	Negative	Positive
CO2 Capture Rate [%]	92.27	92.51
Feed Gas Flow Rate [kg/h]	110.05	118.01
Cleaned Gas Flow Rate [kg/h]	92.93	102.70
CO2 Absorbed [kg/h]	9.09	9.53
Regeneration Energy [MJ/kgCO2]	5.99	6.28

Deviation in Absorber Temperature [°C]

Vapour		Liquid	
Neg	Pos	Neg	Pos
0.62	0.78	0.54	0.26
0.52	0.38	0.59	0.81
0.45	0.45	0.88	0.82
0.52	0.58	0.78	0.52
0.75	0.55	0.42	0.58
0.36	0.64	0.44	0.66

TABLE C.52 EXPERIMENTAL RESULTS FROM RUN 2.2

2.2

Profiles for Absorber Column				
	CO2			
Distance from Bottom [m]	*Concentration [Volume %]*	[%] Captured	*Vapour Temperature [°C]*	*Liquid Temperature [°C]*
Feed/Sump -0.5			25.85	43.52
0.00	9.30	0.00	42.48	44.60
0.54	6.83	28.47	48.78	48.68
1.08	5.64	41.70	47.08	47.14
1.62	3.49	64.77	44.12	43.37
2.16	2.86	71.25	35.39	39.37

Various Steady State Conditions		
	0.86	**[steam quality]**
Steady State Period	13h05 - 13h15	
Steam Flow Rate	19.1	**[kg/h]**
Solvent Flow rate	257.2	**[kg/h]**
Gas Feed Rate	117.4	**[kg/h]**
L/G-ratio	2.2	**[mass/mass]**
Cleaned Gas Flow Rate	112.2	**[kg/h]**
CO2 absorbed	7.7	**[kg/h]**
CO2 Capture Rate [%]	71.25	**[%]**
Regeneration Energy	4.79	**[MJ/kgCO2]**

Deviations in CO2 concentration

Negative	***Positive***
0.030	0.140
0.067	0.233
0.049	0.181
0.134	0.686
0.228	0.228

Deviations in Various Parameters	***Negative***	***Positive***
CO2 Capture Rate [%]	68.8	74.0
Feed Gas Flow Rate [kg/h]	114.3	121.3
Cleaned Gas Flow Rate [kg/h]	107.2	116.1
CO2 Absorbed [kg/h]	7.3	8.3
Regeneration Energy [MJ/kgCO2]	4.4	5.0

Stripper Temp Profiles	**Distance from Bottom [m]**	**Temperature [°C]**	**Normalized Heigh**
Sump	-0.5	98.9	
	0	95.8	0.00
	1	75.2	0.17
	2	76.1	0.33
	3	77.6	0.50
	4	74.3	0.67
	5	58.4	0.83
	6	48.2	1.00

Deviation in Absorber Temperature [°C]

Vapour		Liquid	
Neg	**Pos**	**Neg**	**Pos**
0.55	0.65	0.42	0.48
0.38	0.52	0.80	0.70
0.48	0.82	0.58	0.72
0.48	0.32	0.34	0.56
0.62	0.28	0.57	0.33
0.49	0.61	0.77	0.63

TABLE C.53 EXPERIMENTAL RESULTS FROM RUN 2.3

2.3

Profiles for Absorber Column

	Distance from Bottom [m]	*CO2 Concentration [Volume %]*	[%] Captured	*Vapour Temperature [°C]*	*Liquid Temperature [°C]*
Feed/Sump	-0.5			26.50	40.04
	0.00	9.33	0.00	38.35	40.52
	0.54	8.09	14.48	43.67	43.51
	1.08	7.22	24.36	42.76	42.81
	1.62	5.58	42.50	41.17	40.68
	2.16	4.36	55.65	34.68	37.69

Various Steady State Conditions

Steady State Period	13h55 - 14h00	
Steam Flow Rate	11.528	**[kg/h]**
Solvent Flow rate	266	**[kg/h]**
Gas Feed Rate	119.4	**[kg/h]**
L/G-ratio	2.2	**[mass/mass]**
Cleaned Gas Flow Rate	117.1	**[kg/h]**
CO2 absorbed	6.0	**[kg/h]**
CO2 Capture Rate [%]	55.65	**[%]**
Regeneration Energy	3.83	**[MJ/kgCO2]**
	0.89	**[steam quality]**

Deviations in CO2 concentration

Negative	***Positive***
0.123	0.087
0.174	0.706
0.131	0.189
0.125	0.355
0.007	0.013

Deviations in Various Parameters

	Negative	***Positive***
CO2 Capture Rate [%]	54.9	56.2
Feed Gas Flow Rate [kg/h]	116.8	122.1
Cleaned Gas Flow Rate [kg/h]	112.8	119.7
CO2 Absorbed [kg/h]	5.8	6.3
Regeneration Energy [MJ/kgCO2]	3.6	3.9

Stripper Temp Profiles	**Distance from Bottom [m]**	**Temperature [°C]**	**Normalized Heigh**
Sump	-0.5	96.1	
	0	86.6	0.00
	1	71.4	0.17
	2	72.1	0.33
	3	73.5	0.50
	4	69.0	0.67
	5	52.1	0.83
	6	41.4	1.00

Deviation in Absorber Temperature [°C]

Vapour		Liquid	
Neg	**Pos**	**Neg**	**Pos**
0.502	0.398	0.762	1.040
0.945	0.955	0.983	0.920
1.026	1.174	0.594	1.210
0.535	0.865	0.586	0.910
0.833	0.970	0.818	0.980
0.520	0.680	0.506	0.690

TABLE C.54 EXPERIMENTAL RESULTS FROM RUN 3

3.1

Profiles for Absorber Column				
	Distance from Bottom [m]	*CO2 Concentration [Volume %]*	[%] Captured	*Vapour Temperature [°C]*	*Liquid Temperature [°C]*
Feed/Sump	-0.5			23.83	41.94
	0.00	8.64		39.69	42.77
	0.54			46.16	45.97
	1.08	3.71	62.57	43.95	43.96
	1.62	2.45	75.62	40.99	40.27
	2.16	2.03	79.84	33.13	37.17

Various Steady State Conditions		
	0.8	**[steam quality]**
Steady State Period	22h39	- 22h50
Steam Flow Rate	25.641	**[kg/h]**
Solvent Flow rate	267	**[kg/h]**
Gas Feed Rate	124.3	**[kg/h]**
L/G-ratio	2.1	**[mass/mass]**
Cleaned Gas Flow Rate	111.4	**[kg/h]**
CO2 absorbed	8.5	**[kg/h]**
CO2 Capture Rate [%]	78.06	**[%]**
Regeneration Energy	5.43	**[MJ/kgCO2]**

Deviations in CO2 concentration

Negative	***Positive***
0.037	0.013
0.022	0.028

Deviations in Various Parameters	***Negative***	***Positive***
CO2 Capture Rate [%]	77.8	78.5
Feed Gas Flow Rate [kg/h]	119.7	128.7
Cleaned Gas Flow Rate [kg/h]	106.6	115.0
CO2 Absorbed [kg/h]	8.4	8.6
Regeneration Energy [MJ/kgCO2]	5.3	5.4

Stripper Temp Profiles	**Distance from Bottom [m]**	**Temperature [°C]**	**Normalized Heigh**
Sump	-0.5	98.6	
	0	96.2	0.00
	1	73.5	0.17
	2	74.3	0.33
	3	76.0	0.50
	4	73.4	0.67
	5	58.3	0.83
	6	48.9	1.00

Deviation in Absorber Temperature [°C]

Vapour		**Liquid**	
Neg	**Pos**	**Neg**	**Pos**
0.374	0.526	0.561	0.939
0.813	0.687	0.729	0.871
0.837	1.363	0.932	1.468
0.648	1.152	0.839	1.161
0.614	0.986	0.734	1.066
0.566	0.534	0.532	0.568

TABLE C.55 EXPERIMENTAL RESULTS FROM RUN 4.1

4.1

Profiles for Absorber Column				
Distance from Bottom [m]	*CO2 Concentration [Volume %]*	[%] Captured	*Vapour Temperature [°C]*	*Liquid Temperature [°C]*
Feed/Sump -0.5			26.39	48.76
0.00	9.48	0.00	48.60	51.01
0.54	2.72	73.34	52.82	52.27
1.08	1.51	85.32	47.60	47.29
1.62	0.65	93.74	43.53	42.82
2.16	0.31	97.03	36.92	40.93

Various Steady State Conditions		
Steady State Period	14h00 - 14h15	
Steam Flow Rate	52.404	**[kg/h]**
Solvent Flow rate	249.3	**[kg/h]**
Gas Feed Rate	121.8	**[kg/h]**
L/G-ratio	2.0	**[mass/mass]**
Cleaned Gas Flow Rate	115.4	**[kg/h]**
CO2 absorbed	11.2	**[kg/h]**
CO2 Capture Rate [%]	97.03	**[%]**
Regeneration Energy	10.39	**[MJ/kgCO2]**

Deviations in CO2 concentration Profile [Vol %]

Negative	***Positive***
0.098	0.119
0.103	0.077
0.036	0.014
0.008	0.022
0.070	0.050

Deviations in Various Parameters	*Negative*	*Positive*
CO2 Capture Rate [%]	96.5	97.7
Feed Gas Flow Rate [kg/h]	118.8	125.7
Cleaned Gas Flow Rate [kg/h]	113.0	117.4
CO2 Absorbed [kg/h]	11.0	11.4
Regeneration Energy [MJ/kgCO2]	10.2	10.5

Deviation in Absorber Temperature [°C]

Vapour		Liquid	
Neg	**Pos**	**Neg**	**Pos**
0.607	0.493	0.544	0.556
0.796	0.704	0.786	0.814
0.479	0.521	0.529	0.471
0.503	0.397	0.612	0.388
0.673	0.527	0.677	0.423
0.484	0.516	0.767	0.533

TABLE C.56 EXPERIMENTAL RESULTS FROM RUN 4.2

4.2

Profiles for Absorber Column				
	Distance from Bottom [m]	*CO2 Concentration [Volume %]*	*[%] Captured*	*Vapour Temperature [°C]*	*Liquid Temperature [°C]*
Feed/Sump	-0.5			27.40	48.71
	0.00	9.25	0.00	48.75	50.76
	0.54	2.88	70.86	52.78	52.12
	1.08	1.73	82.74	47.57	47.36
	1.62	0.75	92.62	43.52	42.77
	2.16	0.43	95.74	37.61	41.18

Various Steady State Conditions		
Steady State Period	16h30 - 16h50	
Steam Flow Rate	41.535	**[kg/h]**
Solvent Flow rate	257.2	**[kg/h]**
Gas Feed Rate	127.6	**[kg/h]**
L/G-ratio	2.0	**[mass/mass]**
Cleaned Gas Flow Rate	119.6	**[kg/h]**
CO2 absorbed	11.3	**[kg/h]**
CO2 Capture Rate [%]	95.74	**[%]**
Regeneration Energy	8.18	**[MJ/kgCO2]**

Deviations in CO2 concentration Profile [Vol %]

Negative	***Positive***
0.821	0.565
0.026	0.184
0.041	0.069
0.014	0.016
0.047	0.023

Deviations in Various Parameters	*Negative*	*Positive*
CO2 Capture Rate [%]	95.0	96.4
Feed Gas Flow Rate [kg/h]	123.6	131.6
Cleaned Gas Flow Rate [kg/h]	116.6	122.4
CO2 Absorbed [kg/h]	10.2	12.1
Regeneration Energy [MJ/kgCO2]	7.6	9.0

Deviation in Absorber Temperature [°C]

Vapour		Liquid	
Neg	**Pos**	**Neg**	**Pos**
0.396	0.804	0.615	0.811
0.450	0.351	0.741	0.559
0.424	0.776	0.882	0.618
0.834	0.866	0.544	0.556
0.680	0.620	0.531	0.469
0.595	0.405	0.615	0.485

TABLE C.57 EXPERIMENTAL RESULTS FROM RUN 4.3

4.3

Profiles for Absorber Column				
	Distance from Bottom [m]	*CO2 Concentration [Volume %]*	*[%] Captured*	*Vapour Temperature [°C]*	*Liquid Temperature [°C]*
Feed/Sump	-0.5			27.00	46.00
	0.00	8.49	0.00	44.87	47.34
	0.54	3.53	60.59	49.65	49.19
	1.08	2.27	74.97	45.47	45.30
	1.62	1.06	88.47	41.74	40.93
	2.16	0.77	91.58	35.90	38.99

Various Steady State Conditions		
Steady State Period	18h50 - 19h10	
Steam Flow Rate	27.192	**[kg/h]**
Solvent Flow rate	255	**[kg/h]**
Gas Feed Rate	129.6	**[kg/h]**
L/G-ratio	2.0	**[mass/mass]**
Cleaned Gas Flow Rate	122.8	**[kg/h]**
CO2 absorbed	10.1	**[kg/h]**
CO2 Capture Rate [%]	91.58	**[%]**
Regeneration Energy	6.03	**[MJ/kgCO2]**

Deviations in CO2 concentration Profile [Vol %]

Negative	***Positive***
0.203	0.570
0.053	0.157
0.191	0.139
0.012	0.028
0.028	0.045

Deviations in Various Parameters	*Negative*	*Positive*
CO2 Capture Rate [%]	90.9	92.4
Feed Gas Flow Rate [kg/h]	126.4	132.3
Cleaned Gas Flow Rate [kg/h]	118.8	127.1
CO2 Absorbed [kg/h]	9.7	10.9
Regeneration Energy [MJ/kgCO2]	5.6	6.2

Deviation in Absorber Temperature [°C]

Vapour		Liquid	
Neg	**Pos**	**Neg**	**Pos**
0.303	0.597	0.695	0.505
0.734	0.466	0.860	0.740
1.049	0.951	1.213	0.787
1.135	0.665	1.096	1.204
0.857	1.043	1.065	0.735
0.605	0.895	0.812	0.488

TABLE C.58 SUMMARISING PILOT PLANT RESULTS

% CO_2 Captured	Heat duty of Reboiler [GJ/ton CO_2]
55.65%	3.83
71.25%	4.79
78.06%	5.43
91.58%	6.03
92.40%	6.13
94.60%	9.44
94.94%	11.82
95.08%	13.39
95.66%	13.71
95.74%	8.18
97.03%	10.39

TABLE C.59 ASPEN PLUS(R) SIMULATION RESULTS FOR L/G-RATIO OF 2 - SET UP WITH SAME OPERATING CONDITIONS AS THE PILOT PLANT EXPERIMENTS

Run #	% CO2 Captured	Reboiler Duty [MJ/hr]	CO2 Removed [kg/hr]	Heat duty of Reboiler [GJ/ton CO2]
1	**40%**	**20.85**	**5.63**	3.702
2	**45%**	**24.95**	**6.46**	3.860
3	55%	32.83	8.27	3.968
4	**60%**	**36.64**	**9.20**	3.985
5	65%	40.36	10.08	4.003
6	70%	44.99	11.04	4.075
7	75%	51.31	11.98	4.283
8	80%	60.17	12.84	4.687
9	85%	77.32	13.86	5.579
10	90%	105.73	14.81	7.137
12	92%	132.29	15.20	8.705
13	93%	148.66	15.39	9.658
14	94%	166.84	15.58	10.705
15	95%	192.62	15.79	12.199
16	96%	249.90	15.94	15.678

APPENDIX D: CALIBRATION CERTIFICATES

Drager South Africa (Pty) Ltd
1989/003553/07

Unit 1, Cor Willow Rd & Cecil Morgan St,
Stikland, 7530

P O Box 3677, Tyger Valley, 7536
Tel +27 21 945 4241/5
Fax +27 21 945 4246

St. Peter's Square, Cnr. Waterford Place &
Witkoppen rd. Kleeve Hill Park, Sandton

PO Box 68601, Bryanston, 2021
Tel +27 (0) 11 465 9959
Fax +27 (0) 11 465 6953

Dräger

GAS CALIBRATION CERTIFICATE

NUMBER: C2947

Works Order No: 1401 Product Ref: 5546

Owners Name: University of Stellenbosch

Submitted for test by: University of Stellenbosch

Instrument Type: PIR 7200

Serial Number: ARBH-0185

Sensor Type	Part Number	Serial No	Cal Gas	Batch No	Expiry Date	Alarm 1	Alarm 2	STEL	TWA
IR CO2	n/a	n/a	2% Vol CO2	1266866	Mar 2013	n/a	n/a	n/a	n/a

Calibrated at: Sea Level

Next Calibration: 17 October, 2012

Calibration Verified

Functional Inspection

Visual Checked

CALIBRATED AND CHECKED Wayne Baguley

DRÄGER S.A. (PTY) LTD
Unit 1
Cor Willow & Cecil Morgan St
Stikland - 7530
P O Box 3677, Tyger Valley, 7536
Tel: 021 945 4241 / Fax: 021 945 4246

Signature:

Date: 17 April, 2012

THIS CERTIFICATE IS INVALID UNLESS OVERSTAMPED

The issue of this certificate does not imply any warranty in respect of any instrument as to its fitness for use once the instrument has left the Company's premises save that at the time of calibration it conformed to manufacturer's standard operating specifications under simulated test conditions using the test gases above. This instrument is required to be periodically re-calibrated in accordance with these standard manufacturer specifications.

FIGURE D.124 CALIBRATION CERTIFICATE FOR THE CO_2 ANALYSER

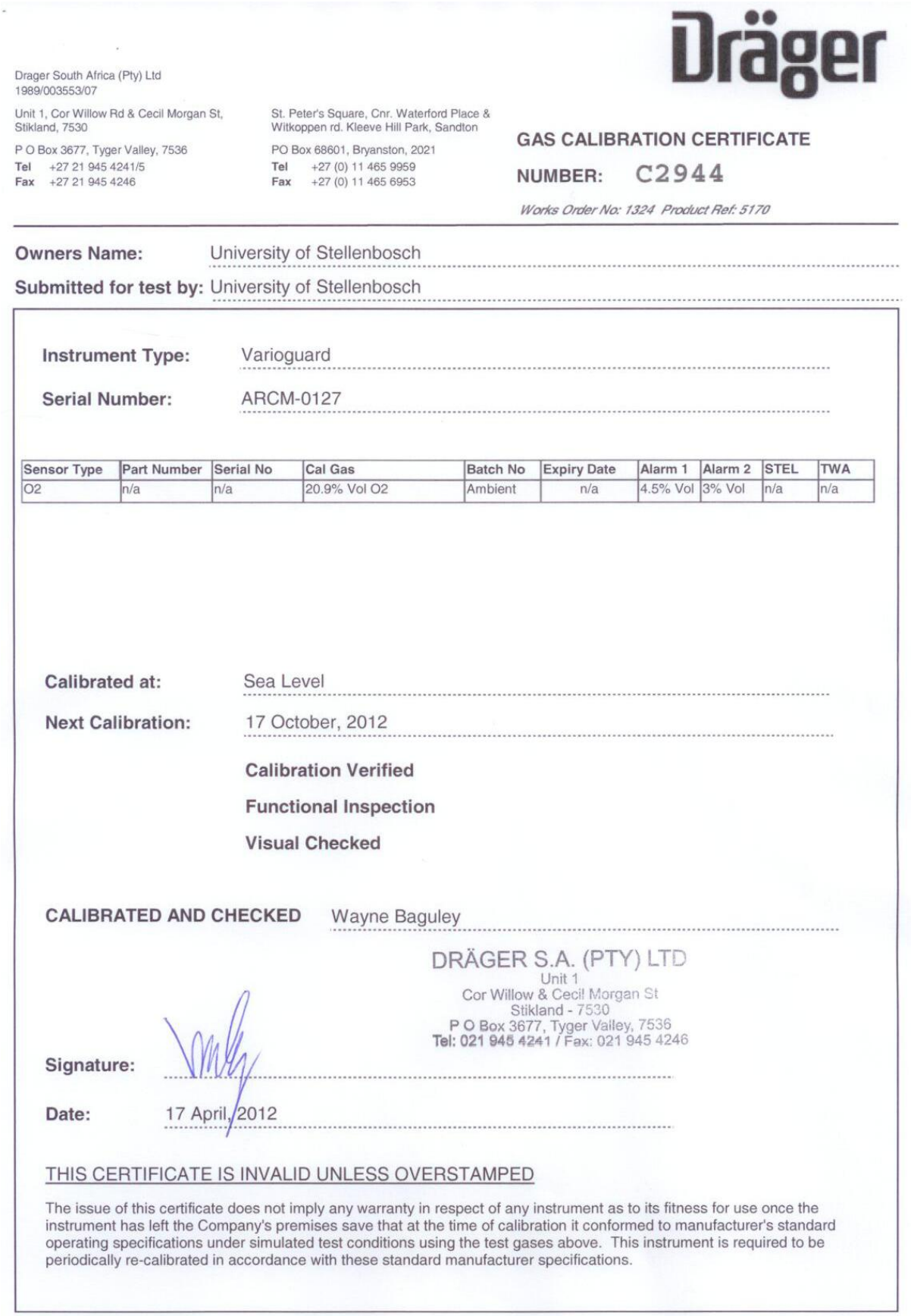

Dräger

Drager South Africa (Pty) Ltd
1989/003553/07

Unit 1, Cor Willow Rd & Cecil Morgan St,
Stikland, 7530

P O Box 3677, Tyger Valley, 7536
Tel +27 21 945 4241/5
Fax +27 21 945 4246

St. Peter's Square, Cnr. Waterford Place &
Witkoppen rd. Kleeve Hill Park, Sandton

PO Box 68601, Bryanston, 2021
Tel +27 (0) 11 465 9959
Fax +27 (0) 11 465 6953

GAS CALIBRATION CERTIFICATE

NUMBER: C2944

Works Order No: 1324 Product Ref: 5170

Owners Name: University of Stellenbosch

Submitted for test by: University of Stellenbosch

Instrument Type: Varioguard

Serial Number: ARCM-0127

Sensor Type	Part Number	Serial No	Cal Gas	Batch No	Expiry Date	Alarm 1	Alarm 2	STEL	TWA
O2	n/a	n/a	20.9% Vol O2	Ambient	n/a	4.5% Vol	3% Vol	n/a	n/a

Calibrated at: Sea Level

Next Calibration: 17 October, 2012

Calibration Verified

Functional Inspection

Visual Checked

CALIBRATED AND CHECKED Wayne Baguley

DRÄGER S.A. (PTY) LTD
Unit 1
Cor Willow & Cecil Morgan St
Stikland - 7530
P O Box 3677, Tyger Valley, 7536
Tel: 021 945 4241 / Fax: 021 945 4246

Signature:

Date: 17 April, 2012

THIS CERTIFICATE IS INVALID UNLESS OVERSTAMPED

The issue of this certificate does not imply any warranty in respect of any instrument as to its fitness for use once the instrument has left the Company's premises save that at the time of calibration it conformed to manufacturer's standard operating specifications under simulated test conditions using the test gases above. This instrument is required to be periodically re-calibrated in accordance with these standard manufacturer specifications.

FIGURE D.125 CALIBRATION CERTIFICATE FOR THE O_2 ANALYSER

ZEST
WEG Group

ZEST ELECTRIC MOTORS (PTY) LTD
Reg. No. 1991/005022/07

47 Galaxy Avenue,
Linbro Business Park, Johannesburg
Private Bag X10011
Sandton, 2146
South Africa
Tel: +27 11 723 6000
Fax: +27 11 723 6001
E-mail: info@zest.co.za
Website: www.zest.co.za

Certificate of Compliance to SANS 60079 – 0&1

(Electrical Apparatus for Explosive Gas Atmospheres)

Part 0 : IEC Requirements

Part 1 : Flameproof Enclosures 'd'

This is to certify that the following WEG motor:

Client	CFW INDUSTRIES (PTY) LTD
Motor Serial Number	1014715415
Customer Tag Number	
Power	7.5KW
Frame Size	132
Speed	2Pole
Mounting	B3/5
Voltage	380Volt
Order Number	PO 96756
Zest Reference	477944
Explosion Protection Certification	Ex d I/IIB T4 SABS MS/11-843

has been manufactured and tested to IEC / SANS 60079 - 0&1, flameproof for use in a Zone 1 or 2 hazardous area.

This motor is certified for the following operational conditions:

- "Direct-on-Line" supply (S1 duty as per IEC 60034)
- Powered by a WEG variable speed drive type CFW09, under the conditions as described in Certificate No. S-XPL/05127 and Zest Electric Motors (Pty) Ltd procedure (Certificate of Compliance No. ZEST 0507)

Any alterations to the design and or construction of the motor, exceeding the motor rating or operating the motor in an area other than that specified will invalidate the explosion protection.

Downloads of certification, Installation and Maintenance Manuals are available on ZEST website: http://www.zest.co.za/zest/downloads.html

Signed	

Date	11 APRIL 2012

CERTEX
CX 0514

SANS 60079-0&1
Ex d

SABS APPROVED

Permit No. 4754/6870

Document Number	ZEST 0002
Revision	NOV 2011

weg

FIGURE D.126 CERTIFICATE FOR THE FIREPROOF MOTOR ON THE RECYCLE GAS BLOWER, E-201

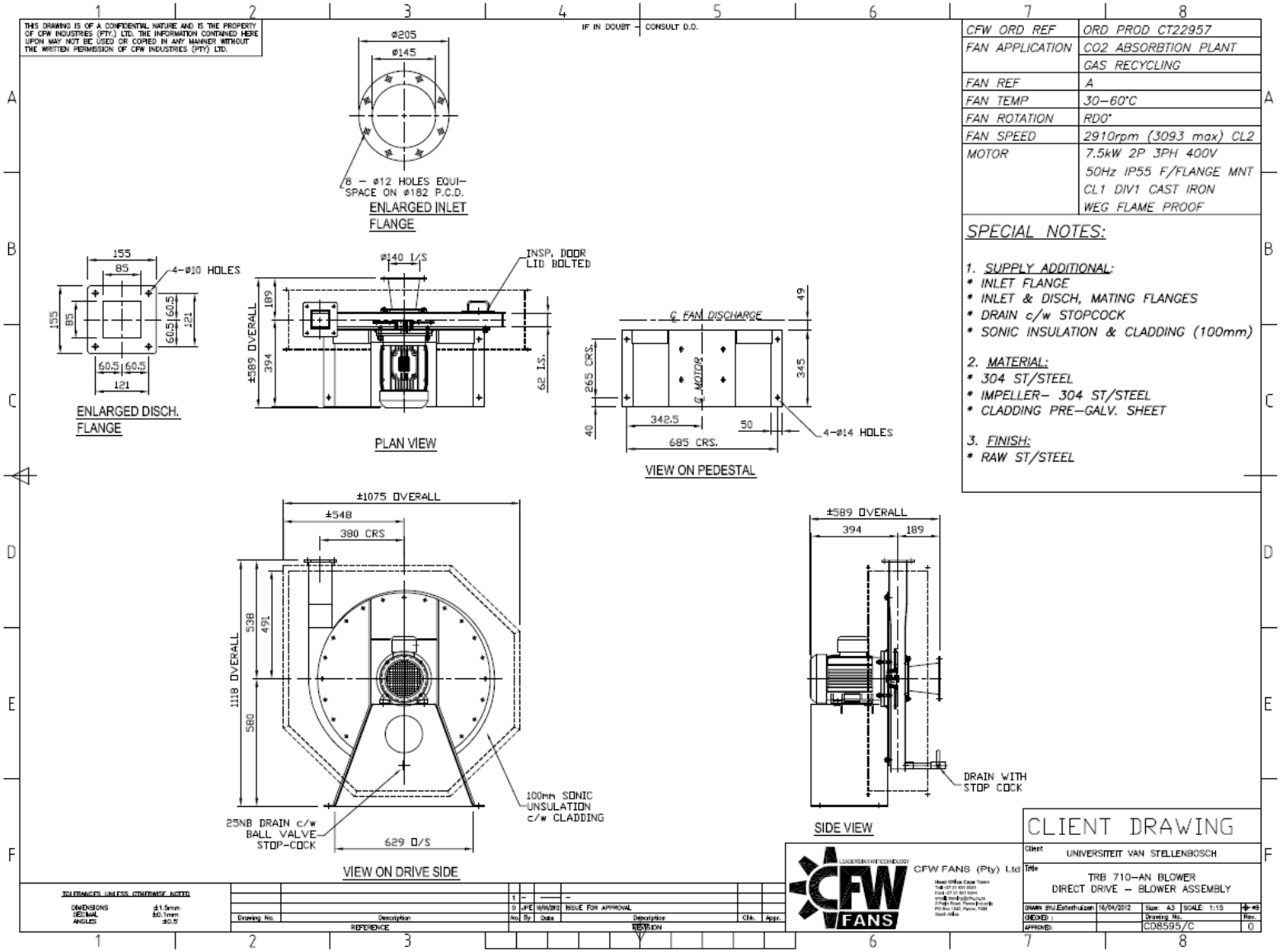

FIGURE D.127 TECHNICAL DRAWINGS OF THE GAS RECYCLE BLOWER, E-201

SIEMENS

QUALITY INSPECTION CERTIFICATE / QUALITÄTSPRÜF-ZERTIFIKAT

SITRANS P Transmitter for Pressure
DS III HART Series

Customer order / Kundenauftrag	: T859/1211
Siemens order / Siemensauftrag	: R007-4503651276
Manufacture order / Werksauftrag	: 956891 / 0030
Product number / Bestell-Nr. (1)	: 7MF4033-1CA00-1DB6
Options / Zusätze (1)	:
Serial number / Fertigungsnummer	: N1-BD14-9087292
Nominal measuring range / Nennmessbereich	: 0.04 ... 4 bar
Max. permissible pressure / Max. Betriebsdruck	: 10 bar
Output / Ausgang	: HART 4 ... 20 mA
Selected measuring range / Eingestellter Messbereich	: 0 ... 4 bar
Displayed unit / Angezeigte Einheit	: mA
Measuring point desc., TAG / Messstellenbeschreibung	: .
Measuring point message / Messstellennachricht	: .

Output Characteristic / Ausgangskennlinie

Input / Eingang (3)		Output / Ausgang [mA] (3)		Deviation / Abweich. [%]	
Pressure [%]	[bar]	Up	Down	Up	Down
0	*0*	*3.9983*	*3.9994*	*-0.0108*	*-0.0036*
50	*2*	*12.0022*	*12.0035*	*0.0138*	*0.0220*
100	*4*	*19.9995*		*-0.0034*	

- The measured values are within the admissible limits. / Die gemessenen Werte liegen innerhalb der Toleranzen.
- Compressive strength test passed. / Druckfestigkeitsprüfung bestanden.
- High-voltage and insulation test passed. / Hochspannungs- und Isolationsprüfung bestanden.

HAGUENAU, 2012-01-04

(2)

Stumpf Sébastien

.....

Works inspector / Werksprüfer

(1) Technical data see operating instructions. / Technische Daten siehe Bedienungsanleitung.
(2) Was created automatically, needs no signature. / Wurde automatisch erstellt, gilt ohne Unterschrift.
(3) PTB traceable calibrated test instruments. / Auf PTB Standart Rückverfolgbarkeit Kalibrierte Prüfgeräte.

1280985 / 6032226
2012-01-04 09:07:24

I IA SC MF-H PI-1 PRO-1 1 / 1 IEC 60770-2

FIGURE D.128 SPECIFICATION SHEET FOR ONE OF THE ABSOLUTE PRESSURE CELLS